AD 758 000

TECHNICAL REPORTS SECTION
NAVAL POSTGRADUATE SCHOOL
MONTEREY, CALIFORNIA 93940

NOLTR 72-209

INTRODUCTION TO A UNIFIED THEORY OF EXPLOSIONS (UTE)

BEST
AVAILABLE COPY

By
F. B. Porzel

14 SEPTEMBER 1972

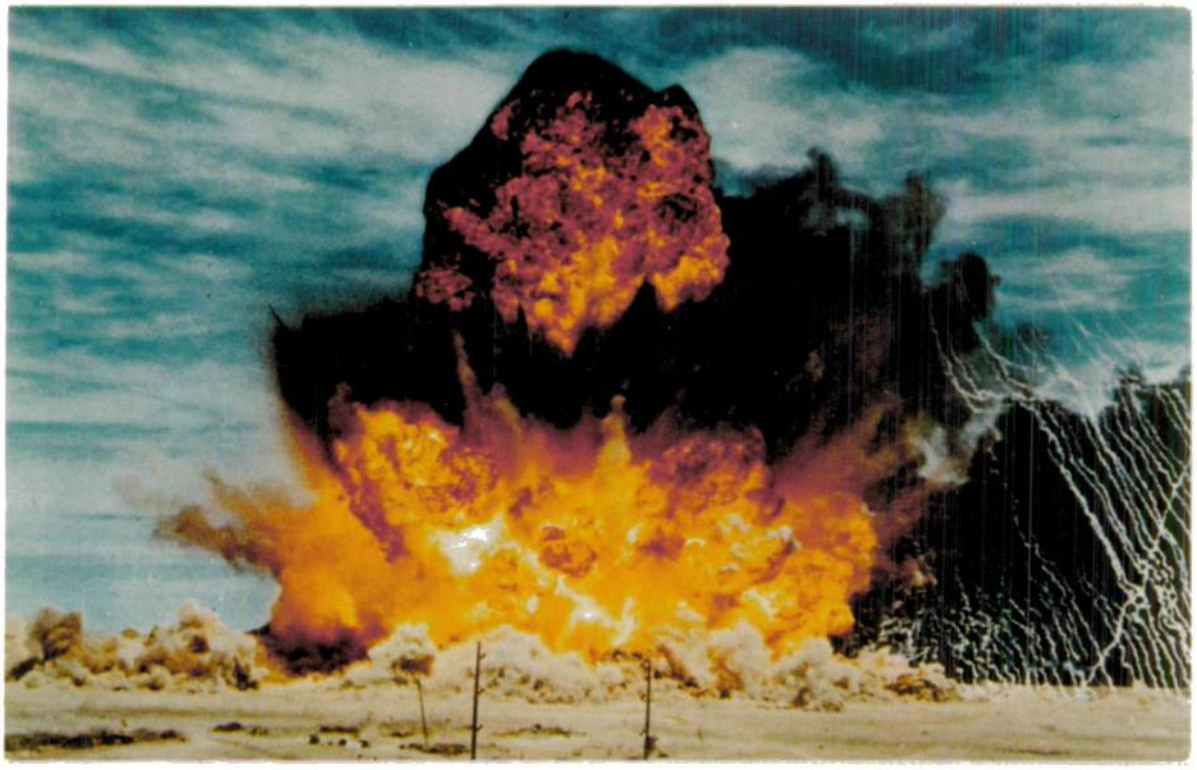
NOL

NAVAL ORDNANCE LABORATORY, WHITE OAK, SILVER SPRING, MARYLAND

NOLTR 72-209

APPROVED FOR PUBLIC RELEASE;
DISTRIBUTION UNLIMITED

500 tons of TNT were detonated on the surface of the earth at the Suffield Experimental Station, Ralston, Alberta, Canada, on the 17th of July, 1964. This was the largest non-nuclear unconfined explosion yet to be detonated.



DEAR READER:

The Good Books say that TNT finally burns to transparent gasses and water vapor.

$$C_7O_6H_5N_3 + \frac{21}{4}\ O_2 \rightarrow 1\tfrac{1}{2}N_2 + 7CO_2 + 2\tfrac{1}{2}H_2O$$

But as so often happens, "It ain't necessarily so".

THE AUTHOR

INTRODUCTION TO A UNIFIED THEORY OF EXPLOSIONS (UTE)

Prepared by:
F. B. Porzel

ABSTRACT: The unified theory of explosions offers simple methods for analyses of blast and absolute hydrodynamic yield of explosions in general and similar energy releases. The concepts and techniques apply at any shock strength, in virtually any medium and ambient conditions, and are adaptable to a gamut of burst geometries and warhead configurations. The methods are conveniently summarized by two separate BASIC machine programs, with complete instructions for prediction and evaluation of explosions in air; machine time and research effort are many times more cost effective than with present machine or hand calculations. The methods are illustrated with nuclear and TNT data. Present results indicate that the concepts and techniques are probably valid within a few percent for measuring yield, predicting peak pressure and distance; results are well within the natural variations of blast effects and well-suited to diagnose non-ideal explosions.

AIR/GROUND EXPLOSIONS DIVISION
EXPLOSIONS RESEARCH DEPARTMENT
NAVAL ORDNANCE LABORATORY
SILVER SPRING, MARYLAND 20910

NOLTR 72-209 14 September 1972

Introduction to a Unified Theory of Explosions (UTE)

This report presents a comprehensive theory of explosions capable of describing many kinds of explosions ranging from spark discharges to cosmic events. Here, however, the emphasis is on explosions in air originating from chemical high explosives and nuclear devices; the primary effect observed is blast.

The Unified Theory of Explosions (UTE) is, as any theory should be, "a closely reasoned set of propositions, derived from and supported by established evidence and intended to serve as an explanation for a group of phenomena". As such, the UTE is intended to serve also as a prediction method for the blast performance of new explosives and warheads and as a diagnostic tool for describing the explosion behavior of current explosives and warheads.

Like many a new theory introduced into an old and established field, some of new methodologies and conclusions of the UTE are in disagreement with current practices and findings. The author presents his arguments and rationale for the differences. Certainly, there will be little disagreement about the significance of the many parameters identified and treated as being common to all explosions; the identification of these parameters certainly is a large step forward in the explosion's field. The utilization of UTE for prediction and diagnostic purposes, it is hoped, will be an even larger step.

Support for this work was provided under many tasks over a period of about three years. NAVORDSYSCOM (ORD 0332) provided the initial funding; subsequent support came from DNA (SPLN now SPSS) and the Long Range Explosives Program directed by Picatinny Arsenal.

ROBERT WILLIAMSON II
Captain, USN
Commander



C. J. ARONSON
By direction

CONTENTS

		Page
INTRODUCTION		viii
1.	Assumptions and Concepts	1
1.1	Foreword	1
1.2	Methods in the Unified Theory of Explosions, UTE	6
1.3	Prompt Blast Energy, PBE	9
1.4	Hydrodynamic Yield, HY	13
1.5	Form Factor F and Generalized Scaling	17
1.6	QZQ Hypothesis	23
1.7	Generalized Modes of Energy Transport	27
1.8	The Mass Effect, MEZ	28
1.9	Average Specific Heat	33
1.10	Transition Pressure Between Strong and Weak Shocks	36
1.11	Natural Units (NU) and Generalized Equation of State, GES	38
1.12	Generalized Divergence, GDV	42
1.13	Applications	44
2.	Direct Evaluation of Blast Energy, DEB	50
2.1	Foreword	50
2.2	Concept for Direct Evaluation of Blast Yield, DEB	51
2.3	DEB506 BASIC Program	57
2.4	Input Data	59
2.5	Input Parameters and Options	60
2.6	Data Modification and Transformations	65
2.7	Waste Heat Calculations	68
2.8	Integration of Waste Heat	75
2.9	Estimates for Total Yield	80
2.10	Printout and Diagnostics	83
3.	Hand Calculation for Prediction and Direct Scaling	89
3.1	Foreword	89
3.2	QZQ Method for Predicting Pressure Distance	91
3.3	Calculating Waste Heat	93
3.4	Fix the Critical Radius	96
3.5	Direct Scaling	100
4.	Direct Scaling of Blast Energy, DSC	105
4.1	Foreword	105
4.2	Concept for Prediction and Direct Scaling of Blasts	106
4.3	The DSC506 BASIC Program	111
4.4	Input Data and Transformations	115
4.5	Input Parameters and Options	122

CONTENTS (Cont'd)

		Page
4.6	Input Options	130
4.7	Subroutines	136
4.8	Measured Data, Theoretical Curve, and Scaling	141
4.9	Summary of Yield	145
5.	Results and Summary	154
5.1	Foreword	154
5.2	Direct Evaluation of Nuclear Composite Data	157
5.3	Direct Evaluation of TNT	170
5.4	Direct Scaling, Nuclear Composite Data	176
5.5	Direct Scaling for TNT	185
5.6	Summary of Results	189
6.	Discussion	192
6.1	Yield of TNT	192
6.2	Absolute Energy vs Equivalent Weight	201
6.3	Flat Pressure-Distance Curve Close-In	205
6.4	Acoustic Decay	207
6.5	Are the Oscillations Real?	210
Alphanumeric References		222
APPENDIX A	--BASIC Machine Language: Conventions and Purposes	A-1
APPENDIX QVP	--Waste Heat Calculations for Ideal Gases and Real Air	QVP-1

ILLUSTRATIONS

Figure	Title	
1.3-1	Prompt Blast Energy and Waste Heat	12
2.2-1	DEB Concept: Direct Evaluation of Blast	56
3-1	Peak Pressure-Distance Prediction, QZ^q = Constant Method	104
4.2-1	Comparison of Weighing Data in DEB and DSC	110
5.2-1	Test of QZQ and MEZ Hypotheses	168
5.2-2	q = DLN Q/DLN Z versus Overpressure	169
5.4-1	Comparison of UTE Predictions with Nuclear and TNT Data	183
5.4-2	Comparison of Nuclear and TNT Measured Yields with Unified Blast Theory	184
6.1-1	Effect of Case Mass on Heat of Detonation in Large Chambers in Inert Gas	200
6.5-1	Possible Distortion Due to Classical Assumption	219
6.5-2	Possible Distortion Due to Failure to Recognize CUSP at Transition Pressure	219

ILLUSTRATIONS (Cont'd)

Figure	Title	Page
6.5-3	Bow Effect: An Oscillation Due to Perturbed Early History	220
6.5-4	A Suggested Relation Between the Delay of Transition and Amplitude of Oscillations.	220
6.5-5	Results of DSC Analysis on Two Nuclear Explosions.	221

TABLES

Table	Title	Page
1-1	Concepts for Unified Theory of Explosions	46
1-2	Modes of Energy Transport and Method of Describing Them in the Unified Theory of Explosions	48
2-1	LIST DEB506	85
2-2	Direct Evaluation of Blast Energy, Unified Theory for Blast	87
2-3	Nomenclature for DEB506	88
3-1	Hand Calculation for Prediction and Direct Scaling	102
4.4-4	Yield and Distance Relations in the Unified Theory of Explosions	121
4-1	LIST FOR DSC506	148
4-2	PRINTOUT FOR DSC506	151
4-3	Nomenclature for DSC506	152
5.2-1	Input Instructions DEB506, Nuclear Data	164
5.2-2	Direct Evaluation of Blast Energy, Unified Theory for Blast	165
5.2-3	Direct Evaluation of Blast Energy, Unified Theory for Blast	166
5.2-4	DEB506, Nuclear Data with Modified Q at High Pressure	167
5.3-1	Input Instructions DEB506, TNT Data.	175
5.3-2	Direct Evaluation of Blast Energy, Unified Theory for Blast	175
5.4-1	Input Instructions, DSC506, Nuclear Data	180
5.4-2	Direct Scaling with Unified Theory for Shock Growth	181
5.4-3	Direct Scaling with Unified Theory for Shock Growth	182
5.5-1	Input Instructions, DSC506, TNT Data	188
5.5-2	Direct Scaling with Unified Theory for Shock Growth	188
6.5	Is the Oscillation Real?	218
QVP-1	Waste Heat for Ideal Gases, Q * DO/PO, Acoustic Approximation	QVP-5
QVP-2	Waste Heat for Ideal Gases, Q * DO/PO, Acoustic Approximation	QVP-6
QVP-3	Waste Heat for Ideal Gases, Q * DO/PO Acoustic Approximation	QVP-7
QVP-4	Waste Heat for Ideal Gases, Q * DO/PO, Standard Adiabat	QVP-8

TABLES (Cont'd)

Table	Title	Page
QVP-5	Waste Heat for Ideal Gases, Q * DO/PO, Standard Adiabat	QVP-9
QVP-6	Waste Heat for Ideal Gases, Q * DO/PO, Standard Adiabat	QVP-10
QVP-7	Waste Heat for Ideal Gases, Q * DO/PO, Standard Adiabat	QVP-11
QVP-8	Waste Heat for Ideal Gases, Q * DO/PO, Standard Adiabat	QVP-12
QVP-9	Waste Heat for Ideal Gases, Q * DO/PO, Standard Adiabat	QVP-13
QVP-10	Waste Heat Q for Real Air	QVP-14
QVP-11	Waste Heat Q for Real Air	QVP-15
QVP-12	Waste Heat Q for Real Air	QVP-16
QVP-13	Waste Heat Q for Real Air	QVP-17
QVP-14	Waste Heat Q for Real Air	QVP-18
QVP-15	Waste Heat Q for Real Air	QVP-19
QVP-16	LIST, QVP506, For Waste Heat of Gases	QVP-20
QVP-17	Nomenclature for QVP506	QVP-22

PREFACE

Explosion evaluation has traditionally been highly empirical. A vigorous spurt of theoretical work during World War II led notably to the scaling laws and some strong shock theory for chemical explosions including that of Kirkwood-Brinkley. Although these efforts were significant advances at the time, they are too primitive for engineering design or to advance the current state-of-the-art. Some advances in theory were made since, but such calculations contain arbitrary adjustable parameters and smoothing techniques such as smearing the shock front, and most current theory omits such significant phenomena as afterburning, mass effect, radial mixing, non-ideal thermodynamics, and a host of surface effects which affect the measurements. Meanwhile, prodigious parallel study of these phenomena on nuclear explosions has been made and awaits application to high explosives.

Unified Theory of Explosions (UTE) is an organized system of about two dozen concepts, models, and techniques. About half of these originated in pioneer nuclear explosions, for prediction of effects, testing and evaluation of results, and, out of the necessity for removing the inadequacies of classical shock theory as they were already recognized at the time.

"Hydrodynamic yield" analysis was routinely used as a primary diagnostic measurement on nuclear test operations, in parallel with the radio-chemical yield. The yields on the first thermonuclear explosion, first deep underwater explosion, and the first contained underground explosion were all determined by what is now UTE. As a group leader in the test division at the Los Alamos Scientific Laboratory until 1954, the present author was a Director for Blast Programs on these and other operations, a rare and great opportunity which provided many insights which make UTE possible now.

Many of the other ideas were later developed while he was the Senior Scientific Advisor at the then Armour Research Foundation, Illinois Institute of Technology, where much of the work was sponsored by the Defense Nuclear Agency and later work was done at the Institute for Defense Analyses.

About three years ago, the author joined the Naval Ordnance Laboratory. Since then, this early work on nuclear explosions was brought to fruition and applied to high explosives as a principal effort of the author.

Francis B. Porzel

FRANCIS B. PORZEL

Naval Ordnance Laboratory
20 August 1971

INTRODUCTION

Review of Explosion Models and Terminology

"An explosion," says reference ENW, "in general, results from a very rapid release of energy within a limited space." This is true regardless of the source of energy: nuclear reaction, conventional high explosive like TNT, detonating gas, absorption of a spurt of light, of x-rays or of other radiation, lightning, electric spark, exploding electric wire, shove of a piston, impact of colliding bodies, rupture of a pressurized tank, or implosion of a paper bag. In each case, nature solves the problem of relieving the stress nowadays in the same way the ancients defined the explosion as "the action of driving out, or issuing forth with violence and noise."

As is well known nowadays, the rapid expansion initiates a shock wave in the surrounding medium -- air, water, or earth. The front of the wave soon develops into a virtually discontinuous rise in pressure, density and material velocity, with a gradual decrease, or oscillations in the same quantities behind the shock front. We will usually refer to the discontinuous rise at the front as the shock and will refer to the longer decrease as the blast wave.

The pressure at the front is as much an effect as it is a cause. True, the discontinuous rise of pressure at the front may be thought as locally causing the instantaneous rise in material velocity. But by and large, it is the inertial motion in the whole interior of

the blast wave which drives the shock ahead. There would be no shock at the front without the outward motion of material on the interior of the wave. Where Lucretius saw only "atoms and the void", he might now say "in reality there is nothing but the momentum of particles in empty space." The distinction between pressure and material velocity is itself mostly an artifice of the human imagination. The purely random directions of momentum constitute pressure; the directionalized parts of momentum constitute the material velocity. Going back to our definition, the explosion is the surge of outward momentum which relieves the energy within the initially limited space in the only direction it can usually do so -- outward toward lower pressures.

Soon after the energy release, the propagation of the shock will of course differ according to:

1. How much energy is released?
2. Within how much space and what shape?
3. In what medium is the space and what medium surrounds it?
4. How rapidly is it released?

The classical assumptions made to answer these question are thus: Taken together, (1) and (2) above imply that explosions scale, i.e., are similar, whenever their energy/ volume ratio, Y/R^3, is the same, hence $Y^{1/3}$ scaling. The shape is assumed spherical -- it provides the largest volume and least average pressure for a given shock area. In the first approximation, the medium is assumed uniform and the energy is released instantaneously.

This is typically the strong shock domain. It seems certain that however the explosion starts, nature will drive as rapidly as

possible to whatever pattern of pressure and motion in the blast wave will relieve the stress most quickly. Thus a similarity in all explosions arises; we already noted a pattern: the peak pressure is at the front and a decrease in pressure follows it. There are special reasonswhy this happens instead of a slow rise in pressure. It is a goal of UTE to find a simple set of reasons and parameters which describe the wave as it approaches similarity, whatever the initial release of energy was like.

Within these assumptions, the simplest model of an explosion as described by von Neumann (see LA 2000) is to treat "the original, central, high pressure area as a point. Clearly, the blast coming from a point, or rather from a negligible volume, can have appreciable effects in the outside atmosphere only if the original pressure is very high. One will expect that, as the original high pressure sphere shrinks to a point, the original pressure will have to rise to infinity. It is easy to see, indeed, how these two are connected. One will want the energy of the original high pressure area to have a fixed value Y_0, and as the original volume containing Y_0 shrinks to zero, the pressure in it will have to rise to infinity. It is clear that of all known phenomena nuclear explosions come nearest to realizing these conditions."

The development of the atomic bomb during World War II perforce included vigorous theoretical efforts to predict its blast, which was recognized as the principal military effect. The essential simplification permitted by the point-source model is the so-called "similarity property" of the solution. Among the theories developed on that basis were the point-source solution of J. von Neumann

(LA 2000), the "small gamma γ-1" theory of H. Bethe (LA 2000) and the classical solution of G. I. Taylor (reference Taylor). All these theories described the blast during fireball growth before breakaway, when the shock pressures are high, characteristically above 100 bars, where the density ratio across the shock is presumed to be constant and thus relatively simple solutions become possible. Although these theories were never put to extensive practical use, they did provide much of our present insight about the behavior of strong shocks. Each of these solutions idealized the explosion in such a way that the shock raduis R grows with time t according to $R \sim t^{0.4}$, or what is the same thing under these classical assumptions, the pressure P behaves as $P \sim R^{-3}$.

Fireball measurements on the first nuclear explosion in New Mexico in 1945 seemed at first to verify the simple similarity solutions (reference Taylor). But by 1950, it was already clear that the similarity relations were inadequate to describe nuclear explosions well enough for diagnostic purposes. The principal reasons for this failure of similarity were summarized in LA 1664 as radiative transport, mass effect, and non-ideal equation of state.

Radiative transport refers to the fact that for temperatures in air above 300,000° C, the fireball grows by transport of radiant energy -- random walk of photons -- faster than it can grow by hydrodynamic transport of energized molecules. Under these conditions, the fireball grows very rapidly, near the speed of light, at first, but slows rapidly so that the radius grows in time like $R \sim t^{0.09}$ instead of $R \sim t^{0.4}$. Below 300,000° C or a shock pressure of 80,000 bars shock transport is faster than radiative transport. The fireball

does grow as a strong shock, but the early history of radiative growth causes the shock radius to be larger than one would expect by purely hydrodynamic growth. Radiative transport probably predominates on the interior of any strong shock, owing to the higher temperature and lower density near the center than at the front. As a result of radiative transport, the pressure, temperature, and density are more uniform in the blast wave than pure hydrodynamics would predict. We refer to this uniformity as an isothermal sphere.

Mass effect (LA 1664) pointed up the physical fact that close enough to any real explosion, including nuclear, the material in the blast wave is obviously not air, as is presupposed in the similarity solutions. It is mostly bomb debris, vaporized tower or warhead parts, material which characteristically weighs thousands of times as much as a comparable volume of uniform air. As a consequence, the early pressures and temperatures are drastically reduced from what a point source model would predict. But the momentum of the debris means a heavier "piston" drives the shock and sustains the peak pressure. Eventually, as more and more air is engulfed by the shock, the mass of debris becomes negligible compared with the air engulfed. The point source assumption becomes increasingly accurate, and the shock reaches the pressures predicted by similarity. (As we shall see, the pressure-distance curves even cross, the "massive" bomb being more efficient.) As a result the pressure-distance curve is initially much flatter, for a massive bomb; it turns down near the point where the air and bomb mass become equal.

Non-ideal equation of state refers to the fact that above 10 bars or so (150 psi) air does not behave like an ideal gas. The behavior

was treated in LA 1664 by a "variable gamma" equation of state; it was these variations with pressures, which negated the ideal gas similarity. But different similarities were possible. Also, as a consequence of real gas effects, hydrodynamic energy is used up and stored at different rates than ideal air.

The analytic solution methods (ANS) described in LA 1664 are an intrinsic part of UTE and were developed to circumvent these failures of similarity scaling. A real equation of state and a bomb mass were included in the blast parameters. No assumptions were made to predict the R vs t curve; rather, radius-time data from fireball measurements were input to the solution and used to deduce the interior wave and thus evaluate the yield.

A conventional chemical explosion, such as the TNT explosion on the frontispiece, clearly requires a much more complex model than a nuclear explosion. A nuclear fireball is often a nearly perfect sphere at comparably late times. Yet, many of the non-ideal properties of TNT are encompassed in the perturbations already found for nuclear explosions, especially mass effect. The difference is drastic, but more a difference in degree than a new type of explosion.

Consider the mass effect. If a small A-bomb, 1KT, were actually high explosive, it would obviously weigh (close to) 1000 tons; the real device is obviously transportable by aircraft or can be shot from a cannon. If we fired a 1KT nuclear device, surrounded with 1000 tons of inert material, a sphere of rock-like material 17 feet in radius, the resulting explosion would resemble the frontispiece, jets and all. To a first approximation, mass and energy are the controlling parameters here. At least, this is a hypothesis to be tested in the

present paper by comparing nuclear and TNT curves.

There are qualitative differences between the mass effect on HE and nuclear. In nuclear bombs the initial temperatures are so high that all debris is gaseous, at least until a late stage where it condenses to smoke. On HE, much of the debris is particulate, smoke and particles evident in the frontispiece. These effects will be discussed later and the differences characterized by parameters for mass and average specific heat.

The equation of state of air is a lesser problem on HE than for nuclear explosions because the initial pressures from HE are lower and in a domain where the ideal gas law does not fail severely. Yet, the non-ideal equation of state of air, which is caused by numerous exothermic and endothermic phase and chemical changes is paralleled by unidynamic analogs in afterburning and waste heat respectively.

By afterburning we refer to the fact that the release of energy may not be instantaneous. It is energy that is released late by chemical or phase changes; it is due to potential energy which is not initially manifest as pressure. Afterburning may arise, as the name suggests, from unburned fuel in oxygen-deficient explosives which can burn only after the debris has mixed with air. (Some fuel seems to be burning in the frontispiece, but much material, which should have burned by this late stage, obviously did not burn.) Afterburning is also possible from reactions which occur too slowly to be part of detonation, or reactions which are possible only at reduced pressures or temperatures. They are paralleled in the nuclear case, although there on an insignificant scale energy-wise, by burning of tower or other equipment originally vaporized by the bomb.

By waste heat we refer to energy which, by one process or another, propagates too slowly or remains as residual heat in the debris on the interior, and is thereby lost to the shock. There is a parallel between the residual heat of bomb debris and the late incandescent fireball of a nuclear explosion. The bookkeeping of energy into two fractions, prompt energy and waste heat, is a central feature of the unified theory of explosions. By generalized waste heat we will mean any process which removes energy from the shock, analagous to the normal partition but in addition to the "shock dissipation".

Radiative transport has no direct counterpart on high explosives, unless we think of the jets as precursors carrying energy ahead of the shock. But there are different remarkable coincidences: The radius of the fireball at the end of the radiative phase scales closely to the charge radius of most high explosives. As we shall see, the long range blast from 1 kiloton nuclear occurs on a distance scale almost 100 times that from 1 pound of TNT. It also happens that the charge radius for the HE is 4 cm, and the isothermal sphere radius is about 4.2 meters. The waste heat in the nuclear case is uniform because it is an isothermal sphere at this stage; in HE it is uniform because the detonation wave presumably left all the material in the same state. Thus if we count the hydrodynamic yield as only that energy actually delivered to air, we can count the energy in one case to the charge radius, and in the other, to the isothermal sphere. The waste heat of material within these distances is not counted as part of the hydrodynamic yield but can be estimated assuming uniformity.

Cased, high-explosive weapons represent another degree of complexity. Yet, as we shall see, the mechanisms already discussed, mass effect, afterburning, and waste heat, readily accommodate to the energy transfer for very fine to massive fragments to air. To a first approximation, the addition of case mass in any form is only a modest change compared with the drastic change already made in going from a point-source to a chemical explosion. If nuclear and bare HE can be correlated by the mass effect, the case mass becomes a trivial extension. We can treat a cased weapon much like a bare charge of the same energy release but with increased mass.

By a weak shock we refer to late times when the shock front is so far removed from the explosion center that the source no longer matters. Virtually, by definition, all explosions then become similar including cased weapons. There is a stronger physical reason than sheer distance or the fact that the total mass of case and debris becomes small compared with the mass of air engulfed. When the shock reaches an overpressure of about 2 bars or 30 psi, a negative phase first develops in the wave where the pressure and sound velocity are both below ambient, and the material velocity may be reversed from the shock. This means that hydrodynamic signals from the interior can no longer overtake the shock front. The blast wave then must "coast" on whatever momentum it already possesses. Of course, if strong energy signals are still coming from within the wave interior, even though the shock pressure is only 2 bars, the negative phase will not develop so soon, the shot will still be "strong" on that basis, and the peak pressure will not decay as fast as scaling would indicate. Sooner or later a negative phase will develop, the shock will become "weak" by definition and ought to become similar to all other "weak shocks".

When the author joined the Los Alamos Scientific Laboratory nearly a quarter century ago, it was a lively controversial question: "Do nuclear explosions scale with HE?". As it turned out within a few years, both sides were right. Explosions do scale at late times over enormous ranges of energy release, 10^{19} times from spark gaps to H-bombs. But this applies only if their very different early "non-scalable" history is taken into account. In general then, we can expect failures in scaling during the strong shock phase, when the shock front is in communication with the interior. We expect similarities during the weak shock phase when the shock is isolated from the interior.

Beyond that, when and how close similarity is approached, we cannot say without more precise conceptual and calculational tools. Lord Kelvin's remark is most apt! "When we cannot measure, our knowledge is meagre and unsatisfactory". The point in UTE is to provide a means of measurement, for just such a richer and better understanding of explosions.

1. Assumptions and Concepts

1.1 Foreword

The unified theory of explosions offers simple concepts and methods for hydrodynamic yield (free field blast energy) and blast analyses for explosions in general and for similar energy releases. They apply at any shock strength, in virtually any medium and ambient conditions, and are adaptable to a gamut of burst geometries and warhead configurations.

In Chapter 1, we amplify the above portion of the abstract phrase by phrase. Each such phrase most typically applies to a specific concept or assumption, which is identified by a section heading and an acronym for short. In the present "introduction" paper the exposition is not complete, but can only be a brief summary for what will require a separate paper later for each topic. Table 1-1 shows the scope of these concepts and how they fit into the UTE.

The main goal of this paper is to describe two machine programs, one described in Chapter 2 for direct evaluation of blast energy (or hydrodynamic yield) and the other in Chapters 3 and 4 on direct scaling of blast energy. In this chapter, we seek only to give enough information to help the reader use the machine programs, without the deluge of reasons why one particular approach was chosen over all the other possible choices which were considered. Analyses for a typical nuclear and a TNT explosion serve as illustrative examples and are given in Chapter 5. Results are summarized in Chapter 5. The more controversial results are discussed in Chapter 6.

The remainder of the Section 1.1 concerns some ideas underlying this unified approach to explosions.

Explosions are of broad interest and often beyond the scope of much classical physics because they involve processes which are:

discontinuous, as at the shock and fireball fronts,
non-conservative and irreversible,
highly non-linear,
not steady-state but violently time-dependent,
initially asymmetrical,
propagated in mixtures in complex and non-uniform media
most significantly, their boundaries are free.

The last means that the shock front conditions are not given as a priori conditions but are virtually the solution being sought in the "shock problem."

Explosions begin as a random smear of suddenly released energy and, as if contrary to "maximum disorder" interpretations of the second Law of Thermodynamics, rapidly drive instead toward a highly organized structure of motion and stress. They are highly reproducible too; in his experience the author finds the main features to scale over a range of 10^{19} times in energy and about 10^{30} times in energy density, covering as broad a range as any law in physics.

Yet, the above list of explosion characteristics denies virtually all the prerequisites usually assumed in modeling physical phenomena: static, continuous, conservative, reversible, linear, etc. It is to be expected then that many of our classical concepts, which were quite adequate for those processes, will be found inadequate for the dynamic phenomena attending real explosions.

This chapter proposes models, assumptions, and concepts, shown in Table 1-1, which so far do appear adequate for blast. These ideas are themselves part of an even broader study of explosions and dynamic processes. Since the 19th century physics has already usurped the word "thermodynamics" for what should have been called "thermostatics," the word "unidynamics" is perhaps suitable for the collective body of those ideas which follow: not aerodynamics, hydrodynamics, or geodynamics, but the dynamics of stuff in general.

Unidynamics combines two common sense goals: simplicity, and generalization.

William of Occam stated the goal best: "essentia non sunt multiplicanda praeter necessitatem." I take this to mean literally "essentials should not be multiplied prior to necessity." There is small practical point in theory that is more exact than the natural variations in the effects it describes, is more complicated than the user can "do for himself" or contains more input parameters than he can afford in money and research effort. Exact solutions often betray what is really the physical naivete of the model, whatever the virtuosity of the performance on an unreal problem.

The second part of the goal, generalization, embodies an idea of "unidynamic analogs." While Nature is infinitely diverse, our finite brains can tolerate only a handful of differential equations which govern their behavior. Nature is seldom so unkind as that a phenomenon depends upon a dozen equally important causes; only a few most important ones usually control it. Every phenomenon is describable by a characteristic form of equation or solution. If any two phenomena happen to have the same basic differential equation or

other characteristic behavior, to that extent they can be described by the same mathematical solution, however else they may differ in outward form or in minor details. We then say they are "unidynamic analogs."

Now, to disregard the similarity that exists among many such analogs, out of lip-service to the rigors of Specialized Scientific Scriptures, is like saying Newton's law of gravity is perforce wrong because "you cannot mix apples and planets." Worse than that, we throw away useful information and waste money and effort on duplicative research effort if we do not recognize that what we see happen in one phenomenon because it follows as a consequence of the mathematical model, must necessarily follow in all the unidynamic analogs as a consequence of the same mathematics. We block, instead of stimulating, cross-fertilization of ideas.

Most of the time we do not seek perfect answers; all we care about is whether some perturbation makes the effect we see go up, go down, or wiggle a little. Table 1-2, discussed later in Section 1.7, is a specific example listing about 30 such perturbations. All but the first two--adiabatic work and kinetic energy--have usually been ignored heretofore in blast theory. Yet most of them are unidynamic analogs which can be described in the unified blast theory by varying a single parameter q.

In summary, the underlying goal in unidynamics and in the unified blast theory is not a precise solution, but to find a simple adequate way of finding and describing which variables most strongly control all explosions. To ask "which one is right?" is a misleading question. They all apply one way or another, but the differences

among many of them are too inconsequential to make a practical difference or to resolve by experiment.

To see first where the theory leads, some end-product methods are briefly noted in Section 1.2, which follows. The ideas which underlie the methods are then summarized in Sections 1.3 to 1.13.

1.2 Methods in the Unified Theory of Explosions, UTE

"Simple methods" in the abstract refers specifically to five techniques; they are end results of UTE.

1. Direct evaluation of Blast Energy, DEB
2. Direct scaling for Blast Energy, DSC
3. Analytic Solution, ANS
4. QR^4 criterion for yield, QR^4
5. Miniequation, MEQ

The first two methods, DEB and DSC, have been firmed into do-it-yourself BASIC machine programs described in Chapters 2 through 4. These programs require a knowledge only of algebra and about ten simple specialized English words and insure that the exposition is complete. (See Appendix "BASIC.") Raw pressure-distance data or other measures of shock strength are input. Input parameters for DEB and DSC include the ambient pressure, density, adiabatic compressibility exponent of the medium, the initial or charge radius and the total weight of the explosive and surrounds. Options for varying other parameters such as specific heat of explosive, initial pressure, etc., are provided but the values are estimated automatically if not explicitly specified by the user. The output for both DEB and DSC is an annotated table analyzing the data and calculating the energy release. DEB makes maximum use of data and evaluates them with a minimum of theory. DSC makes maximum use of theory, predicts a theoretical pressure curve for shock growth for a trial yield, and then compares the measured with predicted results.

The Analytic Solution ANS is the oldest of the UTE methods and is already well documented in the literature (see LA 1664, ARF D125, DASA 1285 (1)), AIAA, 8, No 2.

The absolute energy and wave forms for a blast wave were derived from a given time-of-arrival curve. The method: assume a physically plausible wave form for density $\rho(r/R)$ as a function of distance r at a fixed time when the shock is at distance R; use conservation of mass to deduce the corresponding material velocity wave form u(r); use conservation of momentum to deduce the pressure gradient $\partial P/\partial r$ and then obtain P(r) by integration. Shock front conditions are used to fix constants of integration and other parameters. Knowing $\rho(r)$, u(r), P(r) the hydrodynamic energy of radius R is given directly by integrating over the shock volume.

The analytic solution was routinely used to determine the hydrodynamic yield on nuclear tests and for pioneering the close-in phenomena on the first thermonuclear explosion, IVY Mike (WT 9001); on the first deep underwater explosion, WIGWAM, (WT 1034); and on the first contained underground explosion RAINIER, (WT 1495). A major advance is made by the present theory because the DEB and DSC methods now provide a reliable boundary condition for any input condition from theory instead of requiring actual shock measurements for each explosion, as then required. Also, whereas these early analytic solutions were for interior wave forms and naturally restricted to strong shocks because of their goal--to obtain the hydrodynamic yield of a nuclear explosion--the recent work under the present NOL study applies to all shock strengths at the front and shows highly fruitful extensions for interior wave forms of weak shocks. The latter work is not complete and has not yet been firmed into a BASIC program.

To the user primarily interested in damage or systems analyses, as opposed to blast analysis and diagnoses, two other simplified methods

of UTE, the QR^4 criterion and the mini-equation, offer notable advantages of speed and economy: the predicted radius R for a given shock strength P is a single expression for R(P). Thus the whole blast prediction problem is reduced to a single line, ideally suited for incorporation into a complex operational analysis or study of effects. Briefly these methods are:

QR^4 Figure-of-Merit. The idea is that in free air the product of waste heat Q for a shock (internal energy less the adiabatic work) and the fourth power of the shock radius R is essentially a constant below 50 psi. Most explosions do not scale with original energy release because of their different early histories, and anomalies may persist to low pressures due to long duration energy release or severe energy losses at nearby surfaces. Yet all explosions approach similarity at long enough distances, and QR^4 expresses both the initial yield and the final "efficiency" for relatively ideal media. Because Q is an explicit function of pressure, QR^4= constant is virtually a simple power law relating a pressure, distance, and yield.

Mini-equation (MEQ). For an instantaneous ideal energy release in air, MEQ is a single expression giving the distance R for any shock pressure, initial energy release, ambient pressure, density, and weight of explosive and surrounds.

These QR^4 and MEQ methods will not be described in further detail in this paper, but follow directly from the DEB and DSC methods.

1.3 Prompt Blast Energy, PBE

"Free field blast energy" in the abstract refers to a concept for prompt blast energy PBE in UTE. The end idea is that growth of explosions is directly controlled by the promptly available (undissipated) blast energy Y(R) still remaining within a given shock radius R rather than by its original (fixed) energy Y_o such as is assumed in conventional cube-root scaling. The new theory does not negate cube-root scaling but extends it to presently unscalable cases. Nuclear vs high explosives are a dramatic example and provide a definitive test of the theory; the well known "efficiency" of nuclear explosions--quoted variously from 30% to 70%--demonstrates in fact failure in cube-root scaling for absolute yields.

Rigorous thermodynamic definitions are first devised to separate the total hydrodynamic energy E_T of a pressurized, moving medium into two fractions on the basis of its damage potential. The prompt fraction PBE may be characterized by the static overpressure and the dynamic pressure. As shown in Figure 1.3-1, the static fraction comprises the work done by actual expansion from the present pressure P_i and volume V_i to some final volume V_f and final pressure P_f,

$$W \equiv \int_{V_i}^{V_f} PdV \text{ (actual path)}. \qquad \begin{matrix} 1.3\text{-}1 \\ \text{PBE-}1 \end{matrix}$$

The total prompt energy also includes the kinetic energy per unit mass, due to material velocity u:

$$K = u^2/2.$$

The remaining fraction Q of the total energy E_T

$$E_T \equiv Q + W + K \qquad \begin{matrix} 1.3\text{-}2 \\ PBE\text{-}2 \end{matrix}$$

is defined so as to comprise those modes of energy which either do not enter into the energy transactions at all, (like ionization energy or other components of mc^2) or are transported too slowly to support the blast (like temperature <u>per se</u>).

As implied in Equation 1.3-1 and shown in Figure 1.3-1, Q represents the "ambient energy" $Eo = \int_{V_f}^{\infty} PdV$. Q is different before and after the shock. The well known entropy change across a shock is the main contributor to ΔQ.

The separation of energy into prompt and delayed fractions for dynamic processes instead of using an absolute state variable like entropy is done in UTE for several reasons. First, they are not the same thing; the waste heat ΔQ is an energy and entropy change $S - S_o$ is a heat capacity. We cannot calculate the correspondence between them without knowing the average time history of temperature $\bar{T}$, $\Delta Q = \bar{T}(S-S_o)$, and it is far easier--and less prone to error--to calculate ΔQ directly. Secondly, the flow of hydrodynamic energy is in directions and at rates which are in fact governed by the overpressure, not by the absolute state variables. Third, "time is of the essence"; many separations of energy can occur in adiabatic processes which depend upon which mode of transport is the fastest, having nothing to do with entropy. Fourth, separations of energy occur in explosions which cannot be described by the usual entropy concepts. Finally, PBE avoids other inadequate and ambiguous properties of an absolute state variable like entropy when many different processes are present.

Table 1-2 shows about thirty such modes of energy transport and how the energy transactions are accommodated by PBE and various other concepts in UTE. Classical thermodynamics dealt with only the first mode: $\int PdV$ expansion along an adiabat.

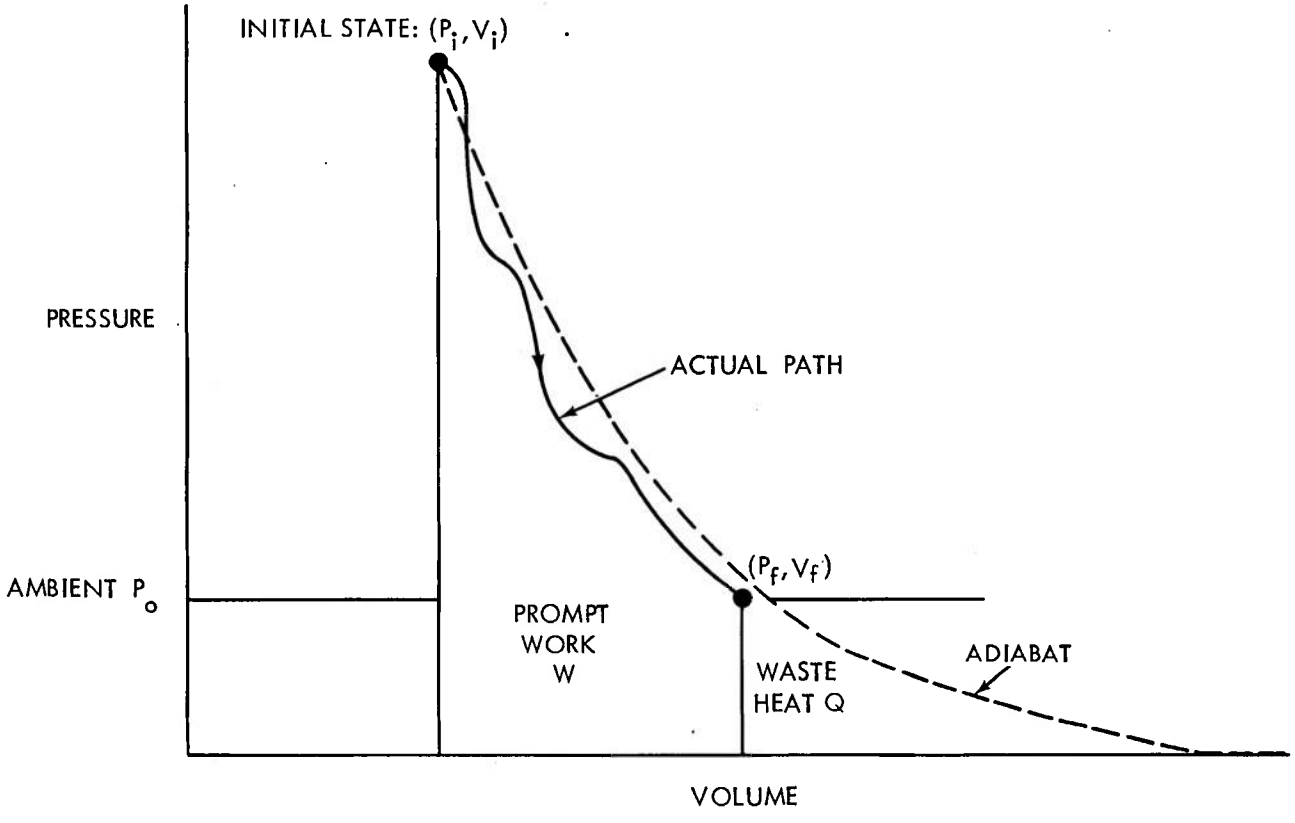


FIG. 1.3-1 PROMPT BLAST ENERGY AND WASTE HEAT.

$$W \equiv \int_{P}^{P_o} P\, dV \quad \text{(actual path)}$$

$$E_I = W + Q$$

1.4 Hydrodynamic Yield, HY

The integral Y(R) of prompt energy in a spherically symmetric wave is defined as

$$Y(R) = 4\pi \int_0^R (W + K)\, r^2 dr \qquad \begin{matrix} 1.4\text{-}1 \\ (HY\text{-}1) \end{matrix}$$

where r is the distance of an interior particle from the center and R is the shock radius. As the shock grows, the energy within the wave is continually converted from prompt energy W + K to delayed energy Q according to

$$\frac{dY}{dR} = -4\pi\, QR^2 \quad . \qquad 1.4\text{-}2$$

Of course, nearly all the dissipation does occur at the shock front as implied here; but if other losses occur on the interior, the energy bookkeeping may still be done on the basis of the shock. Material in shells of shock area $4\pi QR^2$ and thickness dR undergoes an average conversion of Q_τ cal/cm^3; thus

$$Q_{Total} = Q_{Shock}\left[1 + \frac{Q_{interior}}{Q_{shock}}\right] .$$

Eventually, all the original available energy is so converted to delayed energy, and Y = 0 at R = ∞. But Q is not all really "dissipated", it is only delayed. Q is the heat which later radiates from a nuclear fireball, it becomes the source of energy for their firestorms. Q is the bubble energy of an underwater explosion. Q is the principal seismic energy seen at a long distance from an underground explosion--the transverse Love and Rayleigh Waves--and is also the source of the cavity pressures, if any. Q may appear as energy of secondary shocks or even a train of "shocklets."

Hydrodynamic yield is an absolute measure of energy and usually refers to the total blast energy Y_o actually released at the charge surface R_o. Y_o gives a direct measure of energy expressed in nuclear "kilotons" (10^{12} cal) or in nuclear kilograms (1 megacalories = 10^6 calories). We note that an "equivalent weight" is an ambiguous measure of energy because it is relative to an empirical standard like TNT whose heat of explosion may be uncertain by a factor of 2.

From the definition for PBE as the energy delivered to the medium it follows directly that

$$Y_o = 4\pi \int_0^{R_o} (W + K)\, r^2 dr = 4\pi \int_{R_o}^{\infty} QR^2 dR \quad . \qquad \text{(HY-2)}$$

Y_o is essentially the heat of detonation or heat of explosion. However, it does not include the waste heat of explosion products, $4\pi \int_0^{R_o} Qr^2\, dr$. But it does include whatever fraction of the heat of combustion, due to afterburning of debris in surrounding air, burns early enough to support the growing shock front.

Hydrodynamic yield also refers to the prompt energy Y(R) remaining in the blast at any greater radius of shock. Consistent with HY-2,

$$Y(R) = 4\pi \int_c^{R} (W + K)\, r^2 dr = 4\pi \int_{R}^{\infty} QR^2 dR \quad . \qquad \text{(HY-3)}$$

The right hand integral is important because Y(R) provides the means to scale, based on similarities during late times, explosions which

are otherwise unscalable because of their very different histories at early times, say comparing nuclear and TNT.

It will be recognized that the dissipation equation 1.4-2 resembles but is not the same as in the well known Kirkwood-Brinkley theory. Theirs is perhaps the only other shock theory, other than early versions of UTE, which explicitly recognizes some partition of blast energy. However these differences should also be noted:

a. The Kirkwood-Brinkley expression uses the enthalpy change h instead of waste heat Q, which is an internal energy change. $\Delta H = \Delta E + P_o(V_o - V)$ includes $P\Delta V$ work which is not wasted, but delivered to the surrounding air.

b. Instead of the space integral of W + K as in HY-3, Kirkwood-Brinkley would write (in our notation) the time integral

$$Y(R) = 4\pi R^2 \int_{t(R)}^{\infty} P(t)\, u(t)\, dt$$

where P is the absolute pressure, u the material velocity, all at a fixed position R (as if the material did not move).

c. Kirkwood-Brinkley assumed a specific form for P and u on the interior, essentially that $Pu = \text{constant } e^{-kt}$. This is a main limitation on their theory because it is quite arbitrary and does not permit a negative phase in the wave.

d. Q is more general in UTE than h in the Kirkwood-Brinkley theory. Q includes losses other than entropy changes and also can be an average value without requiring a spherically symmetric wave.

Beside the error of using enthalpy instead of waste heat, the preemptive difference here is (b) above: UTE does not require a specification of the interior wave forms. Of course, some other "condition"

is thereby required to solve the hydrodynamic equations instead of Kirkwood-Brinkley wave forms. These in UTE are the form factor F and the QZQ hypothesis in the two sections which follow.

Other significant differences exist between the Kirkwood-Brinkley and UTE theories, but further discussion is deferred until all the UTE concepts have been discussed.

1.5 Form Factor F and Generalized Scaling

The form factor F was a generic and useful concept used in all the early versions of UTE in the analytic solution ANS for hydrodynamic yield of nuclear weapons. (See LA 1664 for free air bursts, WT 1034 for underwater bursts and WT 1495 for underground bursts.)

We can always define a factor F such that

$$Y \equiv \underbrace{\frac{4\Pi}{3} R^3}_{\text{shock volume}} \cdot \underbrace{P}_{\text{pressure at the shock front (energy/unit volume)}} \cdot \underbrace{F}_{\text{average energy on interior relative to peak pressure}}$$

$$\text{Blast energy} = \text{shock volume} \cdot \text{pressure at the shock front (energy/unit volume)} \cdot \text{average energy on interior relative to peak pressure}$$

We recognize that a different F

$$F = \frac{Y}{\frac{4\pi}{3} R^3 P}$$

applies depending on how Y and P are defined.

Probably the most important single experimental fact learned about explosions in the past thirty years is the fact that they scale, and over enormous ranges of yield. This means that there must exist a quantity F which is not unique to a specific explosion, requiring a separate calculation for each, but some average energy, a <u>form factor</u> common to all explosions. If we can determine it for one, we can determine it for all similar explosions.

Several families of scaling laws follow immediately from defining F, one family by demanding that F is some unique function of the shock strength $(\frac{P}{\alpha})$

$$\frac{Y}{\frac{4\pi}{3} R^3 \alpha} = \frac{P}{\alpha} F\left(\frac{P}{\alpha}\right)$$

where α can be any constant. In particular, familiar Sachs scaling employs the initial yield and ambient pressure

$$Y = Y_o$$

$$\alpha = P_o$$

and we observe that this implies

$$\frac{(Y_o/P_o)}{R^3} = \frac{P}{P_o} F\left(\frac{P}{P_o}\right) \quad .$$

The right side is a function of shock strength only. Accordingly, the left side must also be invariant for any fixed value of P/P_o, and we recognize it as the familiar "scaling law" that $R \sim (Y_o/P_o)^{1/3}$.

In particular, strong shock similarity hypothesizes that F = constant and is independent of shock strength. From this follows the classical strong shock similarity condition that, for fixed Y_o and P_o, $P \sim \frac{1}{R^3}$.

The restraint on F for weak shocks follows from acoustic theory. The general wave equation is

$$\nabla^2 \psi - \frac{1}{c^2} \frac{\partial^2 \psi}{\partial t^2} = 0 \quad .$$

For plane waves

$$\frac{\partial^2 \psi}{\partial r^2} - \frac{1}{c^2} \frac{\partial^2 \psi}{\partial t^2} = 0$$

and for a spherical wave, $\nabla^2 = \frac{\partial^2}{\partial r^2} + \frac{2}{r}\frac{\partial}{\partial r}$ so that

$$\frac{\partial^2 \psi}{\partial r^2} + \frac{2}{r}\frac{\partial \psi}{\partial r} - \frac{1}{c^2}\frac{\partial^2 \psi}{\partial t^2} = 0 \quad .$$

As is well known, if ψ is a solution to the plane wave equation the transformation $Z = \frac{\psi}{r}$ gives Z as a solution to the spherical wave. Because

$$\frac{\partial Z}{\partial r} = \frac{1}{r}\frac{\partial \psi}{\partial r} - \frac{\psi}{r^2}$$

$$\frac{\partial^2 Z}{\partial r^2} = \frac{1}{r}\frac{\partial^2 \psi}{\partial r^2} - \frac{2}{r^2}\frac{\partial \psi}{\partial r} + \frac{2\psi}{r^3}$$

$$\frac{2}{r}\frac{\partial Z}{\partial r} = \quad + \frac{2}{r^2}\frac{\partial \psi}{\partial r} - \frac{2\psi}{r^3}$$

and adding: $$\nabla^2 Z = \frac{1}{r}\frac{\partial^2 \psi}{\partial r^2} \quad .$$

Also $\frac{\partial^2 Z}{\partial t^2} = \frac{1}{r}\frac{\partial^2 \psi}{\partial t^2}$ so that the spherical wave can be reduced to a form Z(r,t) identical with a plane wave equation for $\psi(r,t)$

$$\nabla^2 Z = \frac{1}{c^2}\frac{\partial^2 Z}{\partial t^2}$$

$$\frac{1}{r}\frac{\partial^2 \psi}{\partial r^2} = \frac{1}{c^2 r}\frac{\partial^2 \psi}{\partial t^2} \quad .$$

Physically, to say that $Z = \frac{\psi}{r}$ is a solution for the spherical wave, where ψ is a solution for the plane wave, means that at long distances, where r is relatively constant over the wave length, the plane and spherical wave forms will appear similar to an observer at r.

Assume this similarity is the case. We then conclude that since a constant amplitude describes a traveling planar wave, then the overpressure P in an acoustic spherical wave must decay in amplitude like $P \sim \frac{1}{R}$. That being the case, since by definition,

$$\frac{Y_o}{R^3} \sim FP \sim \frac{F}{R} \quad ,$$

it follows that $\frac{Y_o}{R^2} \sim F$ which implies that $F \sim P^2$.

In summary, there are two restraints on F in classical theory:

strong shock similarity: F = constant, $\frac{P}{P_o} >> 1$

acoustic theory: $F \sim P^2$, $\frac{P}{P_o} << 1$.

With regard to scaling, we know as a matter of experience that explosions which have very different early histories do show similar behavior at low pressures. As is well known, nuclear explosions do scale with chemical explosions for low overpressures, but with a relative efficiency more like 30% to 50% for the nuclear. Thus, scaling does not follow Y_o, but we require an "efficiency" to make them scale.

This anomaly, that explosions can scale but not with the original energy, is removed by more generalized scaling in the following way. From HY-3 we see that the prompt energy of the wave and thus the form factor is in fact determinable by the late history; that is

$$Y(R) = 4\pi \int_R^\infty \rho R^2 dR = \frac{4\pi}{3} R^3 PF$$

$$Y(R)/R^3 \sim PF(P)$$

embraces a region which is similar for the two explosions. A major change in "unidynamic scaling" follows: explosions scale according to the available fraction Y(R) and not the original energy Y_o.

A second major change for unidynamic scaling is the choice of a normalizing factor for the pressure.

For many physical reasons, we will define a ψ such that

$$\psi = \frac{\Delta P}{\rho_o C_o^2} \quad .$$

This is a trivial change for scaling an ideal gas because

$$\rho_o C_o^2 = KP_o$$

and since K is a constant also it is immaterial whether the shock strength is normalized to $\rho_o C_o^2$ or to P_o. A breakthrough does occur, as will be discussed in Section 1.11, because ψ as defined above also describes the dissipation for any material at weak shocks and describes many other properties of material. Hence ψ fulfills the requirement for a similar measure of shock strength in nearly any homogeneous gas, solid, or liquid.

We summarize the result so far regarding scaling. Instead of

$$\frac{Yo}{\frac{4\pi}{3} P_o R^3} = \frac{P}{P_o} F\left(\frac{P}{P_o}\right)$$

the unified theory of blast specifies

$$\frac{Y(R)}{\frac{4\pi}{3} \rho_o C_o^2 R^3} = \psi F(\psi)$$

where $\psi = \Delta P / \rho_o C_o^2$. The generality arises from

1) Y(R) instead of Y_o, which permits similarity despite different early history and

2) $\psi = \frac{\Delta P}{\rho_o C_o^2}$ which permits similarity among different homogeneous materials.

Two further relations will be applied to scaling. In the mass effect MEZ, R^3 is replaced by Z^3 which takes mass of explosive and surrounds into account. It removes the restraint of homogeneous material on the scaling law:

3) $Z \equiv (M+R^3)^{1/3}$.

For explosions in a non-uniform atmosphere, IDA P150 suggested a quite successful means of scaling high altitude nuclear explosions: it defined an average ambient pressure

4) $\bar{P}_o = \frac{\int P_o(r)\, r^2 dr}{\int r^2 dr}$

using the standard recipe for an average value. Details are not germane to the present exposition but "mean pressure scaling" is a fourth way of generalizing the scaling law in a non-uniform medium.

In summary, the form factor F and generalized scaling are used in this paper to mean equivalent statements of the same thing. To say two explosions scale is to say they have a common form factor under certain specified restrictions, usually a constant shock strength.

1.6 QZQ Hypothesis

QZQ refers to a controlling hypothesis in UTE that the quantity

$$q \equiv -\frac{d\ln Q}{d\ln R} \cong \text{constant} \qquad \text{QZQ-1}$$

holds under a gamut of explosion conditions. q is a "nearly constant" in unidynamics because it is either virtually constant under ideal conditions or varies slowly or oscillates about a constant under non-ideal conditions. In particular

q = 3.5 for strong shocks, ideal

q = 4.0 for weak shocks, ideal

q = less than, greater than, or oscillates about q (ideal) for non-ideal explosions.

If q = constant then QR^q = constant and two important consequences follow:

(a) The integration for yield Y(R) or Y_o in HY-2 or HY-3 is both trivial (a power law) and is exact. If true, it obviates the need for a machine solution to generate the shock conditions.

(b) The pressure-distance curve is directly defined because Q = Q(P) point for point, once Q(R) is determined.

Regarding justification, the QZQ concept was originally formulated theoretically (ARF TM421). Since then, it has been abundantly verified experimentally (see Figure 5.2-1), so at the present time the validity of the concept can be argued either theoretically or empirically.

The main features of this derivation are summarized as follows. By definition, the original blast yield Y_o is

$$Y_o = 4\pi \int_0^R QR^2 dR + \frac{4\pi}{3} R^3 PF \quad .$$

$$\overbrace{\text{dissipated fraction}} \qquad \overbrace{\text{available fraction}}$$

Since Y_o is a constant, by setting $\frac{1}{4\pi}\frac{dY_o}{dR} = 0$, we obtain

$$0 = QR^2 + R^2 PF + \frac{R^3}{3}\frac{d(PF)}{dR} \quad ;$$

dividing by $R^2 PF$ and rearranging

$$\frac{d\ln PF}{d\ln R} = -3\left[1 + \frac{Q}{PF}\right] \quad . \qquad 1.6\text{-}1$$

Note that if $Q = 0$, then $PF \sim \frac{1}{R^3}$. The similarity condition for strong shocks implies that F = constant and thus $P \sim R^{-3}$. For weak shocks, the resemblance between spherical and plane waves requires that $P \sim R^{-1}$, according to acoustic theory, which implied that $F \sim R^{-2} \sim P^2$. In QZQ, we assume that the essential features of these two similitude principles still apply: F = constant for strong shocks (similarity) and $F \sim P^2$ for weak shocks (plane and spherical waves appear nearly similar).

From thermodynamics we then find that Q/PF in 1.6-1 is a constant for both strong and weak shocks (but not necessarily the same constant). Because, for strong shocks $Q \sim P$ and F = constant; thus Q/PF is constant. For weak shocks, in any material, it turns out that $Q \sim P^3$; but $F \sim P^2$, so $PF \sim P^3$ also and the ratio Q/PF is again constant. If in each domain Q/PF = constant, then it follows that

$$\ln Q = \ln \text{constant} + \ln PF$$

$$\frac{d\ln Q}{d\ln R} = \frac{d\ln PF}{d\ln R}$$

and if $$-\frac{d\ln Q}{d\ln R} \equiv q$$

then from 1.6-1

$$q = +3\left[1 + \frac{Q}{PF}\right]$$

$$q = \frac{3Q}{PF}$$

We may normalize the dissipation equation 1.4-2 by dividing by Y

$$\frac{dY}{Y} = \frac{-4\pi\, QR^2}{\frac{4\pi}{3} R^3 PF}$$

$$\frac{dY}{Y} = \frac{3Q}{PF}\frac{dR}{R}$$

Thus, in domains where $\frac{Q}{PF}$ is constant, $-\frac{d\ln Y}{d\ln R} = q-3$.

The specific values for q at strong and weak shocks are estimated thusly. If the amplitude of acoustic spherical waves decays as 1/R, this implies that $\frac{d\ln Y}{d\ln R} = -1$, then $\frac{3Q}{PF} = 1$ and $q = 3 + \frac{3Q}{PF} = 4$ (weak shock). Similar arguments can be made for strong shocks. Whereas all the shock energy is subject to dissipation for weak shocks (E_K is negligible) when the shock is strong, half of the energy is kinetic and not subject to waste. There would be no waste heat if all the energy were somehow kinetic. More specifically, the analytic solution explicitly calculates F on the interior of a strong shock and we find that over the strong shock domain $\frac{3Q}{PF} \cong 1/2$. Hence $q = 3 + \frac{3Q}{PF} \cong 3.5$ (strong shock).

When the shock radius R is suitably corrected for mass of explosive, denoted by a hypothetical radius Z (see MEZ in Section 1.8),

the quantity QZ^q = constant for any explosion with different values of q and a different constant in each of the two domains. We refer to this as the QZQ concept and it provides the great simplification which makes the integrations for yield Y both easy and accurate.

DEB, direct evaluation, is a maximum-data minimum-assumption method in which Q is calculated from the measured overpressure at each distance R and the integration for Y is done directly (see Chapter 2). DSC, direct scaling, is a minimum-data method in which a theoretical pressure-distance curve is calculated, using the QZQ concept for a given initial energy release Y_o; the measured radius is then compared with the predicted radius for each pressure, the data evaluated point by point by ordinary cube-root scaling (Chapters 3 and 4). The slope q = -dln Q/dln Z is found to change abruptly and the two domains are separated by a characteristic transition pressure, as described later in Section 1.9, "Strong and weak shocks eigenfunctions."

Figure 5.2-1 is a test of the QZQ hypothesis from analyses of nuclear and high explosive data in later chapters.

1.7 Generalized Modes of Energy Transport

"Blast analyses" is mentioned in the abstract because the QZQ concept permits a comparison between the measured values of q and the ideal values 3.5 and 4.0. Table 1-2 "Modes of Energy Transport" lists about 30 possible real effects and how they can be accommodated in UTE. If the difference between observed and ideal q's is statistically significant, the cause may be categorized under typical behavior patterns:

Generalized Waste Heat, GWH:

$q\ (\text{real}) > q\ (\text{ideal})$, endothermic reactions

Generalized Afterburning, GAB:

$q\ (\text{real}) < q\ (\text{ideal})$, exothermic reactions

Body Waves, BOW:

$q\ (\text{real}) - q\ (\text{ideal})$ is periodic (oscillations)

Some real effects may average out spatially (e.g., Mach reflection) or so quickly in time (e.g., radiation precursors which are overtaken by the shock) that the effect is "nearly constant" and may be regarded as a parameter rather than a variable. Other changes are due to gradual shift from cylindrical to spherical symmetry close to a conventional warhead and may be amenable to treatment by a concept of generalized divergence, GDV, which is described later in this chapter.

1.8 The Mass Effect, MEZ

"Explosions in general"--nuclear, sparks, chemical, propellants--can be treated in a uniform way, mainly through the mass effect concept and definition of a hypothetical radius Z. The mass effect is usually significant only for explosions in air or other gases, i.e., when the surrounding medium is much different in density than the explosive.

MEZ was conceived and routinely used by the present author for analysis of nuclear explosions for hydrodynamic yield (LA 1664). It recognizes that no explosion is truly a point source of energy close to the source, as is assumed in virtually all strong shock solutions. Initially, the bomb energy is not carried by the surrounding medium but nearly all as kinetic and internal energy of explosion products and surrounds, material which weighs a thousand times as much as the air engulfed. This energy is only gradually transferred to the surrounding medium by normal physical processes as new material is engulfed and both debris and medium slow down and cool by expansion.

By MEZ, the energy is assumed to be distributed between bomb parts and air (or other medium) in direct proportion to their relative masses, that is

$$\text{Total PBE} = (\text{PBE of Air}) \left[1 + \frac{HM'}{\frac{4\pi}{3} R^3 D_o} \right] \qquad \text{MEZ-1}$$

where M' = the actual weight in air of explosive and surrounds, H = average kinetic and internal energy ratio relative to air, $(4\pi/3)D_o R^3$ = the mass of air of density D_o engulfed at any radius R.

If we multiply the term in brackets by the variable R^3 we can then define a new variable Z such that

$$Z \equiv (R^3 + M)^{1/3} \qquad \text{MEZ-2}$$

where $M = HM'/4.186D_o$. Here Z^3 may be regarded as either a hypothetical volume, as if the energy were distributed over a larger volume, or as a modified gas with more degrees of freedom as represented by the debris. From MEZ-2, the transform $Z^2dZ = R^2dR$ follows for counting dissipation $dY = -4\pi QR^2dR$ for integration of the energy Y in HY-2 and other relations. At long ranges, Z and R become identical, and the mass of explosive is there negligible. Close-in, Z = constant $\cong M^{1/3}$ and is independent of the mass of the air engulfed and shock radius.

The mass effect assumption MEZ is based on the concept "radial mixing." This is a fundamental difference between UTE and all other shock theories as the author knows them, including machine solutions--they do not permit mixing. Radial mixing is a direct consequence of conservation of momentum:

$$\frac{Du}{Dt} = \frac{-1}{\rho}\frac{\partial P}{\partial r}$$

where ρ is density. It states that when materials of vastly different densities, like particulate bomb debris and air, are each exposed to the same pressure gradient $\frac{\partial P}{\partial r}$, the rare materials (small ρ), are slowed down drastically faster than dense fragments (large ρ). Each material is decelerated inversely proportionally to its density. The density ratio between particulate matter and gas is typically 1000:1. It means that denser particulate material must actually migrate through the surrounding lighter gas.

Usually the surrounding medium will also be moving outward violently. The finest debris will reach equilibrium soon and thereafter ride with the material medium of the blast, being first slowed down and later carried along--so to speak--by viscous drag. Coarser debris moving faster than air will reach equilibrium later, being drastically slowed down only when it tries to pass through the shock front into still air ahead; the shock in fact represents the merging of the bow shocks from the initially outermost debris. The very largest fragments give rise to jets. Thus at early times, there is no real shock front, but only a series of fingers; they resemble, but probably are not "Taylor instability." Taylor, himself in treating this problem required the bomb case to blow up uniformly like a balloon. Finally, note that there is no meaning to "bow shocks" or "drag" unless the debris is moving faster than air, and that means radial mixing is occurring.

Radial mixing preempts the use of Lagrangian coordinates for hydrodynamic flow at least close-in, because it implies that the mass-lines cross, which is unthinkable in Lagrangian coordinates. Because the local material velocity is actually multi-valued, Euler's hydrodynamic equation for conservation of mass is not rigorous either in its simple form.

Nor does the energy carried by the bomb case fragments represent a fixed loss as presupposed in the well known Fano and Gurney formulas for cased weapons. Most of the fragment energy is continuously transferred "back" to the surrounding air. I say "back" in quotes because the energy was never in air; the fragment is the mode by which the energy is transferred to the air in the first place. The

Fano and Gurney formulas do apply however, to energy which is wasted irreversibly in case rupture and heating, and also for very large fragments which return energy too late to support the shock. These are all different forms of waste heat.

The mass effect explains why the initial pressures of a chemical explosive are a hundred to a thousand times lower than nuclear explosions at comparable scaled radii: the energy is distributed over a corresponding greater mass. A main result thereby is to make chemical explosions more efficient by suppressing dissipation during their early growth. As we shall see in Chapter 5, a chemical explosion requires only about one-third the initial energy of a nuclear explosion to produce the same pressure-distance curve at much later times. The nuclear explosion is not a hydrodynamic "point-source"; if it were, the dissipation would be infinite at the source and its blast efficiency would be virtually zero relative to TNT or to any real explosion.

The mass effect relation also provides a convenient way to describe any of its analogs, i.e., any effect which decreases (or increases) pressure close-in--flattens (or peaks up) the wave form--in a way which is inversely proportional to shock volume. Among such analogs are:

1) changes in specific heat (see section 1.8)
2) waveform during radiative phase (isothermal sphere)
3) delayed energy release near origin.

The first effect refers to ASH, to be discussed in the following section. The next two may be regarded as an "inertial mass-effect." If, for any reason, the wave shape differs from an ideal wave, material needs first be redistributed before the wave can approach the ideal

form. The redistribution cannot be instantaneous, i.e., it is an inertial effect, and an artificial value of M is a plausible way to permit a gradual approach to similarity, i.e., in proportion to the ratio of perturbed to unperturbed volume.

Figure 5.2-1 is a test of the MEZ hypothesis, showing that nuclear and TNT can be reduced to a common scaling by the use of Z.

1.9 Average Specific Heat

Average Specific Heat (ASH) is a graphic acronym for both explosive "ash" and for "average specific heat" of bomb and explosion debris relative to air. It is symbolized by the parameter H. It is based on the concept of dust-loading in surface effects theory for air blast over ground surfaces (LA 1665). It means to recognize that the physical size of debris affects the mass effect in a different proportion depending on whether or not the particle has reached kinetic and thermal equilibrium with the surrounding air.

The spectrum of significant sizes for bomb and explosive debris may be encompassed by four classes:

Class	Typical Size	Thermal Equilibrium?	Mechanical Equilibrium?
Gas	Molecular	Yes	Yes
Smoke	Macro-molecular to microns	Yes	Yes
Fines	Sand	No	Yes
Coarse	Chunks	No	No

Each class affects the kinetic and internal energy content of the wave differently.

The gaseous debris increases kinetic energy in direct proportion to its mass (H = 1). But it does not affect the pressure (internal energy per unit volume) in proportion to its mass.

Addition of gas lowers temperature, raises density but affects pressure only insofar as it changes the average specific heat at constant volume C_v, and C_v is roughly equal for most materials, about 0.2 cal/gm degree. Only about 10% of a strong shock (for a point source) is kinetic energy, so if the added gas is diatomic only the kinetic energy is affected, and the effective value would be $H \cong 0.1$ in MEZ.

Consistent with the dust-loading idea, the particulate smoke is an energy sink for both heat and kinetic energy. It behaves as if extra degrees of freedom were present, like a polytropic gas, without contributing substantially to the total volume as would additional gas. $H \cong 1$ for this smoke fraction; the effect is directly proportional to mass for both prompt energy and kinetic energy fractions of the wave.

The fines, by definition, are particles fine enough to be in mechanical equilibrium, as if $H = 1$ for kinetic energy, but they are too coarse to be in thermal equilibrium, so $H < 1$, and the excess heat remaining in them is part of a generalized waste heat Q.

The coarsest chunks are neither in thermal nor mechanical equilibrium. Their contained heat is again part of a generalized waste heat Q. But they produce jets at late times and to that extent that they continue to drive the shock by viscous drag; they behave phenomenologically like generalized afterburning GAB.

We note in passing that the time dependent feature of debris size is reasonably encompassed by MEZ and GAB forms of relations: if the recovery of energy is early, the mass effect described it; if the recovery is late, generalized afterburning describes it.

The principal result of ASH is that H is substantially less than 1 as would otherwise be expected, if we did not consider the internal energy of gas and the non-equilibrium fraction of debris. Secondly, the average value of H will change as the shock grows, if only because the partition between kinetic and prompt energy changes. The DEB method permits a variable H and some high explosive data do appear better correlated by a variable H than a constant.

But an average, constant value of H = 0.25 is usually used in DEB and DSC for these reasons:

a. Too few pressure-distance data are close enough to the bomb to be sensitive to H.

b. The blast yield at pressures of interest ($P < 50$ psi) is insensitive to H, behaving like $Y \sim H^{0.2}$.

c. The distribution of particle sizes, nor the actual specific heats are not known well enough to improve on the estimate H = 0.25.

1.10 Transition Pressure Between Strong and Weak Shocks

The UTE concepts and techniques are said to "apply at any shock strength" mainly because the strong and weak shock values $q = 3.5$ and $q = 4.0$ are most readily derived using the approximations $\Delta P/P_o \gg 1$ and $\Delta P/P_o \ll 1$ for the respective ratios of overpressure to ambient. These "asymptotic" values ought to be most realiable at the extreme high and low pressures.

Less obvious, and a serendipitous empirical result, is the abrupt transition--like eigenvalues--from $q = (3 + \frac{1}{2})$ to $q = (3 + 1)$. It occurs near $\Delta P/P_o = 1$ ($\cong$ 15 psi), apparently for four mutually abetting reasons.

First, above $\Delta P/P_o = 3.82$ (about 55 psi at sea level) the material speed just behind the shock is supersonic with respect to the local sound velocity. The flow of hydrodynamic energy is therefore preponderantly forward; hydrodynamic signals cannot even move backward in space, near the shock, until the shock overpressure ratio falls below 3.82. As in all flow problems, we expect profound changes between subsonic and supersonic flow.

Second, around $\Delta P/P_o = 2$, a negative phase first develops in the wave. Until then, energy anywhere on the interior of the wave can eventually reach the front; but thereafter, energy on the deep interior is trapped near the bottom of the negative phase where it can accumulate as a secondary shock. This is a point where delay in average energy transport is crucial; one can accurately speak properly of delayed energy as being "wasted" so far as the shock front is concerned.

Third, near these same shock pressure levels, the prompt energy $Y(R) = (4\pi/3)R^3(P_T - P_o)F$ in the wave rapidly passes from being a quantity which is large compared with the ambient energy of the air engulfed ($Y >> \frac{4\pi}{3} R^3 P_o$) to an ever-dwindling fraction which is lost in an ocean of surrounding air whose mass and ambient energy are growing as R^3.

Fourth, we note that the kinetic energy fraction at the shock is not really subject to waste heat. In uniform free air explosion only internal energy is "wasted." Recall that the initial partition of energy at the shock front in any medium is such that

$$\frac{\text{internal energy increment}}{\text{total energy increment}} = \frac{1/2(P+P_o)(V_o-V)}{(P)\ (V_o-V)} = \frac{P+P_o}{2P}$$

where P here is an absolute pressure. At high overpressures $P >> P_o$, only half the shock energy can possibly be wasted, the kinetic energy half always remains to drive the shock. At low pressure, $P \cong P_o$ and all the shock energy is subject to waste. This gives a fourth reason why we expect a sharp transition near $\Delta P/P_o = 1$; the rate of change in the energy partition at the front changes most significantly near $\frac{\Delta P}{P_o} = 1$.

1.11 Natural Units (NU) and Generalized Equation of State, GES

That "virtually any medium and ambient conditions" can be treated in UTE appears possible through the use of a proposed concept for "natural units" NU using a dimensionless, pressure ratio ψ, and through a generalized equation of state GES.

First regarding ψ, physical considerations of the Maxwell distribution for molecular speeds suggests that sound velocity C_o is essentially the average outward (i.e., divergent) component of molecular speed, and $\rho_o C_o$ measures their random divergent momentum. The quantity $\rho_o C_o^2$ is a corresponding momentum flux; it measures the possible divergence of internal energy. As is also well known, $\rho_o C_o^2$ is also significant in describing the compressibility of a medium. The ambient pressure P_o itself is a fundamental significance because it actually controls direction of the energy flow for the prompt work PBE.

For these reasons we define a dimensionless overpressure ratio ψ such that

$$\psi \equiv \frac{P-P_o}{\rho_o C_o^2} \quad . \qquad \text{NU-1}$$

The name "nautral unit" seems appropriate because ψ is essentially the ratio of prompt internal energy $P-P_o$ to its maximum conceivable rate of divergence $\rho_o C_o^2$.

Further, considering the Rankine-Hugoniot relations in any medium, for weak shocks we find the results

$\psi = (P-P_o)/\rho_o C_o^2$, overpressure ratio

$\psi \cong (\rho/\rho_o) - 1$, overdensity ratio

$\psi \cong u/C_o$, Mach number of material speed

$\psi \cong (U/C_o) - 1$, excess speed of shock.

We also find that the waste heat in any uniform medium is such that

$$Q = \text{Constant} \cdot \psi^3 .$$

From the definition PBE we can always define an α such that

$$W = \int_P^{P_o} PdV = \alpha\,(P-P_o)V$$

Then we found again, in the acoustic approximation, that $\alpha = 1$ and the prompt work W per unit volume V is

$$\psi = \frac{W}{V} .$$

The generalized equation of state GES used with UTE extends the Lennard-Jones potential concept. Without giving detailed justification, let us here assume that all the adiabatic deformation energy E in a body can be expressed by a series of the form

$$E = \Sigma A_i / V^{n_i}$$

where each A_i and n_i are constants, but are not usually integers. They describe the various close-range, long-range, attractive, and repulsive forces due to molecular collisions, Coulomb forces, various multipole moments and van der Waal forces--as many kinds of forces as are needed for accuracy desired. The volume V is directly related to the average inter-molecular distance r. With appropriate changes in the above nomenclature for A_i and N_i, we readily derive that for adiabatic changes

$$P - P_o = \Sigma\left[\frac{A_i}{V^{n_i}} - \frac{A_i}{V_o^{n_i}}\right] = \Sigma\, A_i \left[\left(\frac{\rho}{\rho_o}\right)^{n_i} - 1\right] \qquad \text{GES-1}$$

If we require that $C^2 = dP/d\rho = dP/d\,(1/V)$, this imposes one restraint on the A_i's and N_i's. At any pressure level, certainly near P_o, we can define an average value of $\bar{n}_i \equiv k$. These definitions taken together, we then find that

$$P - P_o = \rho_o C_o^2 \left[\left(\frac{V_o}{V} \right)^k - 1 \right] \qquad \text{GES-2}$$

$$\psi = \frac{1}{k} \left[\left(\frac{V_o}{V} \right)^k - 1 \right] \quad .$$

A final argument for use of the natural unit ψ is because, in the acoustic approximation, ψ then is independent of K because

$$\psi \simeq \frac{1}{k} \left(1 + \frac{\Delta V}{V_o} \right)^k - 1 \simeq \Delta V / V_o \quad .$$

This means the generalized equation of state is also consistent with a natural unit ψ: the overpressure ratio is the same as the density ratio for any material regardless of its adiabatic compressibility.

For all these reasons, we say ψ is a natural unit. The ordinary wave equation becomes directly in the same acoustic approximation

$$\nabla^2 \psi - \frac{1}{C^2} \frac{\partial^2 \psi}{\partial t^2} = 0 \quad .$$

Thus, we do not have to ask, "What is waving?--does ψ refer to pressure, speed, displacement, density?". No matter; they are all ψ, and in the acoustic approximation are linearly related.

We say UTE applies to "any ambient condition" because $\rho_o C_o^2$ also specifies the necessary conditions for scaling. For gases in particular $\rho_o C_o^2 = kP_o$ where k is the adiabatic compressibility. For the same reason, GES-1 reduces to the ordinary adiabat $P = P_o\,(V_o/V)^k$

for ideal gases because

$$P = P_o + \frac{\rho_o C_o^2}{K}\left[\left(\frac{V_o}{V}\right)^k - 1\right] = \left(P_o - \frac{\rho_o C_o^2}{K}\right) + P_o\left(\frac{V_o}{V}\right)^k .$$

For non-uniform atmospheres, earlier work (IDA P150) defined an average ambient pressure $\bar{P}_o$ such that

$$\bar{P}_o = \frac{\int_o^R P_o(r) r^2 dr}{\int_o^R r^2 dr} .$$

A main requirement for this definition was to provide a rigorous expression for subtracting the ambient energy of the medium from the total energy of the blast wave to obtain the prompt energy. This proved to be a key idea in a successful approximation for scaling high altitude nuclear explosions. Since the adiabatic compressibility K of air is constant, especially for rarefied air, it follows that the average values are

$$\overline{\rho_o C_o^2} = k\bar{P}_o$$

which suggests that ψ will also be appropriate for describing many non-uniform media.

1.12 Generalized Divergence, GDV

"Adaptable to a gamut of burst geometries" is an idea already tested, (LA 1664), for propagation of a blast in a non-uniform atmosphere; it is based on a concept of generalized divergence (GDV).

The idea in GDV starts by noting that the space coordinate r in all the hydrodynamic equations either appears as gradients $\frac{\partial P}{\partial r}$, $\frac{\partial \rho}{\partial r}$, $\frac{\partial u}{\partial r}$, etc., or appears alone in the divergence term for conservation of mass

$$u \frac{\partial \rho}{\partial r} + \frac{\partial P}{\partial t} + \frac{\partial u}{\partial r} + \lambda \frac{\rho u}{r} = 0 \qquad \text{GDV-1}$$

where $\lambda = 0$ for plane waves

$= 1$ for cylindrical waves

$= 2$ for spherical waves .

Recall that we can add any constant g we wish to r without changing the gradient, because $\frac{\partial}{\partial r} = \frac{d(r+g)}{dr} \frac{\partial}{\partial (r+g)} = \frac{\partial}{\partial (r+g)}$.

Moreover, since the material cannot know where the origin of expansion is, the physical significance of r in the divergence term can only be as a radius of curvature. Thus, the physical role of r is not as a distance but to describe the local divergence.

Now the curvature for any surface can be approximated by two mutually orthogonal radii of curvatures, r_1 and r_2, including the special value $r = \infty$ for a straight line. If we therefore define r such that

$$\frac{1}{r} = \frac{1}{r_1} + \frac{1}{r_2}$$

we automatically generate $\lambda = 0, 1, 2$, for the plane, cylindrical and spherical cases in the conservation of mass equation.

But we do much more: we can describe the divergence of hybrid geometries, shapes lying between spherical and cylindrical symmetry by the simple device of using a non-integer λ. We can handle 3-D geometries essentially on the basis of spherical ones by treating them as small pieces of a spherical wave. That of course is the problem of focused blast and of non-spherical warheads.

1.13 Applications

Why we can say "gamut of warhead configurations" should now be evident. MEZ provides the means to describe the equilibrium mass effects due to case mass. GWH provides the means to describe the energy losses such as rupture and unrecovered fragment energy. GAB and QZQ provide the means to describe slow energy release, combustible cases, non-equilibrium mass effects, etc. by varying the close-in value of $q = d\ln Q/d\ln Z$ from the ideal value. GDV provides the means to treat hybrid geometries by non-integer parameter λ.

The sometimes quoted partition of nuclear explosion energy into fixed fractions--blast 50%, thermal 35%, prompt radiation 10%, etc.--is naive and misleading numerical nonsense. "Similar energy releases" implies the fundamental behavior; explosions, like many other natural processes, represent evolutions of energy modes one into another rather than fixed partitions of energy. The UTE is intended for just such versatility.

Recall the characteristics of explosions--discontinuous functions, irreversible, non-linear, time-dependent, assymetrical, non-uniform, free boundaries--mentioned at the beginning of this chapter. If an adequate solution to explosive phenomena continues to be found in UTE, it ought to provide useful insights into many other physical phenomena not yet understood. The concepts developed here for the UTE have been applied in fact by the author and found enlightening in a number of areas such as:

Chemical stoichiometry and combustion

Big Bang cosmology

Tornados

Lunar seismology

deBroglie waves and quantum mechanics eigenfunctions

model for gravity and force-at-a-distance

many features of relativity

social phenomena and systems analyses

While most of these are not of interest for immediate military problems--anymore than atomic energy was in 1935--it might prove welcome to both doves and hawks if the fallout from explosion phenomena were to include useful new approaches and insights into the basic nature of these physical phenomena and laws.

TABLE 1-1

Concepts for Unified Theory of Explosions

Simple analytic expressions

DEB Direct evaluation of blast yield

DSC Direct scaling from shock growth

ANS Analytic solution for yield and interior wave forms

MEQ Mini-equation (a single equation for pressure-distance)

QR^4 Figure of merit (criterion) for weak shocks

Blast predictions, hydrodynamic yield and blast diagnostics

PBE Prompt blast energy and waste heat Q

HY Hydrodynamic Yield

F Form factor and generalized scaling

QZQ QZ^q eigenvalues for strong and weak shocks

ISG Interior and shock gradients, and time decay

Any shock strength, burst conditions and media

NU Natural Units

GES Generalized equation of state

EPV Variable epsilon equation of state for nonideal gases

APV Variable alpha coefficient for prompt work

VSV Law of partial volumes

MPS Mean pressure scaling

Explosions in general and allied energy partitions

MEZ Mass effect

ASH Average Specific Heat (of debris relative to medium)

TABLE 1-1 (Cont'd)

GWH Generalized waste heat

GAB Generalized afterburning

BOW Body Waves

NC Nearly constants

HIJ h, i, j functions

Variety of burst geometries and warhead configurations

GDV Generalized divergence for hybrid space

TSS Trapping in secondary shock

CVS Convergence shock

SET Surface effects, thermal

SEM Surface effects, mechanical

GIP Generalized impact problem

TABLE 1-2

Modes of Energy Transport and Method of Describing Them in the Unified Theory of Explosions

Mechanical

$\int$PdV expansion, (random momentum flux)	W in PBE*
Kinetic energy (ordered momentum flux)	K in PBE*
Cavity and bubble energy	GWH
Internal body waves (ringing)	BOW
Dust loading, fine case fragments and explosion products	MEZ
Viscous drag, coarse fragments (non-equilibrium mass effect) jets, bow waves from jets	GAB
Enhanced kinetic energy from massive explosives and cases	MEZ, H in MEZ
Friction at boundary layers and surfaces	GWH
Local turbulence, strong and weak impedance of flow by rough or smooth surfaces	GWH
Macroscale transverse waves, Love and Rayleigh waves (delayed blast energy)	GWH
Free air impedance and scattering	GWH
Case rupture and deformation energies	GWH
Internal friction, slippage of grains under pressure	GWH
Compaction of voids and lattice holes	GWH
Crushing energy and plastic deformation	GWH
Work against gravity and other body forces	GDV

* Acronyms for concepts in the Unified Theory of Explosions are shown in Table 1-1.

W = $\int$PdV work path of actual expansion in the (P,V) plane

K Kinetic energy = 1/2 u^2 per unit mass

TABLE 1-2 (Cont'd)

Electromagnetic and Light	
"Fireball" radiation over entire electromagnetic spectrum	GWH
Excitation of internal modes: vibration, rotation luminescence, fluorescence	APV, GES, GWH
Electron jetting at shock, electromagnetic pulse	GWH, NC
Chemical	
Afterburning of explosive	GAB
Afterburning of combustible fillers, liquid sheaths, bomb cases, porous-fuel surrounds	GAB
Phase changes: endothermic	GWH
exothermic	GAB, BOW, TSS
Heats of vaporization, fusion, transition	HY, GWH
Electric	
Piezoelectric effect (first order, some crystals)	GWH
Reverse electrostriction (second order, all crystals)	GWH
Triboelectric effects (contact potential, rubbing)	GWH
Thermal	
Dust loading, heat transfer to air	H in MEZ
Conductive heat transfer	GWH, NC, TSS
Convective heat transfer	GWH
Thermoelectric effect at phase and grain boundaries	GWH
General	
Relaxation phenomena and effects	GAB, NC, BOW
Case assymetries	GDV, NC
Reflection phenomena	GDV, NC
General purpose blast-fuel warheads (massive effects close-in, afterburning and incendiary action far out)	GWH, GAB, MEZ

2. Direct Evaluation of Blast Energy, DEB

2.1 Foreword

In this chapter we first describe the DEB method for evaluating the blast energy of an explosion. Mainly, it requires only a broad range of some measurement of shock growth, such as pressure versus distance or time-of-arrival. Some specific illustrations of "how it works" are done later in Chapter 5.

The method is conveniently summarized in a BASIC machine program, with instructions suitable for do-it-yourself analyses and learning the method. Listing the program insures that the instructions and logic are complete, that there are no hidden assumptions, and that most of the extraneous ideas have been weeded out. To list the program is hopefully the ultimate in a clear, complete, step-by-step list of procedures. It is simply a modern and efficient means of technical communication.

The chapter is organized as follows:

2.2 Concept for Direct Evaluation of Blast Yield (DEB)

2.3 DEB506 BASIC Program

2.4 Input Data

2.5 Input Parameters and Options

2.6 Data Modification and Transformations

2.7 Waste Heat Calculation

2.8 Integration of Waste Heat

2.9 Estimates for Total Yield

2.10 Printout and Diagnostics

We will refer to Table 2-1, which lists the program, to Table 2-2, which is a printout from a sample run, and to Table 2-3, which defines the terms used in the program.

2.2 Concept for Direct Evaluation of Blast Yield, DEB

The DEB concept proposes that a broad range of measurements of shock growth, peak pressure versus distance for example, is sufficient to determine the absolute hydrodynamic yield Y_o at the surface of any explosive, the blast energy $Y(R)$ at any intermediate measured distance R and the form factor F at that pressure level.

The procedure is illustrated in Figure 2.2-1:

At each measured distance R, the waste heat Q is first calculated from the measured overpressure P. Standard thermodynamics using the Rankine-Hugoniot relations and an adiabatic expansion will define both the prompt blast energy, PBE, and the waste heat Q as will be illustrated in Section 2.7. Appendix QVP gives the results in detail. If other modes of energy transport are present, as listed in Table 1-2 of Chapter 1, then Q is suitably corrected to Q_{TOTAL} at each measured point.

We then have defined $Q[P(R)] = Q_{TOTAL}(R)$. As the shock grows, prompt energy is depleted according to

$$\frac{dY}{dR} = -4\pi\, Q_T R^2$$

and assuming $Y = 0$ at $R = \infty$, we have

$$Y(R) = 4\pi \int_R^\infty Q_T\, R^2\, dR \quad . \qquad \text{HY-1}$$

This completes the necessary prerequisite concepts for DEB. Given a broad enough range of pressure-distance data, any one of many numerical techniques is sufficient to determine Y(R) at any point R and in turn to evaluate the hydrodynamic yield

$$Y_o = 4\pi \int_{R_o}^\infty Q\, R^2 dR \qquad \text{HY-2}$$

at the charge surface R_o.

Thus, DEB was called a maximum-data, minimum-assumption method because in principle no concepts or assumptions, other than PBE, HY, and DEB are necessary if the range of data is broad enough. We do not require a knowledge of interior wave forms as in the Kirkwood-Brinkley theory, how Q varies with R nor the mass of explosive if the data are in sufficient detail. A number of standard explosives--nuclear, TNT, pentolite--afford sufficient data for evaluation using only these assumptions.

Other concepts are used in DEB,

QZQ Optimum Propagation

MEZ Mass Effect

GAB Generalized Afterburning

GWH Generalized Waste Heat

but these are primarily "assumptions for convenience". They make the DEB method more practical by drastically reducing the data requirements, both in range and detail but are not intrinsic.

The QZQ concept, namely that

$$q = -\frac{d\ln Q}{d\ln Z} \equiv \text{constant}$$

permits us to perform the integration in bold steps, requiring relatively few data points, and using the data itself to measure the slope q between adjacent points. The assumption $q = 4$ at long distances provides a means for estimating the contribution to Y from shock growth beyond the farthest distance measured (shown as "estimate, acoustic"in Fig. 2.2-1). Similarly, $q = 3.5$ provides an estimate for the region between the charge surface R_o and the nearest data point ("estimate, close-in" on the figure).

A similar estimate can be made for the waste heat of the explosive itself; but it is not properly part of the blast "yield" since it is energy which is not released to the air.

QZQ relaxes the requirement for data enough so that in principle DEB could be applied with only two data points, albeit approximately: one measurement in the strong shock region of an overpressure ratio $P > 3.8$, extrapolating back to the charge surface with $q = 3.5$ and one measurement in the weak shock region $P < 2$, extrapolating to infinity with $q = 4$. We note in passing that as such, DEB would become the DSC method.

The advantages of integrating backward in DEB mainly accrue because it circumvents serious uncertainties associated with analyzing high-shock pressures and other close-in phenomena, such as

a) Non-ideal equation of state

b) Instrumentation at high pressure

c) Wild fluctuations in measured pressure due to bow shocks, fingering, and jetting from the mass effect.

d) The calculation starts with the most certain boundary condition: $Y = 0$ at $R = \infty$.

e) It provides an absolute value of $Y(R)$ without recourse to interior wave forms or to early history.

The last point is exceedingly useful. We can always define an average form factor F for the blast wave such that

$$Y(R) = \underbrace{\frac{4\pi}{3} R^3}_{\text{volume}} \cdot \underbrace{P}_{\text{peak pressure}} \cdot \underbrace{F}_{\text{average}} \qquad 2.2\text{-}1$$

F thereby expresses the average value of energy in the wave relative to the peak pressure (energy/unit volume) at the front. As noted earlier, F is in fact the implicit quantity sought in machine solution for free field. DEB gives F explicitly from

$$F = \frac{Y}{\frac{4\pi}{3} R^3 P} = \frac{4\pi \int_R^\infty QR^2 dR}{\frac{4\pi}{3} R^3 P}$$

$$F = \frac{3 \int_R^\infty QR^2 dR}{PR^3} \quad .$$

Given F(P), and assuming scaling, the "blast problem" is largely solved and the pressure-distance curve for any other Y(R) is obtained directly by the above equations, 2.2-1 et seq.

The mass effect concept MEZ makes DEB practical but is also not intrinsic to it. Whenever the mass is appreciable, even a crude estimate for the mass of explosive and case makes the quantity $q = -d\ln Q/d\ln Z$ much more constant than $d\ln Q/d\ln R$. If measurements close to the charge radius are available, the improvement in Y_o due to MEZ can only be a few percent even though q varies. But if no measurements exist closer than 10 charge radii or so, letting M = 0 is equivalent to treating the explosion like a nuclear explosion, and the yield Yo at the source will be estimated high by a factor of 2 or more. MEZ is of small consequence at distances greater than 10 charge radii or, as noted, if actual data points are available.

The various modes of energy transport included in GAB or GWH as shown in Table 1-2 are not always appreciable for free air

measurements. One raises the question whether they need be considered. First of all, the measured values of q in DEB will indicate the fact by systematic deviations from 3.5 and 4.0. If we suppose that the measurements being evaluated do represent realistic field condition, and the wave does suffer losses such as those due to surface effects, then the effective blast yield ought probably to be corrected for those losses as measured. In such cases, the difference between q (observed) and q (ideal) in the weak shock region is almost certainly due to surface effects and the corresponding energy loss is readily determined by the expression for yield in direct scaling method. But of course, for practical purposes, any other explosion under similar field conditions will also show the loss and in any case, DEB measures the losses and blast actually present at a given distance in the field under experimental conditions. On the other hand, for comparison with stoichiometry studies, DEB ought to be corrected, if at all reasonably possible, for any non-ideal loss.

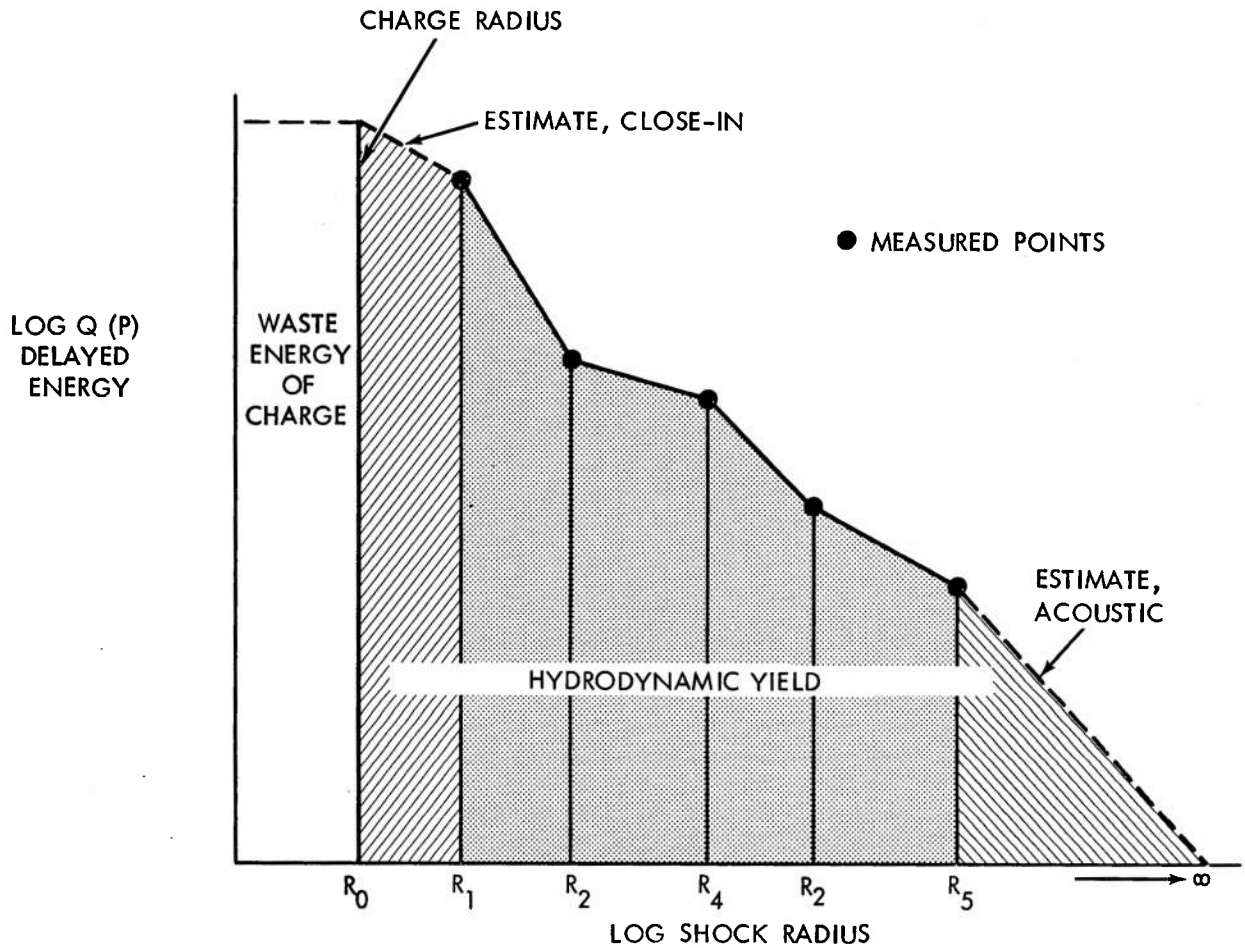


FIG. 2.2-1 DEB CONCEPT: DIRECT EVALUATION OF BLAST.

$$Y(R) = 4\pi \int_{R}^{\infty} Q \; R^2 \; dR$$

2.3 DEB506 BASIC Program

We turn now to using the program DEB506.

To read BASIC requires only a knowledge of algebra, a few conventions, and special meanings for about a dozen English words. An appendix "BASIC Machine Language" is included for the benefit of readers who do not now know BASIC. Only a few minutes may be enough to learn to read BASIC well enough to follow the subsequent discussion.

We refer continually to Table 2-1 which is the LIST of instructions to the machine for DEB506. We will refer also to Table 2-2 which is the printout; the reply of the machine to these instructions. Table 2-3 gives the nomenclature for DEB506.

The line numbers of DEB are shown on the left of the LIST; they run from 100 to 2000. In the discussion which follows, we will refer to line numbers and omit the word "LIST." That is, "100-290" will mean "Line numbers 100 to 290 in the LIST inclusive."

DEB506 is organized as follows (see Table 2-1):

100-290	deal with titling and input instructions
297-360	read the data as input in 1000-1989, transform them to cgs units and route them in the program
400-490	calculate the waste heat Q(P)
499-730	integrate the waste heat to obtain Y and printout the results for each measured data point
799-840	makes an estimate for energy dissipated between the charge surface and the closest data point and for the waste heat of the charge
998-1989	are reserved for inputting pressure-distance data
1990-2000	terminate the calculation

Most of the titling shown on the printout Table 2-2 is obvious. For example, the machine responds to line 100 of the LIST (which see)

by doing exactly what it is told; and the result appears as the title at the top of the printout Table 2-2 (which see). In accord with the remark shown in 104, the user would type:

110 PRINT "name of the data"

The name must be in quotation marks. The result appears as the second line on the printout: "DASA 1559 COMPILATION FOR ONE POUND TNT."

All the English words appearing as table headings, parameters, etc., on the printout are similar responses to instructions when the line numbers are followed by the word PRINT and some statement in quotes. See 180, 190, 240, 250, etc., but note that the instruction such as "105 PRINT" standing alone leaves a blank line--it prints nothing.

The term REM following a line number means "Remark." It is an instruction to the user and has no effect on the program. The remarks in DEB506 are doubtless too cryptic by themselves to be understood at first reading. The remaining sections of this chapter will amplify each remark and explain the calculations. Hopefully thereafter, the user can omit the discussion in the present chapter and the briefer comments in REM on the LIST will be sufficient and even preferable.

2.4 Input Data

In accord with the remarks in 102 and in 998, raw measured overpressure and distance data are input in any units as illustrated in lines 1000 to 1040 in the shown LIST. The numbers actually shown are: pressures in bars, 0.02 is the first pressure; and distance in feet, 100 is the first distance. The format is:
line number, the word DATA, followed by pairs of numbers, pressure first, a comma, the corresponding distance, comma, pressure, comma, corresponding distance, etc.

Because DEB integrates backwards from infinite distance, the data should be entered in decreasing order of distance even if pressures do not thereby increase monotonically. However, if the order of distance is reversed, no particular harm is done, as long as q is a slowly varying function.

Data may be actually input anywhere in the program so long as the word DATA appears after the line number. But DEB intends 1000-1989 for that purpose.

1990 DATA 0,0 is a device for routing the calculation to terminate the program; it should not be altered.

2.5 Input Parameters and Options

Referring to nomenclature in Table 2-3, and the LIST in Table 2-1, the following parameters are the minimum required for the program to RUN:

150 DO, ambient density, gm/cm^3

160 PO, ambient pressure, bars

170 K, the adiabatic compressibility

For DEB506 to RUN with a paucity of data:

210 XO, the charge radius in same units as data

220 M, the mass of explosive and case, kilograms

230 H, the average specific energy

Options are also provided:

260 Q1, the slope dln Q/dln Z close to the charge

270 Q2, the slope dln Q/dln Z beyond the farthest data

The program instructions contain aids for the inputting parameters. The actual line number is usually preceded by a remark; thus, line 140 relates to and precedes 150-170. All the parameters are printed out and the PRINT instruction for that parameter will state what units, if any, were needed for the input. But no special printing instruction will be found for units of ZO, Q1, or Q2 because these numbers are printed in their proper position in columns 2, 4, and 5 of the printout.

For an explosion in any gas which is not diatomic (as is air), the proper adiabatic compressibility K should be inputted in line 170. For all diatomic gases, let K = 1.4 as it now stands. But for an explosion in argon, for example, type:

```
170 LET K = 5/3
```

As written in Table 2-1, DEB contains a high-pressure correction for the non-ideal equation of state of air for overpressure ratios above P = 11.25 as is shown in lines 440, 480, and 490. If the medium is not air, a suitable high-pressure correction ought to be inserted to replace 440, 480, and 490, if it is known. If the high-pressure form is not known, type 440, followed by a carriage return; this will erase the present line 440 and the program will perform the calculation using the ideal gas law just as in lines 450 and 460 for low pressure air. Those expressions are valid for any value of K.

For solids and liquids, the form of waste heat is practically the same but slightly different from those shown. We defer that discussion until Section 2.7.

210, XO, "charge radius" must be in the same units as the data because later lines 310 and 330 convert all distances to centimeters in the same way.

220, M, "weight of explosive and case" means excess mass over air and, therefore, means precisely "weight in air." Thus, for a lighter-than-air gaseous explosive, M would be a negative quantity. For most explosives, M should include all material disintegrated by the explosion. For a nuclear explosion M would thus include the weight of the missile, certainly the cab on a tower shot, etc. An HE missile poses a more difficult judgement but is best expressed by using the word "surrounds." The explosion will reflect from, rather than disintegrate, massive objects in the near vicinity which do not actually surround it, hence, they would not be included in M.

230 H "average specific energy" is not a sensitive parameter. As described in ASH, Section 1.8, it represents the average ratio of

internal and kinetic energy of explosive and bomb debris relative to the surrounding medium. Without more precise information, leave 230 with the value H = 0.25.

The dependence of the estimate for initial yield on the parameter H is solely due to extrapolating the closest data inward to obtain the pressure at the charge surface. The yield is independent of H wherever the pressure is specified by actual measurement. The best way to answer the question, "What uncertainty is introduced?" is to vary H slightly about the ideal value .25 for the specific data and see what differences arise. For the DASA 1559 TNT data shown in Table 2-2 several runs showed these results

Assumed H	Y_o	Waste heat of charge
0	.356	.015
.1	.327	.035
.25	.328	.074
.5	.330	.139
1.0	.332	.269

Thus, for data extending this close to the charge, any guess $.1 \leq H < 1$ makes an insignificant difference in the blast yield Y_o. To ignore mass entirely--by setting H = 0--is equivalent to treating the explosion like a nuclear explosion close-in; the yield is increased 10% thereby because of the very high pressures close in.

An interesting aside: note the waste heat of the charge itself increases in direct proportion to H, nearly doubling the apparent total yield for H = 1, up to 0.332 + 0.269 = 601 megacal/pound or about 1320 cal/gm. About 25% of the yield of TNT comes from afterburning--TNT is an oxygen deficient explosive. The result 1320/1.25 = 1060 cal/gm is

in good agreement with the classical values for heat of detonation. This result suggests that the analysis thereby verifies the classical heat of detonation for TNT. But this order of magnitude estimate for waste heat in the charge is too crude to be that reliable. A more fundamental discrepancy: the classical heat of detonation was not supposed to be affected more than a few percent because of residual heat of charge. Perhaps that is why the classical procedure calculated the stoichiometry as if all the reactions occurred at room temperature and as if the heat of detonation and blast yield were the same. Besides, the close-in pressure measurements do not indicate low pressure as if H=1.

At 260, Q1 provides an option for varying dln Q/dln Z close to the charge, if it is thought to be different from 3.5. One guide would be to use the average value of dln Q/dln Z as it was previously found in nearby data. In Table 2-2, the printout for a samples run of DASA 1559, with H = .25 shows the strong shock slopes for $100 \geq P \geq 3$ to be: 4.03, 3.62, 3.15, 2.95, 2.84, and 3.63. These slopes average 3.37. What we see here may only be experimental scatter due to calculating the slope directly from adjacent points. It could also be real, $q < 3.5$ because of afterburning.

At 230, Q2 provides an option for varying dln Q/dln Z for shock growth beyond the farthest data, if it is thought to be different from 4.0. An easy way to make a better estimate is to average the slopes for weak shocks $P < 3$. The low pressure values of dln Q/dln Z for DASA 1559 are 3.79, 3.59, 4.16, 4.37, 4.24, 4.17, 4.50, 4.03; they average 4.11. There may be some monotonic systematic loss here due to any number of causes we can consider as generalized waste heat; most of the systematic fluctuation seen here is a typical of a body wave

(BOW) or oscillation which may occur for high explosives, but averages out to be null in average effect, like an AC fluctuation on a DC current.

In either extreme of distance, the uncertainties in Q1 and in Q2 have negligible effect on Y_o. Below 0.2 psi, Table 2-2 shows only 0.0048 megacalories are estimated with Q2 = 4 out of an eventual total of 0.330, thus, about 1.5% of the source energy Y_o would be lost if the tail fraction were omitted entirely. Between the charge surface and the first data point at 13.7 cm, the fraction of energy involved is

$$\frac{.330 - .322}{.330} \times 100 = 2.4\%$$

Such would be the error in yield Y_o if we completely neglected all the energy dissipated inside a shock distance of 13.7 cm (about 4 charge radii). It is not worth the effort to try improving over an estimate with the ideal value q = 3.5.

2.6 Data Modification and Transformations

We refer to 297-360, where data are read in and routed.

Line 300 reads the data in pairs as input, starting at line 1000, assigning the first number of each pair as a pressure P, the second number as a measured distance X. Either may be in any units.

Line 320 (or thereabout) converts the pressure P as read to an overpressure ratio by dividing by the ambient pressure in whatever units were used for P in the DATA statements. The user should type:

320 LET P = P/(actual ambient pressure)

Another example: If P were input in absolute psi instead of overpressure, and P_o were 13.6 psi, type

320 LET P = P/13.6 - 1.

Suppose the shock velocity were input at line 1000 instead of pressure P; we have for ideal air,

$$\frac{U}{C_o} = \sqrt{1 + \frac{6}{7}\ \frac{\Delta P}{P_o}}$$

and in our notation for pressure

$$P = \frac{\Delta P}{P_o} = \frac{7}{6}\left[\left(\frac{U}{C_o}\right)^2 - 1\right] .$$

The program would read the input shock velocity as P (not U). If ambient sound velocity C_o = 1100 f/s, then we could type directly

320 LET P = (7/6) * ((P/1100) ↑ 2 - 1) .

As a further example of data modification: Suppose that the time-of-arrival method had been used with a sound velocity later determined to be too high by 0.3%. As a result, all the Mach numbers for shock velocity are too low by 0.3%. It is straightforward to show that the pressures so calculated are too low, especially at low pressures and that a suitable correction in the pressure ratio is shown as line 325 below:

```
325 LET P = 0.007 + 1.006 * P .
```

Line 330 or thereabouts must convert the distances X as read in the DATA statement to either centimeters or meters. Because of the factor 10^6 between nuclear and HE energy and that volumes go like R^3, the program automatically computes both small charge and nuclear data with the same numbers for radii. If the conversion in 330 is intended to mean centimeters, say R = 30.48 * X (using 30.48 cm/ft), the numbers for the yields Y will mean megacalories (10^6 cal). If the conversion in 330 were intended to mean meters, say R = 0.3048 * X or R = X/3.28, then Y would mean the number of kilotons (10^{12} cal). Normally, this factor of 10^6 between HE and nuclear explosions will be clear from context. With tongue in cheek, I cannot forego the comment that a potential user who does not recognize a factor of 10^6 in energy release from the distances would be well advised to get outside help before fooling around with explosives.

As another example of distance conversion: Suppose distances all were measured too short by 5 feet. After reading the data in line 300 but before converting to centimeters in 330, an extra line would correct them thus:

```
328 LET X = X + 5
330 LET X = 30.48 * X
```

Proceeding in the LIST, 350 is the mass effect correction for Z; it reads directly:

$$Z = (R^3 + M \cdot H)^{1/3}$$

The present line 350 is intended to accept a variable H. Note that if the program were refined to let H be a variable, variations would perforce be programmed prior to line 350.

305, 310, and 360 terminate the program when the input data are all read and the machine comes to read P = 0, X = 0 in line 1990. It routes the program to the terminal statements 800 *et seq.* summarizing results.

2.7 Waste Heat Calculations

As listed in Table 2-1, 400-490 calculates the waste heat for air with appropriate approximations for low overpressures at 420 and a non-ideal equation of state for air at 490. For explosions in air, with no corrections for GAB or GWH, or no further modifications are needed, the program is ready to RUN.

We discuss briefly the derivation of these equations and the alternate procedures for other materials. See also Appendix QVP, which gives a program for calculating Q and prints results completely for $10^{-4} < P < 10^{6}$ and at several values of K for $P < 10$.

The typical calculation for waste heat is done in 460. Just before this, 450 is the density ratio computed according to the usual Rankine-Hugoniot relations

$$D = \frac{\rho}{\rho_o} = \frac{\mu\xi + 1}{\xi + \mu}$$

where ρ/ρ_o = density ratio across the shock and ξ is the absolute pressure ratio using

$$\xi = 1 + P$$

$$\mu = \frac{K + 1}{K - 1} \quad .$$

It follows that

$$D = \frac{\frac{K + 1}{K - 1}(1 + P) + 1}{(1 + P) + \frac{K + 1}{K - 1}}$$

$$D = \frac{\frac{K + 1}{K - 1} P + \frac{2K}{K - 1}}{P + \frac{2K}{K - 1}}$$

which is line 450.

460 is a straightforward derivation from classical thermodynamics and the Rankine-Hugoniot relations. For an adiabatic expansion and ideal gas, the prompt energy relation

$$W = \int_{V_i}^{V_f} P dV$$

leads directly to

$$W = \frac{P_i V_i}{K - 1} \left[1 - \left(\frac{V_i}{V_f} \right)^{K - 1} \right] .$$

By whatever process an ideal gas is compressed, the energy added to the material is

$$E_i - E_o = \frac{P_i V_i}{K - 1} - \frac{P_o V_o}{K - 1}$$

so that in ordinary notation, where P is an absolute pressure,

$$Q = E_i - E_o - W$$

$$Q = \frac{P_i V_i}{K - 1} - \frac{P_o V_o}{K - 1} - \frac{P_i V_i}{K - 1} + \frac{P_i V_i}{K - 1} \left(\frac{V_i}{V_f} \right)^{K - 1}$$

$$Q = \frac{P_i V_i}{K - 1} \left(\frac{V_i}{V_f} \right)^{K - 1} - \frac{P_o V_o}{K - 1}$$

$$\frac{Q}{P_o V_o} = \frac{1}{K - 1} \left[\frac{P_i}{P_o} \frac{V_i}{V_o} \left(\frac{V_i}{V_f} \right)^{K - 1} - 1 \right]$$

$$= \frac{1}{K - 1} \left[\frac{P_i}{P_o} \cdot \frac{V_i}{V_o} \left(\frac{P_f}{P_i} \right)^{\frac{K - 1}{K}} - 1 \right] .$$

If $P_f = P_o$, as is the case for most shocks, and noting that $\rho_o = 1/V_o$:

$$\frac{\rho_o Q}{P_o} = \frac{1}{K - 1} \left[\frac{V_i}{V_o} \cdot \left(\frac{P_i}{P_o} \right)^{\frac{1}{K}} - 1 \right] .$$

Showing DEB506 notation on the left and standard notation on the right,

$$Q = \rho_o \, Q/P_o$$

$$D = \frac{V_o}{V_1}$$

$$1 + P = \frac{P_1}{P_o}$$

and we have, as the waste heat for any shocked gas

$$Q = \frac{(1 + P)^{\frac{1}{K}}}{K - 1} \cdot \frac{1}{D} - \frac{1}{K - 1}$$

which is 460.

For low pressures, say $P < 0.02$, Q becomes an exceedingly small difference between two numbers each approximately equal to $1/(K - 1)$. The actual value of Q becomes less than the truncation errors of the machine. By a laborious but straightforward expansion, using the binomial theorem and carrying fourth order terms for any ideal gas

$$\frac{\rho_o Q}{P_o} \cong \frac{K + 1}{12} \left(\frac{P_s - P_o}{\rho_o C_o^2} \right)^3 \left[1 - \frac{3}{2} \frac{(P_s - P_o)}{P_o} + \ldots \right] .$$

This approximation is 420 when expressed in DEB506 notation:

$$Q = \frac{(K + 1)}{12} \left(\frac{P}{K} \right)^3 \left(1 - \frac{3}{2} P \right)$$

Note, as an aside on natural units, that since $\Psi = \frac{P_s - P_o}{\rho_o C_o^2}$,

this last expression is

$$Q = \frac{K+1}{12}\phi^3\left(1 - \frac{3}{2}K\phi\right) \quad .$$

Both 420 (the low pressure approximation) and 460 are valid expressions for the waste heat of any ideal gas. This is an easier requirement than appears at first because the ideal gas law does not fail seriously below 10 bars, and the contributions to yield very close to the charge become small because of the small radius R involved in $Y = 4\pi\int QR^2dR$.

For P > 10 bars or so, air does not follow the ideal gas law. A correlation of theoretical equations of state for real air was given in LADC 1133, reprinted in LA 1664, and was used to determine the hydrodynamic yields of most nuclear explosions. Using these data, the waste heat Q of real air was found well represented by the simple approximate expression

$$\frac{\rho_o Q}{P_o} = 10^{\frac{(22-L)(L-1)}{16}}$$

where $L = \log_{10}(P)$. This expression closely approximates the ideal gas at moderate pressures, and matches it exactly both at 3.4 and 11.25 bars. As an easy comparison, the above formula clearly gives $\rho_o Q/P_o = 1$ at P = 10, where $\log_{10} P = 1$; the ideal gas law gives $\rho_o Q/P_o = 1.0136$. As shown in line 440, the high pressure form is used for P > 11.25.

The accuracy of the high pressure expression is really fixed by the numerical parameters 22 and 16, since these numbers were theoretically derived and appropriately rounded off for uncertainties. As an aside, fitting with precise fireball data from

nuclear explosions suggest the number ought to be 21.75 instead of 22. But we continue to use the value 22 for two reasons. First, we wish to keep the entire present derivation as theoretical as possible, precisely in order to make meaningful comparisons with data later, and we cannot do so if the numbers are already fitted to data. Second, there is no guarantee that the composite or fireball data are that accurate either. The main implication is that there is no serious worry about the equation of state at low pressures of interest. The fractional uncertainty in Q due to a difference in parameter 22 as opposed to 21.75 is then

$$\frac{Q_{theoretical}}{Q_{fitted}} = \frac{10^{\frac{(22-L)(L-1)}{16}}}{10^{\frac{(21.75-L)(L-1)}{16}}}$$

$$\text{relative error} = 10^{\frac{0.25(L-1)}{16}} .$$

At the end of the radiative phase and the beginning of shock growth where P = 75,000 bars, L = 4.88 and Q is therefore uncertain by a factor $10^{\frac{0.25\ (3.88)}{16}} = 1.15$, or 15%. But at 100 bars, about the highest pressure of interest for high explosives, the fraction is $10^{\frac{0.25(1)}{16}} = 1.02$ which is a negligible error. And of course, from the form of the expression, Q is completely insensitive to the exponent 22 at P = 10 bars, where L = 1. In short, although 21.75 is probably a better number, it does not appear worthwhile to change it in the present introductory study from the originally derived theoretical parameter 22.

Tables 10 to 15 of Appendix QVP makes an explicit comparison of Q for both parameters 22 and 21.75 and the ideal gas law.

For gases other than air the high pressure form 490 will not be valid. If the high pressure approximation for that gas is known, corresponding changes should be made at 440 and 480-490. Otherwise, as mentioned in the discussion of input parameters K, in Section 2.5, we can erase 440 by typing "440" and a carriage return. The program will then use the ideal gas law throughout.

For applications to solids and liquids, the whole block from 410 to 490 should be replaced by its counterpart. The relations for Q in a solid or liquid are quite similar. The adiabats are identical if written in the form

$$P = \frac{\rho_o C_o^2}{K-1}\left[\left(\frac{V_o}{V}\right)^K - 1\right] .$$

For pure solids or liquid, $K \cong 7$ and the counterpart of 420 in the low pressure approximation differs only by the factor K from the expression for a gas, that is

$$Q \cong \frac{(K+1)\,K}{12}\,\phi^3$$

The extra K occurs because in solids and liquids, the material returns essentially to its original volume. This expression applies if a gas is allowed to return to its original volume by promptly radiating away its heat. But it is treacherous to push these similarities too far. Most solids contain air voids which drastically alter the waste heat. To offset these difficulties, however, $\phi \ll 1$ for most solids and liquids (except in nuclear explosions) and the behavior is acoustic as above. To calculate waste heat for such materials, the reader is referred to WT 1034, WT 1495, or UNP 434.

For explosions exhibiting marked losses different from waste heat such as surface effects or radiation appropriate corrections to increase or decrease Q can be made following 420, 460, and 490. There are no general rules which ought be cited for the data here.

2.8 Integration of Waste Heat

The generic idea in DEB was given in Section 2.2. Before discussing the program itself, consider again Figure 2.2-1, which shows the specific method of calculation in DEB506. Refer to lines 499-592.

Define a local constant q(Z) such that between adjacent points Z and Z1

$$QZ^q = \text{constant} = Q_o Z_o{}^q \quad .$$

Then the local slope is

$$q = \frac{\ln Q - \ln Q_o}{\ln Z - \ln Z_o} = \frac{\ln (Q/Q_o)}{\ln (Z/Z_o)} \quad .$$

This is essentially the N in line 550, except that 3 is subtracted from it for convenience for reasons noted below.

The integration for Y actually starts with 510 which makes an estimate for shock growth beyond the farthest data point. It is based on a value of $\frac{d\ln Y}{d\ln R} = N = Q2 - 3$ as shown in 275 using the theoretical value Q2 = 4 or with whatever value was input at 270. The expression in 510 follows the more general procedure which is as follows.

Y1 in line 560 is the general increment in Y between some R_1 and R_2:

$$\Delta Y = 4\pi \int_{R_1}^{R_2} QR^2 dR \quad .$$

Because q is assumed constant in the interval R_1 to R_2, $QR^q = Q_1 R_1{}^q$ and

$$\Delta Y = 4\pi Q_1 R_1{}^q \int_{R_1}^{R_2} R^{2-q}\, dR \quad .$$

This is an elementary integral and the form for all increments in Y becomes

$$\Delta Y = \frac{4\pi\ Q_1 R_1^{\,3}}{q-3}\left[1 - \left(\frac{R_1}{R_2}\right)^{q-3}\right]$$

$$\frac{\Delta Y}{P_o} = \frac{4\pi}{3}\frac{3Q_1 R_1^{\,3}}{P_o(q-3)}\left[1 - \left(\frac{R_1}{R_2}\right)^{q-3}\right].$$

The nomenclature of DEB506 is shown on the left in the relations

Y1 = ΔY, the increment in Y

Q = local value of $\rho_o Q/P_o = Q_1$ above, bars (not Q1 in DEB506)

Z = local value of R_1, mass corrected

ZO = previous value of R_2, mass corrected

N = q - 3 .

Combining these terms we have

$$Y1 = \frac{4\pi}{3}\frac{3QZ^3}{N}\left[1 - \left(\frac{Z}{ZO}\right)^{N}\right]$$

which is 560, except for units.

The dimensions of Y1 are thus: Q is proportional to the ambient pressure in bars, since it was calculated by letting $Q = \rho_o Q/P_o$ in Section 2.7. In the above equation, Z/ZO is dimensionless, so is N. The dimensions of Y1 are then

$$Y_1 \sim \frac{4\pi}{3}\,3QZ^3 \text{ bar cm}^3$$

$$Y_1 \sim 3QZ^3\,\frac{4\pi}{3} \text{ bar cm}^3 \cdot \frac{\text{cal}}{\frac{4\pi}{3} \times 10^7 \text{ ergs}} \cdot \frac{10^6 \text{ ergs}}{\text{bar cm}^3}$$

$$Y_1 \sim .3QZ^3$$

Now note that the first increment in line 510 is simply Y1 with ZO = ∞:

$$Y1 \sim 0.3\ QZ^3/N \text{ calories.}$$

Throughout the calculation, Y1 is so carried, in calories.

Line 570 Y = Y + Y1, is the heart of the DEB program. It integrates the prompt energy Y at each measured distance by summing the previous increments Y1. The scaling conversion due to ambient pressure and for energy in megacalories or kilotons is done simply in line 700 by printing out $P_oY/10^6$ instead of Y itself.

The slope $N1 = \frac{d\ln Y}{d\ln R}$ in line 580 is derived thus.

Consider $dY = -4\pi QR^2 dR$

Since $R^2dR = Z^2dZ$

$$\frac{dY}{Y} = -4\pi \frac{QZ^3}{Y} \frac{dZ}{Z} \quad .$$

Now define

$$N1 \equiv -\frac{dY/Y}{dZ/Z} = 4\pi\frac{QZ^3}{Y} \quad .$$

Because QZ^3 is carried in bar cm^3, and Y in calories, again we have

$$N1 = \frac{4\pi}{3} \frac{3QZ^3 \text{ bar cm}^3}{Y \text{ cal}} \frac{\text{cal}}{\frac{4\pi}{3} \times 10^7 \text{ ergs}} \cdot \frac{10^6 \text{ ergs}}{\text{bar cm}^3}$$

$$N1 = 0.3 \frac{QZ^3}{Y}$$

which is 580.

From N1 the form factor F is readily specified; F is defined by

$$Y(R) \equiv \frac{4\pi}{3} R^3 PF$$

The above definition for N1 then becomes

$$N1 = \frac{4\pi QZ^3}{\frac{4\pi}{3} Z^3 PF}$$

$$N1 = \frac{3Q}{PF}$$

According to the arguments in the QZQ hypothesis, N1 ought to be a constant at both extremes of very strong and very weak waves. According to the scaling hypothesis, F should be a function only of shock strength P. According to thermodynamics, Q is also a Q(P), hence Q/P is certainly a function of P. Hence, N1 ~ Q/P and ought to be constant in both extreme values and "scale", i.e., be a function only of shock strength. It is a "nearly constant." Thus, even better than tabulating F, which scales but varies rapidly at low pressures, the tabulation in Column 5 shows N1 is a slowly varying function, 0.5 < N1 < 1 and we can always obtain F readily and directly from

$$F(P) = \frac{3Q}{PN_1} .$$

Here, in dramatically simple form, is the power of the DEB method. As mentioned in Section 1.8, solving the blast wave problem reduces mainly to a matter of solving for the form factor F. Column 5 gives F implicitly in terms of a nearly constant, N1 summarized by

$$\underset{\text{strong shock}}{0.5} \leq \left(N1 = \frac{3Q}{PF}\right) \leq \underset{\text{weak shock}}{1.0} .$$

700 is the actual printout of results. In Columns (1) and (2), P and R are printed as carried in the program. Y is scaled and

converted to megacalories or kilotons as discussed above and appears in Column 3.

For the program it is clear that N + 3 in Column 4 is the local slope dln Q/dln Z. The logarithmic slope for yield versus distance, N1 in Column 5, was derived above for explaining line 580. 710, 720 store the current values of Q, Z, and as the "previous values" Qo, Zo for the next step.

2.9 Estimates for Total Yield

When the input data are used up, the program eventually reads 0,0 in 1990. Lines 310 and 360 then route the calculation to 800.

800 extrapolates Q directly to the charge surface using the ideal exponent of Q1,or whatever number was input at line 200; normally Q1 = 3.5. Z is now the mass corrected charge radius XO.

810 and 820 are straightforward inversions of 480 and 490 which calculate the waste heat of a strong shock; they solve for pressure using the Q obtained in 800. These lines are valid only for air. If the explosion occurs in some other medium, lines 810 and 820 must be changed accordingly.

Having obtained P at the charge surface at 820, the calculation is routed back to 550. Increments in Y and slopes are then treated as for any other point.

We note in passing that the value of P printed out as a result of the last step provides a useful and sensitive check on the values of the parameters Q1, M, and H. The effect of q = Q1 is clear; the steeper Q1, the higher the value of the waste heat Q and the higher pressure at the charge surface.

The pressure at the charge will be inversely proportional to M and H, extrapolating backward from the closest data. All the reasons and restraints are more elaborate than we need discuss here, but consider the mass correction term in brackets

$$Y = \frac{4\pi}{3} R^3 \, PF \left[1 + \frac{HM}{\frac{4\pi}{3} D_o R^3} \right] .$$

If the mass effect correction in brackets is large, as it will be for high explosive charges near the charge surface,

$$Y_o \cong \frac{PF\ HM}{D_o} \quad .$$

Thus,

$$P \sim \frac{D_o Y_o}{FHM} \quad .$$

As we noted previously in connection with the choice of H, variation in H and hence variations of P at the surface do not strongly affect the yield Y_o. D_o and M are known for a given weight of surrounds; in some cases we may not be sure how much of the case enters into the mass effect. F is a constant due to similarity conditions for strong shocks. The physical meaning of H is now clear, a low specific heat H results in high initial pressures.

An order of magnitude estimate for the waste heat of the charge is made at the end of the calculation. This Q of the charge is not included in the estimate for yield Y_o at the initial radius because, in principle at least, it is energy never delivered to the surrounding air as part of the explosive process. It appears as residual heat of debris remaining after the air has returned to P_o, and may be delivered to air by much slower processes of conduction and convection. This order of magnitude estimate is included, not for rigor, but as a reminder and guide why there may be substantial real differences between hydrodynamic yield and total chemical energy release by detonation.

This magnitude is estimated as if all material inside the initial radius--the high explosive itself or the isothermal sphere of a nuclear explosion--undergoes the same waste heat as the adjacent air. It is as if the inner material eventually reached

temperature equilibrium with the surrounding air. It is somewhat a "cart before the horse" argument, done more for convenience than rigor, which is why line 705 prints "of the order".

Line 707 shows the estimate explicitly. Assuming Q = constant as noted by printing out dln Q/dln Z = "0 assumed", then

$$\Delta Q(\text{charge}) = 4\pi \int_0^{Z_o} QR^2 dR$$

$$= \frac{4\pi}{3} QZ_o^3 \quad .$$

This is the quantity printed out by line 707 (except for conversions from bar cm^3 to megacalories). No further calculations were necessary because Q and Z_o were currently stored in the program from the estimates at the initial radius.

This estimate may be substantially different from what one would calculate using the ideal gas law, without mixing, and without radiative transport. But each of these processes do occur. In nuclear explosions, the inner material does radiate, some of its energy is lost by conduction to surrounding air at the edge of the isothermal sphere. For chemical explosions, the mixing assumption implies that powerful conduction and convention losses occur. In both cases the inner material does expand along a path steeper than the classical adiabat, and so the waste heat would be greater. One can argue that the energy is eventually regained by the surrounding air. True, but it remains in the air and conducts too slowly to support the shock or contribute to prompt energy. At any rate no claim is made for accuracy in estimating the waste heat of the charge; it is probably an upper limit but only order-of-magnitude correct.

2.10 Printout and Diagnostics

Table 2-2 is the printout for the list shown in Table 2-1. The heading of the Table ought to verify if inputs and calculations were as intended. As a check:

1. All the parameters shown just below the title, such as ambient pressure, density, etc., should appear with the correct values for the units shown. If not, the tabulated results will probably be in error, however smooth the tabulated entries might appear.

2. In the leading line of the columnar results, $\frac{d\ln Y}{d\ln Z}$, in Col. 5 should be the input N1 = Q2-3 as intended in 270.

3. In the next to final line, "ESTIMATES AT INITIAL RADIUS": $\frac{d\ln Q}{d\ln Z}$ (Col. 4) should have the value Q1 intended in line 250. Also, the measured radius in Column 2 should be the radius XO input at 210, but converted to centimeters or meters.

Columns 1 and 2 of the printout retabulate the measured input pressure-distance data. Column 1 is the overpressure, expressed as a dimensionless ratio to ambient; it is the normal "scaled" pressure. Column 2 is the distance, expressed in centimeters, meters, or whatever instruction was given in line 330. As noted in the heading (cm or m), the numbers in Column 2 usually mean centimeters for chemical explosions or meters for nuclear explosions. However, many other combinations of distance units and yield are primarily expressed as will be discussed in Section 4.4 and summarized in Table 4.4.

Column 3 tabulates the integrated prompt energy Y(R) remaining in the wave at each measured distance R. Y(R) is the main result of DEB. If calculations were done to predict the explosion, carrying them forward as in real time, starting from

some initial hydrodynamic yield Y_o and initial radius R_o, then Y(R) would be the energy remaining in the wave at distance R, still available to drive the shock at further distances. Using DEB, this energy has been evaluated by asking literally, "How much energy was in fact dissipated beyond distance R?".

At the end of the calculation, we find "ESTIMATES AT INITIAL RADIUS" as discussed in Section 2.9. Under pressure in column 1 is the estimate for pressure P_i at the input charge radius R_o and number inputted should appear in Column 2.

The entry under Column 3 in this lines "ESTIMATES"--.330476 in Table 2.2--is the single most diagnostic result of DEB: it is the hydrodynamic yield which is estimated at the charge radius R_o. The preceding number in Column 3--.32218 in Table 2.2--is the firmest number in DEB, being the energy Y(R) at the closest measured pressure. Y_o includes a theoretical estimate for the intervening distance.

Recall that the hydrodynamic yield Y_o is not the heat of detonation. It is even more useful. It is the energy actually released from the explosive to the surrounding medium. If we know the heat of detonation, we would also have to know the loss of energy due to waste heat in the charge, and this is a more uncertain quantity. We circumvent this uncertainty by specifying Y_o instead of the heat of detonation.

This waste heat of the charge is estimated in the line following "LOSS IN CHARGE OR RADIATIVE PHASE IS OF THE ORDER:" at the end of the printout. The entry under Column 3--7.42755 E-2 in Table 2.2--is the waste heat of the charge itself, not the cumulative total energy. The best estimate for the heat of detonation

would be

estimate of Y_o	.330476	megacal
loss in charge	.074275	
estimated total	.405	megacal

This is still not the chemical energy in heat of detonation. Experience shows that Y_o includes a 20% to 25% contribution from afterburning, which implies that the heat of detonation itself was only 320 to 340 megacalories. By way of summary, here again is the advantage of specifying the hydrodynamic yield Y_o instead of the heat of detonation: Y_o does not include the waste heat in the charge, which never does appear in the medium. Y_o does include the afterburning, but only insofar as it supports the blast wave.

Column 4, $q = d\ln Q/d\ln Z$ of the printout can be used for diagnostics by comparing them with the eigenvalues of 4.0 and 3.5 in the strong and weak zones respectively. But before concluding that the scatter is real, consider the possibility that the observed scatter is due in part to calculating the slope from adjacent points. A 7% measured error in pressure is about as small as we reasonably expect from experience on field data. When the pressure is small, $Q \sim P^3$ and the resulting error in Q is 20% or a factor 1.2. If the ratio between distances is 1.5, which is relatively wide spacing and one which therefore ought to give a relatively good average slope, then $\ln Q$ (measured) = $\ln Q$ (real) $\pm$ ln (1.2) and we have

$$q\ (\text{measured}) = \frac{\ln Q_1 \pm \ln 1.2 - \ln Q_o}{\ln 1.5}$$

$$q\ (\text{measured}) - q\ (\text{real}) = \pm \frac{\ln 1.2}{\ln 1.5}$$

$$\Delta q = \pm 0.45$$

Thus, the scatter expected in q is about as much as the 0.5 difference between strong and weak shock eigenvalues. On that basis, DASA 1559 is high quality data because most of the points on Table 2-2 fall within that scatter.

Even trends in data may not be significant because most "data" are not really experimental numbers but are some smooth curve passed through the data. Thus, the "French curve" error can show "trends" as large as ± 0.5 in q.

More discussion of diagnostics is given in Chapter 4, after the exposition of DSC. The diagnostics of DEB and DSC go together: a value of q larger (steeper slope) than its respective eigenvalues in DEB will generally indicate a falling apparent yield Y in DSC; a value of q smaller than its respective eigenvalue means a rising yield. About two dozen reasons exist why q may rise, fall, or oscillate. Many variations are due to the modes of energy transport listed in Table 1-2.

TABLE 2-1

LIST DEB506

```
100   PRINT"DIRECT EVALUATIØN ØF BLAST ENERGY, UNIFIED THEØRY FØR BLAST"
101   REM...FØR QUESTIØNS ØR REFERENCES CALL F.B.PØRZEL,301-495-8101
102   REM..INPUT MEASURED DATA, ANY UNITS. SEE LINE 998
103   REM...INPUT PARAMETERS AND ØPTIØNS  MADE IN LINES 141 TØ 270
104   REM...IDENTIFY THE DATA AS IN LINE 110
105   PRINT
110   PRINT"DASA 1559 CØMPILATIØN FØR ØNE PØUND TNT"
120   REM...LINE 130 SETS YIELD Y=0 AT INFINITY (CØL 3 ØF PRINT ØUT)
130   LET Y=0
140   REM...DESCRIBE ATMØSPHERE: DEFINITIØNS AND UNITS AS IN 180,190
150   LET D0=.00129
160   LET P0=1
170   LET K=1.4
180   PRINT"AMBIENT PRESSURE ="P0"BARS   AMBIENT DENSITY ="D0"GM/CM↑3"
190   PRINT"ADIABATIC EXPØNENT K="K;
200   REM.DESCRIBE BØMB: X0=INITIAL ØR CHARGE RADIUS, SAME UNITS AS DATA
201   REM...M, H AS IN LINES 240,250;  H MEANS KINETIC + HEAT ENERGY
210   LET X0=.1312335
220   LET M=.454
230   LET H=.25
240   PRINT"SPECIFIC ENERGIES, BØMB/MEDIUM="H
250   PRINT "EXPLØSIVES AND SURRØUNDS WEIGH"M"KILØGRAMS, KILØTØNS"
251   LET M= 1000*M/4.186/D0
259   REM..Q1 GIVES ØPTIØN FØR DLNQ/DLNZ BETWEEN CHARGE AND CLØSEST DATA
260   LET Q1=3.5
269   REM..Q2 GIVES ØPTIØN FØR SLØPE BEYØND FARTHEST DATA
270   LET Q2=4
275   LET N=Q2-3
279   PRINT
280   PRINT"ØVERPRESSURE","MEAS.RADIUS","PRØMPT ENERGY","  DLN Q/DLN Z";
281   PRINT"   DLN Y/DLNZ"
290   PRINT"  (RATIØ)","(CM.ØR M)","(MEGACAL,KT)"
297   REM.....DATA READ IN AND RØUTED.....
298   REM...CØNVERT P TØ RATIØ:  MEAS.Ø'P/AMBIENT, SAME UNITS, LINE 320
299   REM...CØNVERT DISTANCE TØ CM ØR METERS IN LINE 330
300   READ P, X
305   IF X>0 THEN 320
310   LET X=X0
320   LET P=P/P0
330   LET R=30.48*X
350   LET Z=(R↑3 + H*M)↑(1/3)
360   IF P=0 THEN 800
```

TABLE 2-1 (Cont'd)

LIST DEB506

```
400   REM.....CALCULATE WASTE HEAT.....
410   IF P>.02 THEN 440
420   LET Q=(K+1)*((P/K)↑3)*(1-1.5*P)/12
430   GØTØ 500
440   IF P>11.25 THEN 480
450   LET D=(P*(K+1)/(K-1)+2*K/(K-1))/(P+2*K/(K-1))
460   LET Q=(1+P)↑(1/K)/D/(K-1)-1/(K-1)
470   GØTØ 500
480   LET L= .43429448*LØG(P)
490   LET Q= 10↑((22-L)*(L-1)/16)
499   REM.....INTEGRATIØN ØF WASTE HEAT.....
500   IF Y>0 THEN 550
510   LET Y=.3*Q*(Z↑3)/N
520   LET N1=N
530   GØTØ 700
550   LET N=LØG(Q/QO)/LØG(ZO/Z) -3
560   LET Y1=.3*Q*(Z↑3)*(1-(Z/ZO)↑N)/N
570   LET Y=Y+Y1
580   LET N1=.3*Q*(Z↑3)/Y
591   LET N= INT(100*N +.5)/100
592   LET N1= INT (100*N1 +.5)/100
700   PRINT P, R, PO*Y/1000000, N+3, N1
702   IF X>XO THEN 710
705   PRINT "LØSS IN CHARGE ØR RADIATIVE PHASE IS ØF THE ØRDER:"
707   PRINTP, " ",PO*Q*(Z↑3)/10↑7, O"ASSUMED"
708   GØTØ 2000
710   LET QO=Q
720   LET ZO=Z
725   LET YO=Y
730   GØTØ 300
799   REM.....SUBRØUTINE FØR ESTIMATING INITIAL PRESSURE....
800   LET Q=QO*(ZO/Z)↑01
810   LET L= .5*(23-SQR(23↑2 -4*(22 +16*.4343*LØG(Q))))
820   LET P= EXP(2.303*L)
830   PRINT"ESTIMATES AT INITIAL RADIUS:"
840   GØTØ 550
998   REM...INPUT DATA IN PAIRS:Ø'PRESS, DISTANCE; LØWER PRESSURES FIRST
1000  DATA      .02, 100,      .05, 49,      .1, 28
1010  DATA .23, 16,      .3, 13.6,      .5, 10
1020  DATA      1, 6.8,       2, 5,      3, 4.2
1030  DATA 6, 3.15,   10, 2.55
1040  DATA 20, 1.85,  50, 1.11,  100, .68
1050  DATA 160, .45
1990  DATA 0,0
2000  END
```

TABLE 2-2

DIRECT EVALUATION ØF BLAST ENERGY, UNIFIED THEØRY FØR BLAST

DASA 1559 CØMPILATIØN FØR ØNE PØUND TNT
AMBIENT PRESSURE = 1 BARS AMBIENT DENSITY = .00129 GM/CM↑3
ADIABATIC EXPØNENT K= 1.4 SPECIFIC ENERGIES, BØMB/MEDIUM= .25
EXPLØSIVES AND SURRØUNDS WEIGH .454 KILØGRAMS, KILØTØNS

ØVERPRESSURE (RATIØ)	MEAS.RADIUS (CM.ØR M)	PRØMPT ENERGY (MEGACAL,KT)	DLN Q/DLN Z	DLN Y/DLNZ
.02	3048.	4.80479E-3	4	1
.05	1493.52	9.41375E-3	3.79	.9
.1	853.44	1.50223E-2	3.59	.78
.23	487.68	2.42835E-2	4.16	.93
.3	414.528	2.83759E-2	4.37	.99
.5	304.8	3.88944E-2	4.24	1.06
1	207.264	5.89187E-2	4.17	1.1
2	152.4	8.39986E-2	4.5	1.22
3	128.016	.103324	4.03	1.18
6	96.012	.141054	3.62	1.03
10	77.724	.17121	3.15	.87
20	56.388	.215541	2.95	.68
50	33.8328	.273077	2.84	.51
100	20.7264	.307334	3.63	.52
160	13.716	.32218	6.98	.68
ESTIMATES AT INITIAL RADIUS:				
179.407	4.	.330476	3.5	.67
LØSS IN CHARGE ØR RADIATIVE PHASE IS ØF THE ØRDER:				
179.407		7.42755E-2	0 ASSUMED	

Table 2-3

NOMENCLATURE FOR DEB506

D = current value of shock density, as a ratio to ambient

DO = ambient density, input as gm/cm^3

H = "dynamic specific energy", i.e., the average ratio of internal and kinetic energy of explosive and bomb parts to an equal mass of surrounding air, both at the same velocity and temperatures. A good guess is 0.25, but results are not sensitive if .1<H<1.

K = $(d\ln (P+P_o)/d\ln D)_Q$, adiabatic compressibility of medium

L = $\log_{10} P$

M = weight of bomb and surrounds in air initially, input as gm/cm^3. Line 251 transforms to $M = \frac{H \cdot M}{\frac{4\pi}{3} DO}$, a constant

N = current value of $d\ln Q/d\ln Z - 3$

N1 = $d\ln Y/d\ln Z$, current value

PO = ambient pressure, bars

P = overpressure, input in any units, transformed to a ratio to ambient in line 320 or thereabouts

Q = waste heat, local value in ratio

QO = waste heat, value at preceding data point in run

Q = optional value for $d\ln Q/d\ln Z$ between XO, and closest data

Q2 = optional value for $d\ln Q/d\ln Z$ beyond farthest data

R = shock radius, local value in cm

X = shock radius, input in any units, transformed to cm in meters in line 330

XO = charge or initial radius, same units as data

Y = hydrodynamic yield, current value

Y1 = increment of waste heat, current value

Z = mass effect transform of R, current value

ZO = mass effect transform of R, preceding value

3. Hand Calculation for Prediction and Direct Scaling

3.1 Foreword

The QZQ method is simple enough for a hand-calculated prediction of a pressure-distance curve and subsequent evaluation of data by direct scaling. About three hours are so required, compared with a second or so machine-time using the BASIC program for DSC506. However, several hours would also be required to write and debug a suitable machine program. So, for a single set of data, without access to a machine or to a stored program or tape, hand calculations may be preferable and even faster.

For direct scaling, we will use for illustration only a few values from the composite curve of nuclear data reported in ARF D125:

Pressure (bars)	Distance (meters)
10,000	8.1
1,000	15.5
100	32.3
10	75.6
3	122.5
2	146.8
1	206.0
.5	301.0

The nuclear composite data used here (ARF D125) for comparison were compiled around 1958 and still represent the latest experimental data because this was near the end of nuclear testing in air. In the fireball region, $P > 70$ bars, profuse and highly accurate data were available from fireball measurements; these data were used to

determine the hydrodynamic yield by the analytic solution method (LA 1664, WT 9001). Below 70 bars, much field data were available, although of poorer quality than the fireball time-of-arrival measurements. But here the shock wave behavior was already well described by IBM Problem M (LA 1664), an early machine calculation done circa 1946 at the Los Alamos Scientific Laboratory.

Of course, many other compilations could have been used, and comparisons will be made in future studies with UTE. The ARF D125 data were used because the author knows they do represent raw data, cover an exceptionally broad range, were an authoritative compilation related directly to hydrodynamic yield, and were unclassified.

3.2 QZQ Method for Predicting Pressure Distance

The scheme for predicting the peak pressure-distance curve is illustrated in Figure 3-1.

For some arbitrary transition pressure P_c, from strong to weak shock, first calculate the corresponding waste heat Q_c. For a given yield Y_o, the eigenvalues q_1 and q_2, and the initial radius R_o, we can then solve an implicit equation for transition radius R_c corresponding to the pressure P_c.

From theory, we expect that Q versus R is defined by two straight lines as shown in Figure 3-1. At any pressure P, we can calculate the corresponding waste heat Q(P). It follows that the radius Z(P) is then given by

$$Z(P) = Z_c \left(\frac{Q_c}{Q(P)}\right)^{1/q} \qquad \text{QZQ-1}$$

The hydrodynamic yield Yo is thus defined by

$$Yo \equiv 4\pi \int_{Z_o}^{\infty} QZ^2 dZ$$

$$Yo = 4\pi\left[\int_{Z_o}^{Z_c} QZ^2 dZ + \int_{Z_c}^{\infty} QZ^2 dZ\right]$$

Then, assuming two branches, one for strong and another for weak shocks as shown above with QZ^q = constant in each branch, the shock trajectory is completely specified by fixing Z_c from the results of this integration.

Writing constants A and B for strong and weak shock values of QZ^q = constant = $Q_c Z_c^q$,

$$\frac{Yo}{4\pi} = A \int_{Z_o}^{Z_c} Z^{2-q}\, dZ + B \int_{Z_c}^{\infty} Z^{2-q}\, dZ \quad .$$

Noting that $q > 3$, that $AZ_c^{-q_1} = Q_c = BZ_c^{-q_2}$, and changing signs

$$\frac{Yo}{4\pi} = \frac{A}{3-q_1}\left[Z_c^{3-q_1} - Z_o^{3-q_1} \right] + \frac{BZ_c^{3-q_2}}{q_2-3}$$

$$\frac{Yo}{4\pi} = Q_c Z_c^{3} \left[\frac{\left(\frac{Z_c}{Z_o}\right)^{q_1-3}}{q_1-3} - 1 + \frac{1}{q_2-3} \right]$$

Finally, the total energy of the blast using two branch model is given by

$$Yo = \frac{4\pi\, Q_c Z_c^{3}}{q_1-3} \left[\left(\frac{Z_c}{Z_o}\right)^{q_1-3} - \frac{q_2 - q_1}{q_2 - 3} \right] \qquad \text{QZQ-2}$$

where, in summary

Q_c = waste heat at transition pressure

Z_o = initial radius: at transition from radiative to shock transport ($\cong$ 4.2 meters for 1 kiloton)

Z_c = transition radius: strong shock to weak

Y_o = hydrodynamic yield at Z_o

$q_1 = 3.5$

$q_2 = 4.0$

These values q_1 and q_2 apply for ideal explosions and for most real explosions, but may be varied for non-ideal explosions.

3.3 Calculating Waste Heat

The work is greatly facilitated if a table of waste heat Q versus pressure P is available (see Appendix QVP). This is the only tedious part of the hand calculation; the machine does it automatically for DEB or DSC.

We will not assume such a table is available and illustrate the calculation of waste heat from air in three ranges of pressure: high pressure, moderate, and acoustic region.

The calculation, for waste heat Q in an ideal gas and for an adiabatic expansion is well known, was reviewed in Chapter 2. The modifications for weak and strong shocks were also listed in DEB. Only minor changes are needed for hand calculations.

Recall that the definition of prompt energy

$$W = \int_{P_1}^{P_o} PdV \text{ (actual path)}$$

P = absolute pressure

led to the expression, for a gas at state (P, V)

$$W = \frac{PV}{K-1}\left[1 - \left(\frac{P_o}{P}\right)^{\frac{K-1}{K}}\right] .$$

The waste energy Q in the process starting at energy E_o, raised to energy E and decaying back to P_o is thus

$$Q = E - E_o - \frac{PV}{K-1}\left[1 - \left(\frac{P_o}{P}\right)^{\frac{K-1}{K}}\right].$$

For an ideal gas, K is a constant, also

$$E = \frac{PV}{K-1} \ , \ E_o = \frac{P_o V_o}{K-1}$$

and in dimensionless form the expression for moderate pressures is

$$Q = \frac{\rho_o Q^*}{P_o} = \frac{1}{K-1} \left[\frac{(P/P_o)^{1/K}}{D} - 1 \right] \qquad \text{QVP-3}$$

where $D = V_o/V$.

In general, for non-ideal gases, signifying K_o for the ideal value, $K < K_o$ and

$$E > \frac{PV}{K_o - 1}$$

and Q will be larger than indicated here.

If the compression is done by a shock, the familiar Rankine-Hugoniot condition gives

$$D \equiv \frac{V_o}{V} = \frac{\frac{K+1}{K-1} P + P_o}{P + \frac{K+1}{K-1} P_o}$$

and for K = 1.4, and P an absolute pressure

$$D = \frac{6P + P_o}{P + 6P_o} \ .$$

For P > 10 bars the ideal gas law does not apply. Based on the equation of state for air in LADC 1133, the one by which nuclear yields were actually evaluated, a suitable approximation is

$$Q \text{ (bars)} = 10^{\left(\frac{(22 - L)(L - 1)}{16}\right)} \qquad \text{QVP-4}$$

where $L = \log_{10} (P)$

This expression closely approximates the ideal gas law below and matches exactly at 11.25 bars and at 3.4 bars.

At the other extreme of weak shocks, for $P \ll 1$, certainly for $P < .02$, the ideal gas law form for waste heat QVP-3 is a small difference between much larger numbers. A suitable approximation in the acoustic range is

$$Q = \frac{K + 1}{12}\left(\frac{P}{K}\right)^3(1 - 1.5\ P) \qquad \text{QVP-5}$$

For $P = .1$, as used in the illustration, the pressure is slightly high for the acoustic approximation to be accurate (we demand $P \ll 1$) but using it we obtain

$$Q = .2\left(\frac{.1}{1.4}\right)^3 \quad (.85) = .17\ (10^{-3})\ (.365) = .062 \times 10^{-3} \text{ bars}$$

The exact result is 6.31×10^{-5}, given in the first line of Table 6, Appendix QVP.

3.4 Fix the Critical Radius

The problem is to solve for the transition radius for Z_c in the expression QZQ-2 which we rewrite as

$$Yo = \frac{4\pi}{3} \frac{3}{q_1 - 3} Q_c Z_o^3 \left(\frac{Z_c}{Z_o}\right)^3 \left[\left(\frac{Z_c}{Z_o}\right)^{q_1 - 3} - \frac{q_2 - q_1}{q_2 - 3}\right] \qquad \text{QZQ-2}$$

For a nuclear explosion, negligible mass is assumed, so Z and R are identical. That is

$$Z = \left[M + R^3\right]^{1/3} \cong R \text{ for } M << R^3$$

The starting radius of a nuclear explosion is chosen as R_o = 4.2 meters; it marks the end of the radiative phase and is a theoretical estimate with a transition pressure of 80,000 bars. Rather than neglect the waste heat in the radiative phase, for illustration let us compute it as if the air were ideal and all pressurized to 80,000 bars.

From the waste heat calculations, the fraction of energy wasted during the radiative phase is, for an ideal gas, with K = 1.4

$$\frac{Q}{E} = \left(\frac{P_o}{P}\right)^{\frac{K-1}{K}} \left(\frac{1}{80,000}\right)^{2/7} = \frac{1}{25} = 0.04$$

Accordingly we can set Y = .96 KT at R_o = 4.2 meters instead of Y_o = 1.0.

Let us choose P_c = 2 bars as the transition pressure from strong to weak shock. P_c may well vary from one explosion to another

but 2 bars is chosen as a geometric mean among the several likely choices cited earlier:

1) P = 3.8 bars marks the point where sound velocity C is equal to the material velocity u just behind the wave, and the flow first becomes subsonic behind the wave.

2) P = 1 bar is a natural place to separate the domains when $\Delta P > P_o$ or $\Delta P < P_o$; also it marks the point of maximum change in the partition between kinetic and internal energy.

3) Also around 2 bars, a negative phase first develops in the blast wave behind the shock, thus preventing further hydrodynamic energy from reaching the shock front.

Using $\xi = P + 1 = 3$, and $K = 1.4$ for air, the density-ratio for P = 2 is

$$D = \frac{\frac{K+1}{K-1}\xi + 1}{\xi + \frac{K+1}{K-1}} = \frac{6(3)+1}{3+6} = \frac{19}{9} = 2.1111$$

Using the moderate pressure ideal gas expression for the waste heat and a slide rule

$$Q_c = \frac{1}{K-1}\left[\frac{\xi}{D^{1/K}} - 1\right]$$

$$Q_c = 2.5\left[\frac{3}{2.1111^{1/1.4}} - 1\right] = 0.096 \text{ bars}$$

The exact result is in Table 7, Appendix QVP, which gives the number as .0956.

We now solve for the transition radius R_c using QZQ-2. The starting radius gives

$$R_o^3 = (4.2)^3 = 74 \text{ meters}^3$$

The conversion from kiloton = 10^{12} cal to bar meters^3 is

$$Y = Y(KT)\ \frac{4\pi}{3} \times 10^{19}\ \frac{\text{ergs}}{KT} \cdot \frac{\text{cm}^3\ \text{bar}}{10^6\ \text{ergs}} \cdot \frac{\text{meter}^3}{10^6 \text{cm}^3}$$

$$Y\ (\text{bar meters}^3) = Y(KT) \qquad \frac{4\pi}{3} \cdot 10^7$$

With the values $Q_c = .096$, $R_o^3 = 74$, $q_1 = 3.5$, $q_2 = 4.0$ and writing $X = \frac{R_c}{R_o}$ the energy balance QZQ-2 becomes, for $Y_o = .96$ KT

$$Y_o = \frac{4\pi}{3}\ \frac{3}{q_1 - 3}\ Q_c \cdot Z_o^3\ X^3 \left[X^{0.5} - 0.5\right]$$

$$\frac{4\pi}{3}\ (.96) \times 10^7 = \frac{4\pi}{3}\ \frac{3}{0.5}\ (.096)\ \ (74)\ \ X^3 \left[X^{0.5} - .5\right]$$

$$226000 = X^3\ \ (X^{0.5} - 0.5)$$

Solve for X by integration and interpolation as shown in the tabulation for trial values of X

X	X^3		$\left[X^{0.5} - .5\right]$
35 :	42875	·	[5.416]= 233000
34.7:			226000
34:	39304	·	[5.330] = 209000

We then have X = 34.7 as the solution, and

$$R_c = X\ R_o = 34.7 \times 4.2 = 146 \text{ meters} \quad .$$

The corresponding constants for strong and weak shocks become

Strong: $QR^{3.5} = .096\ (1.46 \times 10^2)^{7/2} = .36 \times 10^7$

Weak: $QR^{4.0} = .096\ (1.46 \times 10^2)^4 = .446 \times 10^8$

For hand calculations it is more convenient to use the numbers for R_c and Q_c directly as calculated

$$R = R_c \left(\frac{Q_c}{Q}\right)^{1/q}$$

whence for any other value of Q

$$R_{calc} = 146 \left(\frac{.096}{Q}\right)^{1/3.5} \quad \text{strong shocks}$$

$$R_{calc} = 146 \left(\frac{.096}{Q}\right)^{1/4.0} \quad \text{weak shocks}$$

3.5 Direct Scaling

Using the values for R_c and Q_c just determined, the calculations for predicting the pressure-distance curve and scaling are shown in Tables 3-1 and 3-2, together with the equations used. They are the expressions derived in the preceding sections 3.2, 3.3 and 3.4.

In the tables, strong shock calculations are separated from those for weak shock. In each case a pressure is chosen (Col.1) and the corresponding waste heat Q calculated in two (or three) columns. From the previous section we have

R_c = Transition Radius--146 meters

Q_c = Transition waste heat--.096 bars

After the column headed Q are two columns which give the values of

$$\frac{R_{calc}}{R_c} = \left(\frac{Q_c}{Q}\right)^{1/q} = \left(\frac{.096}{Q}\right)^{1/q} \quad \text{or}$$

R calc follows directly; the formulas are again shown on the table.

For scaling, the scaled yield is simply

$$\frac{Y_{observed}}{Y_{calc}} = \left(\frac{R_{Meas}}{R_{calc}}\right)^3$$

from standard scaling procedure; it is shown in the last column.

The average relative yield from scaling was determined separately in the high pressure region giving Y = (1.) and low pressure region Y = (1.03).

The individual values of scaled yield and the overall average (1.015) are so close to 1.0 that any prognostication for differences as likely to be meaningless. The maximum excursion, .94 relative yield

at P = 100, means less than 2% in distance; it is the width of a major line on ordinary log-log paper. This rather excellent correlation is particularly satisfying because these data were compiled 15 years before the present calculation was done, 10 years before QZ^q = constant was realized.

Table 3-1

Hand Calculation for Prediction and Direct Scaling

Strong Shock

$$QR^{3.5} = .36 \times 10^{7} \qquad R_{calc} = 146\left(\frac{.096}{Q}\right)^{1/3.5}$$

$$Q = 10^{\frac{(L-22)(6-1)}{16}} \quad \text{where } L = \log_{10} P$$

Pressure P	$\log_{10} P$ L	Waste Heat Q	Q/.096	$(Q/.096)^{1/3.5}$	Shock Radius R_{cal}	Shock Radius R_{meas}	Scaled Yield $(R_c/R_m)^3$
3		.19	1.98	1.216	120.5	122.5	1.06
10	1	1	10.4	1.95	75.0	75.6	1.03
100	2	17.7	184	4.45	33.0	32.3	.94
1000	3	235	2450	9.30	15.7	15.5	.97
10000	4	2400	25000	18.0	8.1	8.1	1.00
						Average	1.00

Table 3-1 (Cont'd)

Weak Shock

$QR^4 = .446 \times 10^8$ $\qquad R_{calc} = 146 \left(\cdot\frac{096}{Q}\right)^{1/4}$

$$Q = 2.5 \left[\frac{(1+P)^{1/k}}{D} - 1\right] \cong \frac{K+1}{12} \left(\frac{P}{K}\right)^3 (1-1.5P)$$

Pressure P	Density D	$(1+P)^{1/k}$	Waste Heat Q	(.096/Q)	$(.096/Q)^{1/4}$	Shock Radius R_{calc}	Shock Radius R_{meas}	Scaled Yield $(R_c/R_m)^3$
2	2.111	2.192	.096	1	1	146	146.8	1.02
1	1.625	1.64	.0231	4.15	1.43	209	206	1.05
.5	1.3333	1.3363	.00562	17.1	2.04	298	301	1.03
.1			$.062 \times 10^{-3}$	1550	6.25	913	905	1.03
							Average	1.03

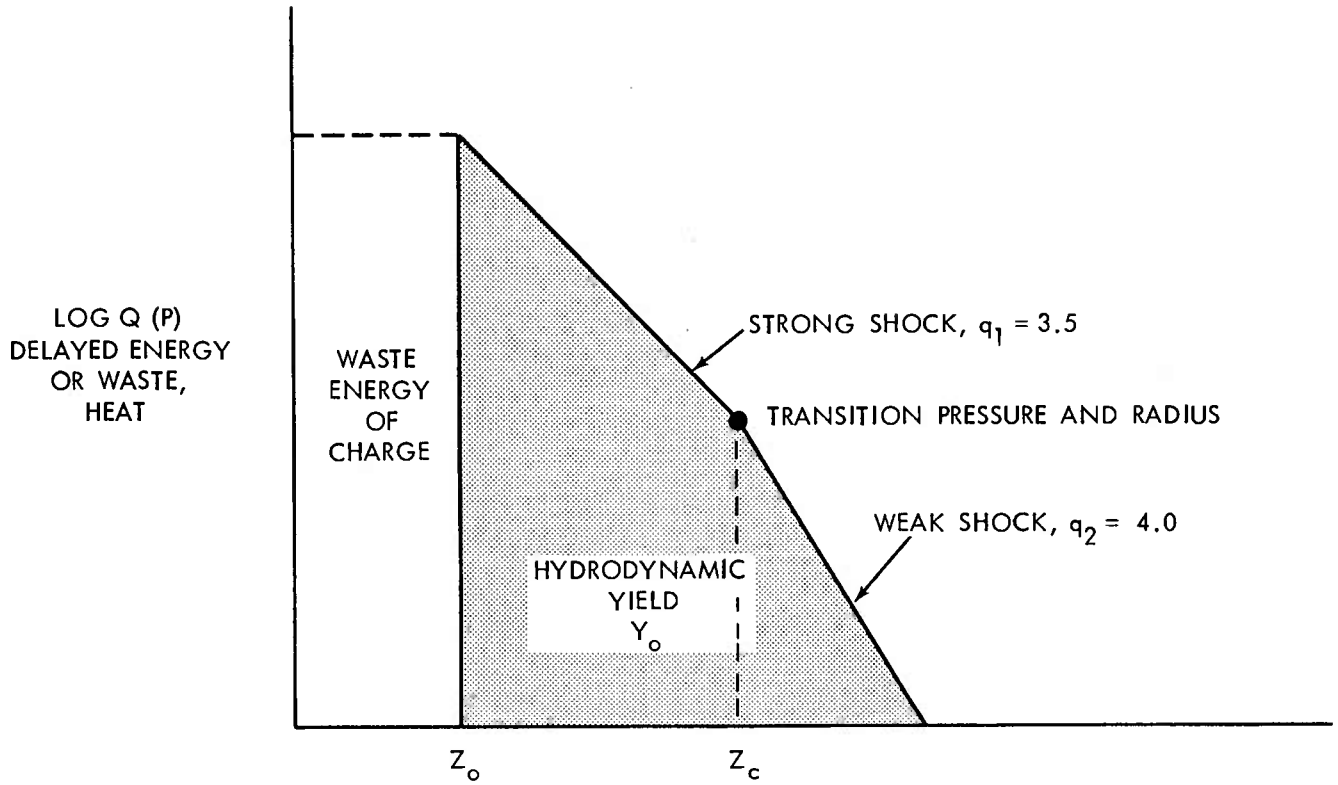


FIG. 3-1 PEAK PRESSURE - DISTANCE PREDICTION, $Q\ Z^q$ = CONSTANT METHOD.

$$Y_o = 4\pi \int_{Z_o}^{Z_c} Q\ Z^2\ dZ + 4\pi \int_{Z_c}^{\infty} Q\ Z^2\ dZ$$

$$Z \equiv (M+R^3)^{1/3}$$

4. Direct Scaling of Blast Energy DSC

4.1 Foreword

In this chapter we describe a specific machine program DSC506 for scaling the hydrodynamic yield of an explosion. At each pressure level, a direct comparison is made of the measured distance with the distance calculated for an idealized explosion of a specified energy release, charge radius, specific heat and other parameters. The procedure is essentially as was done by hand calculation in Chapter 3 for a point source explosion, excepting that DSC506 includes the mass effect of the explosive.

The chapter is organized as follows:

4.2 Concept for direct scaling of blast
4.3 DSC506 BASIC Program
4.4 Input Data
4.5 Input Parameters and Options
4.6 Subroutine for Calculating Initial Pressure
4.7 Subroutine for Calculating the Transition Radius
4.8 Scaling Procedure
4.9 Estimate for Total Yield

Like the corresponding sections of Chapter 2 for the DEB method, this chapter gives a detailed exposition of the DSC method including variations.

Chapter 5 follows with direct illustrations of both methods. The quickest way to see how each method is used is to refer to the input instructions shown in

Table 5.2-1 for nuclear data and DEB506

Table 5.3-1 for HE data and DEB506

Table 5.4-1 for nuclear data and DSC506

Table 5.5-1 for HE data and DSC506

4.2 Concept for Prediction and Direct Scaling of Blasts

As described in the previous chapter, we assume that the waste heat Q versus distance Z can be described in two branches:

$$\text{strong shock:} \quad Q = Q_c \left(\frac{Z_c}{Z}\right)^{q_1} \qquad 4.2\text{-}1$$

$$\text{weak shock:} \quad Q = Q_c \left(\frac{Z_c}{Z}\right)^{q_2}$$

where

Q = waste heat, energy per unit volume of unshocked air

Q_c = waste heat at transition pressure

Z = $(R^3 + M \cdot H)^{1/3}$, the mass-corrected shock radius

Z_c = transition radius Z

q_1 = strong shock exponent ($\cong 3.5$)

q_2 = weak shock exponent ($\cong 4.0$)

For the purposes of calculation, the value of the waste heat Q_c at the transition pressure and the two exponents q_1 and q_2 are assumed values, but are of course chosen on the basis of theoretical considerations and experience.

Again, as in Chapter 3 these assumptions are sufficient to define a hydrodynamic energy Y_o according to

$$Y_o = 4\pi \int_{Z_o}^{Z_c} QZ^2 dZ + 4\pi \int_{Z_c}^{\infty} QZ^2 dZ \qquad 4.2\text{-}2$$

in which we solve for the transition radius Z_c by iteration. At each measured pressure P we calculate Q and then use the relations 4.2-1 to solve for the measured value of Z.

The relative yield is then obtained by direct scaling:

$$\text{Relative yield} = \left(\frac{Z_{\text{measured}}}{Z_{\text{calculated}}} \right)^3 \qquad 4.2\text{-}3$$

By contrast with DEB, which was a maximum-data, minimum-theory method, DSC is a minimum-data, maximum-theory method. We say "maximum theory" because, as just shown, a theoretical curve is calculated before making any comparisons with data.

We say "minimum data" because a single point is in principle sufficient for making an estimate of yield by a comparison with the theoretical radius at the same pressure level. In fact, each point in the DSC method is treated separately from all other points and each measurement is weighted equally in determining Y_o as their average value.

"Maximum theory" means also the DSC procedure may be used entirely for prediction. The calculational device for doing so is discussed later in section 4.4 under "Input Data." (It is simple: If we wish to predict a distance for a given pressure without a corresponding measurement, insert the number "0" in place of the measured distance.)

DSC differs significantly from DEB by the way in which the separate data points are weighted in evaluating the yield. This is described in Figure 4.2-1. In DEB, the measured points are used to define the curve as shown by the circles on Figure 4.2-1. As a consequence, a cluster of data points may serve to define the curve exactly at that region but affects only a relatively small region of growth of the shock. But an isolated point, as shown on the figure,

may distort a large region of the curve and correspondingly affect the calculated value of the yield Y_o. In DSC each measured pressure point is weighted equally; the clustered points count proportionally more than the isolated point.

Normally, there should be no significant difference between the values of the yield so obtained by either method. DEB is more correct in principle because Y_o depends on the shape of the curve. But DSC is more correct in practice, because each measured point is weighted equally. On the whole, DSC is probably less biased on actually measured data. DEB is probably less biased when making comparisons with another measured curve since in the latter case it is possible to choose an erroneous clustering of points which could impair the DSC method. However, with moderate care, it is easy to choose a balanced distribution of pressures for comparisons, such as shock strengths 1, 2, 5, 10, 20, 50, etc., which will usually result in a consistent yield with either method.

Many of the features of DEB apply to DSC. For example, the QZQ concept permits us to perform the integration in bold steps, requiring a relatively few number of measured pressures.

Optimum propagation concepts used both in DEB and DSC--such as MEZ (mass effect), GAB (Generalized Afterburning), GWH (Generalized Waste Heat)--which are "assumptions for convenience " in DEB are intrinsic to the DSC method.

DSC provides options in fixing the theoretical curve:

QZQ by varying P_c, q_1, q_2

MEZ by varying H

GAB by varying q_1

GWH by varying q_2, q_1

These options will be discussed in Section 4.5. The salient point is that DSC provides a comparison not only with the "ideal" explosion, in which

$$H \cong .25$$

$$q_1 = 3.5$$

$$q_2 = 4.0$$

$$P_c \cong 3.78$$

but is also a means of finding a best fit to the measured curve by varying these parameters. Thus DSC is also a way of describing a non-ideal explosive, and how much it differs from an ideal one. Similarly, it gives a quantitative description of the effects of real surfaces and real atmospheres on the propagation of the explosion.

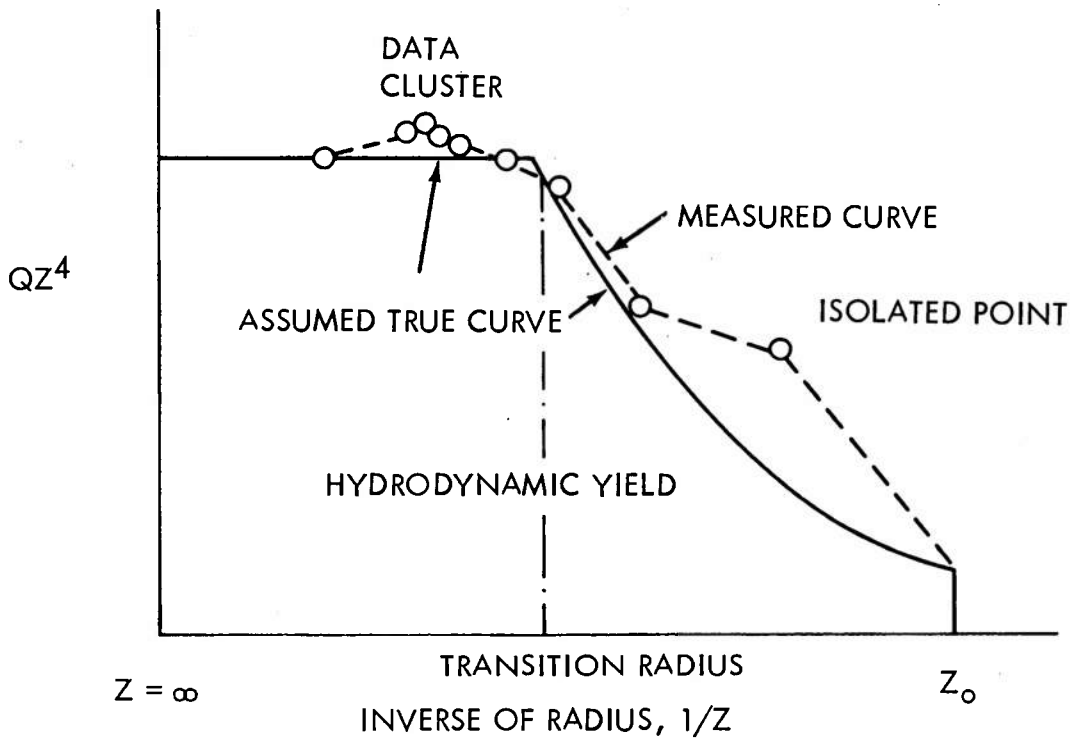


FIG. 4.2-1 COMPARISON OF WEIGHTING DATA IN DEB AND DSC

The ordinate is shown here as QZ^4 because the yield

$$Y_o = 4 \int_{Z_o}^{\infty} QZ^2 dZ$$

is equivalent to

$$Y_o = 4 \int_{0}^{1/Z_o} (QZ^4)\ d(\frac{1}{Z})$$

In DEB, the data are used to define the curve; clustering has no significant effect, but an isolated point can distort a large region of the curve. In DSC each measured point is weighted equally; the cluster counts more than the isolated point, in direct proportion to their numbers.

4.3 The DSC506 BASIC Program

The same purposes are served by DSC506 for the direct scaling method as was served by DEB506 for the direct evaluation method: complete, succinct instructions, step-by-step procedure, convenient and accurate print-out; in short, an objective evaluation.

The tables to which we will refer in describing the program are:

Table 4-1 LIST FOR DSC506

Table 4-2 PRINTOUT OF DSC506

Table 4-3 NOMENCLATURE FOR DSC506

The main logical steps in the DSC506 program are:

1. Calculate a theoretical curve for given input conditions such as yield, ambient pressure, etc.

2. Read the input data, which describe the shock growth by a pair of numbers, and transform each pair to an overpressure ratio and distance in metric units.

3. Calculate the theoretical radius at each measured overpressure.

4. Compare the measured distance X with the theoretical distance R, and scale the apparent yield by the ratio $(X/R)^3$. With a mass effect present, the corresponding values of measured Z and calculated Z are compared.

5. Summarize the results by computing an average yield and standard deviation.

These are essentially the same steps as were performed in Chapter 3 by hand calculation.

In addition to these main steps, DSC506 provides the following options:

1. Accommodate a massive explosion by means of the mass effect concept MEZ, varying M and H.

2. Vary q_1 and q_2 to accommodate a host of non-scaling effects both close-in and far-out.

3. Vary the specific energy H, to account for the different physical properties of explosive debris relative to air, and to calculate the corresponding initial pressure at the charge surface.

4. Provide options to specify an initial pressure P1 at the charge surface and calculate H, or to specify both P and H and calculate the mass M.

5. Vary the transition pressure P2, which separates strong from weak blast propagation.

Sequentially, the DSC506 may be described in blocks of line numbers as follows. We refer to Table 4-1, which is the program LIST.

Lines

100-110 Titles the program and data

111-120 General instructions for input parameters

140-240 Input parameters

240-278 Prints input parameters and the parameters for corresponding theoretical curve Q vs Z, all as the table heading of the printout.

280-294 Calculates pressure P1, at initial radius (if P1 is not specified)

296-469 Data are read in, and transformed to an overpressure ratio (relative to ambient pressure) and to a distance in metric units.

Lines

470-695 Calculate the theoretical radius at each pressure level, scale, and tabulate the apparent yield.

700-750 Subroutine to calculate H, for a given initial pressure P1.

760-880 Subroutine to calculate waste heat Q for real air (or another ideal gas) from an input pressure P

900-990 Subroutine to calculate the theoretical curve from given input parameters Q1, Q2, and P2

998-1899 Data statements are essentially pressure P vs distance X, but may be any pair from which P and X may be derived analytically

1900-2000 Summary and termination of the program

We have tried to make the LIST (Table 4-1) self-explanatory. Table 4-3 gives the nomenclature for additional reference. Throughout the LIST, additional remarks are made, shown by a line number followed by "REM"- for example:

```
540 REM ... TO REJECT DATA, APPLY CONDITION LIKE 550
                BEFORE LINE 620
```

Such cryptic remarks may not be clear on first reading, but hopefully, after an exposition in this chapter, the brief instruction is probably more desirable than repeating a lengthy discussion each time the run is used.

Whenever it is run, DSC first prints out the heading shown at the tope of the PRINTOUT, Table 4-2, as instructed in line 100 of the LIST, Table 4-1. Following the remark made in line 111, the data are identified in line 110 by the instruction thus:

```
110 PRINT "Title of data etc."
```

in one line. If more than one line is needed for the title, begin at an earlier line, say 109; otherwise, the new line 111 will erase the present remark in line 111. Be sure to include a new line 110 as part of the new title; otherwise, the old title will continue to be printed out, if not superseded.

We turn now to the detailed instruction for input data and parameters.

4.4 Input Data and Transformations

Raw input data describing the shock growth are input to DSC506, in pairs of numbers; an intensive variable first, like pressure; an extensive variable second, like distance. The remarks shown in lines 998 and 999 summarize the requirements:

```
998   REM...INPUT DATA:  ANY UNITS, SEQUENCE OR FORM IN LINES
            1000-1899
999   REM...PRESSURE OR OTHER INTENSITY VARIABLE FIRST, THEN
            DISTANCE
```

Subsequently, these data are read into the program beginning at line 300. Lines 296-299 summarize the necessary conversions by which the input data in lines 1000-1899 are converted to units which are used in the calculation.

```
296   REM...DATA READ IN AND TRANSFORMED, LINES 300-469.
297   REM...CONVERT TO O'PRESSURE AND DISTANCE IF OTHER
            VARIABLES READ IN
298   REM...CONVERT P TO RATIO:  MEAS.O'P/AMBIENT, SAME UNITS,
            LINE 320
299   REM...CONVERT DISTANCE TO CM ( Y=KG) OR METERS (Y=KT),
            LINE 330
```

As with DEB, data may be input anywhere in the program using the format:

```
LINE NUMBER
    1000    DATA  number, number, number, etc.
```

The computer will scan the program and read the data in the order as they appear in the LIST, interpreting the first number as the equivalent of a pressure; the second, as the corresponding distance; the

third and fourth numbers as another pressure and distance, and so forth. However, the DSC506 intends that lines 1000-1899 are reserved for the purpose of inputting raw data. Wherever put, data formats are as shown, a line number followed by the word "DATA' followed by numbers separated by commas (as in DEB).

As will be discussed later, it is not mandatory that the data be actually input as pressure-distance pairs, although this was the way in which the program was designed. The minimum requirements are that the data define two variables from which the pressure and the distance may be derived. As we shall show later, time of arrival data would be suitable input data for DSC506. For the time being, however, let us assume that the data input are in fact pressure and distance.

Data may input in any units, provided they are later transformed to metric units within the program. Some versatility accrues to DSC506 because the computer does not know the actual units of the data; thus the same set of numbers input to the program may imply many different but corresponding energy releases. The main intent here is that if the input distances are converted to centimeters then the yield implied will be in megacalories (10^6 calories). If the input distances are intended to mean meters, then the resulting yields are given in kilotons (10^{12} calories). Whatever the units, the yield is proportional to the volume of the explosion R^3; it follows that if the distance is increased by a factor of 10, the yield is correspondingly is increased by a factor of 1000.

These relations are summarized for yields from 1 to 10^{21} calories in Table 4.4-4. This table is a generalization of the

tabular headings for Column 2 and 3 of the printout which reads "centimeters or meters" and for the line reading "trial yield" in the heading of the program which reads "megacalories (= kilogram nuclear) or KT".

There is not much practical point in units smaller than the gram nuclear or larger than the megatons nuclear. For energies in the range of a few numbers of calories, where the explosion would be scaled in fractions of a millimeter, the explosion is so small that scaling fails for physical reasons. The "promptest" energy, say in a spark gap, then is as ultraviolet light whose mean free path is no longer small compared with the dimensions of the shock wave--the typical mean free path for radiation in the range from 0 to 2000 angstroms is like 0.01 centimeters. On the other hand, for a hypothetical explosion as large as a gigaton or teraton, where the shock dimensions would be measured in kilometers, the earth's atmosphere would itself be non-uniform and too thin to maintain spherical symmetry; we are then in a domain in which the explosion presumably blows a hole through the atmosphere into the near vacuum of outer space.

A practical reason for using these units for DSC506 is because a megacalorie explosion, whose characteristic dimensions are measured in centimeters, corresponds roughly to 2 or 3 pounds of high explosive. For nuclear explosions the kiloton is universally used as a unit and a meter is a natural unit of measurement. It is fortuitous but highly useful that the natural sizes of these familiar explosions differ by a factor of a million in yield, 10^6 calories as compared with 10^{12}, and the scaling factor of a hundred applies between them, centimeters as compared with meters.

As noted earlier, when the program comes to line 300, it will successively scan whatever numbers appear anywhere in the list and are preceded by the work "DATA." It will interpret the first of each pair as a pressure (or some other intensity equivalent), and the second as a corresponding distance. As noted in lines 296 to 299, these are to be converted to metric units somewhere between lines 300 and 469. This conversion can be as follows: We wish to convert the pressure from whatever units they were initially input into a pressure ratio to ambient. If the data were input as psi (pounds per square inch) and the measurements were made at one bar atmospheric pressure (14.504 lbs per square inch) then we would write

320 LET P = P/14.504.

As in DEB, of course, a wide variety of other procedures may be used to convert the input data to a pressure ratio. For example, one might first convert to bars and then divide by the ambient pressure in bars, if that were given in line 160. The present instruction LET P = P/PO seems most convenient; it is most likely that if the data were measured in psi the ambient pressure would be recorded in the same way.

Distances are converted to the proper metric units in accord with Table 4.4-4 in lines such as is suggested in 330 LET X = x * 30.48. This example converts distances X in feet to centimeters (30.48 centimeters per foot) and the corresponding yields would be output in megacalories or kilogram nuclear equivalent. On the other hand, if distances X in feet are converted to meters, then yield output would be interpreted in kilotons.

In DEB, it was necessary to enter the data pairs in the order of decreasing distance. In DSC, data pairs may be input in any order because DSC first computes a theoretical curve for specific input parameters. At each point, it calculates the theoretical radius for a given pressure level and compares the measured radius directly. This comparison does not depend upon previous measurements as was the case for DEB. Aesthetically, one may wish to input the data for DSC in descending order of pressure because the program starts by printing the pressure at the initial radius. But this is not a stringent requirement. This printout is routed by lines 290 and 294; if we wished to printout the initial pressure at the end of the program, those two lines could be deleted and the machine instructed to printout the initial pressure somewhere around line 1908 as part of the terminal instructions for example:

1908 PRINT P1, "INITIAL PRESSURE," R.

Or that same instruction could be placed at line 986, before 990 RETURN, and P1 would then appear above the column headings "overpressure."

As noted in line 998, the input data may be input in any form; this is provided the peak pressure ratio can be derived from the variables stated. For example, suppose the shock velocity were input in feet per second as measured in air and the ambient sound velocity were 1100 feet per second. To the extent that the ideal gas law applies, it follows that:

$$\frac{U}{C_o} = \sqrt{1 + \frac{6}{7} P} \qquad 4.4\text{-}1$$

$$P = \frac{7}{6}\left[\left(\frac{U}{C_o}\right)^2 - 1\right]$$

The corresponding instruction in 320 would be:

320 LET P = (7/6) * ((P/1100)^2 -1)

More elaborate procedures are of course possible. The time of arrival curve might be input from which the shock velocity might be deduced, and the peak pressure ratio obtained following the procedure just described. In many such cases, however, it will be necessary to input the data in some ordered sequence, unlike the case above in which the intensity variable can be read directly from the data input, independent of the ordering.

Line 1990 reading "DATA 0,0" must never be altered. It is a routing instruction which at line 310 directs the program to terminate. The program will automatically terminate whenever the computer reads a zero pressure.

We turn now to a discussion of input parameters.

Table 4.4-4

Yield and Distance Relations in the Unified Theory of Explosions

$Y \sim R^3$

Distance	Yield	
	Nuclear	Calories
10^{-4} meters	milligram mg	1
millimeter mm	gram g	10^3
centimeter cm	kilogram kg	10^6
decimeter dm	ton T	10^9
meter m	kiloton KT	10^{12}
decameter dkm	megaton MT	10^{15}
hectometer hm	gigaton GT	10^{18}
kilometer km	teraton TT	10^{21}

4.5 Input Parameters and Options

Referring to the nomenclature in Table 4-3 and the LIST in Table 4-1, the following parameters are the minimum required for the DSC program to RUN:

Input Parameters

140 YO Trial Yield, units consistent with input distances

160 PO Ambient pressure, bars

170 K Adiabatic compressibility

180 DO Ambient density, gm/cm^3

190 R Initial radius, cm

210 P2 Transition overpressure, bars .

In addition, the following options are provided:

OPTIONS

200 H Specific energy ratio, bomb parts/medium

or 200 P1 Initial pressure

220 Q1 = dln Q/dln Z, strong shock

230 Q2 = dln Q/dln Z, weak shock

240 M = Mass of explosive and surrounds, Kg or KT, consistent with yield.

As with DEB, the program LIST contains two aids for inputting parameters. The actual line number may be preceded by some relevant remark. Also, all of the input parameters are printed out, and many of the instructions to print that parameter will state what units, if any, were needed for the input. The remarks in lines 111 to 120 refer specifically to the input parameters and options, and these instructions will probably be complete enough for later reference after the exposition in the section.

The first of the input instructions is the trial or reference yield which appears as

140 LET YO = 0.328 .

Referring to the print out in Table 4-2, this number will then be printed out at the top of the print out in line 3 immediately following the title of the data. The units are to be understood as megacalories, kilotons, or whatever unit was chosen appropriate to the distances input as shown in the previous Section 4.4 and Table 4.4-4.

YO can be merely a reference yield with no attempt to find a best fit of the data for yield. If the data are to be compared with 1 lb of TNT for example, then $Y_o = 0.32$, implying 320,000 calories, is appropriate for comparison with 1 lb of TNT because that is the number we find by experience as a yield for TNT. On the other hand, if we are comparing with a 1 KT nuclear explosions then the entry $Y_o = 1$ would be appropriate for such a comparison if we neglect the energy dissipated during the radiative phase.

A subsequent line 161 will correct the value of YO to units used in the calculation (centimeters^3 or meters^3) based on whatever ambient pressure is input in line 160.

When we wish to find a best fit to the data, a new trial yield is usually required and the run should be iterated. Referring to the printout, note that the final line in Table 4-2 suggests what new trial yield to be used. We defer for the moment the meaning of the qualification "when scaling applies"; this value of Y_o should be used for the "new trial yield". The example in Table 4-2 does not require a new yield; it is already close enough to the trial yield.

The ambient pressure in bars is inserted thus:

160 LET PO = 1.

Of course, the ambient pressure is available in any other units; it is just as convenient to let the program make the calculation, for example:

Ambient Pressure	Command
13.5 psi	160 LET PO = 13.5/14.504
0.9 atmosphere	160 LET PO = 0.9 * 1.0133
30 inches of Hg	160 LET PO = 30 * 0.03386

Similar commands may be formulated for any other equivalents or combinations of them.

Adiabatic compressibility of the medium is thusly:

170 LET K = 1.4

and permits DSC to be used for gases other than air. These same qualifications for other gases apply here as was previously discussed for DEB: As listed in Table 4-1, DSC506 contains a subroutine starting at line 760 to calculate the waste heat and this subroutine calculates the non-ideal behavior of air in lines 840 and 850. If the medium is not air, a suitable high pressure correction ought to be inserted in lines 840 and 850, together with a suitable branching point at line 810. If the high pressure form is not known, type "810", followed by a carriage return. This will erase the present line 810 and the program will calculate the waste heat using the ideal gas approximation as in the previous lines 760 to 820 inclusive.

For solids and liquids, the form of waste heat is not far different from those shown. We refer to the discussion in Section 2.7 under DEB.

The ambient density in grams/centimeter^3 is inserted thus

180 LET DO = 0.00129.

The number shown 0.00129, is the cgs value for a standard atmosphere. Similar remarks apply here, as in connection with ambient pressure, that this line is a convenient place to let the program calculate the ambient density if the cgs units are not conveniently available. Ambient density is not a sensitive parameter; it is involved only in the mass effect correction. An error in DO is almost negligible for the purpose of calculating hydrodynamics yield or the far-out pressure-distance curve. The initial pressures, however, will be inversely proportional to DO. For these reasons, an approximate value for DO is quite suitable. For example, if the ambient temperature was $59^{\circ}F = 460 + 59 = 519^{\circ}$ absolute then it would be suitable to use the ideal gas law and write

180 LET DO = 0.00129 * PO * (460/519) .

As with instructions for computing PO, the resulting number will appear in the table headings. We can use the symbol PO in 180 for calculating DO when so desired because the value PO for ambient pressure in bars will already have been inserted in line 160.

Often the sound velocity may be known. If so and because the ambient pressure PO and adiabatic compressibility K are already specified in lines 160 and 170, we may use the relation for an ideal gas

$$C_o^2 = \left(\frac{dP}{dP}\right)_Q = \frac{KP}{D_o}$$

Thus, for example, if the ambient sound velocity were 1100 ft per second, which is 1100 * 30.48 cm/sec, we could write

```
180 LET DO = K * PO/(1100 * 30.48)↑ 2.
```

The initial radius of the explosion, presumed to be the charge radius in centimeters or meters, is inserted thus

```
190 LET R = 4.2
```

We say initial radius, rather than charge radius, because R may be any arbitrary radius at which the calculation is to be started. R may differ from the charge radius in a number of ways: R may be any of the following:

a. Radius of the "isothermal sphere," at the end of radiative phase of a nuclear explosion. A reasonable estimate for such a radius is 4.2 meters on a scaled basis of 1 kiloton. It happens to be about the same as the charge radius of from a comparable high explosive charge (4 cm for 1 pound, at a density 1.69 gm/cm^3).

b. Equivalent spherical radius from a cylindrical or other nonspherical high explosive charge.

c. Radius at which the shock may first be assumed to have fully formed from a highly massive charge or to have approached symmetry from an initially nonspherical charge.

d. Radius at which all the explosive energy may be presumed to be released.

e. Starting radius from the spark gap explosion.

In each of these cases, the estimate as presently written does not include energy dissipated prior to the radius R. The loss in the charge was listed separatly in DEB, mainly because the hydrodynamic yield does not include the waste heat of the charge. It

would be simple to add such a dissipation to the estimate of DSC but because these histories of explosions may differ markedly, it is probably better that these corrections be applied by the user on the basis of individual characteristics.

For massive charges, the specification of an initial radius R is not strictly necessary. This follows directly from the definition of the mass correction

$$Z^3 = R^3 \left[1 + \frac{MH}{\frac{4\pi}{3} D_o R^3}\right] = \left[R^3 + \frac{MH}{\frac{4\pi}{3} D_o}\right]$$

where M is the actual weight of explosive, H is the average specific energy of bomb parts relative to air, a number smaller than but comparable to 1. Because a spherical charge of radius X_o, and density D_1 will weigh

$$M = \frac{4\pi}{3} D_1 X_o^3$$

it follows that near the charge

$$Z_o^3 = R_o^3 + H \frac{D1}{DO} R_o^3 = R_o^3 \left[1 + H \frac{D_1}{D_o}\right]$$

Because $D_1 >> D_o$, like 1,000, the actual starting radius R_o is immaterial since $D_1 X_o^3 = M/(4\pi/3)$ and if

$$Z_o^3 \cong H \frac{D1}{DO} R_o^3$$

then

$$Z^3 \cong \frac{HM}{\frac{4\pi}{3} D_o} = \text{constant}$$

In the calculation we redefine M like an M^*

$$M^* = \frac{M}{\frac{4\pi}{3} DO}$$

so that regardless of the actual charge radius R_o input,

$$ZO = (HM^*)^{1/3}$$

For most chemical explosives $D_1 = 1{,}000\ D_o$ so a negligible error in Y_o would be made even if R = 0 were inserted in line 190.

The mass of explosives and surrounds input thus:

240 LET M = .454

The units involved are shown in 245 for printing out the heading "EXPLOSIVE AND SURROUNDS WEIGHT ".454 KG, KT." This double label means that the actual weight of explosives and surrounds are to be in mass units which are consistent with the energy units. Thus for 1 lb charge of high explosive, .454 Kg, M is input as shown, M = .454. For a 1,000 lb nuclear bomb and distances intended as meters, if such were the case, M = 454 kilograms = .000454 kilotons and we would have written M = .000454.

The question arises what should be included in the mass of surrounds. The intent is to include all material which is either vaporized or severely fractured by the explosive: that is material which initially absorbs kinetic and internal energy of the explosive and later surrenders that energy back to the blast wave. If the fragments are so large or of such nature that they can never surrender any appreciate fraction of their energy back to the blast wave, they should not be included. Whatever energy they carry off is considered part of the waste heat of the explosive charge itself. This division

is not a critical judgment because the late behavior of the explosive is fairly insensitive to the mass of the explosive. As we shall see, the thousand fold change in density from air in a point source explosion (as in a nuclear explosion) to the initial densities of a high explosive makes only a factor of three or so difference in the eventual yield and "efficiency" of the explosion. Since $3 \simeq 1{,}000^{1/6}$, this relation expresses the fact that Y is roughly proportional to $M^{1/6}$. No ambiguity arises here for the case of missiles or bombs; the mass should include the entire mass of the weapon.

Although the far out performance is insensitive to the mass, the close-in pressure is inversely proportional to mass. Thus the mass may be diagnosed from the close-in behavior of the explosion itself. In other words, we can choose a value of M such that a desired initial pressure is obtained holding yield constant.

4.6 Input Options

A number of options are provided in the input parameters for DSC506. They are primarily for the purposes of diagnostics. The value of each of these options is reasonably well known for ideal explosions. But there are many cases in which the data themselves may be used to provide a different estimate of the parameter than may be expected a priori. Among these options are:

200 H, specific energy ratio, bomb parts/medium, or

200 P1, initial overpressure, bars

210 P2, transition overpressure, bars

220 Q1, dln Q/dln Z, strong shock

230 Q2, dln Q/dln Z, weak shock

Line 200 actually provides a three way option among the initial pressure P1 of the explosion, the average value H of specific energy of bomb parts relative to the air engulfed, and the mass of explosive M. If the initial pressure P1 at the charge surface or other initial radius is known, say 150 bars, we may prescribe

200 LET P1 = 150.

The program will then calculate the corresponding value of H, and the result will appear in the heading as "SPECIFIC ENERGY, BOMB/MEDIUM H=." If the specific energy H is known and input

200 LET H = .50

this input information will again be printed out in the title, and the program will calculate initial pressure, which then will appear in the print-out as the first line under "OVERPRESSURE" and "CALCULATED RADIUS." If neither H nor P1 is specified in line 200 then the program will retain the value H = .25 as previously instructed in line

195; the point in the apparent replication is, that if a different value H is later specified in line 200 it will override line 195.

The third option: If we have let M = 0 in line 240, but have specified an initial pressure in 200, the program will retain H = .25, calculate the mass and print out the result as "INERTIAL MASS ENERGY M=." It means the explosion behaves "as if the mass were" the value shown. The distinction is made between inertial mass-energy and actual weight of explosive because it may be possible to suppress the initial peak pressure of an explosion in many ways without dissipating the energy permanently as waste test; a "fatter" wave form, meaning one whose pressure rises behind the shock due to non-instantaneous energy release, is an example. Such a wave form cannot achieve its ideal shape--highly peaked near the front, decaying rapidly toward the interior--in an instant; inertial mass is a way of letting it approach the ideal case gradually, inversely to blast volume.

Let us note also that H is used as a constant in DSC506 not necessarily for want of detailed information but mostly as a considered choice between simplicity and detail. It is a splendid example of Occam's Razor. Referring to the discussion of the ASH concept for average specific heat in Chapter 1, recall that the explosive and surrounds may consist of vapor, smoke, fines, or coarse material. These represent a progression from vapor which is in both thermal and mechanical equilibrium with the surrounding air, to coarse particles which produce jets but are in neither thermalnor mechanical equilibrium with air. Each of these contributes differently, depending upon whether they contribute to the kinetic energy, to thermal and mechanical energy, or to both. One expects and can calculate a difference

between the behavior of vapor and smoke, each of which are in thermal equilibrium with the surrounding air. In a point source explosion, the internal energy represents about 90% of the energy of the blast, the kinetic energy about 10%. This too affects the value of H. Little is presently known of the detailed partition for most explosives.

It is relatively straightforward to provide for such variations in H in the DSC program and such variations of DEB and DSC have been used. But we previously saw that the result of yields are quite insensitive to the value of M and because MH always appears as a product in DSC506, it is clear that results are also insensitive to H. We use H = constant for four reasons:

a. Results are insensitive to numerical value of H ($Y \sim H^{1/6}$).

b. The actual numerical values are not known for the near-infinite spectrum of explosive products.

c. Accuracy, it probably being more accurate to integrate the equation for yield exactly using a constant value of H, than to involve some approximate integral with a variable value of H.

d. It is probably simpler to adjust H as a diagnostic than to out-guess the a priori numerical value .25.

The transition pressure P2 specified at line 210 marks the change from strong to weak shocks. Recalling the discussion in Chapter 1, a number of profound changes occur at shock overpressures ratios P, between 4 times ambient and ambient among which are:

1. Transition from supersonic to subsonic flow just behind the shock front:

$$u > c \text{ for } P/P_o > 3.82, \text{ strong shock}$$

$$u < c \text{ for } P/P_o < 3.82, \text{ weak shock}$$

2. Negative phase develops; more precisely, there exists an r such that

$$u(r) + c(r) > U(R) \text{ for } P > P2$$

$$u(r) + c(r) < U(R) \text{ for } P < P2$$

3. The available energy is $Y(R) \sim 1/R^{1/2}$ and ambient energy of air engulfed is $E_o \sim R^3$ so that this ratio

$$\frac{Y(R)}{E_o} \sim \frac{1}{R^{3.5}}$$

rapidly passes from $Y(R) >> E_o$ at strong shock strengths and small radii to $Y(R) << E_o$ at weak shock strengths and larger radii. In other words, the energy of the blast passes rapidly from swamping out the surrounding air, to being lost in an ocean of surrounding air.

4. The ratio of internal energy E_i change to total shock energy E_t is

$$\frac{E_i - E_o}{E_t - E_o} = \frac{\frac{1}{2}(P_{abs} + P_o)(V_o - V)}{P_{abs}\,(V_o - V)} = \frac{1 + P/2}{1 + P}$$

which rapidly passes from the fraction

$$\frac{(E_i - E_o)}{E_t - E_o} = \begin{cases} 1/2 \text{ for strong shocks} \\ 1 \text{ for weak shocks} \end{cases}$$

All affect P2, and each of the above causes is not necessarily independent. That is, the negative phase probably develops(2, above) mainly because the material velocity does become small compared with sound velocity (1, above). If all explosions scaled perfectly, P2 might be a constant pressure and for an instantaneous energy release, as from a nuclear explosion, the transition P2 does seem to occur around the theoretical pressure ratio of 3.82 bars which marks the

transition from supersonic flow just behind the shock at high pressures to subsonic flow for low pressures.

These phenomena are further complicated in HE explosions by afterburning within the blast wave which perforce "fattens" the interior wave form and thus increases the local sound velocity on the interior of the wave somewhat above what it would have been for an instantaneous energy release. As a consequence, the fireball region can continue to support the leading parts of the blast wave. The positive duration lengthens, the negative phase is somewhat delayed, and the peak pressure is supported longer than it would have been for an ideal explosion. Another possibility is that in the vicinity of a ground surface the shock velocity itself may be somewhat slowed down due to surface roughness or viscosity at the front, permitting signals from the interior to reach the front which might not have reached it had the shock front been running at full speed. Both decrease P2.

For these and other reasons, the option is provided in line 210 for an arbitrary pressure P2. Again, however, the principal value of this option is a diagnostic because the value P2 may be altered or adjusted to fit the data, telling us much about the phenomenology. But the final yields are virtually insensitive to the choice of P2; any value between 1 and 4 is probably reasonably acceptable for determining yield.

Options are also provided for the decay constant Q1 and Q2 of waste heat with distance in lines 220 and 230. The standard values are already input:

```
220 LET Q1 = 3.5
230 LET Q2 = 4.0
```

these being the values for strong shocks and weak shocks respectively.

For predictions, or in the absence of better information, the standard values should be used. To say that explosions scale is to say that Q1 and Q2 are reproducible. But explosions do not scale, for the nearly 30 effects cited in Table 1-2 of Chapter 1 on modes of energy transport. There is no a priori reason to suppose that for all explosions all the energy released is released either instantaneously or on a short enough time-scale to be compatible with hydrodynamic scaling. For these reasons we need a simplified descriptor, and provide for a variation in Q1. Similarly, during the weak shock phase, many surface effects and other losses can occur to the shock wave; some value of Q2 larger than 4 is an adequate way to describe those losses.

Whatever the physical reasons, the variations in Q1 and Q2 are a convenient way to fit a set of measured data by an explicit number. The resulting values of Q1 and Q2 thereby furnish useful diagnostic information to describe the wave which is much more meaningful than other possible ways of fitting the data, such as a terminated Laurent series or an arbitrary power-law for the pressure-distance curve.

This completes the list of necessary input parameters and options to DSC506. If these and the input data have been properly entered, we are then in the position to run the program which is accomplished simply by typing the statement "RUN".

Other options are provided such as rejecting unwanted data. These options are more conveniently considered in the discussion which follows concerning the operation of the program itself.

4.7 Subroutines

Referring to the list in Table 4-1 and to the printout in Table 4-2, by this time we have reached line 245 which instructs the program to printout the weight of explosives and surrounds. This appears on the 6th line in the heading for DSC506 printout in Table 4-2.

At line 250 a branch point occurs in the calculation, depending upon whether the initial pressure P1 has been specified or whether the specific energy has been specified in line 200. If H has been specified, then P1 = 0 and the program goes to 260, prints out the value of H, calculates the working values of M (262) and Z0 (266) for the mass effect corrections. It then goes to line 900, a subroutine for calculating the transition radius and parameters.

The subroutine at line 900 for calculating the transition radius follows the method of hand calculations discussed in Chapter 3. Lines 901 to 955 are an iterative solution of the energy relation

$$Y_o = 4\pi\, QZ_o^3 \left[\frac{(Z_c/Z_o)^{q_1}}{q_1 - 3} - \frac{(q_2 - q_1)(Z_c/Z_o)^3}{(q_2 - 3)(q_1 - 3)} \right] \qquad 4.7\text{-}1$$

Because Q is in bars and Y_o in calories $= \frac{4}{3}\pi\ 10\ \frac{\text{bar cm}^3}{\text{cal}}$, we then define temporarily a dimensionless number A

$$A = \frac{Y_o}{0.3\ QZ_o^3} = \frac{V^{q_1}}{q_1 - 3} - BV^3 \qquad 4.7\text{-}2$$

where $V = Z_c/Z_o$, and $B = (q_2 - q_1)/((q_2 - 3)(q_1 - 3))$. These definitions for A and B appear in lines 901 and 910. Line 920 is merely an appropriate trial value for V. The quantity T in line 930 is a trial

value for the right side of equation 4.7-2; in line 940 T is compared with A until it agrees within .01%, as tested in line 940. The quantity V1 in line 945 is an increment based on the first derivative of equation 4.7-2 using a correction of the form

$$V1 = \Delta V = \frac{dV}{dY_o} \Delta Y_o$$

$$V1 = \frac{(A - T)}{\frac{dY_o}{dV}}$$

$$V1 = \frac{(A - T)}{\frac{q_1 V^{q_1 - 1}}{q_1 - 3} - 3BV^2}$$

When the iteration has been accomplished to the desired degree of accuracy the program redefines A and B in lines 960 and 970 as the constants:

$$A = Q_c Z_c^{q_1} \qquad 4.7\text{-}3$$

$$B = Q_c Z_c^{q_2} \qquad 4.7\text{-}4$$

where $Z_c = V Z_o$ at the successful value of V. As instructed in lines 980 and 985 these relations are printed out at the top of the printout including the values for q_1, q_2, the transition pressure P2, transition waste heat Q_c, and the transition radius Z_c.

The program then returns to line 268 and as instructed in 270, 271, and 275 prints out the column headings "overpressure etc." shown

in Table 4-2. Note that 270 ends in a semi-colon and the present instruction in line 271 is simply to print a blank. The point in printing a blank is to give the user the option of printing an additional column heading if he so desires in column 5 of the printout. If we wish to printout waste heat in column 5 for example, the instruction would be 271 PRINT "WASTE HEAT." The corresponding PRINT instruction in 690 would also be modified to add Q.

If the initial pressure P1 was not specified in line 200, then the pressure at the initial radius is calculated in a subroutine, lines 280 through 290. As previously noted in the discussion for DEB, the waste heat Q for nonideal air is described by a high pressure approximation of the form

$$Q = 10^{(22 - L)(L - 1)/16} \qquad 4.7\text{-}5$$

where $L = \log_{10} P$.

This equality appears in lines 840 and 850. In the present subroutine for calculating the initial pressure, line 281 first calculates the waste heat Q at the initial radius Z_o and the following two lines, 283 and 285, are the inverse of equation 4.7-5, for solving P1 given Q. The result is stored as P1 in line 287 and later printed out under the proper column headings for P and R in line 670.

So much if initial pressure had not been specified at the branch point line 250.

If the initial pressure P1 is already specified at line 250, the corresponding value of H is calculated out in the subroutine 700-750. In that case, the initial waste heat Q calculated for pressure P1 will already have been calculated and stored as Q0 by lines

204, 206, and 208. The initial value of V, required in 4.7-2, is therefore known and specified by line 710. Z in line 720 is defined as

$$Z3 = Z_o^3$$

and we recognize that line 720 is the inverse of equation 4.7-2. 725 and 730 are inversions of the definitions.

$$M_1 = \frac{1000\ M}{\frac{4\pi}{3}\ DO}$$

$$Z_o = (R_o^3 + M_1 H_1)^{1/3}$$

whence, in 738,

$$H = \frac{Z_o^3 - R_o^3}{M_1}$$

Having calculated (and stored) H, at 750 the program returns to 253, and then to 960. Since V is already known, the iteration to solve for it (900-955) is by-passed; at 960 the program calculates the constants A and B as previously described by equations 4.7-3 and 4.7-4. The transition pressure, waste heat radius, constants A and B, etc., are again printed out. But H is now a derived variable which appropriately will appear afterward, and is printed out by 260.

The column headings are printed out (270-275). In case P1 is already known there is no need to calculate the pressure at the initial radius and as shown at line 278 the program jumps to line 292 and 294, and then to 670, where it prints out the initial values of pressure and radius in the proper columns, as instructed in line 670.

For completeness we note that line 760 through 850 are a subroutine for calculating the waste heat. This is identical to the subroutine used previously and discussed under the DEB method.

The program is now ready to read and record data.

4.8 Measured Data, Theoretical Curve, and Scaling

Data are read into the program in pairs of numbers at lines 300; the first number is typically interpreted as a pressure, the second as a measured distance. In whatever form the data may have been entered, subsequent transformations of the data between lines 300 and 469 are used when required to translate them to an overpressure ratio and to a distance in appropriate metric units.

The purpose of line 310 (if P=0) is to alert the program to summarize the data after all the input data have been read. This is accomplished by providing the data point 1990 DATA 0,0.

The transformations shown in lines 320 and 330 of the illustrative LIST in Table 4-1 are for the case of pressures already input in bars, distances in feet, and interpreting the yield in megacalories.

As presently written, line 470 makes the program by-pass an attempt to "scale" any measured points in which the pressure exceeds the calculated initial pressure. That is, no provision is made for the possibility of a peak pressure curve which increases with distance close to the charge. Such a case is probably possible for a particular kind of energy release, perhaps one slow enough. When such a high pressure is read, the program does print it out, but notes as shown in line 480, that the point is not scalable and goes on to the next measured pressure.

Such a non-scalable measured pressure can be made scalable by raising the initial pressure in any of several ways:

1. State the same or higher pressure in line 200
2. Lower H in 200
3. Lower M in 240.

As one expects from the remark in line 499, lines 505 to 620 are the heart of the DSC program. The theoretical shock radius is calculated in 530, measured data are scaled in 620 to the theoretical predictions and the resulting apparent yield printed-out in line 690.

The theoretical radius is always calculated using

$$\text{Const} = A,\ q = Q_1 \text{ for } P > P_2$$

$$\text{Const} = B,\ q = Q_2 \text{ for } P < P_2$$

in the expression $$Z = \left(\frac{\text{const}}{Q}\right)^{1/q} \qquad 4.8\text{-}1$$

This is also the pressure-distance predictor for DSC506 using whatever values for the input constants A and B, Q_1 and Q_2 as shown for the pressure levels above or below the assumed transition pressure P2. Equation 4.8-1 is also the theoretical value of Z used for scaling. The radius R corresponding to that value of Z is calculated in line 530 and will be printed out as the theoretical radius in Column 3. Note, however, that Z, not R, is the value which enters in to the scaling in line 620, which is equivalent to the statement

$$Y1 = \frac{\text{apparent yield}}{Y_o} = \left(\frac{Z_{\text{measured}}}{Z_{\text{calculated}}}\right)^3 = \frac{M + X^3}{M + R^3} \qquad 4.8\text{-}2$$

Because Y1 is normalized to Y_o, it is also a direct measure of the variance, stated as a fraction.

Before explaining the remark about rejecting data in line 540, let us note that line 630 stores a running total Y2 of the relative yields Y1; this is the sum from which the mean value of yield will eventually be determined. Line 640 counts how many data points have actually been used for the running total Y2.

Line 650 is the running sums of the variances Y1 of the data according to the well known formula for σ^2

$$\sigma^2 = \sum \frac{(Y_i - \bar{Y})^2}{I}$$

$$= \frac{1}{I} \sum Y_i^2 - \frac{2}{I} \bar{Y} \sum Y_i + \frac{I\bar{Y}^2}{I}$$

$$= \frac{1}{I} \sum Y_1^2 - \frac{2}{I} \bar{Y} I\bar{Y} + \bar{Y}^2$$

$$\sigma^2 = \frac{1}{I} \sum Y_i^2 - \bar{Y}^2 \qquad 4.8\text{-}3$$

The variance σ^2 is S1 in line 1903 and in the printout for standard deviation in line 1910. Note that the running sum, $S = \sum Y1^2$ is carried along by line 650 as the calculation proceeds. A powerful advantage of this familiar transformation is seen here: we are able to calculate the variance as in 4.8-3 without knowing the mean $\bar{Y}$, i.e., until we reach line 1910.

Most of the printout instruction in line 690 is obvious. The relative yields Y1 are then rounded off to two decimal places, partly for clarity and partly because there is no meaning to yields more precise than 1%--it would correspond to a discrepancy between measured and calculated pressure of only .3%.

As previously noted in line 540, data may be excluded from the weighting of average yield by applying a condition like 550 anywhere before line 620. This option 550 for by-passing scaling serves several purposes:

1. To make pressure-distance predictions at pressures where no measured data are available.
2. To reject data believed to be erroneous; the point is not counted.
3. To select special regions for weighting.

For example, to predict the curve for selected pressures 100, 50, 20, 10, 5, 2, 1, 5, 2, 1, write the input data as

1000 DATA 100, 0 50, 0, 20, 0, 10, 0, etc., then write 550 just as it appears in the present LIST

550 if X = 0 THEN 670.

To select only data inside the range 10-1 bar for weighting the averages, one could write

550 IF P > 10 then 670

551 IF P < 1 then 670

To reject a specific point, say P = 15.267, write

550 IF P = 15.267 then 670.

In each of these cases, the program will print the pressure and corresponding distance in line 670, but will exclude it when calculating the mean yield.

4.9 Summary of Yield

When all the input data have been read, as was instructed in line 300, the program will eventually come to read P = 0 at line 1990. Then, as directed in line 310 the analysis will be summarized by lines 1900 to 1930 inclusive. The summary includes the average yield, the standard deviation, and a new trial yield.

The purpose of line 1900 itself is to by-pass the calculation when using the program for predictions only (I=0) or if only one point is being used for evaluation (I=1). Otherwise, the machine would print a program error "dividing by zero" when it reached either line 1903 (I=0) or 1905 (I-1=0).

The variance of the sample is calculated in line 1903 which is equation 4.8-3. Recall that Y2 is a running total of relative yield so that $\bar{Y}$ = Y2/I gives the average relative yield. 1903 is the actual standard deviation of the sample itself. But it is well known that the standard deviation, as calculated from the mean of a sample, is favored by that particular mean and is a smaller value than the standard variance of infinite population. Line 1905 is a well-established estimate for the variance of a population (S1 on the left side of 1905) based on the variance of the particular sample (S1 on the right side of 1905).

Line 1907 transforms the yield Y0 from bar cm^3 or bar $meter^3$ back to kilograms or kilotons. It is interesting to note that this simple inclusion of P0 in line 1907 is all that is involved in the ambient atmospheric part P_o of the standard Sachs scaling $(\frac{Y}{P_o})^{1/3}$.

The mean yield as printed out according to line 1910 is actually the average yield of the samples counted--and printed out--

in column 4 of the printout. The standard deviation shown in percent is the standard deviation of infinite population, not of the sample itself. If we wished to obtain the standard deviation of the sample, we could by-pass line 1905 by writing

1904 GO TO 1905 (By-pass 1905)

or simply

1905 (Erasing 1905)

For reassurance, the next line of the printout, as instructed in line 1920, states the actual number of samples used in obtaining the mean yield.

The final line in the printout is a "NEW TRIAL YIELD" in the event we wish to obtain the best possible fit for yield to the data. Superficially, one might suppose that the mean yield would be the best new value to insert. Such will be the case for point source explosions and also if the initial pressure has been specified. As a rule, however, scaling applies if and only if the initial energy densities are the same between two explosions, that is, if the ratio Y_o/M is constant. In adjusting for a yield, however, we usually hold M fixed because the mass of the explosive is known; consequently, when a new yield is selected, it does not really scale with the previous trial because now we have a <u>different</u> energy in the <u>same</u> mass of explosive. If the energy is initially increased, the rate of dissipation initially will be higher, more energy will be lost during the early phases, and relatively more energy will be required to produce the farout pressure than simple cube root scaling would inidicate. Of course, Y2/I in line 1930 is the mean relative yield and if it were not for the mass effect, mean yield would be the proper new value to try. That is,

$$\text{New Y1} = \text{Old YO} \left(\frac{Y_2}{I}\right)^{1.0}$$

The extra .28 shown in the exponent 1.28 at the end of line 1930, is a semi-empirical correction which expresses the extra dissipation of more energetic sources. This exponent varies with energy density but the exponent 1.28 is appropriate for the density of most chemical explosions. As previously mentioned, if the initial pressure P1 was specified, then the mean yield itself is probably a better estimate for a new trial yield. One will find that the calculated value of H or M will increase if Y is increased but P1 held fixed.

TABLE 4-1

LIST FOR DSC506

```
100   PRINT"DIRECT SCALING WITH UNIFIED THEØRY FØR SHØCK GRØWTH"
105   PRINT
110   PRINT"DASA 1559 CØMPILATIØN FØR ØNE PØUND TNT"
111   REM..TITLE DATA IN 110. INPUT DATA, PARAMET RS AND ØPTIØNS THUS:
112   REM.. INPUT DATA LINES 1000-1899. SEE ALSØ 296-299, 998-999
113   REM..LINE 140, TRIAL YIELD YØ.  SEE 150 FØR UNITS
114   REM..160-180 STATE AMBIENT CØNDITIØNS; SEE 185,186 FØR UNITS
115   REM..190,INIT.RADIUS R(CM,M)..210, TRANSITIØN Ø'PRESS. P2(BARS)
116   REM..220, 230: Q1= D LNQ/D LNZ STRØNG SHØCK; Q2 FØR WEAK SHØCK
117   REM..240 M=WEIGHT ØF EXPLØSIVE AND SURRØUNDS, KG ØR KT.SEE 245
118   REM..200 TYPE EITHER INITIAL Ø'PRESS P1 (BARS) ØR H (SEE 260)
119   REM..PRØGRAM USES H=.25 IF NEITHER P1 ØR H IS SPECIFIED (SEE 195)
120   REM..PRØGRAM SØLVES FØR M IF P1 IS GIVEN BUT M=0 IN 240.....
140   LET YØ=.328
150   PRINT"TRIAL YIELD YØ="YØ" MEGACALØRIE (= KG.NUCLEAR) ØR KT"
160   LET PØ=1
161   LET YØ=YØ*1000000/PØ
170   LET K=1.4
180   LET DØ =.00129
185   PRINT"AMBIENT PRESSURE="PØ"BARS  AMBIENT DENSITY ="DØ"GM/CM↑3"
186   PRINT "ADIABATIC CØMPRESSIBILITY EXPØNENT K="K
190   LET R=4
195   LET H=.25
200   LET H=.25
202   IF P1=0 THEN 210
204   LET P=P1
206   GØSUB 760
208   LET QØ=0
210   LET P2=2
212   LET P=P2
215   GØSUB 760
220   LET Q1= 3.5
230   LET Q2=4
240   LET M=.454
245   PRINT "EXPLØSIVE AND SURRØUNDS WEIGH"M"KG,KT"
250   IF P1=0 THEN 260
253   GØSUB 700
256   GØSUB 960
260   PRINT"SPECIFIC ENERGY, BØMB/MEDIUM H="H
262   LET M= 1000*H*M/4.186/DØ
264   IF P1>0 THEN 269
266   LET ZØ= (M+R↑3)↑(1/3)
268   GØSUB 900
269   PRINT
270   PRINT"ØVERPRESSURE","MEAS.RADIUS","CALC.RADIUS","RELATIVE YIELD";
271   PRINT"  "
275   PRINT"(RATIØ)","(CM.ØR M.)","(CM.ØR M.)"
278   IF P1>0 THEN 292
```

TABLE 4-1 (Cont'd)

LIST FOR DSC506

```
280   REM.....CALCULATE PRESSURE AT INITIAL RADIUS.....
281   LET Q=A/Z0↑Q1
283   LET L=.5*(23-SQR(23↑2-4*(22 +16*.4343*LØG(Q))))
285   LET P= EXP(2.303*L)
287   LET P1=P
290   GØTØ 670
292   LET P=P1
294   GØTØ 670
296   REM..DATA READ IN AND TRANSFØRMED, LINES 300-469.
297   REM..CØNVERT TØ Ø'PRESSURE AND DISTANCE IF ØTHER VARIABLES READ IN
298   REM...CØNVERT P TØ RATIØ: MEAS.Ø'P/AMBIENT,SAME UNITS,LINE 320
299   REM...CØNVERT DISTANCE TØ CM (Y=KG) ØR METERS (Y=KT),LINE 330
300   READ P,X
310   IF P= 0 THEN 1900
320   LET P=P/P0
330   LET X=30.48*X
470   IF P<=P1 THEN 500
480   PRINT P, X, "  ","NØT SCALABLE"
490   GØTØ 300
499   REM..CALCULATE SHØCK RADIUS (530), SCALING(620), PRINTØUT (690)
500   GØSUB 760
505   IF P<P2 THEN 520
510   LET Z=(A/Q)↑(1/Q1)
515   GØTØ 530
520   LET Z=(B/Q)↑(1/Q2)
530   LET R=(Z↑3-M)↑(1/3)
540   REM...TØ REJECT DATA, APPLY CØNDITIØN LIKE 550 BEFØRE LINE 620
550   IF X=0 THEN 670
620   LET Y1= (M+X↑3)/(Z↑3)
630   LET Y2=Y2+Y1
640   LET I=I+1
650   LET S=S+Y1↑2
660   GØTØ 690
670   PRINT P, "   ",R
680   GØTØ 300
690   PRINTP,X,R,INT(100*Y1 +.5)/100
695   GØTØ 300
700   REM...SUBRØUTINE FØR CALCULATING H ØR INERTIAL MASS-ENERGY.....
710   LET V= (Q0/Q)↑(1/Q1)
720   LET Z3=YO/.3/Q/((V↑Q1)/(Q1-3) -(Q2-Q1)*(V↑3)/(Q2-3)/(Q1-3))
725   IF M>0 THEN 738
730   LET M=((Z3-R↑3)/H)*(4.186*DO/1000)
733   PRINT"INERTIAL MASS-ENERGY M="M"KG,KT"
736   GØTØ 740
738   LET H=(Z3-R↑3)*4.186*DO/M/1000
740   LET ZO=Z3↑(1/3)
750   RETURN
```

TABLE 4-1 (Cont'd)

LIST FOR DSC506

```
760   REM....SUBRØUTINE TØ CALCULATE WASTE HEAT.....
770   LET D=(P*(K+1) +2*K)/(P*(K-1) +2*K)
780   IF P>.025 THEN 810
790   LET Q= (K+1)*((P/K)↑3)*(1-1.5*P)/12
800   GØTØ 880
810   IF P>3.4 THEN 840
820   LET Q=((1+P)↑(1/K)/D- 1)/(K-1)
830   GØTØ 880
840   LET L=.43429448*LØG(P)
850   LET Q=10 ↑((22-L)*(L-1)/16)
880   RETURN
900   REM .....SUBRØUTINE FØR TRANSITIØN RADIUS AND PARAMETERS
901   LET A=Y0/(.3*Q*Z0↑3)
910   LET B= (02-01)/(02-3)/(01-3)
920   LET V= 4
930   LET T= (V↑01)/(01-3) - B*V↑3
940   IF ABS(T/A-1)<.0001 THEN 960
945   LET V1= (A-T)/(01*(V↑(01-1))/(01-3) -3 *B*V↑2)
950   LET V=V+V1
955   GØTØ 930
960   LET A= Q*(V*Z0)↑01
970   LET B=Q*(V*Z0)↑02
980   PRINT "STRØNG SHØCK, QZ↑"Q1"="A" WEAK, QZ↑"Q2"="B
985   PRINT"TRANSITIØN PRESSURE="P2"BARS, Q="Q"BARS, ZC="V*Z0"CM.,M"
990   RETURN
998   REM...INPUT DATA: ANY UNITS, SEQUENCE ØR FØRM IN LINES 1000-1899
999   REM...PRESSURE ØR ØTHER INTENSITY VARIABLE FIRST, THEN DISTANCE
1000  DATA 160, .45,  100, .68
1010  DATA 50, 1.11
1020  DATA 20, 1.85, 10, 2.55, 6, 3.15
1030  DATA 3, 4.2,  2, 5,  1, 6.8
1040  DATA .5, 10,   .3, 13.6,  .23, 16
1050  DATA .1, 28,   .05, 49,   .02, 100
1900  IF I<2 THEN 2000
1903  LET S1=S/I -(Y2/I)↑2
1905  LET S1=S1*I/(I-1)
1907  LET Y0=Y0*P0/1000000
1910  PRINT"MEAN YIELD="Y2*Y0/I" KG,KT  STD DEV PCT="100*SQR(S1)
1920  PRINT"BASED ØN "I" SAMPLES"
1930  PRINT "NEW TRIAL YIELD (WHEN SCALING APPLIES):"Y0*(Y2/I)↑1.28
1940  GØTØ 2000
1990  DATA 0,0
2000  END
```

TABLE 4-2

PRINTOUT FOR DSC506

```
DIRECT SCALING WITH UNIFIED THEORY FOR SHOCK GROWTH

DASA 1559 COMPILATION FOR ONE POUND TNT
TRIAL YIELD YO= .328      MEGACALORIE (= KG.NUCLEAR) OR KT
AMBIENT PRESSURE= 1     BARS  AMBIENT DENSITY = .00129  GM/CM↑3
ADIABATIC COMPRESSIBILITY EXPONENT K= 1.4
EXPLOSIVE AND SURROUNDS WEIGH .454     KG,KT
SPECIFIC ENERGY, BOMB/MEDIUM H= .25
STRONG SHOCK, QZ↑ 3.5       = 3.66886E+6     WEAK, QZ↑ 4      = 4.44632E+7
TRANSITION PRESSURE = 2     BARS, Q= 9.55525E-2    BARS, ZC= 146.872 CM.,M

OVERPRESSURE   MEAS.RADIUS     CALC.RADIUS     RELATIVE YIELD
(RATIO)        (CM.OR M.)      (CM.OR M.)
 170.032                        4
 160             13.716         11.0714          1.05
 100             20.7264        24.6068          .83
 50              33.8328        37.4514          .81
 20              56.388         55.9652          1.02
 10              77.724         73.826           1.16
 6               96.012         90.2765          1.2
 3               128.016        119.87X          1.22
 2               152.4          146.547          1.12
 1               207.264        207.069          1
 .5              304.8          309.449          .96
 .3              414.528        428.814          .9
 .23             487.68         512.167          .86
 .1              853.44         916.225          .81
 .05             1493.52        1513.89          .96
 .02             3048.          2977.65          1.07
MEAN YIELD= .327599  KG,KT  STD DEV PCT= 13.781
BASED ON  15    SAMPLES
NEW TRIAL YIELD (WHEN SCALING APPLIES): .327487
**READY.
```

Table 4-3
NOMENCLATURE FOR DSC506

A = A dummy variable for normalized yield in lines 901-970. After 960 it used and printed out as the coefficient in the expression $Q = A/Z^{Q1}$ for strong shocks.

B = A dummy variable in lines 902-970. After 970, used and printed out as the coefficient in the expression $Q = B/Z^{Q2}$ for weak shocks.

D = Current value of density, ratio to ambient

DO = Ambient density, input as gm/cm^3

H = "dynamic specific energy", i.e., the average ratio of internal and kinetic energy of explosive and bomb parts to an equal mass of surrounding air, both at the same velocity and temperatures. H is not a sensitive parameter.

I = Counter of data samples being used to find mean relative yield. I is by-passed if the data are not scalable (see 480), or is to be rejected from sampling (see 540, 550, 670).

K = $(d\ln (P+P_o)/d\ln D)_Q$, adiabatic compressibility of medium

L = $\log_{10}P$

M = mass of bomb and surrounds, input as Kilograms or kilotons. See line 250 for transform $M = \frac{H \cdot M}{\frac{4\pi}{3} DO}$

PO = ambient pressure, bars

P = overpressure, input in any units but late transformed to ratio to ambient in line 320

P1 = initial overpressure in bars

P2 = transition pressure, bars. P2 = 3.78 for point source explosion, somewhat less, P2 $\cong$ 2 for massive explosions.

TABLE 4-3 (Cont'd)

NOMENCLATURE FOR DSC506

Q = waste heat, local value in bars

Q1 = optional value, dln Q/dln Z for P>P2 if the ideal value 3.5 is not desired

Q2 = optional value dln Q/dln Z for P→0, if the ideal value 40 is not desired

R = calculated shock radius, local value in cm; input as initial radius of explosion

S = running sum, ΣY_1^2 for calculating variance (see 650)

S1 = variance of the relative yield (see 1900) corrected for sample size in 1905

T = trial value of normalized yield A in subroutine for transition radius ZC (see 930)

V = trial value V=ZC/Z0 in subroutine for transition radius ZC

V1 = increment for V in subroutine solving for transition radius ZC. As it appears in 945, $V1 = \frac{dV}{dT} \Delta T$

X = measured shock radius, input in any units, but transformed to cm or meters around line 330

Y = hydrodynamic yield, current value

Y0 = hydrodynamic yield, initial value, at charge radius, i.e., $Y_o = Y(Z_o)$

Y1 = local scaled yield, relative to Y0 (see 620)

Y2 = running total of relative yield Y1 (see 630)

Z = mass effect transform of R, local value

Z0 = mass effect transform of R, at the initial radius (see line 255)

5. Results and Summary

5.1 Foreword

In this chapter we show results and compare them for both the direct evaluation method (DEB) and the direct scaling method (DSC) and for both nuclear and TNT data. This combination of methods and data provides a critical test of the unified explosion theory (UTE).

The nuclear data make a kind of control for the mass effect (MEZ) and afterburning (GAB) concepts, because they represent a nearly point-source, instantaneous energy release. The nuclear data also provide a critical test of the equation of state for air, because the ideal gas law fails markedly at pressures above 10 bars or so. In a nuclear explosion the radiative phase ends and the shock starts near a pressure at 10^5 bars; the waste heat Q for real air at such pressures is about 10 times that of ideal air. (See Table 15, Appendix QVP) The high explosive data severely test the mass effect assumption (MEZ) because initially the energy is contained in material which weighs a thousand times that of air engulfed at a comparable radius. On the other hand, only a narrow region of high explosive data occurs at pressures above 100 bars or so (1500 psi), so the equation of state of air is on the average more nearly ideal and the equation of state introduces but small uncertainty. (See Table 11, Appendix QVP)

Contrasting the two methods, DEB was characterized earlier as a minimum-assumption, maximum-data method, whereas DSC was characterized as a minimum-data, maximum-theory method. We say this for DEB partly because, in principle, the total blast energy Yo of an explosive may be evaluated with virtually no assumptions about the way a shock is propagated, provided the range of data is broad enough. A more

trenchant observation is that the diagnostic parameter q = dln Q/dln Z is obtained directly from the data using DEB; thus there is no danger of prejudgement from theory. On the other hand, DSC requires few data, or none at all in the sense that a prediction is made a priori to reading the data. A single point is sufficient to obtain a "scaled yield" using DSC. Finally taken together, a comparison of the results from DEB and DSC for total yield Yo on the same data will provide an internal measure of the uncertainty between methods.

The nuclear data selected was previously discussed in Chapter 3, and came from an unclassified tabulation in ARF D125, a study done for the Los Alamos Scientific Laboratory in 1958. At pressures above 70 bars, these data were obtained from profuse and highly accurate measurements of fireball growth taken for the purpose of evaluating the hydrodynamic yield for nuclear explosions in air. The "analytic solution" method, used for those analyses, is part of the present unified explosion theory and this early work provided much of the background and insight from which DEB and DSC is derived.

The high explosive data used are for TNT, as correlated in DASA 1559, because as its title "Self-Consistent Blast Wave Parameters" suggests, it is already a comprehensive, critical survey of theoretical and experimental data for TNT, precisely as desired for an objective test of the present theory. The various results reported by Brode with the artifical viscosity method were rejected in DASA 1559 because "Unfortunately, Brode's data could not be adjusted to provide exact agreement with the experimental data....the results seem to lack internal consistency as evidenced by values of the same parameter that differ by more than 10% when read from different curves....it is

not possible to determine whether this inconsistency is inherent in the calculation or is due to careless plotting." DASA 1559 is essentially a marriage between the NOL WUNDY artifical viscosity code (NOLTR 62-168) and a comprehensive summary of several dozen sources of experimental data. "In general, the theoretically predicted magnetudes of these parameters were significantly lower than the experimental values at the same scaled distances, requiring the application of additional correction factors in order to bring the theory into agreement with experiment."

The correction factor for overpressure in DASA 1559 is 1.2 at pressures of practical interest, WUNDY being lower than the data. When the pressure is decaying typically like $R^{-1.5}$, $(n = +1.5)$ a factor of 1.2 in pressure implies, a factor $(1.2)^{\frac{3}{n}} = 1.44$ in equivalent weight. 1.44 is thus a measure of uncertainty between WUNDY and experiment and of the state of the art prior to the present theory.

Other compilations for high explosive data were analyzed, could have been reported here, and will be reported in subsequent papers. One such is Goodman's comprehensive compilation for pentolite; results are similar to these reported here for TNT, except that the standard deviation of relative yield was about 22% on Goodman's pentolite data in comparison with 14% for the DASA 1559 data. This does not necessarily mean that TNT is more reproducible than pentolite, the result may be due to the fact that the DASA 1559 TNT data are already smoothed by pegging them to the WUNDY curve; whereas Goodman's results are all uncorrelated experimental results.

In summary the nuclear data in ARF D125 and the high explosive data in DASA 1559 are used because they are unclassified, cover a broad range, and incorporate most recent compilations available.

5.2 Direct Evaluation of Nuclear Composite Data

Table 5.2-1 shows the input instructions for evaluation of the nuclear composite data. Table 5.2-2 shows the printout from DEB506 with these input instructions. Tables 5.2-3 and 5.2-4 are variations in parameters for eliminating the energy loss in the radiative phase.

In Table 5.2-1, the initial instruction, line 110, identifies the data.

The initial radius XO = 4.2 in line 210 means meters because we wish the results for yield to be in kilotons. This radius corresponds to the end of the radiative phase and the beginning of true shock propagation. Allowance is made at the end of the run for that fraction of energy which is dissipated during the radiative phase. This fraction of energy can be estimated from the equation for waste heat, but the topic is more suitable for discussion later in Chapter 6, dealing with questions. For the present chapter on results, instead, we presently define hydrodynamic yield to mean energy actually released to air as a shock wave.

The mass M is first set to 0 in line 220 for this run. Strictly speaking a nuclear weapon does have a finite mass. However, the data in ARF D125 had been chosen to characterize weapons of high yield to mass ratios, these most nearly approximating a point source. If M = 0, the input value of H = .25 shown in line 230, Table 5.2-1 is immaterial.

Lines 320 and 330 for pressure and distance

```
320 LET P = P/PO
330 LET R = X
```

appear redundant, because the data are already input in bars and meters

as is required for the program. However, these lines as shown for completeness and insure that no transformations of data are inadvertently made from a stored LIST of a previous run of DEB in which data may have been transformed from psi and/or feet.

The input data listed in lines 1000 to 1200 inclusive are in bars (the first number) and meters (second number). These data could have been typed in far fewer lines, but typing a single data pair for a single line makes it easier to enter, alter, or delete specific points. It is only a suggestion; it is not recommended generally.

Table 5.2-2 shows the printout from DEB506 for these input instructions.

The ambient conditions printed at the top of the table are all standard conditions; as such, they are part of the standard DEB506 LIST and changes were not required in the input instructions. Other parameters, H and M, as actually input, do appear at the top of Table 5.2-2.

Columns (1) and (2) show the overpressure and measured radius, just as they were input.

Column (4) is the actual slope q = dln Q/dln Z measured from adjacent data points. Because M = 0, $Z = (M + R^3)^{1/3} = R$ for this run, and Column (4) is dln Q/dln R directly. The initial entry q = 4 at P = .07 is the theoretical acoustic value. The final slope q = 3.5 at the initial radius of 4.2 is the theoretical strong shock value.

Column (3) shows the integrated yield Y(R) at each distance. In Column (3) note that the energy in the first line, which estimates the available energy remaining at .07 bars, (about 1 psi) is only 0.0117 KT out of approximately Yo = 0.94 kiloton at the initial radius;

thus the energy dissipated beyond 1200 meters or below 0.07 bars is about 1% of the total. The final yield is therefore not sensitive to the choice of whatever q_2 = dln Q/dln Z is used to describe the shock behavior in the acoustic range beyond the measurements. The point is interesting in itself: much damage can still occur beyond the 1 psi level, yet only 1% of the shock energy is left.

The estimate for yield at the initial radius is Yo = 0.94 KT. It is readily estimated that 5 to 15% of the original energy would become unavailable because of an isothermal expansion during the radiative phase, due to hydrodynamics alone and depending on whether the ideal or real equation of state is used. Of course, other losses would also occur due to various kinds of radiations, but we see that the total energy, which could be accounted for by hydrodynamics alone is within a few percent of a theoretical kiloton.

We note also in Column (3) that only 70% of the energy remains at the closest data point, a pressure P = 13600 bars. Therefore about 24% was dissipated between the end of the radiative phase (.94 KT) and the first data point (.70 KT). This raises the question how sensitive hydrodynamic yield is the choice of q = dln Q/dln Z in this region. A similar run of the same data, using q = 3.25 close-in instead of q = 3.5, gave a total yield of 0.922 instead of 0.939 and a starting pressure of 110139 instead of 130948. This difference, only 1.7%, is assurance that although a substantial fraction of energy is involved in the estimates, the final yield is not sensitive to the choice of q in the early region.

This insensitivity of Y to choice of q follows from the power law form of the energy. For small enough changes in distance, the integral is independent of q. Consider

$$\Delta Y = 4\pi \int_{R_1}^{R_2} QR^2 dR$$

$$= 4\pi\, Q_2 R_2^{-q} \int_{R_1}^{R_2} R^{2-q}\, dR$$

$$= 4\pi \frac{Q_2 R_2^{-q}}{3-q} \left[R_2^{3-q} - R_1^{3-q} \right]$$

$$= 4\pi \frac{Q_2 R_2^{3}}{(q-3)} \left[\frac{R_2}{R_1}^{q-3} - 1 \right] .$$

Then for $(R_2/R_1) = 1 + \Delta$, Δ a small quantity,

$$\Delta Y = 4\pi \frac{Q_2 R_2^{3}}{q-3} \left[(1 + \Delta)^{q-3} - 1 \right] .$$

By the binomial expansion,

$$\Delta Y = 4\pi \frac{Q_2 R_2^{3}}{q-3} \left[1 + (q-3)\,\Delta + \frac{(q-3)(q-4)}{2!}\,\Delta^2 + \ldots - 1 \right]$$

$$= 4\pi\, Q_2 R_2^{3}\, \Delta \left[1 + \frac{(q-4)}{2}\,\Delta + \ldots \right]$$

which is independent of a q for $\Delta \ll 1$ and also for $q = 4$.

Referring to the bottom of Table 5.2-2, we find that the loss of energy during the radiative phase is of the order .16 KT. Taken

together with the estimate for yield, .94 KT, at the initial radius gives a total of 1.10 KT which is 10% high. But as previously noted, the initial pressure of 130948 bars is about twice as high as is realistic, and is due to demanding zero mass in the bomb. When 30% of the energy is dissipated inside 7.32 meters, above 13600 bars, far above ordinary fireball measurements, it is not surprising, and in fact quite reassuring, to see that so drastic an error in initial parameter as setting M = 0 results in only a 10% discrepancy in overall yield.

Tables 5.2-3 and 5.2-4 study two further variations in parameters for these same nuclear data evaluated with DEB.

In Table 5.2-3 a mass of .001 kilotons = 1 ton = 2000 lbs was arbitrarily added to the explosion, because it is no secret that bombs do have weight and so does the missile or tower which carries it. About the only perceptible change in result from the point-source calculation in Table 5.2-2 is an estimated pressure of 76500 bars at the initial radius of 4.2 meters (instead of 130948) and a yield there of .903 KT instead of .94 KT. This latter pressure is now in good agreement with the earlier calculations estimating 80000 bars for the fireball pressure at the end of the radiative phase (LA 2000, LA1664, ARF D125). The loss of energy in the radiative phase remains about the same (.17 KT); despite the lower pressure, more material is being heated and the total energy release is estimated at .903 + .171 = 1.074 KT. Again, this is reassuring if anything, considering it involves estimates at pressures beyond what can be measured. At 13600 bars itself the yield changed only from .7027 to .7039 KT, less than 0.2% in yield or 0.06 % in radius. None of the measurements were that close.

Table 5.2-4 tests sensitivity to the equation of state by varying the parameter 22 in the high pressure approximation for waste heat

$$Q = 10^{\frac{(22 - L)(L - 1)}{16}}$$

The integer 22 clearly means to represent some better but uncertain parameter lying between 21.5 and 22.5, and its average uncertainty a priori is ±.25. Accordingly, the input for Table 5.2-4 changed the parameter from 22 to 21.75 and retained a mass M = 1 ton. Now we find an estimated pressure of 79135 bars and a yield of .849 KT at the end of the radiative phase. The loss in the radiative phase is now of the order .153 KT for a total of 1.002 KT. Both the initial yield and pressure are thus in splendid agreement with the facts as best we know them.

Recall that the error of the input data themselves must be at least 1% in radius because the numbers were rounded off to two and three significant figures and data were complied on log pressure vs log distance plots (ARF D125). Hence the yields derived from them are probably uncertain to 3 or 5%. This is well within the discrepancies discussed above. Let us assume the input data are perfect. The following conclusions still seem warranted, despite the large fraction of energy dissipated close to a nuclear explosion.

1) The error in DEB lies well within the natural uncertainties in q, M, and the equation of state.

2) The hydrodynamic yield at 13600 bars lies between .67 and .703 KT whatever we reasonably assume about the value of the parameters.

3) Uncertainty in Q due to equation of state has a completely negligible effect on the hydrodynamic yield for pressures as low as those of high explosions.

4) Whatever the uncertainty in heat of detonation at the source, a realistic choice of available energy Y at some larger distance still results in accurate predictions at still larger distances.

Figure 5.2-1 is a test of the hypothesis that

$$QZ^q = \text{constant}.$$

The diamonds show the waste heat with log Q as the ordinate and with the distance log Z as the abcissa. The abcissa is also the shock radius directly because M = 0, and is read directly in meters for the nuclear explosion.

The test here is to see if the data do fall on two straight lines as expected from theory: a slope q = 3.5 for strong shocks ($P > P_c$) and a slope of q = -4 for weak shocks ($P < P_c$). Here we have a confirmation for a point source explosion, extending over 10^9 times in Q. As nearly as one can judge, the slope changes abruptly near Q = 0.2 bars which implies transition pressure of P_c = 3 bars, just below the pressure 3.82 at which the flow first becomes sonic.

The full line in Figure 5.2-2 is a more magnified test of the theory. The ordinate shows the slope q as measured in Table 5.2-2, plotted as a function of log P. A bar graph is used because the slope is measured for the interval between data points. Because the slope is calculated between closely spaced adjacent distances, considerable scatter is to be expected. Several standard procedures are available to smooth the fit, if one were desired, but so far smoothing has not been found necessary to obtain an accurate yield with data spaced as they are here.

TABLE 5.2-1

Input Instructions DEB506, Nuclear Data

```
110   PRINT"NUCLEAR COMPOSITE, LA 1664 (IBM M) AND ARF D128 DATA"
210   LET X0=4.2
220   LET M=  0
230   LET H= .25
320   LET P=P/P0
330   LET R=X
1000  DATA .07, 1200
1010  DATA .1, 905
1020  DATA .2, 544
1030  DATA  .5,  302
1040  DATA 1, 206
1050  DATA     2    ,   147.4
1060  DATA 3,     122.5
1070  DATA 4,        108.5
1080  DATA     5    ,    98.8
1090  DATA 6,         91.5
1100  DATA 8,         82.4
1110  DATA 10, 75.6
1120  DATA    20    ,    57.3
1130  DATA    50    ,    41
1140  DATA   100, 32.3
1150  DATA   200, 25.6
1160  DATA 510, 19.2
1170  DATA   870, 16.5
1180  DATA  1550, 13.7
1190  DATA  3750, 10.7
1200  DATA  13600,  7.32
```

TABLE 5.2-2

DIRECT EVALUATION OF BLAST ENERGY, UNIFIED THEORY FOR BLAST

NUCLEAR COMPOSITE, LA 1664 (IBM M) AND ARF D128 DATA
AMBIENT PRESSURE = 1 BARS AMBIENT DENSITY = .00129 GM/CM↑3
ADIABATIC EXPONENT K= 1.4 SPECIFIC ENERGIES, BOMB/MEDIUM= .25
EXPLOSIVES AND SURROUNDS WEIGH 0 KILOGRAMS, KILOTONS

OVERPRESSURE (RATIO)	MEAS.RADIUS (CM.OR M)	PROMPT ENERGY (MEGACAL,KT)	DLN Q/DLN Z	DLN Y/DLNZ
.07	1200	1.17014E-2	4	1
.1	905	1.53213E-2	3.64	.92
.2	544	2.41884E-2	3.82	.88
.5	302	4.16666E-2	4.07	.96
1	206	.06108	4.19	1.04
2	147.4	8.67296E-2	4.11	1.06
3	122.5	.104979	3.77	1.01
4	108.5	.118376	3.7	.97
5	98.8	.129398	3.47	.93
6	91.5	.138727	3.27	.89
8	82.4	.151971	3.56	.86
10	75.6	.163253	3.15	.81
20	57.3	.200687	3.17	.69
50	41	.25043	3.42	.64
100	32.3	.290822	3.51	.62
200	25.6	.33506	3.48	.6
510	19.2	.398795	3.66	.61
870	16.5	.438047	3.82	.63
1550	13.7	.490605	3.27	.59
3750	10.7	.568108	3.63	.6
13600	7.32	.702749	3.24	.53
ESTIMATES AT INITIAL RADIUS:				
130948.	4.2	.940514	3.5	.52
LOSS IN CHARGE OR RADIATIVE PHASE IS OF THE ORDER:				
130948.		.163396	0 ASSUMED	

TABLE 5.2-3

DIRECT EVALUATION ØF BLAST ENERGY, UNIFIED THEØRY FØR BLAST

NUCLEAR CØMPØSITE, LA 1664 (IBM M) AND ARF D128 DATA
AMBIENT PRESSURE = 1 BARS AMBIENT DENSITY = .00129 GM/CM↑3
ADIABATIC EXPØNENT K= 1.4 SPECIFIC ENERGIES, BØMB/MEDIUM= .25
EXPLØSIVES AND SURRØUNDS WEIGH .001 KILØGRAMS, KILØTØNS

ØVERPRESSURE (RATIØ)	MEAS.RADIUS (CM.ØR M)	PRØMPT ENERGY (MEGACAL,KT)	DLN Ø/DLN Z	DLN Y/DLNZ
.07	1200	1.17014E-2	4	1
.1	905	1.53213E-2	3.64	.92
.2	544	2.41884E-2	3.82	.88
.5	302	4.16666E-2	4.07	.96
1	206	.06108	4.19	1.04
2	147.4	8.67296E-2	4.11	1.06
3	122.5	.104979	3.77	1.01
4	108.5	.118376	3.7	.97
5	98.8	.129398	3.47	.93
6	91.5	.138727	3.27	.89
8	82.4	.151971	3.56	.86
10	75.6	.163253	3.15	.81
20	57.3	.200688	3.18	.69
50	41	.250433	3.42	.64
100	32.3	.290826	3.51	.62
200	25.6	.335068	3.49	.6
510	19.2	.398824	3.67	.61
870	16.5	.438083	3.85	.64
1550	13.7	.490662	3.32	.6
3750	10.7	.568275	3.72	.62
13600	7.32	.703931	3.47	.59
ESTIMATES AT INITIAL RADIUS:				
76546.2	4.2	.903546	3.5	.57
LØSS IN CHARGE ØR RADIATIVE PHASE IS ØF THE ØRDER:				
76546.2		.171647	0 ASSUMED	

TABLE 5.2-4

DEB506, Nuclear Data with Modified Q at High Pressure

```
490 LET Q=10↑((21.75-L)*(L-1)/16)
810 LET L=.5*(22.75-SQR(22.75↑2 -4*(21.75 +16*.4343*LOG(Q))))
RUN
```

```
DIRECT EVALUATION OF BLAST ENERGY, UNIFIED THEORY FOR BLAST

NUCLEAR COMPOSITE, LA 1664 (IBM M) AND ARF D128 DATA
AMBIENT PRESSURE = 1     BARS    AMBIENT DENSITY = .00129  GM/CM↑3
ADIABATIC EXPONENT K= 1.4      SPECIFIC ENERGIES, BOMB/MEDIUM= .25
EXPLOSIVES AND SURROUNDS WEIGH .001     KILOGRAMS, KILOTONS
```

OVERPRESSURE (RATIO)	MEAS.RADIUS (CM.OR M)	PROMPT ENERGY (MEGACAL,KT)	DLN Q/DLN Z	DLN Y/DLNZ
.07	1200	1.17014E-2	4	1
.1	905	1.53213E-2	3.64	.92
.2	544	2.41884E-2	3.82	.88
.5	302	4.16666E-2	4.07	.96
1	206	.06108	4.19	1.04
2	147.4	8.67296E-2	4.11	1.06
3	122.5	.104979	3.77	1.01
4	108.5	.118376	3.7	.97
5	98.8	.129398	3.47	.93
6	91.5	.138727	3.27	.89
8	82.4	.151971	3.56	.86
10	75.6	.163253	3.15	.81
20	57.3	.200484	3.14	.68
50	41	.249334	3.38	.62
100	32.3	.288508	3.46	.6
200	25.6	.330952	3.44	.58
510	19.2	.391335	3.62	.59
870	16.5	.428098	3.8	.61
1550	13.7	.47691	3.27	.57
3750	10.7	.548135	3.67	.58
13600	7.32	.670522	3.41	.55
ESTIMATES AT INITIAL RADIUS:				
79135.8	4.2	.848855	3.5	.54
LOSS IN CHARGE OR RADIATIVE PHASE IS OF THE ORDER:				
79135.8		.153347	0 ASSUMED	

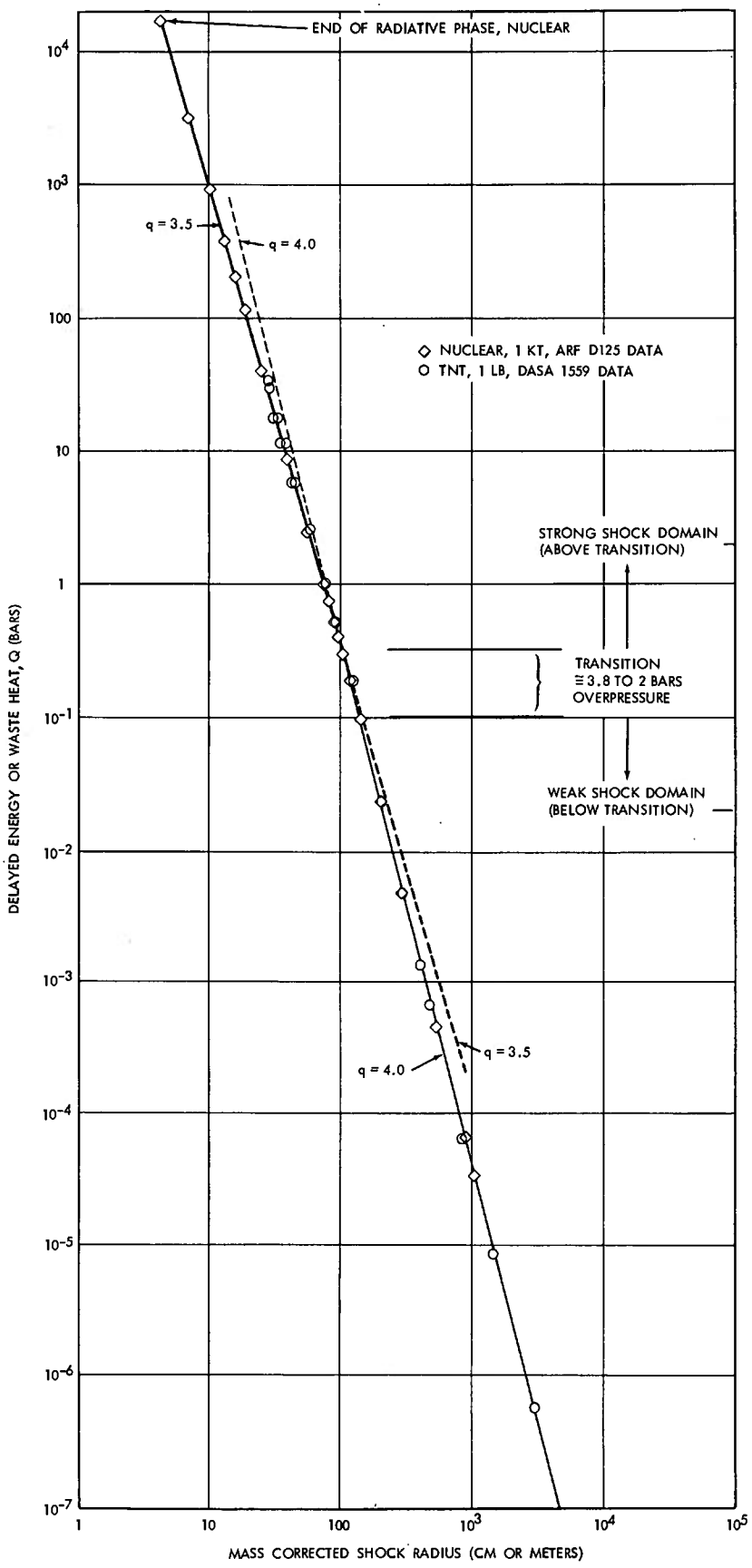


FIG. 5.2-1 TEST OF QZQ AND MEZ HYPOTHESES
QZ^q = CONSTANT q = 3.5 FOR STRONG SHOCK
q = 4.0 FOR WEAK SHOCK
$Z = (M+R^3)^{1/3}$

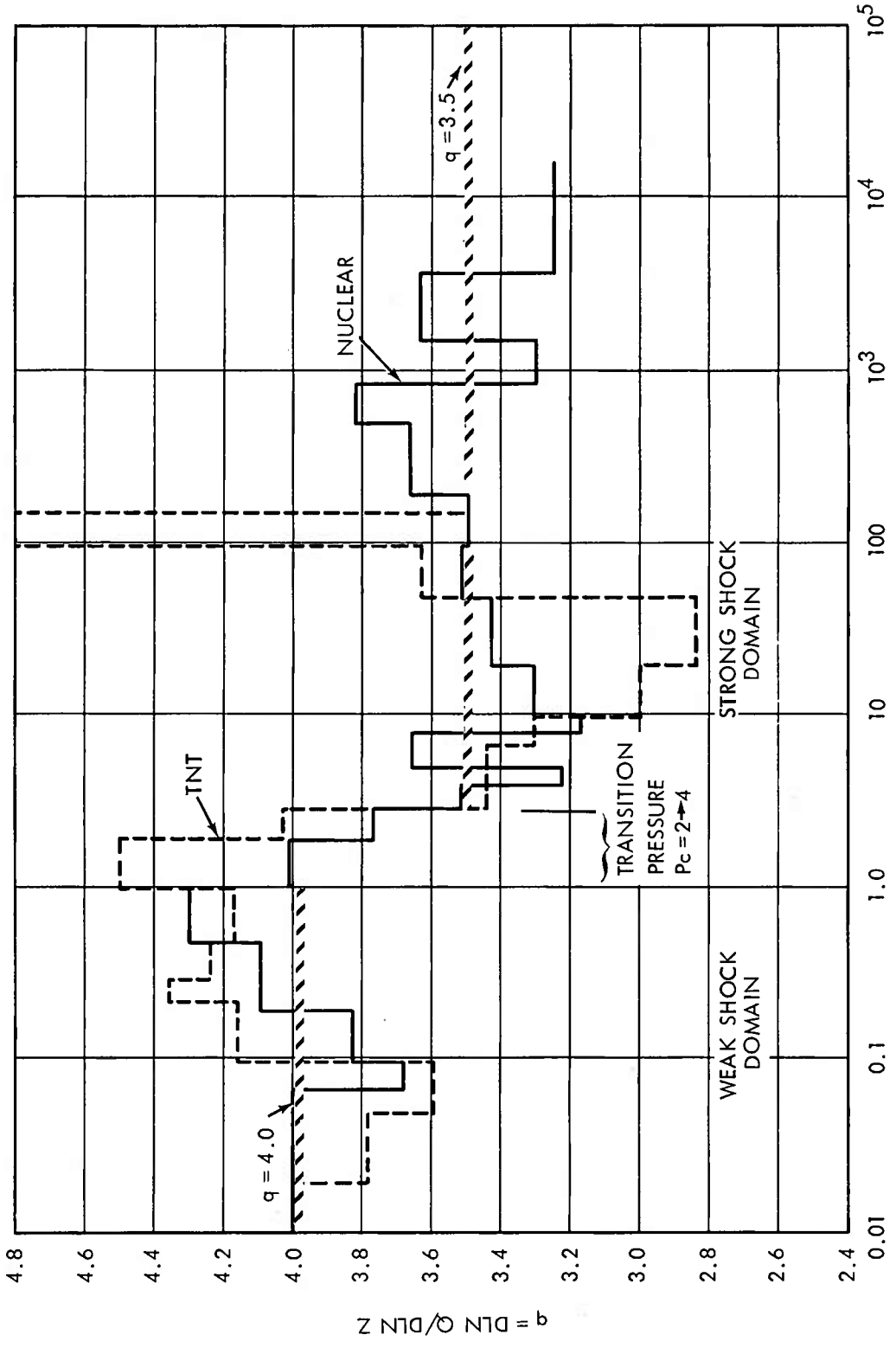


FIG. 5.2-2 q = DLN Q/DLN Z VERSUS OVERPRESSURE.

The ideal values are q = 3.5 for $P > P_c$, q = 4.0 for $P < P_c$.

5.3 Direct Evaluation of TNT

Table 5.3-1 shows the input instructions for evaluation of one pound of TNT using selected points from the DASA 1559 curve. This table corresponds to Table 5.2-1 for nuclear data; both are inputs to the same program DEB506.

The particular charge radius shown in line 210, XO = 0.13123, was so written merely to make the initial radius come out exactly 4 centimeters. The mass M = .454 is the number of kilograms in one pound. The explosive density thereby implied is about 1.7 gm/cm^3, but as previously noted, the shock growth is virtually independent of charge radius, and hence to charge density D_o. This insensitivity to R_o applies whenever $M = \frac{\text{mass}}{\frac{4\pi}{3} D_o X_o^3} \gg 1$ because the mass effect correction is

$$Z_o \equiv \left[R_o^3 + H \cdot M\right]^{1/3} \cong (HM)^{1/3} \text{ whenever } H \cdot M \gg R_o^3.$$

DEB506 is designed to accommodate a variable specific energy H. Here we use a constant H (line 230) for reasons cited in ASH in Chapter 1: diagnostics are easier and the variations in H are of the same order as the natural uncertainties of explosives. That is, the data do not yet warrant the sophistication of variable H.

The final yield evaluated by DEB is virtually insensitive to H, because Q and R are sufficient to evaluate the energy being dissipated where data exist. H is involved only in estimating the value of Z at the initial radius and in turn the contribution to Yo from shock growth between the closest data and the charge surface. H = 0.25 is a best guess from first principles. Moreover, if an initial pressure at the charge surface is known, as we shall see later, DSC506 provides

the means to calculate H, and H = .25 was chosen here mainly as a result of that analysis, and to be consistent in comparison of DEB with DSC.

The data in lines 1,000 to 1,050 are input with pressure in bars and distances in feet.

Line 330 in the instructions transforms the measured shock distances from feet, as they were input, to centimeters. Accordingly, the yield will appear in megacalories or nuclear kilograms. As another example, for a million = 10^6 pounds = 500 tons of TNT, the distance would be converted to meters by letting R = 0.3048*X and we would understand the yield to mean in nuclear kilotons.

Table 5.3-2 shows the printout from DEB506 for the DASA 1559 data.

Again, the input parameters are printed out at the top of the table. The entire calculation is summarized at the bottom by the extimate of yield Yo = 0.328 megacalories at the initial radius. Of this energy, we note in the first line of Column (3) that 0.0048 megacalories is available at a pressure of 0.02 bars, about 0.3 psi. This is $\frac{.0048}{.328}$ x 100 = 1.5% of the total; a choice of $q_2 = 4.5$ instead of 4.0 would have resulted in a correction of 1% tail fraction instead, because the tail fraction is $\Delta Y = \frac{4\pi\, Q_f R^3}{q_2 - 3}$. Thus, the total energy is insensitive to a choice of q_2.

A slightly larger but still small fraction of the total energy is involved in the close-in correction: we have as prompt energy to start: 0.328 megacalories at R = 4, P_1 = 179,

and 0.320 megacalories at R = 13.7, P = 160.

This implies a fraction $\frac{.008 \times 100}{.328} = 2.5\%$ dissipated in the early interval. A number of similar runs were done which compare thus:

Input Parameter		Outputs	
Q1	H	Pi	YO
3.5	.25	179.4	0.32814
3.5	.5	169.8	0.32988
3.25	.25	178.0	0.32810
3.25	.5	169.0	0.32986

These spread in yield Yo is about $\frac{.0018 \times 100}{.329} = .5\%$, due almost entirely to the variation in H.

Also plotted on Figure 5.2-1, the circles show the waste heat Q and distances Z taken from the same run as Table 5.3-2 for both H = .5 and H = .25. They are compared directly with nuclear data, excepting that the abcissa now reads in centimeters for TNT.

The test here is again to see if the data fall on two straight lines as the theory predicts: a slope of -3.5 for strong shocks (P > 3.0 bars or so) and a slope of -4 for weak shocks (P < 3.0 bars or so).

The figure speaks for itself. Now we have a confirmation over a range of 10^{10} times in waste heat Q, involving a million-fold change in explosion energy from one pound to one kiloton, and a 1,000 fold change in the initial energy density between nuclear and HE. Without the mass effect correction, the uppermost points for TNT would not be near Z = 35, where they are now, but nearly a full decade to the left near the charge radius R = 4.

In Figure 5.2-1, note that:

1. In the weak shock region, the 1 KT nuclear curve falls almost exactly in 1 lb TNT. Because nuclear data are in meters, and TNT in centimeters, the scaling factor between them is almost exactly 100. The result is partly fortuitous, highly convenient, has been realized for a long time, but perhaps not quite so assuredly as shown here.

2. In the strong shock region, most TNT points lie on the correct slope, parallel to the nuclear curve, but tend to be displaced by about 20% energy-wise to the right. This appears as evidence of afterburning. During early times, the TNT curve is continually supported by heat of combustion from within. But once the negative phase develops around the transition pressure, the combustion energy can no longer reach the shock front and the afterburning energy is trapped behind the secondary shock. Thereafter the TNT blast coasts on, like reduced energy, being unsupported from the interior.

The dashed lines on Figure 5.2-2 show, in more detail than Figure 5.2-1, the local behavior of the slope q as a function of pressure for TNT. Here, as with the nuclear data, the general trends are confirmed: $q \cong 4.0$ for weak shocks and $q \cong 3.5$ for strong shocks. Although the average values agree with the idealized behavior, now we see that the scatter about these values is as large as the difference between them. As noted previously however, the departure may not be significant: an error of 7% in pressure, at low pressure, makes a difference of $\pm$ .5 in the slope q.

The dashed lines on the figure suggest an oscillation about the ideal value. A similar oscillation appears for the nuclear data,

but is of so much smaller amplitude as to suggest the oscillation is experimental trend and is not real for instantaneous point source of energy. Some physical reasons for the departures are

1. BOW (Body Wave Oscillation) below 2 bars
2. Variation in H at high pressure.
3. Afterburning, $q_1 < 3.5$ for $P < 50$

But there is insufficient evidence in these data alone to prove the oscillation is real. Further discussion on this point is deferred until the next chapter.

The single measurement at 160 bars, leading to a slope q of 6.98 is probably not realistic. It represents the highest point in the DASA 1559 curve. It is doubtful if a pressure this high could have been measured directly; the data probably came from time-of-arrival measurement and read high. There is much evidence, suggested by the mass effect and discussed briefly in Section 1.8, to suggest that the time-of-arrival curve does not represent a spherically symmetric shock but isolated early arrival jets. It is also possible that the actual data did flatten off; but the smooth curve was drawn in accord with the widespread preconception that P decreases monotonically with distance in this region. It is also possible, although the authors of DASA 1559 do not show these details, that close-in data are really WUNDY theoretical results as extracted from NOLTR 62-168. According to the mass effect, we then would expect WUNDY to read high because the code did not permit radial mixing.

TABLE 5.3-1

Input Instructions DEB506, TNT Data

```
110   PRINT"DASA 1559 CØMPILATIØN FØR ØNE PØUND TNT"
210   LET XO=.1312335
220   LET M=.454
230   LET H=.25
320   LET P=P/PO
330   LET R=30.48*X
1000  DATA      .02, 100,     .05, 49,     .1, 28
1010  DATA .23, 16,      .3, 13.6,      .5, 10
1020  DATA      1, 6.8,       2, 5,      3, 4.2
1030  DATA 6, 3.15,   10, 2.55
1040  DATA 20, 1.85,  50, 1.11,  100, .68
1050  DATA 160, .45
*
```

TABLE 5.3-2

DIRECT EVALUATIØN ØF BLAST ENERGY, UNIFIED THEØRY FØR BLAST

DASA 1559 CØMPILATIØN FØR ØNE PØUND TNT
AMBIENT PRESSURE = 1 BARS AMBIENT DENSITY = .00129 GM/CM↑3
ADIABATIC EXPØNENT K= 1.4 SPECIFIC ENERGIES, BØMB/MEDIUM= .25
EXPLØSIVE + SURRØUNDS WEIGH .454 KILØGRAMS

ØVERPRESSURE (RATIØ)	MEAS.RADIUS (CM.ØR M)	PRØMPT ENERGY (MEGACAL,KT)	DLN Ø/DLN Z	DLN Y/DLNZ
.02	3048.	4.80479E-3	4	1
.05	1493.52	9.41375E-3	3.79	.9
.1	853.44	1.50223E-2	3.59	.78
.23	487.68	2.42835E-2	4.16	.93
.3	414.528	2.83759E-2	4.37	.99
.5	304.8	3.88944E-2	4.24	1.06
1	207.264	5.89187E-2	4.17	1.1
2	152.4	8.39986E-2	4.5	1.22
3	128.016	.103324	4.03	1.18
6	96.012	.140086	3.44	.99
10	77.724	.169245	3.31	.87
20	56.388	.213205	3	.69
50	33.8328	.27074	2.84	.51
100	20.7264	.304997	3.63	.52
160	13.716	.319843	6.98	.68
ESTIMATES AT INITIAL RADIUS:				
179.407	4.	.32814	3.5	.68
LØSS IN CHARGE ØR RADIATIVE PHASE IS ØF THE ØRDER:				
179.407		7.42755E-2	0 ASSUMED	

5.4 Direct Scaling, Nuclear Composite Data

Table 5.4-1 shows the instructions to DSC506 for direct scaling of nuclear composite data.

The trial yield in line 140, Yo = 0.965, is chosen from a previous run. These same data evaluated with DEB gave Yo = 0.940 KT. On an absolute basis, using 5% as the ideal gas estimate for energy dissipated in the radiative phase, we could have started with 0.95 KT. Either way, the result of the first run would suggest a new trial yield of 0.965 KT, with M = 0.

The average specific energy H = .25 is inconsequential inasmuch as M = 0. However, typing H = .25 in line 200 leaves the initial pressure undefined, and the program is thereby instructed to calculate P_1 on the basis of M = 0 and H = .25.

The selection of P2 = 2 in 210 is expected theoretically but was verified by DEB for these same data on the original graph of Figure 5.2-2; there, q = 4 for $1 > P > 2$ but q = 3.77 for $2 < P < 3$.

In lines 220-240, the parameters Q1 = 3.5, Q2 = 4.0, M = 0 are all standard for an ideal point-source explosion.

Again, lines 320 and 330 for transformation of P and X appear redundant; but these entries insure that different instructions are not left over from a previous run.

The data in lines 1000-1170 are input with P in bars and distances in meters. Hence, yields are interpreted in kilotons.

The printout from DSC506 for these instructions is given in Table 5.4-2. The input parameters are shown at the top starting with the trial yield Y1 = 0.965.

In the instruction we set M = 0, and the initial pressure was not specified, hence, the program computes an initial pressure. It is shown as the first entry P = 143496 bars at 4.2 meters as if it were a truly massless explosion. It is about twice as high as is real, for three reasons:

1. The real explosion during the radiative phase is an isothermal isobaric sphere, the wave form is flat and not sharply peaked at the front like a purely hydrodynamic blast wave. The "square wave" contains about twice as much energy, relative to the shock pressure, as does a peaked blast wave. For a given hydrodynamic energy, the peak pressure in an isothermal sphere would therefore be about half as high as in a strong blast wave.

2. A nuclear bomb is never truly massless, if not because of the bomb itself, then because of the surrounds: tower, cab, or missile carrying it. The mass will suppress temperature and pressure.

3. At these pressures, much energy is present as radiation pressure, ionization, dissociation, etc., energy which will shortly be returned to the blast as the material cools. It is an "inertial mass effect" which behaves like mass, in storing energy.

The yield, with M = 0 is 0.965, is good enough agreement with one kiloton, but is high considering that five to fifteen percent of the energy may be dissipated during the radiative phase.

If we initially set M = 0, but specify the initial pressure at R_o, say 80,000 bars, the program will solve for an effective mass, as shown in Table 5.4-3. This is an "effective mass" which appears as the "inertial mass-energy" in the heading of the table, .0008 KT = 800 Kg. For this run, the average yield is 0.904 KT, compared with

0.965 for DSC for M = 0, and with 0.935 KT from the DEB evaluation of the same data. This agreement, with a few percent in yield, means an uncertainty about 1 or 2% in shock radius and is quite acceptable. It is within round-off errors of the original data. There is of course, no assurance either that the ARF D125 data are more accurate than that. Except for the first data point at P = 13600, the differences between the calculated radius and theoretical radius in either Table 5.4-2 or 5.4-3 are too small to plot; at P = 13,600, one run calculates R = 7.26, the other R = 7.47, the measured value is 7.32.

Also, except for the first point, there is no significant difference in the relative yield for any point for the two cases shown in Tables 5.4-2 and 5.4-3. In both cases the standard deviation is about 4.7% in yield, or about 1.5% in distance.

Figure 5.4-1 is a familiar pressure distance plot. The nuclear data from either Table 5.4-2 or 5.4-3 are plotted as diamonds. The theory is plotted as a full line. If continued, the uppermost part of the curve would branch for the two cases of Table 5.4-2 and Table 5.4-3; one for truly point source termination at 143496 bars at R = 4.2, the other with an initial pressure of 80,000 bars. But wherever data exist, below 13,000 bars, and because of the exceedingly good agreement between theory and data, no difference is seen between theory and experiment. This usual comparison, log P vs log R, is too coarse to show the difference.

This significant development should not be overlooked. It is nearly universal practice to compare explosives mainly by showing their pressure distance curves as in Figure 5.4-1. But here we see

agreement between the unified explosion theory and data in which the differences are too small to portray on a log P vs log R plot.

A more sensitive plot is shown in Figure 5.4-2 which gives the scaled relative yield, measured/ideal, as a function of overpressure ratios. The full line shows data from Column (4) of Tables 5.4-3 (and 5.4-2, except at the two higher pressures).

Reminiscent of the oscillation of q in Figure 5.2-2, we see an apparent oscillation here about the correct value relative Y = 1.0. Whether this difference is real or merely due to scatter is not clear. To accept the oscillation as real is hazardous, partly because the "input data" are themselves points taken from a curve passed through measured data; they are not really raw data. The average value of the input curve is doubtless correct--it averaged the data--and the trial yields for Tables 5.4-2 and 5.4-3 represent a UTE fitted average to the input curve. No matter how smooth a curve is passed through the original data, the local value cannot everywhere be perfect, compared with the true curve. Whatever the real curve is, the "French curve" drawn through it is an average and will perforce be high as often as it is low. It will perforce appear to oscillate, but the oscillation may only be due to curve fitting.

TABLE 5.4-1

Input Instructions, DSC506, Nuclear Data

```
110    PRINT"NUCLEAR CØMPØSITE, LA 1664 (IBM M) AND ARF D128 DATA"
140 LET YO= .965
190    LET R=4.2
195    LET H=.25
200    LET H=.25
210    LET P2=2
220    LET Q1= 3.5
230    LET Q2=4
240    LET M= 0
320    LET P=P/PO
330    LET X=X
1000   DATA 13600, 7.32
1010   DATA 3750, 10.7,    1550, 13.7
1020   DATA 870, 16.5,  510, 19.2,  200, 25.6, 100,32.2
1030   DATA 50, 41, 20, 57.3, 10, 75.1
1040   DATA 8, 82.4,  6, 91.5,  5, 98.8, 4, 108.5
1130   DATA 3, 122.5,    2, 147.4
1140   DATA 1, 208
1150   DATA .5, 302
1160   DATA .2, 544
1170   DATA .1, 905,     07, 1200
```

TABLE 5.4-2

DIRECT SCALING WITH UNIFIED THEØRY FØR SHØCK GRØWTH

NUCLEAR CØMPØSITE, LA 1664 (IBM M) AND ARF D128 DATA
TRIAL YIELD YO= .965 MEGACALØRIE (= KG.NUCLEAR) ØR KT
AMBIENT PRESSURE= 1 BARS AMBIENT DENSITY = .00129 GM/CM↑3
ADIABATIC CØMPRESSIBILITY EXPØNENT K= 1.4
EXPLØSIVE AND SURRØJNDS WEIGH 0 KG,KT
SPECIFIC ENERGY, BØMB/MEDIUM H= .25
STRØNG SHØCK, ØZ↑ 3.5 = 3.60142E+6 WEAK, ØZ↑ 4 = 4.35304E+7
TRANSITIØN PRESSURE= 2 BARS, Q= 9.55525E-2 BARS, ZC= 146.096 CM.,M

ØVERPRESSURE (RATIØ)	MEAS.RADIUS (CM.ØR M.)	CALC.RADIUS (CM.ØR M.)	RELATIVE YIELD
143496.		4.2	
13600	7.32	7.4738	.94
3750	10.7	10.6251	1.02
1550	13.7	13.727	.99
870	16.5	16.3355	1.03
510	19.2	19.2756	.99
200	25.6	26.0386	.95
100	32.2	32.8198	.94
50	41	41.6763	.95
20	57.3	57.811	.97
10	75.1	74.6927	1.02
8	82.4	81.2432	1.04
6	91.5	90.6464	1.03
5	98.8	97.2261	1.05
4	108.5	106.007	1.07
3	122.5	119.723	1.07
2	147.4	146.096	1.03
1	208	206.136	1.03
.5	302	307.886	.94
.2	544	560.381	.91
.1	905	911.39	.98
.07	1200	1178.43	1.06

MEAN YIELD= .966074 KG,KT STD DEV PCT= 4.73684
BASED ØN 21 SAMPLES
NEW TRIAL YIELD (WHEN SCALING APPLIES): .966375

TABLE 5.4-3

DIRECT SCALING WITH UNIFIED THEØRY FØR SHØCK GRØWTH

NUCLEAR CØMPØSITE, LA 1664 (IBM M) AND ARF D128 DATA
TRIAL YIELD YO= .905 MEGACALØRIE (= KG.NUCLEAR) ØR KT
AMBIENT PRESSURE= 1 BARS AMBIENT DENSITY = .00129 GM/CM↑3
ADIABATIC CØMPRESSIBILITY EXPØNENT K= 1.4
EXPLØSIVE AND SURRØUNDS WEIGH 0 KG,KT
INERTIAL MASS-ENERGY M= 8.18254E-4 KG,KT
STRØNG SHØCK, QZ↑ 3.5 = 3.64162E+6 WEAK, QZ↑ 4 = 4.40862E+7
TRANSITIØN PRESSURE= 2 BARS, Q= 9.55525E-2 BARS, ZC= 146.56 CM.,M
SPECIFIC ENERGY, BØMB/MEDIUM H= .25

ØVERPRESSURE (RATIØ)	MEAS.RADIUS (CM.ØR M.)	CALC.RADIUS (CM.ØR M.)	RELATIVE YIELD
80000		4.2	
13600	7.32	7.26582	1.02
3750	10.7	10.5465	1.04
1550	13.7	13.7037	1
870	16.5	16.3402	1.03
510	19.2	19.303	.98
200	25.6	26.1028	.94
100	32.2	32.9124	.94
50	41	41.8014	.94
20	57.3	57.9908	.96
10	75.1	74.9277	1.01
8	82.4	81.4994	1.03
6	91.5	90.9328	1.02
5	98.8	97.5336	1.04
4	108.5	106.342	1.06
3	122.5	120.103	1.06
2	147.4	146.559	1.02
1	208	206.791	1.02
.5	302	308.864	.93
.2	544	562.161	.91
.1	905	914.285	.97
.07	1200	1182.18	1.05

MEAN YIELD= .904054 KG,KT STD DEV PCT= 4.60223
BASED ØN 21 SAMPLES
NEW TRIAL YIELD (WHEN SCALING APPLIES): .903789

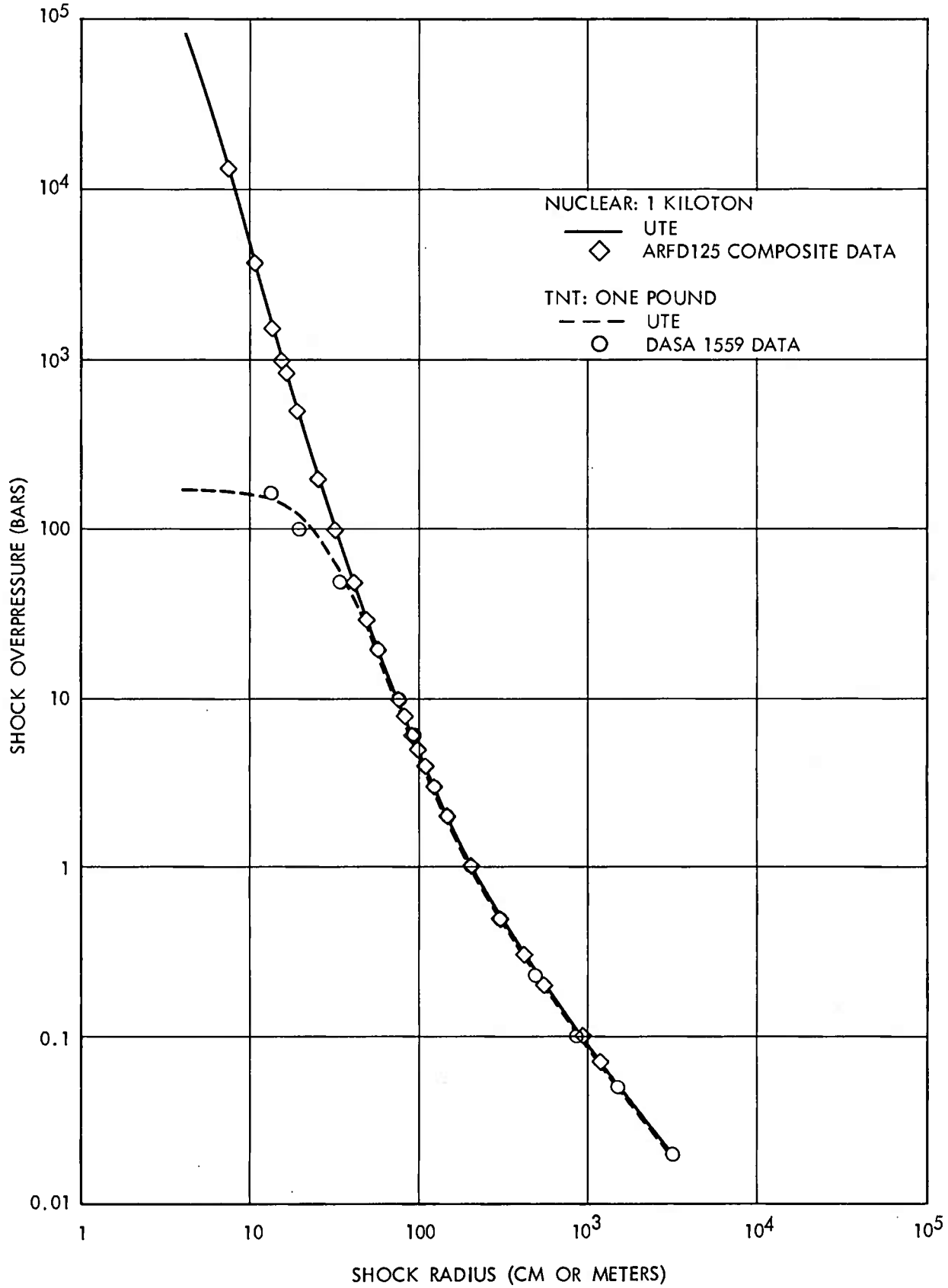


FIG. 5.4-1 COMPARISON OF UTE PREDICTIONS WITH NUCLEAR AND TNT DATA.

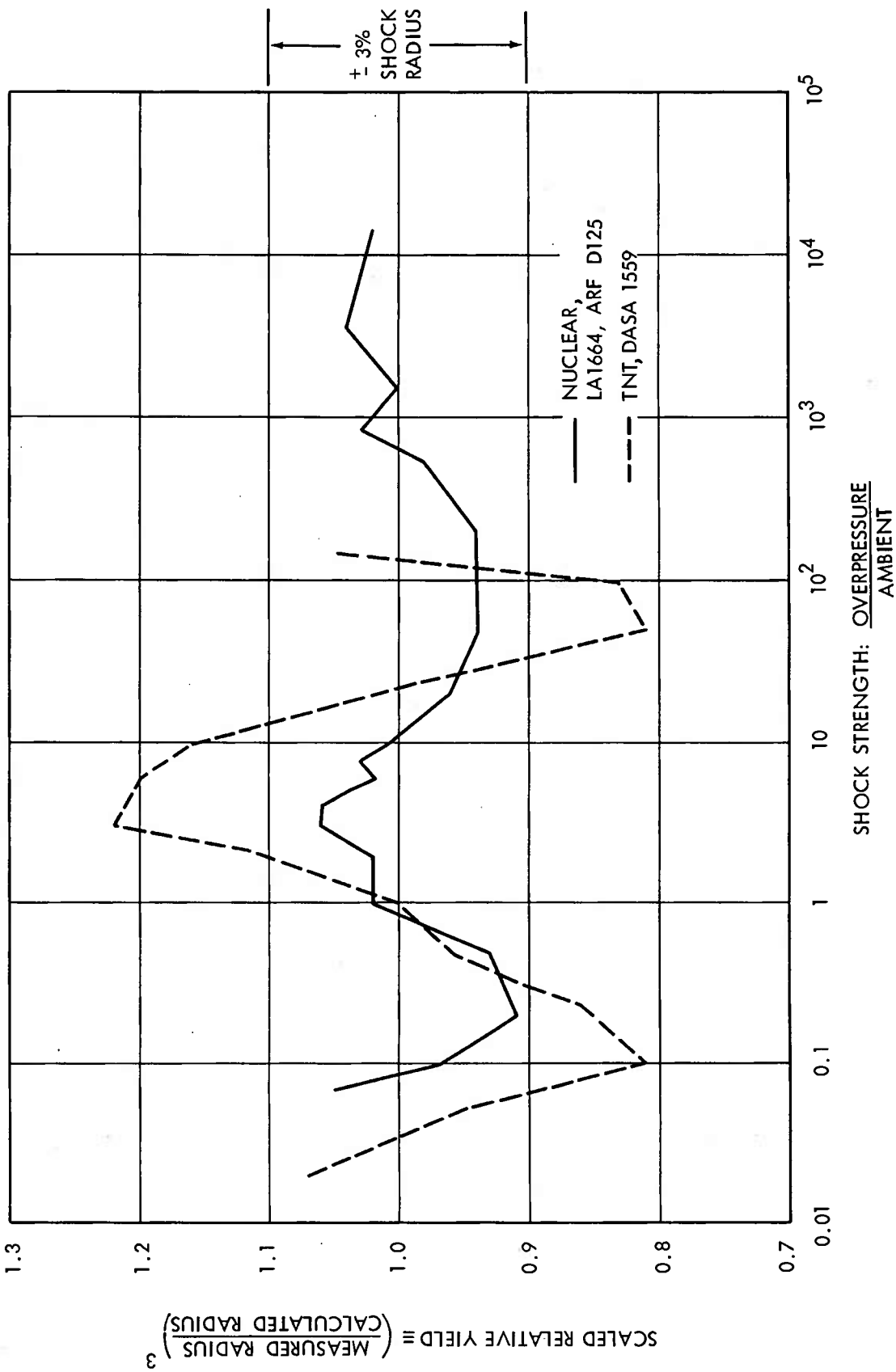


FIG. 5.4-2 COMPARISON OF NUCLEAR AND TNT MEASURED YIELDS WITH UNIFIELD BLAST THEORY.
Familiar scatter in blast, about 7% in pressure, is roughly 3-5% in radius, 10-15% in yield.

5.5 Direct Scaling for TNT

The set of input instructions to DSC506 for scaling of the DASA 1559 data for TNT is Table 5.5-1. Standard atmospheric conditions are assumed again, and do not appear in the input.

The trial yield YO = 0.328 megacalories is already known from DEB. The initial radius R = 4 is again the charge radius in centimeters. As shown, H = .25 at line 200 is redundant with 195, but the entry at 200 insures that an initial pressure is not specified for this run in line 200 (a P1 might have been left over from a previous run). It requires the machine to calculate P1. Typing "200" would do as well to erase a previous entry. Other values of H might have been used. The transition pressure P2 = 2 is chosen to be consistent with the nuclear data. Q1 = 3.5, Q2 = 4 are ideal values; M = 0.454 means kilograms and is one pound.

The printout from DSC506 for these instructions is shown as Table 5.5 -2.

The mean yield and a suggested new trial yield is 0.3275; both are in splendid agreement with DEB number for the same data, .328. Pressures near the charge surface from chemical explosions are much reduced from nuclear, 170 compared with 80,000 bars, and for that reason, the yield is not subject to so large an uncertainty due to choice of initial conditions.

The agreement between DEB and DSC for DASA 1559 data is fortuitously close, mostly because the data are uniformly spaced. A similar run with a transition pressures of 3 bars resulted in a fitted yield of 0.333 megacalories for DSC, a difference of 2% in yield with DEB. The initial pressures are slightly more sensitive:

	P_i	Yo
DSC	170.0	0.3275
DEB	179.4	0.3281

The reason for the difference: DSC is an absolute calculation using the trial YO and a fitted curve for the whole strong shock region as shown at the top of the table, $QZ^{3.5} = 3.67 \times 10^{6}$ for the strong shock. Whereas, the initial pressure on DEB is no more accurate than the closest point; the initial pressure is extrapolated inward from the closest data point, which was 160 bars at 13.7 cm. We see in DSC that this point is about 5% high in yield compared with the rest, and DEB naturally would extrapolate high, to 179 bars at the origin instead of 170 as in DSC.

The standard deviation 13.78% in yield, implies 4.5% in radius and 7-9% in overpressure. This is about equal to common experience for scatter in pressure measurements. Speculation regarding the variation are therefore hazardous.

The circles on Figure 5.4-1 for pressure-distance are the measured data from the TNT printout. The dashed line is the calculated radius taken from Table 5.5-2. The flattening of the pressure-distance at small distances is striking compared with the nuclear data in the same region. Scaling is another striking feature on Figure 5.4-1, as was noted previously in Figure 5.2-1; because the nuclear data are in meters, TNT in centimeters, the scaling factor between them is almost exactly 100.

A finer measure of the 100-fold scaling at long distance is the calculated value of the constant QZ^{4} for the weak shock branch

of the nuclear and TNT curves. These are read directly from the printouts in headings for Tables 5.4-2, 5.4-3, and 5.5-1.

	Transition Pressure	Mass KT	QZ^4
Nuclear	2	0.0008	4.409×10^7
	2	0	4.353×10^7
TNT	2	0.454	4.446×10^7
	3	0.454	4.226×10^7

The maximum spread here is 5% in QZ^4; this quantity is proportional to $Y^{4/3}$. For a given value of pressure, Q or any other measure of shock intensity, the difference in radius Z is like $(1.05)^{1/4} \simeq 1\%$.

On Figure 5.4-2 the dashed line shows the relative yield from Column (4) of the DSC analysis for TNT. As previously noted for the nuclear case, an oscillation appears to occur about the ideal value with a minimum near P = 0.2 and a maximum near P = 2. The amplitude is about three times as large as for the nuclear curve, but the phasing appears similar. More of that in Chapter 6.

TABLE 5.5-1

Input Instructions, DSC506, TNT Data

```
110   PRINT"DASA 1559 CØMPILATIØN FØR ØNE PØUND TNT"
140   LET YO= .328
190   LET R=4
195   LET H=.25
200   LET H=.25
210   LET P2=2
220   LET 01= 3.5
230   LET 02=4
240   LET M=.454
1000  DATA 160, .45,  100, .68
1010  DATA 50, 1.11
1020  DATA 20, 1.85, 10, 2.55, 6, 3.15
1030  DATA 3, 4.2,  2, 5,  1, 6.8
1040  DATA .5, 10,   .3, 13.6,  .23, 16
1050  DATA .1, 28,   .05, 49,   .02, 100
```

TABLE 5.5-2

```
DIRECT SCALING WITH UNIFIED THEØRY FØR SHØCK GRØWTH

DASA 1559 CØMPILATIØN FØR ØNE PØUND TNT
TRIAL YIELD YO= .328      MEGACALØRIE (= KG.NUCLEAR) ØR KT
AMBIENT PRESSURE= 1    BARS  AMBIENT DENSITY = .00129  GM/CM↑3
ADIABATIC CØMPRESSIBILITY EXPØNENT K= 1.4
EXPLØSIVE AND SURRØUNDS WEIGH .454    KG,KT
SPECIFIC ENERGY, BØMB/MEDIUM H= .25
STRØNG SHØCK, QZ↑ 3.5      = 3.66886E+6    WEAK, QZ↑ 4     = 4.44632E+7
TRANSITIØN PRESSURE= 2    BARS, Q= 9.55525E-2   BARS, ZC= 146.872 CM.,M

ØVERPRESSURE   MEAS.RADIUS     CALC.RADIUS     RELATIVE YIELD
(RATIØ)        (CM.ØR M.)      (CM.ØR M.)
 170.032                        4
 160             13.716         11.0714          1.05
 100             20.7264        24.6068          .83
 50              33.8328        37.4514          .81
 20              56.388         55.9652          1.02
 10              77.724         73.826           1.16
 6               96.012         90.2765          1.2
 3               128.016        119.87X          1.22
 2               152.4          146.547          1.12
 1               207.264        207.069          1
 .5              304.8          309.449          .96
 .3              414.528        428.814          .9
 .23             487.68         512.167          .86
 .1              853.44         916.225          .81
 .05             1493.52        1513.89          .96
 .02             3048.          2977.65          1.07
MEAN YIELD= .327599  KG,KT  STD DEV PCT= 13.781
BASED ØN  15    SAMPLES
NEW TRIAL YIELD (WHEN SCALING APPLIES): .327487
```

5.6 Summary of Results

From the analysis in Chapter 5 of nuclear and TNT data with DEB and DSC, these conclusions are suggested:

1. Either method provides an absolute measure of blast yield directly from the measured data; there is no need to risk the uncertainties in an empirical standard, or fitting the data to an arbitrary curve for analysis.

2. Both methods give consistent yields with each other, and the observed standard deviations (1% to 4% in predicted radius) are within the familiar experience of scatter in pressure-distance data.

3. The yield from a 1 KT nuclear explosion 0.90 ± .05 KT is as expected at the end of the radiative phase, and is probably correct within a few percent when corrected for loss in the radiative phase. The yield for one pound of TNT at the charge surface is 0.328 megacalories or about 720 cal/gm by either method.

4. Below a shock strength of 20 or a blast overpressure of 300 psi, the scaling factor between 1 pound of TNT and 1 kiloton nuclear is almost exactly 100. Both curves can be superimposed if 1 KT nuclear is plotted in meters and 1 pound TNT is plotted in centimeters.

5. Based on measured energy released and due to the suppression of close-in pressure by the mass effect, the chemical explosion is about 3 times as efficient as a nuclear explosion.

6. The QZQ hypothesis is apparently confirmed over a range of 10^{10} times in waste heat, Q, a million times in yield from one pound to 1 kiloton, and a thousand times in initial energy density per unit mass.

7. At long distances, for $P/P_o < 1$, all explosions decay as $\frac{\Delta P}{P_o} \sim R^{-4/3}$, in a near ideal medium.

8. A machine time of about 1 second is required to analyze a pressure-distance curve and about one minute to printout the full table of shock front results by either method using time-sharing remote access teletype. This compares with many hours for artificial viscosity codes with exclusive use of the full computer; these codes of course give interior wave forms as well as shock front behavior.

9. Below a transition pressure like 2 bars or 30 psi, either the quantity QR^4 or YR are constants at long distances for any explosion. Both are proportional to $Y^{4/3}$, and provides a convenient measure of explosion performance:

$$QR^4 = 4.4 \times 10^7 \left(\frac{Y}{Yo}\right)^{4/3}$$

$$YR = 18.4 \times 10^7 \left(Y/Yo\right)^{4/3}.$$

The units for QR^4 are bar cm^4 for Yo in megacalories, or bar $meters^4$ for Yo in KT. The units for YR or megacalories, cm, and kiloton meters respectively.

10. Options for analysis of non-ideal explosions are provided--q = dln Q/dln Z, specific heat H, transition pressure P_2, initial pressure P_1. The analysis therein of nuclear and TNT data showed that the values expected from theory are satisfactory.

11. The final yields are insensitive to uncertainties the input options.

12. Due to the high density in all chemical explosives relative to surrounding air, the pressure-distance curves are initially flat near the charge surface and out to several charge radii.

13. No conclusion is made whether the apparent oscillations observed are real or due to experimental and analytical errors, except to note they are of the same order as natural scatter in pressure-distance data.

14. The programs appear versatile enough to treat a wide variety of different explosions through a simple change in parameters. (Recall Tables 1-1 and 1-2.)

15. The shock front conditions are precisely defined and succinctly stated on the printout. The artificial viscosity method does give much detail on the interior--much more than may be needed or wanted--but the shock itself is smeared out and the peak values are ambiguous.

6. Discussion

Among the more controversial results of Chapter 5 are:

1. Yield of TNT

   720 cal/gm instead of the classic 1000 cal/gm

2. Absolute standard for chemical explosives:

   megacalories or kilograms nuclear vs equivalent weight

3. Pressure-distance curve near the charge:

   $d\ln P/d\ln R = 0$ instead of -3 according to classical similarity solutions

4. Acoustic decay of pressure with distance:

   $d\ln P/d\ln R = -4/3$ instead of -1 or $-(1 + 1/2 \ln R)$

5. Oscillation about the theoretical curve:

   is scatter in data purely random, or a real defect due to simplified calculation.

6.1 Yield of TNT

The number 1,000 cal/gm for the heat of detonation of TNT is so traditional that it cannot be lightly dismissed. It is perhaps the best known number in explosive research. No less than a President of the United States (President Truman, August 1945) introduced the term "kiloton"--which is based on that value--in reporting to the American public that Hiroshima and Nagosaki bombs were equivalent to 20,000 tons of TNT.

We summarize the yields obtained in Chapter 5:

	Nuclear (1 KT)	TNT (1 lb)
Direct evaluation method	0.904 KT	0.328 megacal
Direct scaling method	0.904-0.965 KT	0.327 megacal

Here we have two methods, each giving consistent results with each other for explosives which differ a million-fold in energy and a thousand times in initial energy density. The standard deviations are well within normal experimental scatter.

For one pound of TNT (454 grams), the blast energy of TNT is:

$$\frac{328000}{454} = 720 \text{ cal/gm.}$$

This includes approximately a 25% contribution from afterburning previously demonstrated by Filler in chamber experiments (see Ref. 1SC57), by Swisdak in the conical shock tube (NOLTR 69-61), and in several experiments using nitrogen-filled balloons. This leaves about 600 cal/gm released at the charge surface, well below the classical value of 1000 cal/gm and about half the modern RUBY code value of 1260 cal/gm (NOLTR 63-216). But it is in excellent agreement (600 cal) with the "CO-H_2O-CO_2 arbitrary" such as discussed by Kamlet and Ablard (JCP 48). Whatever the reasons for the discrepancy, the energy delivered to the blast wave is found to be about 700 cal/gm and is the number required to scale TNT with nuclear blast, or other explosives.

I believe the yield for TNT indicated by UTE---= 720 cal/gm with afterburning, 600 cal/gm without--is essentially correct and that the discrepancy with the classical value 1080 cal/gm is explained for the following reasons:

1. The hydrodynamic yields are all consistent as is evidenced in the above Table.

2. Photography belies the idealized stoichiometry assumed for detonation products of TNT.

3. Hydrodynamic yield does not include the waste heat and residual motion of explosive debris.

4. Confinement in a small bomb calorimeter does not reproduce a freely expanding explosion in air.

5. When the heat of detonation of TNT is measured in a large calorimeter, and corrected for the waste heat of the explosive debris (in accord with points 2, 3, 4 above), the hydrodynamic yield is found to be less than 650 cal/gm, consistent with the UTE number.

6. No known burning process is near 100% efficient.

7. Abundant evidence is seen of energy losses due to turbulence, cloud rise, jetting.

8. The formation of a negative phase decouples the blast wave near the front from late time energy production on the interior.

9. Dynamic considerations of stoichiometry.

10. We are here reporting the first absolute measurement of a completely unconfined high-explosive energy release.

11. There is insufficient evidence to show that all the classical chemical reactions of TNT occur swiftly enough to be realized as blast energy.

Widely available photographs*, taken a few seconds after a TNT explosion, completely belie the idealized model of a spherically symmetrical, adiabatically-expanded and cooled ball of carbon dioxide, water vapor, and nitrogen. The classical stoichiometry is:

*An excellent postcard C1487 is printed as a "Travel-time Product, by Grant-Mann Lithographers LTD, Vancouver, B.C., Canada; it shows 500 tons of TNT detonated at the surface of the earth at Suffield Experimental Station, Ralston, Alberta, Canada." Figure 16 in DRES 207 is also a color photograph.

Detonation:

$$C_7H_5N_3O_6 \rightarrow 1\tfrac{1}{2}N_2 + 2\tfrac{1}{2}\ H_2O + 1\ 3/4\ CO_2 + 5\tfrac{1}{4}C$$

Burning:

$$C_7H_5N_3O_6 + \frac{21}{4}\ O_2 \rightarrow 1\tfrac{1}{2}N_2 + 2\tfrac{1}{2}\ H_2O + 7\ CO_2$$

Because the shock itself is usually far out of these photographs, and much burning still occurring, the explosion is far from being an instantaneous energy release as is assumed in the usual stoichiometry. The fireball is still a violently turbulent, jetting mass of free carbon, a great orange cloud of incandescent or still-burning debris on the outside, and a white hot core of inner debris shows through. Of course, much of the heat at late times is due to burning in air: the heat of combustion of TNT is about 4 times the heat of detonation. The enormous waste heat and asymmetry of the debris is clear even from black and white photographs.

The classical detonation theory did not overlook waste heat altogether; the confusion arises because it was generally supposed that the waste heat represented only 2 or 3% of the heat of detonation and from assuming the products are gaseous. Yet, a gram of smoke at an average specific heat of 0.4 cal/gm/degree and average temerature of only 1,000°C would represent 400 cal, which is of the order of the discrepancy under consideration.

Small bomb calorimetry doubtless indicates an energy release of 1,080 cal/gm but is misleading because of the confinement. Owing to reflection from the walls, the hydrodynamic energy in the outgoing shock is stopped, reflected, and intimately mixed with highly heated debris from the fireball. The energy partition we sought to describe

in free air by separating prompt blast energy from the other internal energy is largely negated by the calorimetric mixing. Moreover, there is no assurance that the same chemical reactions occur at the high confined pressures and temperatures of a small calorimeter as occur for debris moving outward in free air. The absolute pressure on the deep interior of an explosion in free air is often near zero; in a small calorimeter are more like initial detonation pressures. In summary: small bomb calorimetry simply does not relate well to a free air explosion or to a thinly cased explosive.

Large bomb calorimetry, such as described by Filler (ISC 6), permits the explosive debris to expand down to a few atmospheres or so, and more nearly relates to an explosion in free air. Afterburning can be eliminated by use of an inert atmosphere such as argon or a vacuum.

When such large calorimetric experiments are performed, they show a 40% or so enhancement of energy release due to a thick case, and Figure 6.1-1 summarizes the results of various investigators by plotting the heat of detonation as a function of the mass ratio: shell case/explosive, S/X. Most significantly, the heat of detonation of bare charges and thin cases--up to S/X = 1--are more like 800 to 850 cal/gm or less. The classic "correct" value of 1080 cal/gm is not achieved unless very thick cases are used, S/X $\cong$ 7. The implication is clear that the small bomb calorimeter does not reproduce a free air explosion, but represents the stoichiometry of an even thicker bomb case--a case so thick that the calorimeter does not rupture.

We also note that all calorimeters perforce measure the waste heat of the explosive debris, as well as the prompt energy actually

delivered to air which appears in the blast wave as hydrodynamic yield.

If an estimate of hydrodynamic yield from calorimetric measurements is based on the data shown in Figure 6.1-1 and evidence from photography, the bookkeeping of energy is summarized by:

Representative heat of detonation, thin case TNT in large calorimeter		800 cal/gm
Waste heat of free carbon in debris		-170 cal/cm
Waste heat of gaseous products		- 40 cal
Hydrodynamic yield	$\simeq$	590 cal/gm

This estimate is in excellent agreement with the UTE result: 720 cal/gm with afterburning, and estimated as 600 cal/gm without afterburning. The highest heat of detonation on Figure 6.1-1 is 860 cal/gm, but the waste heat estimates are both conservative. Hence, it seems safe to say from calorimetric evidence that the hydrodynamic yield of a bare charge of TNT in free air is less than 650 cal/gm.

It is generally conceded that the case effect seen in Figure 6.1-1 in a calorimeter is due to enhanced thermochemistry due to prolonged confinement and thus a longer time for the reactions to occur. But even if this enhancement of thermochemistry does occur, it does not mean that the blast energy delivered to air is correspondingly increased. I have personally observed many times fresh fragments from artillery shells. They are intensely shattered, which must have required much energy. Intense heating is evident from their "tempering colors" of iron oxides from straw to purple, showing that the fragments reached temperatures of 400° to 600° F or 200° to 300° C, (see Reference MEH, Page 6-25). Assuming a specific heat of .12 cal/gm, a

thick case of 8 gms of case/gm of TNT (corresponding to S/X = 8) and a temperature rise of 300°C, then

$$Q = m\, C_v \cdot \Delta T$$
$$= 8 \cdot (.12) \times 300 = 300 \text{ cal}/_{\text{gm TNT}}$$

Thus the entire enhancement of 300 cal/gm would be used up in heating the shell fragments. In a calorimeter, this heat is aggravated by collision of fragments on the walls and transferred back to air.

Coming to reason (6) as why I believe that a TNT explosion does not produce ideal stoichiometry, no known burning process is anywhere near 100% efficient. A well-adjusted oil burner may achieve 60% or 70%. Dacon has listed a great many different possible paths for the thermal decomposition of TNT (Ref. JPC 74). The detonation process is, if anything, even more complex.

Photographs show much evidence of residual motion of the expanding debris. The energy lost in cloud rise could be aggravated by the fact that the pressure measurements are almost always made at the earth's surface, in a direction away from the energy transport in cloud rise.

Categorically, the formation of a negative phase around a shock strength of $\Delta P/Po = 2$, decouples the shock front from many of the late-time energy losses or gains just discussed: heat of combustion, turbulence, calorimetry. Some heat of combustion clearly does get through to the shock front, else we would not see the 20-25% increase in air shock compared with detonations of TNT or pentolite in inert atmosphere. Filler's calorimeter experiment confirmed--within 10%--that 3,500 cal/gm is the heat of combustion in a large calorimeter,

so the bulk of such combustion energy must clearly be too late to support the shock. The DEB results show that about 0.1 megacalories or 1/3 the original energy Yo still remains at the transition pressure. If we imagined that the negative phase did not form, that the shock could continue to be supported and to propagate with $q = 3.5$, instead of $q = 4$, the acoustic energy would be 0.2 megacalories instead of 0.1 megacalories. This is an increase of 33%, raising the heat of detonation proper from about 600 calories to 800 calories. It is not enough to explain the classical heat of detonation, let alone the heat of combustion, in comparison with hydrodynamic yield.

Finally, we report that dynamic considerations of stoichiometry--following the unified theory of explosions--suggest that the lower values of blast yield, as measured here, are probably more realistic than the higher values. Given several possible paths its seems reasonable to assume that natural phenomena will follow whatever path locally produces or requires the least stress or pressure; from this it follows that a detonation, if stable, represents the minimum production of prompt blast energy. This is a fundamental difference with the RUBY code, which maximizes the free energy of the explosion. There are other differences: the prompt blast energy W is not the same as free energy. Further discussion carries us beyond the intent of this paper, which is only an introduction to a new point of view.

In summary, the yields obtained here for TNT do not agree with classical detonation theory or the modern RUBY code but do agree with other theoretical points of view; with experimental data, and with photography.

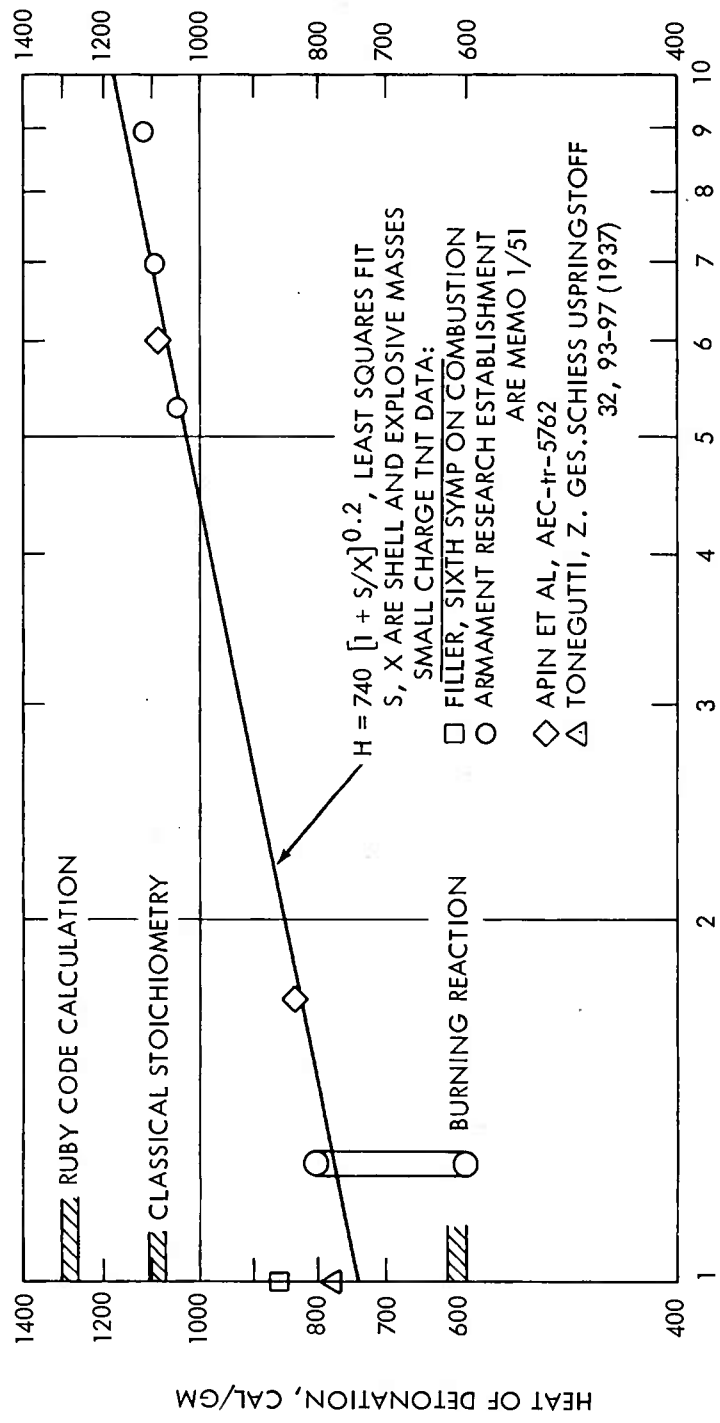


FIG. 6.1-1 EFFECT OF CASE MASS ON HEAT OF DETONATION IN LARGE CHAMBERS IN INERT GAS (after Filler's work).

These data suggest -- albeit insufficient to prove -- that the true heat of detonation of TNT is 740 cal/gm approximately, for an unconfined explosion, without afterburning, but including waste heat of debris. The power law follows from scaling considerations: $dY/dM \sim Y/M$ and cannot depend upon time alone, otherwise large cased charges would not scale. The effect here is analagous to, but independent of, the increased blast efficiency for increased mass, $Y \sim (1 + S/X).28$ approximately. Either way, as Filler notes, the increase is just opposite to the Fano formulae, whereby increased mass is said to deplete the blast energy. The above results are not decisive because the charges were small, even though well-boostered, like 1/4 pound; as such they may merely prove that the role of the case around a small charge is the same as the self-tamping of a large charge.

6.2 Absolute Energy vs Equivalent Weight

The current almost universal practice is to report explosion energy on a basis of equivalent weight to some reference explosive, usually TNT.

The megacalorie = 10^6 cal = 10^{-6} KT = 1 kilogram nuclear is here suggested as a proper, adequate measure of blast energy for chemical explosions. Absolute measures of energy have been the practice for nearly a quarter century on nuclear explosions. The reasons for an absolute measure of energy are even more compelling for chemical explosions than for nuclear explosion, where the hydrodynamics and stoichiometry are simpler and much more straightforward.

As mentioned earlier in the paper, the nuclear kiloton originated at Los Alamos on the basis that TNT releases 1,000 cal/gm: 10^3 cal/gm = 10^6 cal/kgm = 10^9 cal/ton = 10^{12} cal/kiloton. But we observe that the "tons" here meant metric tons, 2208 pounds, more like a long ton and not an English ton as is generally supposed. Beyond that, 1 KT = 10^{12} cal $\cong 4.19 \times 10^{19}$ ergs was a definition with no connection to the energy release of TNT.

One might rationalize that the definition 1 kiloton = 10^{12} calories was intended to imply $.5 \times 10^6$ cal/pound = 1100 cal/gm for TNT. In that case the discrepancy is worse. Besides, the rationalization is not historically correct. A kiloton was defined as 10^{12} cal because it is a round number.

There is another strong modern reason for that choice of a kiloton, because of a coincidence in the number for mechanical equivalent of heat to work. A spectrum of numbers has been variously reported: Joule in 1878 found 1 cal = 4.177×10^7 ergs and Schuster and

Gannon in 1898 found 1 cal = 4.196×10^7 ergs. The currently accepted best value is probably: 1 gram calorie (mean) = 4.186 joules (see Ref. HCP). Now it happens in hydrodynamic calculations that the coefficient $\frac{4\pi}{3}$ often appears in an expression for yield such as in

$$Y = \underbrace{\frac{4\pi}{3} R^3}_{\text{shock volume}} Pf$$

Dividing, we find $\frac{4\pi}{3} = \frac{4(3.1416)}{3} = 4.1888$.
Hence, within 0.07% of the accepted value 4.186 and well within the spread 4.177 to 4.196 we can define interchangeably

$$1 \text{ kiloton} \equiv \frac{4\pi}{3} \times 10^{19} \text{ ergs} \cong 10^{12} \text{ calories}.$$

If pressures are expressed in bars ($= 10^6$ ergs/cm^3) and Y in KT or Kg, the simplification used in DEB and DSC directly follows:

$$Y(KT) = 10^{13} \text{ bar cm}^3$$
$$Y(KT) = 10^7 \text{ bar meter}^3$$
$$Y(KG) = 10^7 \text{ bar cm}^3$$
$$Y(KG) = 10 \text{ bar meter}^3$$

In summary, the radiochemical yields of 1 KT = 4.19×10^{19} ergs and the hydrodynamic yield of 1 KT = $\frac{4\pi}{3} \times 10^{19}$ ergs are virtually identical absolute numbers which have nothing to do with TNT.

Equivalent weight is useful, if it is constant. There is no question that similar explosions do scale. Unfortunately, too few explosions are that similar; equivalent weight varies with pressure. Explosions do scale in the weak shock region, but each has a different efficiency due to its different early history and chemistry. Filler

has suggested that proof firings would be more meaningful if the explosives were surrounded with a mass roughly approximating that of the weapon case than if bare charges are tested.

Some form of reference explosive will always be useful to use as an experimental control. But some preemptive difficulties with an empirical standard are:

1. The standard itself is unknown; any anomalies in the standard explosive, like afterburning, then appear as corresponding anomalies occur in any test explosive with which the standard is compared but will seem low where the standard is high, etc.

2. There is only small assurance that the standard is reproducible and much to suggest it is not.

3. An empirical standard itself must necessarily be fitted to a curve to compare it with data; this introduces unknown biases from curve fittings.

4. Direct comparison of pressure-distance curves on log - log paper is too crude for modern precision in blast measurements, yet the empirical "standard" is perforce a plotted curve and never better.

The DEB and DSC methods do not require abandoning the equivalent weight: they improve on it. Both the standard and test explosives can be readily evaluated. The comparison of numbers on DEB for the two explosives gives an average equivalent weight, averaged over the entire history of each curve. The relative yields in Column 4 of DSC or plotted as in Figure 5.4-2 gives the equivalent weight of each explosive--the standard and the test explosive--relative to the theoretical explosion; hence, relative to each other.

DEB gives the absolute energy directly. Using generalizations mentioned earlier in this paper, the unified theory of explosions can be modified to predict virtually any real explosion within a few percent in yield using DSC methods with simple changes in parameters. The theory then offers an absolute measure and description of blast energy; it does so not on the basis of what our prejudgements from nuclear or chemical stoichiometry say should have happened (in a calorimeter), but consistent with what is actually observed on the explosion under field conditions. Moreover, the departure from scaling is quantitatively and meaningfully described by the parameters (e.g., $q_2 = 4.5$ instead of 4.0) not just a vague discrepancy or merely generating another curve for equivalent weight as a function of shock strength, and another, and another as has been going on for a hundred years.

6.3 Flat Pressure-Distance Curve Close-In

A striking feature here on Figure 5.4-1 is the suppression of the TNT curve at close distances due to the mass effect of the explosive.

The flatness-no decay in pressure with distance--dramatically demonstrates that the energy initially carried by the explosive products--and by the case fragments as well--are not lost permanently as implied by the Fano or Gurney formulas. The fragment energy is gradually, but rapidly transferred to the air. The mass of air engulfed grows rapidly, like R^3, and when the explosion has grown to 10 charge radii or so, the expanded debris is then comparable in mass to the air engulfed. Thereafter, the explosion rapidly approaches similarity to a point source. This close-in flattening was predicted and was found on nuclear explosions also, but of course, at a much higher pressure levels and smaller radii (Ref: LA 1664).

A discrepancy here is that most experimental curves and theoretical curves of which the author is aware all show a monotonic decreasing pressure near the source. But I assert that whenever pressures are actually measured, they show the suppressed pressures close in.

I believe that the curves showing a sharp monotonic decrease in pressure close-in are in error for these reasons:

1. Close-in measurements are usually obtained from time-of-arrival data. TOA methods perforce measure the fastest signal to arrive and these usually are the bow shock from debris. A jet does not represent the average energy per unit volume near the front as

presupposed by "shock pressure." In other words, a time-of-arrival method is not representative unless the shock is fully formed and is spherically symmetrical.

2. The supposition that $P \sim R^{-3}$ close-in is the strong shock similarity condition for a point source. In the early days, the mass effect was not merely neglected in classical theory, as an approximation; there seems no realization that mass made a difference at all. Beyond that, close-in data are usually so scattered that one can draw nearly any curve he pleases through the data to support almost any preconception--and often did.

3. Machine calculations do not allow particulate material to migrate through surrounding air as conservation of momentum demands and as the photographs clearly show. Instead, a definite separation between bomb debris and the air ahead is classically supposed and is intrinsic to Lagrangian mass coordinates. A consequence of this "no-mixing assumption"--where MEZ presupposes mixing--is a "snow plow" effect tending to compress air ahead of the debris. The snow-plow effect inordinately raises the pressures close-in to the charge. But by ten charge radii or so, as the mass effect dies out, pressures approach similarity to point-source values.

Incidentally, this same effect partly explains why the various machine calculations for TNT, all using much higher initial energy than UTE--say 1,000 cal instead of 720--still agrees with the UTE curve far out. The difference is partly due to much higher dissipation of energy due to higher close-in pressures; the flattened curve in UTE represents considerably less yield.

6.4 Acoustic Decay

The argument for a "classical" decay of a weak shock as dln P/dln R = -1 rests on a proof--discussed earlier--that the transformation

$$Z = \frac{\psi}{r}$$

reduces the spherical wave equation

$$\frac{\partial^2 Z}{\partial r^2} + \frac{2Z}{r} - \frac{1}{C^2}\frac{\partial^2 Z}{\partial t^2} = 0$$

to the familiar form for a plane wave

$$\frac{\partial^2 \psi}{\partial r^2} - \frac{1}{C^2}\frac{\partial^2 \psi}{\partial t^2} = 0 \quad .$$

Thus, the familiar properties of a plane traveling wave, such as P_{max} = constant, becomes

$$P(r) = \frac{\text{constant}}{r} \quad .$$

Introducing dissipation, Kirkwood and Brinkley (Ref. PR 71) derived a weak shock decay of the form, C a constant

$$P = \frac{\text{constant}}{R\sqrt{\ln R/C}} \quad .$$

Bethe arrived at the same approximation using a different concept; spreading of the positive phase (Ref. LA 2000). But this decay law is not intrinsically different from R^{-1} because:

$$\ln P = \ln \text{constant} - \ln R - \ln (\ln (R/C))^{\frac{1}{2}}$$

$$\frac{d\ln P}{d\ln R} = -1 - \frac{1}{2\ln(R/C)}$$

$$\lim_{R\to\infty} \frac{d\ln P}{d\ln R} = -1$$

just as in acoustic theory.

On the other hand, introducing dissipation in UTE requires that $Q \sim R^{-4}$ at long distances. If so, at weak pressures, $Q \sim P^3$ so that $P \sim R^{-4/3}$. The idea lies in a derived expression in the QZQ concept that for weak shocks

$$\frac{d\ln P}{d\ln R} = -1 \quad \left[1 + \frac{Q}{PF}\right] .$$

At long distances $Q \sim P^3$ from thermodynamics but $F \sim P^2$ from similarity arguments so that

$$\lim_{P\to 0} \left(\frac{Q}{PF}\right) = \text{constant.}$$

Similar arguments apply at strong shocks, that $\frac{Q}{PF}$ is a constant but not necessarily the same as for weak shocks. In UTE the specific values are

$$\frac{3Q}{PF} = \tfrac{1}{2} \text{ for } P > P_2$$

$$\frac{3Q}{PF} = 1 \text{ for } P < P_2 .$$

At weak shocks it follows that $\frac{Q}{PF} = \frac{1}{3}$ and therefore $\frac{d\ln P}{d\ln R} = -\ 1 + \frac{1}{3} = -4/3$.

An alternate way of stating the argument: the classical result from scaling gives $P \sim Yo^{1/3}/R$ in the acoustic domain. By introducing dissipation, we expect $Y \sim 1/R$ instead of being constant Yo; then if scaling follows the available energy, it implies that $P \sim Y^{1/3}/R \sim 1/R^{4/3}$ as argued above.

Figure 5.2-1 tested this idea of constant q over a spread nearly 10^{12} in Q. Granted, the figure is no rigorous proof that $\frac{d\ln P}{d\ln R} = -\frac{4}{3}$ at weak enough shocks. But similar to a remark made previously about suppression of pressure close-in: all the experimental data say the pressure decays at least as fast as $R^{-4/3}$, all the other theories say it approaches R^{-1}. Yet I know of no actual actual pressure-measurements which do not suggest a steep decay at least like $P \sim R^{-1.25}$ or usually $P \sim R^{-1.40}$ far out.

Sadwin and Christian (NOLTR 71-105) recently reported long range pressure measurements from blasting caps down to 10^{-4} bars which are plotted by a curve of the form $P \sim R^{-1.42}$. This is in good agreement with results reported by Kingery and Pannill in BRL MR 1518 in which surface bursts of TNT up to 100 tons were fitted at long distances by curves of the form $P \sim R^{-1.407}$. These experimental exponents of 1.407 and 1.42 involve surface losses, as well as free air dissipation and for these reasons are considered in good agreement with the UTE value $d\ln P/d\ln R = -4/3$. By contrast the Kirkwood-Brinkley theory is of the form $P \sim \frac{1}{R}\left[\ln \frac{R}{8.3}\right]^{-1/2}$ and at this pressure level would give $\frac{d\ln P}{d\ln R} \simeq -1.07$.

6.5 Are the Oscillations Real?

By oscillation I refer to an apparently sinusoidal behavior in:

Figure 5.2-2 for dln Q/dln Z vs P

Figure 5.4-2 for relative yield vs P.

In Figure 5.4-2 the slope q appears to be a minimum like 3.7 near 0.1 bars, rises to a maximum like 4.3 near 1 bar, and again is well below the idealized value q = 3.5 near 10 bars. It appears as a cycle whose half-period is 10 fold in pressure, i.e., the slope behaves like $\sin(\pi \log_{10} \frac{P}{10})$. Similarly in Figure 5.4-2 the relative yield is a minimum like 0.8--0.9 near 0.2 bars, is a maximum like 1.06--1.2 near 2 bars, and a minimum near 100 bars. Real or not, this is the pattern under discussion.

This oscillation and the possibility of an oversimplification in the UTE has been the most vexing question in the development of the theory. The other questions just discussed--yield of TNT, absolute yield, dln P/dln R = 0 near source, dln P/dlnR = -4/3 far out--are all "controversial" mostly because they are at odds with earlier traditional opinions. But the unified blast theory itself is unequivocal about those questions; it takes the position that the earlier viewpoints are just preconceptions which turned out to be wrong.

The oscillation is a more vexing question because the unified blast theory is equivocal and admits both possibilities, that the effect is real or unreal. And of course, the theory itself could be wrong in the sense that the effect is real but for different reasons than the theory gives. The controversy here devolves upon the fact

that the oscillation is too small to resolve by presently available data. A comprehensive statistical analysis of many sets of data will be required.

The pro's and con's of this question are conveniently listed in Table 6.5; the arguments are listed in juxtaposition deliberately to show the conflict in each facet of the problem. By these pro's and con's, I mean as follows:

1. Curve-fitting. One possibility is that because of the widespread impression that $\lim_{P \to 0} d\ln P/d\ln R = -1$, any attempt to pass a smooth curve through the data, but approaching a final slope of 1 will result in a low fit just before the end of the data; this is indicated in Figure 6.5-1. We might identify the lowness of the experimental curve near 0.2 bar $\cong$ 3 psi to this effect. In support of this hypothesis, that the fitted vurves are spurious near 1 psi, whenever data are actually obtained much below 1 psi, the slope remains much steeper than -1.0 and does not approach the value of 1.

Coming to 1b in Table 6.5, at present UTE assumes that the slope q changes discontinuously at the transition pressure. The plot of QZQ in Figure 5.2-1 indicates also that the break in slope near the transition pressure is quite abrupt. But the waste heat Q itself is a monotonic increasing function of P. Hence, the slope of $d\ln P/d\ln R$ itself would also change discontinuously, as in a cusp at the transition pressure because the slope q increases abruptly.

$$\frac{d\ln P}{d\ln R} = \frac{d\ln P}{d\ln Q} \quad \frac{d\ln Q}{d\ln R}$$

$$\frac{d\ln P}{d\ln R} = \frac{-q}{\frac{d\ln Q}{d\ln P}} .$$

This is indicated, but greatly exaggerated in Figure 6.5-2. In support of this hypothesis that the slope changes discontinuously near P_2, I do find it convenient to fit data with a different French curve above the transition pressure than below.

To counter the curve-fitting hypothesis, the body wave is physically plausible and expected mechanism. We note that although the theory suggests different slopes q = 3.5 and q = 4.0 in the limit for strong and weak shocks respectively, the sharp break at the transition pressure is empirical. There is no theoretical reason why the slope could not change continuously from one assumed value to another, although strong physical reasons exist for the change to occur within the range $1 < \Delta P/P_o < 4$.

Historically the body wave oscillations is one of the oldest features of the unified blast theory and is illustrated in Figure 6.5-3. It was conceived in 1954 for predicting the way in which an underwater nuclear explosion (the ideal wave) and a chemical explosion (pressures initially suppressed) would approach some final similarity, or relative efficiency, to each other.

Some oscillation or ringing may be understood, even for a point-source instantaneous energy release. There is no reason to believe that the cycle of <u>shock</u> compression from ambient pressure P_o, to a shock pressure P_s, followed by an <u>adiabatic</u> expansion will result in exactly zero material velocity when the material expands finally back to ambient pressure P_o. The theory shows (Ref. LA 1664) that the pressure and material velocity are out of phase and the blast wave

oscillates for the same reason as an AC current oscillates. The existence of a negative phase confirms that an "overshoot" occurs. If there remains residual motion of the fireball, the development of such a negative phase does cut off the supply of energy flux W = Pu from the deep interior of the blast. The leading part of the blast is thus isolated and an oscillation could result as the wave form adjusts itself to a new, reduced energy.

Afterburning in oxygen-deficient chemical explosives tends to sustain the strong shock phase by raising pressures on the interior, thus delaying the transition. Similarly, an exceptionally strong mass effect would "continue to push" by inertia, and phenomenologically is equivalent to afterburning. However, in either case, once the negative phase does develop, the approach to the acoustic case ought to be accompanied by larger amplitude of ringing than in the absence of afterburning or mass effect. This idea is qualitatively shown in Figure 6.5-4. If the negative phase developed near the idealized transition pressures, only a moderate oscillation might appear as in the full line. If the negative phase is artificially delayed until B, the extra energy is dissipated in the region ABC, which results in lower pressure and lower dissipation in region DCE. In support of the variations in apparent yield the real one due to body wave ringing, we do observe that the ringing is noticed on afterburning explosives, and less so on balanced explosives and hardly at all on nuclear explosions.

Coming to item 2 in Table 6.5, scatter in data. To date it has never been possible to show that the deviation is statistically significant: the variance of the data is too large.

A general limitation on statistics could apply. Without knowing whether an alternating current was real or not--say a man from Mars--one might well "prove" that the AC deviations observed in voltage were not significant because they were always found to be of the same order as the excursions from the DC component. Similarly, there is no surprise if we have properly fitted a curve and find as much of the curve is low as it is high. Because the true curve is unknown, any arbitrary curve drawn through selecting points is bound to weave back and forth, with the same average value as the true curve.

Nonetheless, and now we are down on the "yes" side No. 2 of Table 6.5, many unbalanced explosives have been analyzed with UTE. The pattern seen in Figures 5.2-2 and 5.4-2 is recognized in a reproducible way. The peak in relative yield always occurs in the range $1.5 < P/P_o < 3.5$. The minimum relative yield always occurs in the range $0.1 < P/P_o < .4$. It seems difficult to accept that this reproducibility is an accident.

The simplest explanation of all for the oscillation is No. 3 under NO: the theory is wrong. The author has an understandable distaste for this explanation.

In defense of the theory, the oscillation does not appear on the best data available, i.e., on fireball measurements of nuclear explosions. Figure 6.5-5 shows an example using the relative yield of two such explosions analyzed by DSC. That the absolute yields checked to a percent or so on each is interesting but not trenchant. That the standard deviation was only 1.6% and that the relative yield is constant down to 50 bars is significant. The deviations we do see are consistent with round-off errors in the data themselves. They do

not show the low relative yield like .94 in the range $30 < P < 200$ seen in Figure 5.4-2 for the nuclear composite. It is difficult to believe that such a splendid correlation as is found with the best nuclear data could be a coincidence, and the theory has been accidentially verified. The explanation seems plausible enough; the 6% variations in relative yield, 2% in radius, is a thoroughly reasonable error in curve reading which went into the tabulation value of ARF D125 data.

The test of the QZQ hypothesis in Figure 5.2-1 is further convincing evidence that the UTE theory is basically correct. In view of that high degree of correlation, over the range 10^{10} in Q, it is easy to argue that all departures from $\frac{d\ln Q}{d\ln Z}$ = constant are accidental.

There is a way to resolve these pro's and con's. We are now down to Item 4 under "Yes": The oscillation is physically real and mathematically imaginary.

The basic theoretical argument was that

$$\frac{d\ln Q}{d\ln Z} = \text{constant}.$$

There is no reason why the constant cannot be complex. In fact, we know that solution $\Psi(x,t)$ to the wave equation is complex, and that spherical solutions are of the form $\Psi(r,t)/r$. If we assume the decay constant for Q is also complex:

that

$$\frac{d\ln Q}{d\ln Z} = \frac{d\ln Q}{d\ln P}\frac{d\ln P}{d\ln Z} = -q \pm ib.$$

we then have

$$\ln Q = -q \ln R \pm ib \ln R$$

$$Q = \frac{\text{const } e^{ib \ln R}}{R^q}$$

This satisfies all the requirements for explaining what we see: an oscillation of small amplitude b superimposed on the general decay R^{-q}. The periodicity we saw in the various figures occurred in terms of log P, and because $\frac{d \ln P}{d \ln R} \simeq$ const, it means they would also be periodic in ln R or in ln Z.

Hence, in answer to the question, "Is the oscillation real?", we can say literally, that variations in $\frac{d \ln Q}{d \ln Z}$ are complex: part real and part imaginary. The real part is $\frac{d \ln Q}{d \ln Z}$, seen constant as in Figure 5.2-2; the imaginary part is a real oscillation about $q = 4$.

This seems a fitting place to explain why an "Introduction" to a Unified Theory of Explosions seemed an appropriate title.

As mentioned previously, the body wave oscillation was conceived in 1954 for underwater explosions preparing the theory for Operation WIGWAM. It was apparent in air data at NOL early in the development of the UTE. It will be a simple matter to accommodate it into DSC506 and solve for the amplitude b of an oscillating q. We already know empirically the imaginary part will have on amplitude about 0.25 for non-balanced explosives.

In view of these prognostications, the reader may well ask why the complex q has not been done in this paper. It was not done for several reasons:

1. The title of the paper and its main goal is an introduction to a unified theory of explosions; variable q is more appropriate as an extension to the present paper.

2. It seems more enlightening to assume constant q, and measure the amplitude of the departures than to prejudge the problem by assuming a form for the perturbation.

3. Essential non-sunt multiplicanda praeter necessitatem.

The first two points are perhaps clear enough. Regarding 3, which is Occam's Razor, we note any theory could be fit by proliferating enough parameters.

The virial equation of state is a case in point: $PV = RT + AT^2 + BT^3 + CT^4$ was long used to describe what can be described much better with a single well-placed constant K as used in

$$P - P_o = \frac{\rho_o C_o^2}{K}\left[\left(\frac{V_o}{V}\right)^k - 1\right].$$

A main advantage of the Unified Theory of Explosion is its simplicity. For most applications, the oscillation of ± 15% in yield means ± 5% in radius and is an unnecessary refinement: it is of the same order as the natural uncertainty of the data. Perhaps the oscillation will prove to be a main result of the natural variations, the effect being obscured because it occurs at slightly different phasing. Occam said it best. Until the phasing can be predicted, until we can use better than 5% accuracy in radius, why complicate the theory prior to necessity?

Table 6.5

IS THE OSCILLATION REAL?

No	Yes
1. Due to curve-fitting	1. Due to body wave
a. $P \sim R^{-1}$ prejudgement	a. negative phase cut-off
b. failure to recognize break	b. afterburning
	c. mass effect
2. Due to scatter in data	2. Seems a consistently recognizable pattern
3. Due to systematic error in UTE	3. Oscillation does not appear in the best fireball data
4. $\frac{d \ln Q}{d \ln Z} = q$ (a constant) over a 10^{12} range in Q	4. $\frac{d \ln Q}{d \ln Z} = q + ib$

Conclusion: The oscillation is complex: part real and part (mathematically) imaginary.

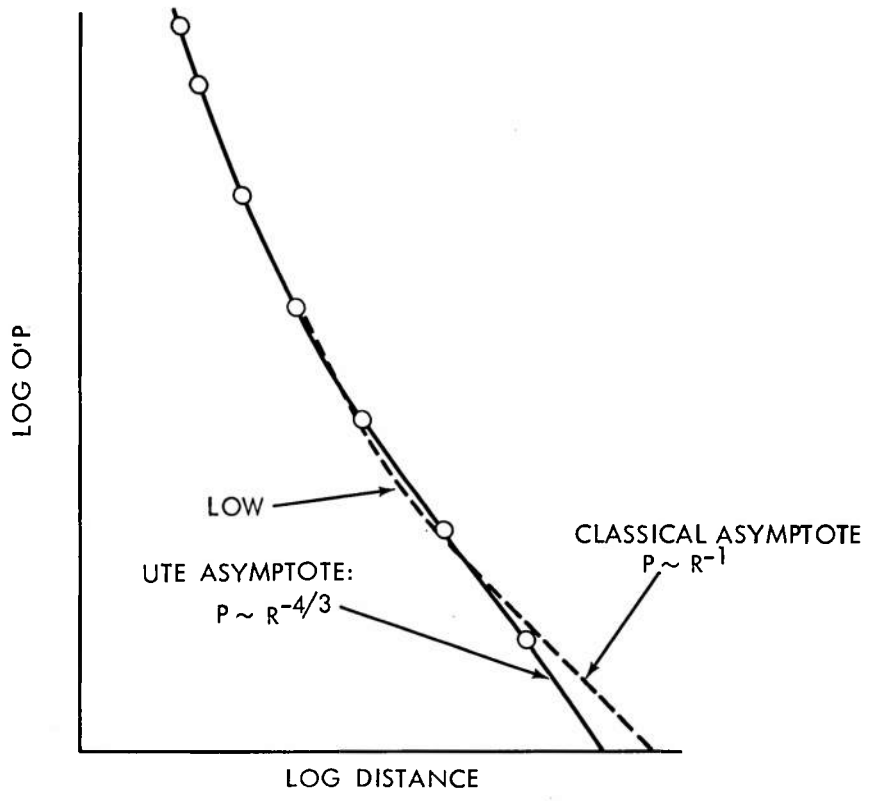


FIG. 6.5-1 POSSIBLE DISTORTION DUE TO CLASSICAL ASSUMPTION.
If drawn with $P \sim R^{-1}$ at long distances, a fitted curve is forced to be low just before the end of the data.

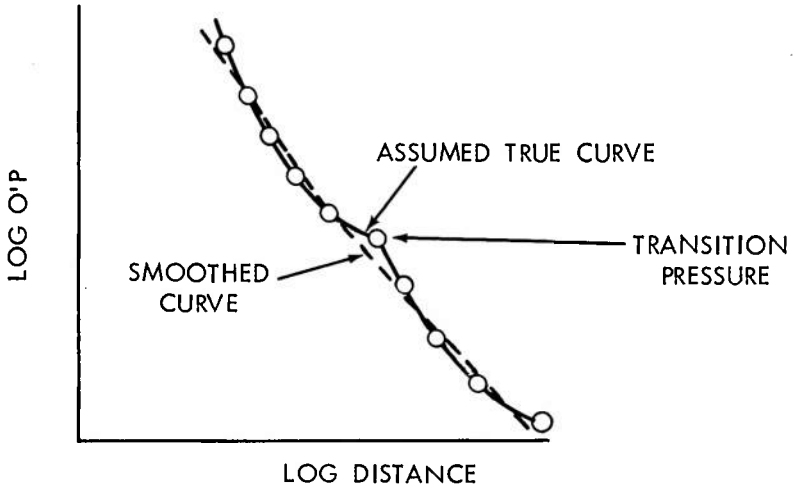


FIG. 6.5-2 POSSIBLE DISTORTION DUE TO FAILURE TO RECOGNIZE CUSP AT TRANSITION PRESSURE.
As a result, a fitted curve oscillates near the cusp.

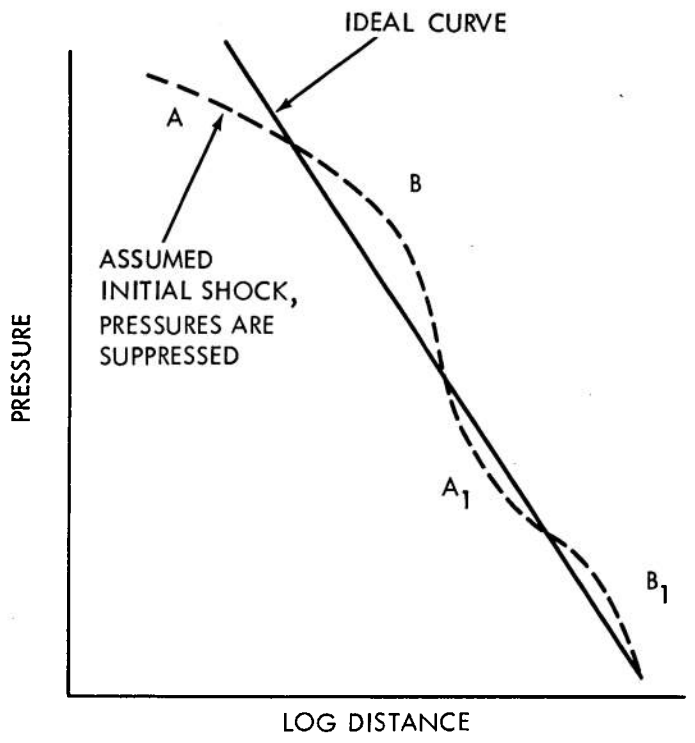


FIG. 6.5-3 BOW EFFECT: AN OSCILLATION DUE TO PERTURBED EARLY HISTORY. Whenever the real curve lies below the ideal curve (A), shock dissipation is lower than normal, and peak pressure tends to be relatively sustained. Whenever the real curve lies above ideal (B), shock dissipation and decay are relatively greater. Critical damping can occur, but as in most physical processes, the real curve usually approaches the ideal curve by a series of damped oscillation (A_1, B_1)

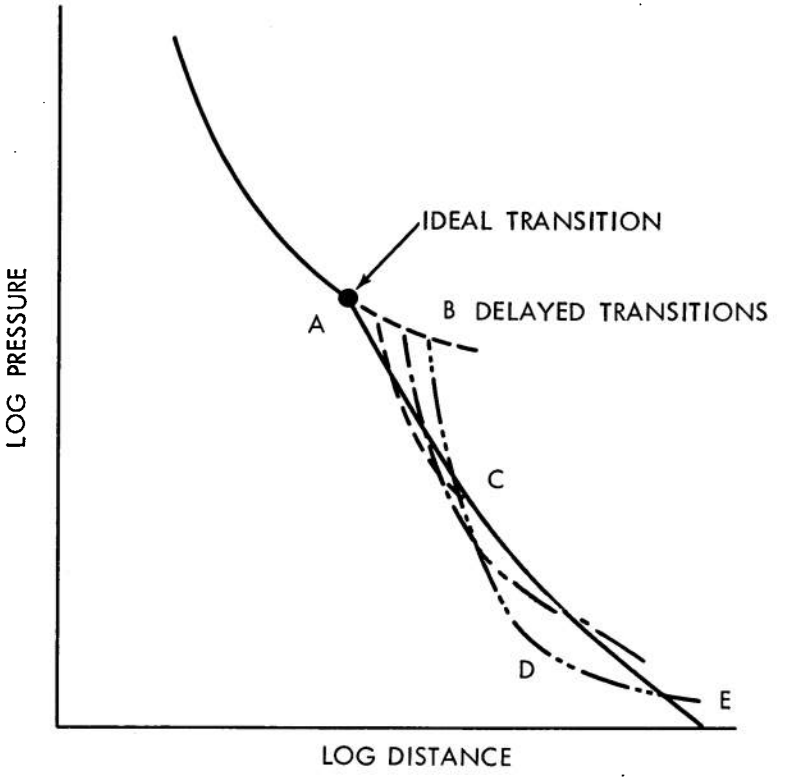


FIG. 6.5-4 A SUGGESTED RELATION BETWEEN THE DELAY OF TRANSITION AND AMPLITUDE OF OSCILLATIONS.
The longer the delay, the greater the oscillation.

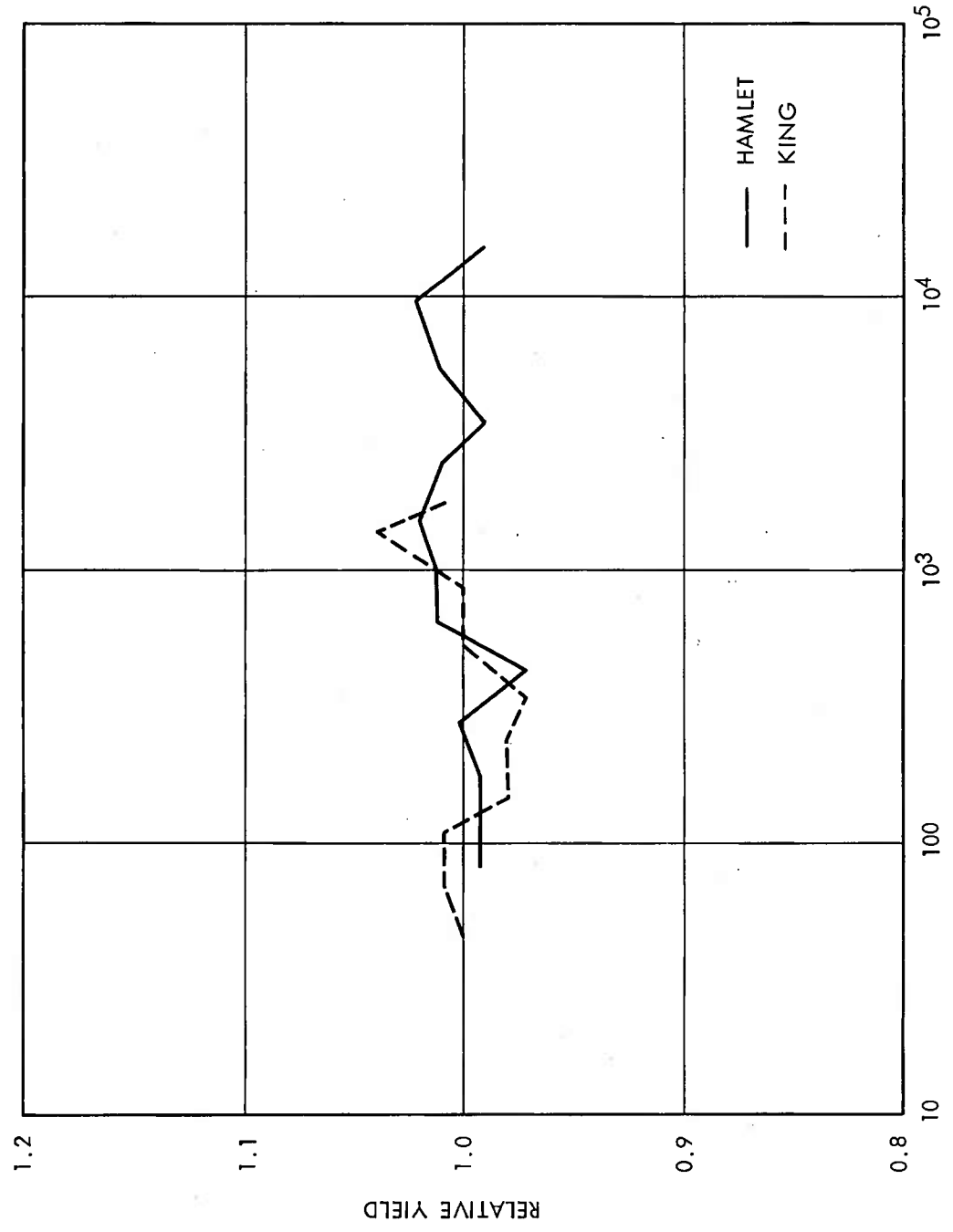


FIG. 6.5-5 RESULTS OF DSC ANALYSIS ON TWO NUCLEAR EXPLOSIONS.
The mean values of yield are well within experimental error and standard deviations are about 1.6% in yield, 0.5% in radius -- like round-off errors of data.

ALPHANUMERIC REFERENCES

AIAA Bach, G. C. and Lee, J. H. S., "An Analytical Solution for Blast Waves", AIAA Journal, Vol. 8, No. 2, pp. 271-275, February 1970

ARF D125 Porzel, F. B. and Parsons, W. D., "Analytic Solution for Wave Forms and Energy Release of a Point Source", Final Rpt, Armour Research Foundation Project D125 for the Los Alamos Scientific Laboratory, ARF D125 (1958)

The first formal application of DEB to explosions in air is given in Appendix A of this paper. It applied the waste heat approach previously found successful in WT 1034 for water and in WT 1495 for rock. However, Q was calculated differently from the present procedures.

ARF TM421 Porzel, F. B., "New Concepts for Control and Use of Nuclear Explosions", Armour Research Foundation for American Society of Civil Engineering (1959) and Second Plowshare Symposium, San Francisco, May 1959

BRL MR1518 Kingery, C. N. and Pannill, B. F., "Peak Overpressure versus Scaled Distance for TNT Surface Bursts", Ballistic Research Laboratory Memorandum Report No. 1518, Apr 1964, (AD 443102)

C1487 Post Card, "500 Tons of TNT", See frontispiece. The author has a limited supply of the original colored post cards and will send one on a request. Write, F. B. Porzel, Code 241, Naval Ordnance Laboratory, Silver Spring, Md. 20910

DASA 1285 "Nuclear Geoplosics, Part One--Theory of Directly Induced Ground Motion", Defense Nuclear Agency, formerly Defense Atomic Support Agency, edited by J. Naar, May 1964 (see Chapter 4 therein).

DASA 1559 Mills, Fisch, Jezek, and Baker, "Self-Consistent Blast Wave Parameters," Aircraft Armaments Inc. (AAI), for Defense Nuclear Agency, then Defense Atomic Support Agency, Oct 1964

DRES 207 Dewey, J. M., "The Air Velocity and Density in Blast Waves from TNT Explosions," Suffield Rpt 207, Defense Research Board, Canada

ENW "Effects of Nuclear Weapons," U. S. Government Printing Office, as reprinted in 1964

ISC 57 Filler, W. S., "Post Detonation Pressure and Thermal Studies of Solid High Explosives in a Closed Chamber," Sixth International Symp on Combustion, Reinhold, N. Y., 1957

IDA P150 Porzel, F. B., "Mean Pressure Method for Scaling Explosions in a Non-Uniform Atmosphere," Institute for Defense Analyses, Oct 1964

HCP Handbook of Chemistry and Physics, Chemical Rubber Publishing Company

JAP 26 Brode, H. L.: Numerical Solutions of Spherical Blast Waves. Journal of Applied Physics, Vol. 26, No. 6 pp. 766-775, Jun 1955

JPC 74 Dacons, J. C., Adolph, H. G., and Kamlet, M. J., "Some Novel Observations Concerning Thermal Decomposition," Journal of Physical Chemistry, 74, 3035 1970

JCP 48 Kamlet, M. J., and Ablard, J. E., Journal of Chemical Physics, 48, p. 36-42

LA 1664 Porzel, F. B., "Height of Burst for Atomic Bombs, (1954), Part 1, The Free Air Curve", Los Alamos Scientific Laboratory, May 1954

Chapters 2.2, 2.3 therein, give details of the ANS method. For a number of years ANS was one of two absolute methods used as standard diagnostic techniques for determining the absolute yield on tests of nuclear weapons. Radio chemistry was the other method. Appendix A therein tabulates the results of IBM run, the earliest and still perhaps the most accurate of machine solutions to the blast wave; one of the very few not using artificial viscosity.

LA 1665 Porzel, F. B., "Height of Burst for Atomic Bombs (1954) Part II, Theory of Surface Effects", Los Alamos Scientific Laboratory, May 1954

This is a comprehensive analysis of the interaction of nuclear blast with a real ground surface. Effects are categorized into two classes: thermal effects due to thermal radiation exploding the ground surface and drastically heating the nearby surface layer of air prior to shock arrival, and mechanical effects in the blast wave, due to dust-loading, turbulence, surface viscosity absorption of energy by ground shock. The main effect of each is a severe reduction of peak pressure at the shock front.

LA 2000 Bethe, Fuchs, Hirsehfilder, Magee, Peierls, von Neumann, "Blast Wave", Los Alamos Scientific Laboratory, Mar 1958

LADC 1133 Porzel, F. B., and Baker, W. D., "Thermodynamic Properties of Air," Los Alamos Scientific Laboratory, Sept 1951

Graphs were given for the properties of air for states along the shock front and within the blast wave, based on what is now referred to as the "variable epsilon theory." The concept was used to correlate extensive calculations for the equation of state of real air, as by Hirschfelder and Curtiss in their 1948 paper, "Thermodynamic Properties of Air II," also by Bethe, Peierls, et al in LA 2000 and in OSRD 3550.

These graphs are now available, along with an exposition of the theory in Section 2.2.2 of LA 1664 and Figures 2.2.2-1 to 2.2.2-4 therein.

MEH Marks, "Mechanical Engineers Handbook," Mcgraw Hill, 6th Edition, 1958

NOL Internal Memorandum Porzel, F. B., "BASIC Program for Blast Energy of an Explosive using the Prompt Energy Theory," Naval Ordnance Laboratory, 14 Feb 1969. An interim theoretical prediction for point source explosions is used as the reference curve for the DSC Method, using the mini-equation method MEQ.

NOLTR 62-168 Lehto, D., and Lutzky, M.: One Dimensional Hydrodynamic Code for Nuclear-Explosion Calculations. Naval Ordnance Laboratory, White Oak, Md., May 1964

NOLTR 63-216 Price, D., and Hurwitz, H., "Ruby Code Calculations of Detonation Properties I. C-H-N-O Systems," Naval Ordnance Laboratory, White Oak, Md., 1 Nov 1963

NOLTR 69-61 Swisdak, M. M., Jr., "A Comparison of Explosives in a Conical Shock Tube, Apr 1969

NOLTR 71-105 Sadwin, L., and Christian, E. A., "Characteristics of the Shock Wave Generated in Air by a Blasting Cap," Naval Ordnance Laboratory, White Oak, Md., 18 Jun 1971

OSRD 3550 "Tables of the properties of air along the Hugoniot curve and the adiabatics terminating in the Hugoniot curve", by S. R. Brinkley, Jr., J. G. Kirkwood, and J. M. Richardson, Report OSRD-3550

OSRD 5137 Brinkley, Stuart R., Jr., and Kirkwood, John G., "Tables and Graphs of the Theoretical Peak Pressures, Energies and Positive Impulses of Blast Waves in Air," OSRD 5137, Div. 2., NRDC and OSRD circa 1944. Calculations for a point source for explosives are carried out following methods later reported in Phys. Rev., 71. The initial energy release and pressure are obtained by curve-fitting to measured data. The heat of detonation so obtained for TNT is 1170 cal/gm and about 60% high if compared with values presently obtained for Y_o on TNT using either DEB or DSC analyses.

Ph. Rev. 71 Brinkley, Stuart R., Jr., and Kirkwood, John G., "Theory of the Propagation of Shock Waves," The Physical Review, Phys. Rev. 71, 606, 1947.

This is the classical Kirkwood-Brinkley paper on this subject. The method is more like ANS than DEB or

DSC; an arbitrary wave form is assumed for energy flux vs time at a fixed distance. Like DEB, the dissipation equation is used to partition energy, but with a somewhat different terms: "h" there is the enthalpy increment instead of a generalized waste heat Q as in DEB; D(R) there corresponds to Y(R) in DEB, but is then set equal to the time integral of energy flux at fixed distance R instead being the space integral of energy at a fixed time as in DEB.

RM 1824 Brode, H. L.: Point Source Explosion in Air, The Rand Corporation, Research Memorandum RM-1824-AEC, Dec 3, 1956

RM 1965 Brode, H. L.: A Calculation of the Blast Wave from a Spherical Charge of TNT. The Rand Corporation Report RM-1965, Aug 1957

RM 1974 Brode, H. L.: Theoretical Solutions of Spherical Shock Tube Blasts. The Rand Corporation, Research Memorandum, RM-1974, Sept 1957 (ASTIA AD 206491)

UNP434 Porzel, F. B., "Some Hydrodynamic Problems of Reactor Containment," Second UN Conference on Peaceful Uses of Atomic Energy, UN Paper 434, Geneva, 1958

von Neumann, J. "The Point Source Solution", Collected works of J. von Neumann, Vol VI. Pergammon Press, Oxford, England, 1963, Mac Millan, New York

WT 1495 Porzel, F. B. and Anderson, D. C., "Close-in Time-of-Arrival Measurements for Yield of Underground RAINIER Shot", Final Report, Project 25.1, Operation PLUMBOB, WT 1495, 1959. RAINIER was the first contained underground nuclear explosion done at Nevada Test Site in 1957. As in WT 1034, both DEB and ANS methods were used to obtain the official yield of 1.7 KT. As a point of practical interest regarding the importance of Q, at 18 meters (55 feet) from the explosion the dissipated fraction of initial energy (the DEB part) was .78, the remaining energy (the ASB part) was .22; thus, most of the energy was already dissipated at a radius (55 feet) corresponding to the final cavity radius of the explosion.

Taylor Taylor, G. I., "The Formation of a Blast Wave by a Very Intense Explosion, Theoretical Discussion", Proceedings of the Royal Society (London), Series A, Vol. 201, 1950, pp. 159-174.

APPENDIX A

BASIC Machine Language: Conventions and Purposes

A.1 Foreword

The principal means for communicating the logic of the unified theory of explosions in this paper is the LIST or program instructions. Eight positive reasons for this approach are discussed briefly below.

There is only one--and a minor--disadvantage: not everyone understands the machine language BASIC. True, to write a program in BASIC requires skill and practice, mainly in knowing how to use the few precise words to which the machine will respond. But to read BASIC is a minor obstacle because it requires learning only a few conventions and words which are not already obvious to a reader of English.

The proposal here is that the BASIC instructions, reasonably annotated, provides a new effective means of technical exposition because of advantages which greatly outweigh the inconvenience of learning the few new terms. Nearly a century ago, Willard Gibbs aptly wrote, "But mathematics too is a language" for reasons which nowadays seems so obvious as to be overlooked. Machine languages are no longer special purpose tools. Some universities, University of Maryland for example, now accept a machine language as fulfillment of the language requirement for a PhD.

First we list the benefits in Section B-2 then the modest cost (a few new terms) in B-3.

A.2 Benefits of Exposition in BASIC

Among the positive reasons for choosing to express the arguments for DEB and DSC in BASIC are the following:

1. Completeness. The program LIST insures that all elements of the derivation have been stated. There can be no hidden steps, "fudge factors" or tacit assumptions. The LIST demonstrates that the information is complete enough for an idiot (the machine) to follow.

2. Succinct. Excess verbiage is deleted, except for clearly labelled remarks. No one wants a treatise, when a dictionary serves the purpose.

3. Clarity. The logic is guaranteed to be stated in workable order. Parameters are readily identified by statements which read

LET H = (Number),

data identified by the word DATA followed by numbers and variables by expressions involving variables (letters) on the right hand side.

4. Accuracy. There is virtually no chance of significant typographical errors in the LIST or in the printed results. No proofreading is necessary for the LIST or for the tabulated results.

5. Accessibility. A stored program can make the nearest teletype not only the reference library, but a robot who will retrieve and then execute the program--if one is stored.

6. Utility. The LIST is a step-by-step procedure for performing the calculation. The nearest teletype performs the calculation without requiring the user even to review the equations.

7. Record-Keeping. The print out is an accurate, permanent record of results, suitable for final copy of a report.

8. Versatility. The program may be readily modified to print out all other computed quantities and to generalize the parameters when they have broader meaning.

A.3 BASIC Conventions:

Among the main conventions in BASIC used DSC and DEB are these:

1. The asterisk * means "multiply by"; thus A*B means AB in ordinary algebra.

2. An upward arrow ↑ means "raise to a power"; thus A ↑ 3 means A^3.

3. A number immediately following a letter means a subscript; thus Q3 means Q_3.

4. The right hand side of an equation is reserved for variables whose values are already known. To the left of the equal sign must be a single letter whose value is to be calculated as instructed on the right hand side. Thus once that A and B are known, LET C = A * B means C = AB in algebra.

A new convention arises: the same letter may appear on both sides of the equal sign, with the new value on the left and the old value on the right. Thus

LET M = M*H means $M_2 = M_1 H$,

or "take the old value of M," multiply it by H and store the product as the new value of M.

5. REM means a "remark," is for the benefit of the reader, and has no effect on the program.

6. INT (X) means "integer value of X"; it truncates the decimal part of the number X; thus INT (3.78) = 3.

7. Ø as printed by the teletype means letter O; O means numeral zero.

Other than the above specialized terms, the rest is basic English and algebra:

1. DEB and DSC use about eight English words which mean just what they say:

PRINT

LET

IF ... THEN

GO TO

DATA

END

2. The symbol for division is the usual /; successive slashes are read in the normal order left to right. That is,

A/B/C means (A/B)/C not A/(B/C).

3. Only parentheses are used and are necessarily in pairs, as is usual; thus

((A+B)/C+D)*(E+F) means $\left[\frac{(A+B)}{C} + D\right]\left[E+F\right]$

4. The sequence of logic follows the line numbers as written.

APPENDIX QVP

Waste Heat Calculations for Ideal Gases and Real Air

QVP506 is a BASIC program which calculates the waste heat for real air and for ideal gases using the conventional adiabatic expansion path. Tables 1-15 give the results. The quantity tabulated is always the waste heat normalized to ambient pressure and specific volume, the dimensionless quantity Q/P_oV_o, and rounded off to three significant figures.

The LIST and nomenclature for the program are Tables 16 and 17 of this Appendix. The theory was discussed briefly in Sections 1.3 and 2.7.

There are three sets of tabulated results:

1. Tables 1-3, acoustic approximation, ideal gases
2. Tables 4-9, moderate pressures, ideal gases
3. Tables 10-15, high pressure, real air

In the first two sets, the tables show Q for gases of 4, 3, 2, and 1 atoms per molecule using the classical value of ratios for specific heat of n atoms, $K = (2n + 3)/(2n + 1)$. These values for K are tabulated in the headings of the columns. Tables 10-15, for high pressures, apply only to air.

The acoustic approximation is used in the first set of tables:

$$Q = \frac{K+1}{12} \left(\frac{P}{K}\right)^3 (1 - 1.5P)$$

as is shown by line 320 of the LIST and at the head of each Table 1-4. Normally, this approximation applies only below P = 0.01 but higher pressures up to P = 0.1 are given in Table 3 for comparison with the exact formula in Tables 4-9.

The classical adiabat is used in the second set of tables for $0.001 < P < 1000$. The equations for density ratio D and waste heat Q are shown in 350 and 360 as:

$$D = \frac{\frac{K+1}{K-1} P + \frac{2K}{K-1}}{P + \frac{2K}{K-1}}$$

$$Q = \frac{1}{K-1} \left[\left(\frac{1+P}{D} \right)^{1/K} - 1 \right] .$$

At low pressures, the term for Q in brackets is a small difference between two numbers close to 1. A comparison of Table 2 for P = 0.001 and the acoustic approximation with Table 4 for P = 0.001 and the standard adiabat shows no significant difference between them. But Q itself is of the order 10^{-11}; the NOL computer carries 14 decimal places. If the computer--or hand calculation--were carried to only 6 significant figures, the acoustic approximation would be necessary up to P = 0.1. A comparison of Table 3, at P = 0.095, K = 11/9 and the acoustic approximation gives $Q = 7.46 \times 10^{-5}$. Whereas, Table 5, for P = 0.095, K = 11/9 using the exact formula gives $Q = 7.58 \times 10^{-5}$. Hence the error in the acoustic formula is (7.58 - 7.46) x 100/7.5 = 1.6%. This is remarkably close agreement at P = 0.095, considering that the acoustic approximation will fail completely, and go negative for $P > 1/1.5$ (because of the correction term (1 - 1.5 P) in the acoustic formula).

Approximate expressions for real air apply for P > 10 bars, above which the ideal gas law fails. Two values of Q are shown in Tables 10-15: both are of the same form as shown in line 390.

$$Q = 10^{\frac{(22-L)(L-1)}{16}}$$

Line 390 is a theoretically derived expression, where the parameters 22 and 16 have been rounded off because the theory was no more certain than these whole numbers. Line 398 is an empirical correction, suggested by nuclear fireball data, in which the parameter 22 is replaced by 21.75. A comparison of these values measures the sensitivity of Q to this parameter, Tables 10 to 15 also provide a comparison with the ideal gas law.

In Tables 10 to 15 note that:

1. All three expressions--ideal, parameter 22, parameter 21.75-are in reasonable agreement--5% or better, near P = 3 and up to P = 20. At P = 3, the respective values for Q are

.192, .198, .202.

2. Exact agreement occurs near P = 3.5.

3. Exact agreement occurs 11 < P < 12, (it is actually near P = 11.25).

4. The ideal gas law fails markedly for P > 20. Near P = 200, about the highest pressures of interest for chemical explosives, the ideal gas law gives a Q about 40% of the real air value, Q = 16 compared with Q = 40.

5. Near P = 200 there is only a minor difference between the two real gas approximations, Q = 40 compared with Q = 38.1, a spread of 5%. Thus the equation of state poses no uncertainty for chemical explosives, provided the real gas laws are used.

6. For pressures near the end of the radiative phase for nuclear explosions, P = 75000 bars, the two approximate formulas differ by about 15%, Q = 14000 compared with Q = 12200. At P = 10000,

about the highest pressures of interest even in fireball measurements, the spread is about 10%. No serious uncertainty appears for most practical purposes on analysis of fireball data. We note, however, that the ideal gas law fails by a factor of 10 in the domain of the radiative phase.

For pressures $P > 10^5$, the hydrodynamic analyses are inadequate and the tables do not apply; energy transport is controlled by radiation. The last table, giving Q for $P \rightarrow 10^6$ is mostly for analytic, not practical interest.

Given the nomenclature (Table 17) the LIST (Table 16) is almost self-explanatory.

The definition shown in lines 40 to 60

```
40  LET N = .43429448
50  LET J = 2
60  DEFFNI(Q)=INT(10↑(N*LOG(Q)-INT(N*LOG(Q))+J)+.5)*10↑INT(N*LOG(Q)-J)
```

is a device for rounding off Q to J + 1 significant figures, noting that

$$\log_{10}(Q) = 0.43429448 \log_e(Q)$$

and based on the identity

$$Q = 10^{\log_{10} Q}$$

TABLE QVP-1

WASTE HEAT FØR IDEAL GASES, Q*DØ/PO, ACØUSTIC APPRØXIMATIØN

$$Q = \frac{K+1}{12} \left(\frac{P}{K}\right)^3 \left(1 - 1.5P\right)$$

ØVERPRESSURE RATIØ	WASTE HEAT, Q*DO/PO			
	TETRATØMIC	TRIATØMIC	DIATØMIC	MØNØATØMIC
(PS-PO)/PO	K=11/9	K=9/7	K=7/5	K=5/3
.0001	1.01000E-13	8.96000E-14	7.29000E-14	4.80000E-14
.00011	1.35000E-13	1.19000E-13	9.70000E-14	6.39000E-14
.00012	1.75000E-13	1.55000E-13	1.26000E-13	8.29000E-14
.00013	2.23000E-13	1.97000E-13	1.60000E-13	1.05000E-13
.00014	2.78000E-13	2.46000E-13	2.00000E-13	1.32000E-13
.00015	3.42000E-13	3.02000E-13	2.46000E-13	1.62000E-13
.00016	4.15000E-13	3.67000E-13	2.98000E-13	1.97000E-13
.00017	4.98000E-13	4.40000E-13	3.58000E-13	2.36000E-13
.00018	5.91000E-13	5.23000E-13	4.25000E-13	2.80000E-13
.00019	6.95000E-13	6.15000E-13	5.00000E-13	3.29000E-13
.0002	8.11000E-13	7.17000E-13	5.83000E-13	3.84000E-13
.00022	1.08000E-12	9.54000E-13	7.76000E-13	5.11000E-13
.00024	1.40000E-12	1.24000E-12	1.01000E-12	6.63000E-13
.00026	1.78000E-12	1.57000E-12	1.28000E-12	8.43000E-13
.00028	2.23000E-12	1.97000E-12	1.60000E-12	1.05000E-12
.0003	2.74000E-12	2.42000E-12	1.97000E-12	1.30000E-12
.00032	3.32000E-12	2.94000E-12	2.39000E-12	1.57000E-12
.00034	3.98000E-12	3.52000E-12	2.86000E-12	1.89000E-12
.00036	4.73000E-12	4.18000E-12	3.40000E-12	2.24000E-12
.00038	5.56000E-12	4.91000E-12	4.00000E-12	2.63000E-12
.0004	6.49000E-12	5.73000E-12	4.66000E-12	3.07000E-12
.00045	9.24000E-12	8.16000E-12	6.64000E-12	4.37000E-12
.0005	1.27000E-11	1.12000E-11	9.10000E-12	6.00000E-12
.00055	1.69000E-11	1.49000E-11	1.21000E-11	7.98000E-12
.0006	2.19000E-11	1.93000E-11	1.57000E-11	1.04000E-11
.00065	2.78000E-11	2.46000E-11	2.00000E-11	1.32000E-11
.0007	3.48000E-11	3.07000E-11	2.50000E-11	1.64000E-11
.00075	4.27000E-11	3.78000E-11	3.07000E-11	2.02000E-11
.0008	5.19000E-11	4.58000E-11	3.73000E-11	2.45000E-11
.00085	6.22000E-11	5.50000E-11	4.47000E-11	2.94000E-11
.0009	7.38000E-11	6.52000E-11	5.31000E-11	3.49000E-11
.00095	8.68000E-11	7.67000E-11	6.24000E-11	4.11000E-11

TABLE QVP-2

WASTE HEAT FØR IDEAL GASES, Q*DØ/PO, ACØUSTIC APPRØXIMATIØN

$$Q = \frac{K+1}{12}\left(\frac{P}{K}\right)^3 \left(1 - 1.5P\right)$$

ØVERPRESSURE RATIØ (PS-PO)/PO	WASTE HEAT, Q*DO/PO TETRATØMIC K=11/9	TRIATØMIC K=9/7	DIATØMIC K=7/5	MØNØATØMIC K=5/3
.001	1.01000E-10	8.95000E-11	7.28000E-11	4.79000E-11
.0011	1.35000E-10	1.19000E-10	9.69000E-11	6.38000E-11
.0012	1.75000E-10	1.55000E-10	1.26000E-10	8.28000E-11
.0013	2.22000E-10	1.97000E-10	1.60000E-10	1.05000E-10
.0014	2.78000E-10	2.45000E-10	2.00000E-10	1.31000E-10
.0015	3.42000E-10	3.02000E-10	2.45000E-10	1.62000E-10
.0016	4.14000E-10	3.66000E-10	2.98000E-10	1.96000E-10
.0017	4.97000E-10	4.39000E-10	3.57000E-10	2.35000E-10
.0018	5.90000E-10	5.21000E-10	4.24000E-10	2.79000E-10
.0019	6.94000E-10	6.13000E-10	4.99000E-10	3.28000E-10
.002	8.09000E-10	7.15000E-10	5.81000E-10	3.83000E-10
.0022	1.08000E-9	9.51000E-10	7.74000E-10	5.09000E-10
.0024	1.40000E-9	1.23000E-9	1.00000E-9	6.61000E-10
.0026	1.78000E-9	1.57000E-9	1.28000E-9	8.40000E-10
.0028	2.22000E-9	1.96000E-9	1.59000E-9	1.05000E-9
.003	2.73000E-9	2.41000E-9	1.96000E-9	1.29000E-9
.0032	3.31000E-9	2.92000E-9	2.38000E-9	1.57000E-9
.0034	3.97000E-9	3.50000E-9	2.85000E-9	1.88000E-9
.0036	4.71000E-9	4.16000E-9	3.38000E-9	2.23000E-9
.0038	5.53000E-9	4.89000E-9	3.98000E-9	2.62000E-9
.004	6.45000E-9	5.70000E-9	4.64000E-9	3.05000E-9
.0045	9.18000E-9	8.11000E-9	6.60000E-9	4.34000E-9
.005	1.26000E-8	1.11000E-8	9.04000E-9	5.96000E-9
.0055	1.67000E-8	1.48000E-8	1.20000E-8	7.92000E-9
.006	2.17000E-8	1.92000E-8	1.56000E-8	1.03000E-8
.0065	2.76000E-8	2.44000E-8	1.98000E-8	1.31000E-8
.007	3.44000E-8	3.04000E-8	2.47000E-8	1.63000E-8
.0075	4.23000E-8	3.74000E-8	3.04000E-8	2.00000E-8
.008	5.13000E-8	4.53000E-8	3.69000E-8	2.43000E-8
.0085	6.15000E-8	5.43000E-8	4.42000E-8	2.91000E-8
.009	7.29000E-8	6.45000E-8	5.24000E-8	3.45000E-8
.0095	8.57000E-8	7.57000E-8	6.16000E-8	4.06000E-8

TABLE QVP-3

WASTE HEAT FOR IDEAL GASES, Q*D0/P0, ACOUSTIC APPROXIMATION

$$Q = \frac{K+1}{12}\left(\frac{P}{K}\right)^3 (1 - 1.5P)$$

OVERPRESSURE RATIO (PS-P0)/P0	WASTE HEAT, Q*D0/P0 TETRATOMIC K=11/9	TRIATOMIC K=9/7	DIATOMIC K=7/5	MONOATOMIC K=5/3
.01	9.99000E-8	8.83000E-8	7.18000E-8	4.73000E-8
.011	1.33000E-7	1.17000E-7	9.54000E-8	6.28000E-8
.012	1.72000E-7	1.52000E-7	1.24000E-7	8.15000E-8
.013	2.18000E-7	1.93000E-7	1.57000E-7	1.03000E-7
.014	2.72000E-7	2.41000E-7	1.96000E-7	1.29000E-7
.015	3.35000E-7	2.96000E-7	2.40000E-7	1.58000E-7
.016	4.05000E-7	3.58000E-7	2.91000E-7	1.92000E-7
.017	4.86000E-7	4.29000E-7	3.49000E-7	2.30000E-7
.018	5.76000E-7	5.09000E-7	4.14000E-7	2.72000E-7
.019	6.76000E-7	5.97000E-7	4.86000E-7	3.20000E-7
.02	7.87000E-7	6.95000E-7	5.66000E-7	3.72000E-7
.022	1.04000E-6	9.23000E-7	7.50000E-7	4.94000E-7
.024	1.35000E-6	1.19000E-6	9.71000E-7	6.40000E-7
.026	1.71000E-6	1.51000E-6	1.23000E-6	8.11000E-7
.028	2.13000E-6	1.88000E-6	1.53000E-6	1.01000E-6
.03	2.62000E-6	2.31000E-6	1.88000E-6	1.24000E-6
.032	3.16000E-6	2.80000E-6	2.27000E-6	1.50000E-6
.034	3.78000E-6	3.34000E-6	2.72000E-6	1.79000E-6
.036	4.48000E-6	3.96000E-6	3.22000E-6	2.12000E-6
.038	5.25000E-6	4.64000E-6	3.77000E-6	2.48000E-6
.04	6.10000E-6	5.39000E-6	4.38000E-6	2.89000E-6
.045	8.62000E-6	7.62000E-6	6.19000E-6	4.08000E-6
.05	1.17000E-5	1.04000E-5	8.43000E-6	5.55000E-6
.055	1.55000E-5	1.37000E-5	1.11000E-5	7.33000E-6
.06	1.99000E-5	1.76000E-5	1.43000E-5	9.43000E-6
.065	2.51000E-5	2.22000E-5	1.81000E-5	1.19000E-5
.07	3.11000E-5	2.75000E-5	2.24000E-5	1.47000E-5
.075	.000038	3.36000E-5	2.73000E-5	.000018
.08	4.57000E-5	4.04000E-5	3.28000E-5	2.16000E-5
.085	5.43000E-5	.000048	3.91000E-5	2.57000E-5
.09	.000064	5.65000E-5	.000046	3.03000E-5
.095	7.46000E-5	6.59000E-5	5.36000E-5	3.53000E-5

TABLE QVP-4

WASTE HEAT FØR IDEAL GASES, Q*DO/PO, STANDARD ADIABAT

$$Q = \frac{1}{K-1}\left[\frac{(1+P)^{1/K}}{D} - 1\right]$$

ØVERPRESSURE RATIØ (PS-PO)/PO	WASTE HEAT, Q*DO/PO TETRATØMIC K=11/9	TRIATØMIC K=9/7	DIATØMIC K=7/5	MØNØATØMIC K=5/3
.001	1.01000E-10	8.95000E-11	7.28000E-11	4.79000E-11
.0011	1.35000E-10	1.19000E-10	9.68000E-11	6.38000E-11
.0012	1.75000E-10	1.55000E-10	1.26000E-10	8.28000E-11
.0013	2.22000E-10	1.96000E-10	1.60000E-10	1.05000E-10
.0014	2.78000E-10	2.45000E-10	2.00000E-10	1.31000E-10
.0015	3.42000E-10	3.02000E-10	2.45000E-10	1.62000E-10
.0016	4.14000E-10	3.66000E-10	2.98000E-10	1.96000E-10
.0017	4.97000E-10	4.39000E-10	3.57000E-10	2.35000E-10
.0018	5.90000E-10	5.21000E-10	4.24000E-10	2.79000E-10
.0019	6.94000E-10	6.13000E-10	4.99000E-10	3.28000E-10
.002	8.09000E-10	7.15000E-10	5.81000E-10	3.83000E-10
.0022	1.08000E-9	9.51000E-10	7.74000E-10	5.09000E-10
.0024	1.40000E-9	1.23000E-9	1.00000E-9	6.61000E-10
.0026	1.78000E-9	1.57000E-9	1.28000E-9	8.40000E-10
.0028	2.22000E-9	1.96000E-9	1.59000E-9	1.05000E-9
.003	2.73000E-9	2.41000E-9	1.96000E-9	1.29000E-9
.0032	3.31000E-9	2.92000E-9	2.38000E-9	1.57000E-9
.0034	3.97000E-9	3.50000E-9	2.85000E-9	1.88000E-9
.0036	4.71000E-9	4.16000E-9	3.38000E-9	2.23000E-9
.0038	5.53000E-9	4.89000E-9	3.98000E-9	2.62000E-9
.004	6.45000E-9	5.70000E-9	4.64000E-9	3.05000E-9
.0045	9.18000E-9	8.11000E-9	6.60000E-9	4.34000E-9
.005	1.26000E-8	1.11000E-8	9.04000E-9	5.96000E-9
.0055	1.67000E-8	1.48000E-8	1.20000E-8	7.92000E-9
.006	2.17000E-8	1.92000E-8	1.56000E-8	1.03000E-8
.0065	2.76000E-8	2.44000E-8	1.98000E-8	1.31000E-8
.007	3.44000E-8	3.04000E-8	2.47000E-8	1.63000E-8
.0075	4.23000E-8	3.74000E-8	3.04000E-8	2.00000E-8
.008	5.13000E-8	4.53000E-8	3.69000E-8	2.43000E-8
.0085	6.15000E-8	5.43000E-8	4.42000E-8	2.91000E-8
.009	7.30000E-8	6.45000E-8	5.24000E-8	3.45000E-8
.0095	8.57000E-8	7.58000E-8	6.16000E-8	4.06000E-8

TABLE QVP-5

WASTE HEAT FØR IDEAL GASES, Q*DO/PO, STANDARD ADIABAT

$$Q = \frac{1}{K-1}\left[\frac{(1+P)^{1/K}}{D} - 1\right]$$

ØVERPRESSURE RATIØ (PS-PO)/PO	WASTE HEAT, Q*DO/PO TETRATØMIC K=11/9	TRIATØMIC K=9/7	DIATØMIC K=7/5	MØNØATØMIC K=5/3
.01	9.99000E-8	8.83000E-8	7.18000E-8	4.73000E-8
.011	1.33000E-7	1.17000E-7	9.54000E-8	6.28000E-8
.012	1.72000E-7	1.52000E-7	1.24000E-7	8.15000E-8
.013	2.19000E-7	1.93000E-7	1.57000E-7	1.03000E-7
.014	2.73000E-7	2.41000E-7	1.96000E-7	1.29000E-7
.015	3.35000E-7	2.96000E-7	2.41000E-7	1.58000E-7
.016	4.06000E-7	3.58000E-7	2.92000E-7	1.92000E-7
.017	4.86000E-7	4.29000E-7	3.49000E-7	2.30000E-7
.018	5.76000E-7	5.09000E-7	4.14000E-7	2.73000E-7
.019	6.76000E-7	5.98000E-7	4.86000E-7	3.20000E-7
.02	7.88000E-7	6.96000E-7	5.66000E-7	3.73000E-7
.022	1.05000E-6	9.24000E-7	7.51000E-7	4.95000E-7
.024	1.35000E-6	1.20000E-6	9.72000E-7	6.40000E-7
.026	1.72000E-6	1.52000E-6	1.23000E-6	8.12000E-7
.028	2.14000E-6	1.89000E-6	1.53000E-6	1.01000E-6
.03	2.62000E-6	2.31000E-6	1.88000E-6	1.24000E-6
.032	3.17000E-6	2.80000E-6	2.28000E-6	1.50000E-6
.034	3.79000E-6	3.35000E-6	2.72000E-6	1.79000E-6
.036	4.49000E-6	3.96000E-6	3.22000E-6	2.12000E-6
.038	5.26000E-6	4.65000E-6	3.78000E-6	2.49000E-6
.04	6.12000E-6	5.41000E-6	4.40000E-6	2.90000E-6
.045	8.65000E-6	7.64000E-6	6.22000E-6	4.09000E-6
.05	1.18000E-5	1.04000E-5	8.46000E-6	5.57000E-6
.055	1.56000E-5	1.38000E-5	1.12000E-5	7.37000E-6
.06	2.01000E-5	1.77000E-5	1.44000E-5	9.49000E-6
.065	2.53000E-5	2.24000E-5	1.82000E-5	.000012
.07	3.14000E-5	2.78000E-5	2.26000E-5	1.49000E-5
.075	3.84000E-5	3.39000E-5	2.76000E-5	1.82000E-5
.08	4.62000E-5	4.09000E-5	3.32000E-5	2.19000E-5
.085	5.51000E-5	4.87000E-5	3.96000E-5	2.61000E-5
.09	6.49000E-5	5.74000E-5	4.66000E-5	3.07000E-5
.095	7.58000E-5	.000067	5.45000E-5	3.59000E-5

TABLE QVP-6

WASTE HEAT FØR IDEAL GASES, Q*DO/PO, STANDARD ADIABAT

$$Q = \frac{1}{K-1}\left[\frac{(1+P)^{1/K}}{D} - 1\right]$$

ØVERPRESSURE RATIØ (PS-PO)/PO	WASTE HEAT, Q*DO/PO TETRATØMIC K=11/9	TRIATØMIC K=9/7	DIATØMIC K=7/5	MØNØATØMIC K=5/3
.1	8.78000E-5	7.76000E-5	6.31000E-5	4.15000E-5
.11	.000115	.000102	8.28000E-5	5.45000E-5
.12	.000148	.00013	.000106	6.98000E-5
.13	.000185	.000164	.000133	8.76000E-5
.14	.000228	.000202	.000164	.000108
.15	.000277	.000245	.000199	.000131
.16	.000332	.000293	.000238	.000157
.17	.000393	.000347	.000282	.000186
.18	.00046	.000406	.00033	.000217
.19	.000534	.000472	.000383	.000252
.2	.000615	.000543	.000441	00029
.22	.000798	.000704	.000573	.000377
.24	.00101	.000892	.000725	.000477
.26	.00125	.00111	.000899	.000591
.28	.00153	.00135	.0011	.00072
.3	.00183	.00162	.00131	.000864
.32	.00217	.00192	.00156	.00102
.34	.00254	.00225	.00182	.0012
.36	.00295	.0026	.00212	.00139
.38	.00339	.00299	.00243	.0016
.4	.00387	.00341	.00277	.00182
.45	.00521	.00459	.00373	.00245
.5	.00677	.00597	.00484	.00318
.55	.00855	.00754	.00611	.00401
.6	.0105	.0093	.00754	.00494
.65	.0128	.0112	.00912	.00597
.7	.0152	.0134	.0108	.0071
.75	.0178	.0157	.0127	.00831
.8	.0206	.0182	.0147	.00962
.85	.0237	.0208	.0169	.011
.9	.0269	.0237	.0192	.0125
.95	.0303	.0267	.0216	.0141

TABLE QVP-7

WASTE HEAT FØR IDEAL GASES, Q*DO/PO, STANDARD ADIABAT

$$Q = \frac{1}{K-1}\left[\frac{(1+P)^{1/K}}{D} - 1\right]$$

ØVERPRESSURE RATIØ (PS-PO)/PO	WASTE HEAT, Q*DO/PO TETRATØMIC K=11/9	TRIATØMIC K=9/7	DIATØMIC K=7/5	MØNØATØMIC K=5/3
1.	.0339	.0298	.0241	.0157
1.1	.0416	.0366	.0295	.0192
1.2	.05	.0439	.0354	.023
1.3	.059	.0518	.0418	.0271
1.4	.0685	.0602	.0485	.0314
1.5	.0786	.069	.0555	.0359
1.6	.0893	.0783	.0629	.0407
1.7	.1	.088	.0707	.0456
1.8	.112	.098	.0787	.0507
1.9	.124	.108	.087	.056
2.	.136	.119	.0956	.0614
2.2	.162	.142	.113	.0727
2.4	.189	.165	.132	.0844
2.6	.217	.19	.151	.0965
2.8	.247	.215	.171	.109
3.	.277	.241	.192	.122
3.2	.308	.268	.213	.135
3.4	.34	.295	.234	.148
3.6	.372	.323	.256	.161
3.8	.405	.352	.278	.175
4	.439	.38	.3	.188
4.5	.525	.454	.358	.223
5.	.613	.529	.416	.258
5.5	.703	.606	.475	.293
6.	.795	.684	.534	.329
6.5	.888	.763	.594	.364
7.	.981	.842	.655	.399
7.5	1.08	.922	.715	.435
8.	1.17	1.	.775	.47
8.5	1.27	1.08	.836	.504
9.	1.36	1.16	.896	.539
9.5	1.46	1.24	.957	.574

TABLE QVP-8

WASTE HEAT FØR IDEAL GASES, Q*DO/PO, STANDARD ADIABAT

$$Q = \frac{1}{K-1}\left[\frac{(1+P)^{1/K}}{D} - 1\right]$$

ØVERPRESSURE RATIØ (PS-PO)/PO	WASTE HEAT, Q*DO/PO TETRATØMIC K=11/9	TRIATØMIC K=9/7	DIATØMIC K=7/5	MØNØATØMIC K=5/3
10.	1.56	1.32	1.02	.608
11.	1.75	1.49	1.14	.675
12.	1.94	1.65	1.26	.742
13.	2.14	1.81	1.37	.808
14.	2.33	1.97	1.49	.872
15.	2.52	2.13	1.61	.936
16.	2.72	2.28	1.72	.999
17.	2.91	2.44	1.84	1.06
18.	3.1	2.6	1.95	1.12
19.	3.29	2.76	2.06	1.18
20.	3.48	2.91	2.18	1.24
22.	3.86	3.22	2.4	1.36
24.	4.24	3.53	2.62	1.47
26.	4.61	3.83	2.83	1.58
28.	4.98	4.13	3.04	1.69
30.	5.35	4.42	3.25	1.8
32.	5.72	4.72	3.45	1.9
34.	6.08	5.01	3.66	2.
36.	6.44	5.3	3.86	2.1
38.	6.8	5.58	4.05	2.2
40	7.15	5.86	4.25	2.3
45.	8.04	6.56	4.73	2.53
50.	8.9	7.25	5.2	2.76
55.	9.76	7.92	5.65	2.98
60.	10.6	8.58	6.1	3.19
65.	11.4	9.24	6.54	3.39
70.	12.3	9.88	6.97	3.59
75.	13.1	10.5	7.39	3.79
80.	13.9	11.1	7.81	3.98
85.	14.7	11.8	8.22	4.17
90.	15.5	12.4	8.62	4.35
95.	16.3	13.	9.02	4.53

TABLE QVP-9

WASTE HEAT FØR IDEAL GASES, Q*DO/PO, STANDARD ADIABAT

$$Q = \frac{1}{K-1}\left[\frac{(1+P)^{1/K}}{D} - 1\right]$$

ØVERPRESSURE RATIØ (PS-PO)/PO	WASTE HEAT, Q*DO/PO TETRATØMIC K=11/9	TRIATØMIC K=9/7	DIATØMIC K=7/5	MØNØATØMIC K=5/3
100.	17.1	13.6	9.41	4.7
110.	18.6	14.8	10.2	5.04
120.	20.1	15.9	10.9	5.37
130.	21.6	17.1	11.7	5.69
140.	23.1	18.2	12.4	6.
150.	24.6	19.3	13.1	6.3
160.	26.	20.4	13.8	6.59
170.	27.5	21.5	14.5	6.88
180.	28.9	22.5	15.1	7.16
190.	30.3	23.6	15.8	7.43
200.	31.7	24.6	16.4	7.7
220.	34.4	26.7	17.7	8.23
240.	37.1	28.7	19.	8.73
260.	39.8	30.7	20.2	9.22
280.	42.5	32.6	21.4	9.69
300.	45.1	34.5	22.5	10.2
320.	47.6	36.4	23.7	10.6
340.	50.2	38.3	24.8	11.
360.	52.7	40.1	25.9	11.5
380.	55.2	41.9	27.	11.9
400	57.7	43.7	28.1	12.3
450.	63.8	48.1	30.7	13.3
500.	69.7	52.4	33.2	14.2
550.	75.6	56.6	35.7	15.2
600.	81.4	60.8	38.1	16.
650.	87.1	64.8	40.5	16.9
700.	92.7	68.8	42.8	17.7
750.	98.2	72.7	45.1	18.5
800.	104	76.6	47.3	19.3
850.	109	80.4	49.4	20.1
900.	114	84.2	51.6	20.8
950.	120	87.9	53.7	21.5

TABLE QVP-10

WASTE HEAT Q FØR REAL AIR

$$\frac{Q}{P_o V_o} = 10^{\frac{(22-L)(L-1)}{16}} , 10^{\frac{(21.75-L)(L-1)}{16}}$$

$$L = \log_{10} (P)$$

ØVERPRESSURE RATIØ (P	IDEAL AIR	WASTE HEAT, Q/POVO PARAMETER 22	PARAMETER 21.75
1.	.0241	.0422	.0437
1.1	.0295	.0483	.05
1.2	.0354	.0548	.0566
1.3	.0418	.0614	.0634
1.4	.0485	.0682	.0703
1.5	.0555	.0752	.0775
1.6	.0629	.0824	.0848
1.7	.0707	.0897	.0923
1.8	.0787	.0972	.0999
1.9	.087	.105	.108
2.	.0956	.113	.116
2.2	.113	.129	.132
2.4	.132	.145	.149
2.6	.151	.162	.166
2.8	.171	.18	.184
3.	.192	.198	.202
3.2	.213	.216	.22
3.4	.234	.235	.239
3.6	.256	.254	.258
3.8	.278	.274	.278
4	.3	.294	.298
4.5	.358	.345	.349
5.	.416	.397	.402
5.5	.475	.452	.456
6.	.534	.508	.512
6.5	.594	.565	.569
7.	.655	.624	.627
7.5	.715	.684	.687
8.	.775	.745	.748
8.5	.836	.807	.809
9.	.896	.871	.872
9.5	.957	.935	.936

TABLE QVP-11

WASTE HEAT Q FØR REAL AIR

$$\frac{Q}{P_o V_o} = 10^{\frac{(22-L)(L-1)}{16}} , \; 10^{\frac{(21.75-L)(L-1)}{16}}$$

$$L = \log_{10}(P)$$

ØVERPRESSURE RATIØ (P	IDEAL AIR	WASTE HEAT, Q/POVO PARAMETER 22	PARAMETER 21.75
10.	1.02	1.	1.
11.	1.14	1.13	1.13
12.	1.26	1.27	1.27
13.	1.37	1.41	1.4
14.	1.49	1.55	1.54
15.	1.61	1.7	1.68
16.	1.72	1.84	1.83
17.	1.84	1.99	1.97
18.	1.95	2.14	2.12
19.	2.06	2.3	2.27
20.	2.18	2.45	2.43
22.	2.4	2.77	2.73
24.	2.62	3.09	3.05
26.	2.83	3.42	3.37
28.	3.04	3.75	3.69
30.	3.25	4.09	4.02
32.	3.45	4.44	4.36
34.	3.66	4.79	4.69
36.	3.86	5.14	5.04
38.	4.05	5.49	5.38
40	4.25	5.86	5.73
45.	4.73	6.77	6.61
50.	5.2	7.71	7.52
55.	5.65	8.66	8.43
60.	6.1	9.63	9.36
65.	6.54	10.6	10.3
70.	6.97	11.6	11.3
75.	7.39	12.6	12.2
80.	7.81	13.6	13.2
85.	8.22	14.7	14.2
90.	8.62	15.7	15.2
95.	9.02	16.7	16.2

TABLE QVP-12

WASTE HEAT Q FØR REAL AIR

$$\frac{Q}{P_o V_o} = 10^{\frac{(22-L)(L-1)}{16}} , \; 10^{\frac{(21.75-L)(L-1)}{16}}$$

$$L = \log_{10}(P)$$

ØVERPRESSURE RATIØ (P	IDEAL AIR	WASTE HEAT, Q/POVO PARAMETER 22	PARAMETER 21.75
100.	9.41	17.8	17.2
110.	10.2	19.9	19.2
120.	10.9	22.1	21.2
130.	11.7	24.2	23.3
140.	12.4	26.4	25.4
150.	13.1	28.7	27.5
160.	13.8	30.9	29.6
170.	14.5	33.1	31.7
180.	15.1	35.4	33.8
190.	15.8	37.7	36.
200.	16.4	40.	38.1
220.	17.7	44.6	42.5
240.	19.	49.3	46.9
260.	20.2	54.	51.3
280.	21.4	58.7	55.7
300.	22.5	63.4	60.2
320.	23.7	68.2	64.6
340.	24.8	73.	69.1
360.	25.9	77.9	73.6
380.	27.	82.7	78.1
400	28.1	87.6	82.7
450.	30.7	99.8	94.
500.	33.2	112	105
550.	35.7	124	117
600.	38.1	137	128
650.	40.5	149	140
700.	42.8	162	151
750.	45.1	174	163
800.	47.3	187	174
850.	49.4	199	186
900.	51.6	212	198
950.	53.7	225	209

TABLE QVP-13

WASTE HEAT Q FØR REAL AIR

$$\frac{Q}{P_o V_o} = 10^{\frac{(22-L)(L-1)}{16}} , \; 10^{\frac{(21.75-L)(L-1)}{16}}$$

$$L = \log_{10}(P)$$

ØVERPRESSURE RATIØ (P	IDEAL AIR	WASTE HEAT, Q/POVO PARAMETER 22	PARAMETER 21.75
1000.	55.8	237	221
1100.	59.8	262	244
1200.	63.8	288	267
1300.	67.7	313	290
1400.	71.5	338	313
1500.	75.2	363	336
1600.	78.8	388	359
1700.	82.4	414	382
1800.	85.9	439	404
1900.	89.4	464	427
2000.	92.8	489	450
2200.	99.5	539	495
2400.	106	589	540
2600.	112	638	585
2800.	119	688	630
3000.	125	737	675
3200.	131	787	719
3400.	137	836	763
3600.	142	885	807
3800.	148	933	851
4000	154	982	894
4500.	167	1100	1000
5000.	181	1220	1110
5500.	193	1340	1210
6000.	206	1460	1320
6500.	218	1580	1420
7000.	230	1690	1530
7500.	242	1810	1630
8000.	253	1920	1730
8500.	265	2030	1830
9000.	276	2150	1930
9500.	287	2260	2030

TABLE QVP-14

WASTE HEAT Q FØR REAL AIR $\frac{Q}{P_o V_o} = 10^{\frac{(22-L)(L-1)}{16}}$, $10^{\frac{(21.75-L)(L-1)}{16}}$

$L = \log_{10}(P)$

ØVERPRESSURE RATIØ (P	IDEAL AIR	WASTE HEAT, Q/POVO PARAMETER 22	PARAMETER 21.75
10000.	298	2370	2130
11000.	319	2590	2320
12000.	339	2810	2520
13000.	359	3030	2710
14000.	379	3240	2890
15000.	398	3450	3080
16000.	417	3660	3260
17000.	436	3870	3450
18000.	454	4080	3630
19000.	472	4280	3800
20000.	490	4480	3980
22000.	524	4880	4330
24000.	558	5280	4670
26000.	591	5670	5010
28000.	623	6050	5340
30000.	655	6430	5670
32000.	686	6800	6000
34000.	716	7170	6320
36000.	746	7540	6630
38000.	776	7900	6940
40000	805	8260	7250
45000.	876	9140	8010
50000.	944	9990	8750
55000.	1010	10800	9470
60000.	1080	11700	10200
65000.	1140	12500	10900
70000.	1200	13300	11500
75000.	1260	14000	12200
80000.	1320	14800	12900
85000.	1380	15600	13500
90000.	1440	16300	14200
95000.	1490	17100	14800

TABLE QVP-15

WASTE HEAT Q FØR REAL AIR

$$\frac{Q}{P_o V_o} = 10^{\frac{(22-L)(L-1)}{16}} \quad , \quad 10^{\frac{(21.75-L)(L-1)}{16}}$$

$$L = \log_{10}(P)$$

ØVERPRESSURE RATIØ (P	IDEAL AIR	WASTE HEAT, Q/POVO PARAMETER 22	PARAMETER 21.75
100000.	1550	17800	15400
110000.	1660	19200	16600
120000.	1770	20600	17800
130000.	1870	22000	18900
140000.	1970	23300	20100
150000.	2070	24600	21200
160000.	2170	25900	22300
170000.	2270	27200	23300
180000.	2360	28400	24400
190000.	2450	29600	25400
200000.	2550	30800	26400
220000.	2730	33200	28400
240000.	2900	35500	30300
260000.	3070	37700	32200
280000.	3240	39900	34000
300000.	3400	42000	35800
320000.	3560	44100	37500
340000.	3720	46200	39200
360000.	3880	48200	40900
380000.	4030	50100	42500
400000	4180	52100	44100
450000.	4550	56800	48000
500000.	4900	61300	51800
550000.	5250	65700	55400
600000.	5580	69900	58800
650000.	5910	74000	62200
700000.	6230	78000	65500
750000.	6550	81900	68700
800000.	6860	85700	71800
850000.	7160	89400	74800
900000.	7460	93000	77800
950000.	7750	96500	80700

TABLE QVP-16

LIST, QVP506, FOR WASTE HEAT OF GASES

```
0     LET S=0
1     REM  LET S=0 IN LINE 0 RØUTES CALCULATIØN FØR IDEAL GAS
2     REM  LET S=1 RØUTES CALCULATIØN FØR REAL AIR.  MANY ØPTIØNS ARE
3     REM  AVAILABLE TØ RØUTE FØR SPECIAL CASES, E.G.
4     REM   IF P<.01 THEN 320, IF P>380 THEN 380 ETC.
10    LET A(1)=1
20    LET A(2)=2
30    LET A(3)=5
32    LET K(1)=11/9
33    LET K(2)=9/7
34    LETK(3)= 7/5
35    LET K(4)=5/3
40    LET N=.43429448
50    LET  J=2
60    DEFFNI(Q)=INT(10↑(N*LØG(Q)-INT(N*LØG(0))+J)+.5)*10↑INT(N*LØG(Q)-J)
90    IF S>0 THEN 100
95    PRINT"WASTE HEAT FØR IDEAL GASES, STANDARD ADIABATIC EXPANSIØN"
96    GØTØ 101
100   PRINT"WASTE HEAT Q FØR REAL AIR"
101   PRINT
102   PRINT
103   PRINT
104   PRINT
105   PRINT
140   PRINT"ØVERPRESSURE","     "     ,"WASTE HEAT, Q/POVO"
145   IF S>0 THEN 170
150   PRINT"RATIØ","TETRATØMIC","TRIATØMIC","DIATØMIC","MØNØATØMIC"
155   PRINT"(PS-PO)/PO","K=11/9","K=9/7","K=7/5","K=5/3"
160   GØTØ 199
170   PRINT"RATIØ","IDEAL AIR","PARAMETER","PARAMETER"
180   PRINT"(PS-PO)/PO","K=7/5","    =22","    =21.75"
```

TABLE QVP-16 (Con'd)

LIST, QVP506, FOR WASTE HEAT OF GASES

```
190    LET K=1.4
199    PRINT
200    FØR C=-3 TØ 2
220    FØR I=1 TØ 3
230    FØR X=.8 TØ 1.9 STEP .1
240    IF I=3 THEN 260
250    IF X<.99 THEN 410
260    LET P=X*A(I)*10↑C
270    PRINT P,
280    IF S>0 THEN 300
290    FØR M= 1 TØ 4
295    LET K=K(M)
300    GØTØ 350
310    IF P>.01 THEN 350
320    LET Q=(K+1)/12*((P/K)↑3)*(1-1.5*P)
330    GØTØ 400
340    PRINT
350    LET D= (P*(K+1)/(K-1) + 2*K/(K-1))/(P +2*K/(K-1))
360    LET Q=((1+P)↑(1/K))/D/(K-1) -1/(K-1)
370    PRINT FNI(Q),
375    IF S=0 THEN 405
380    LET L=.43429448*LØG(P)
390    LET Q= 10↑((22-L)*(L-1)/16)
395    PRINT FNI(Q),
398    LET Q= 10↑((21.75-L)*(L-1)/16)
400    PRINT FNI(Q)
402    IF S>0 THEN 410
405    NEXT M
410    NEXT X
420    PRINT
430    NEXT I
440    PRINT
450    NEXT C
**READY.
```

TABLE QVP-17

NOMENCLATURE FOR QVP506

A(I) = multipliers of the basic sequence 1, 1.1, 1.2, 1.3, 1.4, 1.5, 1.6, 1.7, 1.8, 1.9 for generating pressures as listed

C = counter for multiplying P by factor 10^C

D = shock density ratio, defined as in DEB506 or DSC506

FNI(Ø) = equation for rounding off Q, Ø = $\log_{10}(Q)$, to J+1 significant figures

I = integer counter

J = parameter, for use with FNI(Ø) for rounding off Q. To J+1 significant figures

L = $\text{Log}_{10}(P)$

K,K(I) = adabatic exponent $K = \left(\frac{d\ln P}{d\ln \rho}\right)_Q$

M = counter for K(1), K(2), K(3), K(4)

Q = normalized waste heat, i.e., Q/P_oV_o

Ø = dummy variable in FNI(Ø)

P = overpressure ratio to ambient

L1, L2, L3 = respective values for Ø = $\log_{10}$ (Q)

x = counter for increments of pressure in the basic sequence 0.8, 0.9, 1.0 ...1.9

DISTRIBUTION

	Copies
Commander Naval Ordnance Systems Command Washington, D. C. 20360	
Attn: NORD-9132 , NORD-0523 NORD-0332 NORD-034 NORD-082 NORD-035 NORD-05411 NORD-033	2 7
Commander Naval Air Systems Command Washington, D. C. 20360	
Attn: NAIR-604 NAIR-350 NAIR-52023 NAIR-53233	 4
Commander Naval Ship Systems Command Washington, D. C. 20360	
Attn: NSHP-2021 NSHP-6423 NSHP-0331 NSHP-0342 NSHP-0412	 5
Officer-in-Charge Naval School Civil Engineering Corps Officers Naval Construction Battalion Port Hueneme, California 93041	
Commander Naval Ship Engineering Center Prince Georges Center Hyattsville, Maryland 20782	
Attn: NSEC-6105	4
Commander Naval Ship Research and Development Center Bethesda, Maryland 20034	
Attn: Library, E. Habib, H. Rich, F. Weinberger	5
Chief of Naval Research Department of the Navy Washington, D. C. 20390	
Attn: Code 811	2
Code 493, Code 418, Code 104	3

DISTRIBUTION (Con'd)

	Copies
Headquarters Naval Material Command Washington, D. C. 20360 Attn: 03L	
Commanding Officer Nuclear Weapons Training Center, Atlantic Naval Base Norfolk, Virginia 23500 Attn: Nuclear Warfare Department	
Commanding Officer Nuclear Weapons Training, Pacific Naval Station North Island San Diego, California 92100	2
Commanding Officer Naval Damage Control Training Center Naval Base Philadephia, Pennsylvania 19100 Attn: ABC Defense Course	
Commander Naval Weapons Center China Lake, California 93555 Attn: Library, R. E. Boyer, Dr. Mallory, Dr. J. Pearson	4
Commanding Officer Naval Civil Engineering Laboratory Port Hueneme, California 93043 Attn: Code L31, R. J. Odello (Code L51)	2
Chief of Naval Operations Department of the Navy Washington, D. C. 20350 Attn: OP-985 OP-03EG	2
Director of Naval Intelligence Department of the Navy Washington, D. C. 20350 Attn: OP-922V	
Commander Naval Weapons Evaluation Facility Kirtland AFB, New Mexico 87117 Attn: Library, (WEVS)	2

DISTRIBUTION (Con'd)

	Copies
Commanding Officer Naval Ordnance Station Indian Head, Maryland 20640 Attn: Library	
Commander Naval Weapons Laboratory Dahlgren, Virginia 22448 Attn: Terminal Ballistics Department Technical Library	1 2
Commander, Naval Facilities Engineering Command Headquarters Washington, D. C. 20390 Attn: Code 03	
Superintendent Naval Postgraduate School Monterey, California 93940	
Underwater Explosions Research Division Naval Ship Research and Development Center Portsmouth, Virginia 23709	
Commander Naval Air Development Center Warminster, Pennsylvania 18974	
Director Naval Research Laboratory Washington, D. C. 20390 Attn: Technical Information Section	
Chief of Research and Development Department of the Army Washington, D. C. 20310 Attn: Lt. Gen. W. Gribble Atomic Division	 2
Commanding General USA Missile Command Huntsville, Alabama 35801	
Commanding General White Sands Missile Range White Sands, New Mexico 88002 Attn: STEWS-AMTED-2	
Chief of Engineers Department of the Army Washington, D. C. 20310 Attn: ENGCW-NE, ENGTE-E,ENGMC-E	 3

DISTRIBUTION (Con'd)

	Copies
Commanding General U. S. Army Materiel Command Washington, D. C. 20310 Attn: AMCRD-DE-N	2
Commanding Officer U. S. Army Combat Developments Command Institute of Nuclear Studies Ft. Bliss, Texas 79916	
Commanding Officer Aberdeen Proving Ground Aberdeen, Maryland 21005 Attn: BRL for Director, J. J. Meszaros W. J. Taylor, R. E. Shear, B. Cummings C. N. Kingery, J. H. Keefer, R. E. Reisler	7
Commanding General The Engineer Center Ft. Belvoir, Virginia 22060 Attn: Asst. Commandant, Engineer School	
Commanding Officer Picatinny Arsenal Dover, N. J. 07801 Attn: SMUPA-G,-W,-VL,-VE,-VC,-DD,-DM -DR,-DR4,-DW,-TX,-TW,-V	7 6
Director U. S. Army Corps of Engineers Waterways Experiment Station Vicksburg, Mississippi 39180 Attn: Library, John Strange, G. Arbuthnot	3
Commanding Officer U.S. Army Mobility Equipment R&D Center Ft. Belvoir, Virginia 22060 Attn: Technical Document Center	3
Commandant Army War College Carlisle Barracks, Pennsylvania 17013 Attn: Library	
Commanding Officer Army Engineer Nuclear Cratering Group Lawrence Livermore Laboratory Livermore, California 94550 Attn: Document Control, CAPT Johnson	2

DISTRIBUTION (Con'd)

Copies

Commanding General
Army Safeguard System Command
P. O Box 1500
Huntsville, Alabama 35807
Attn: SAFSC-DB, Ltc. W. Alfonte

Commanding Officer
Army Safeguard System Evaluation Agency
White Sands Missile Range, New Mexico 88002
Attn: LT R. M. Walker

Commandant
Army Command & General Staff College
Fort Leavenworth, Kansas 66027
Attn: Acquisitions, Library Division

Commanding Officer
Frankford Arsenal
Bridge and Tacony Streets
Philadelphia, Pennsylvania 19137

AFWL
Kirtland AFB, New Mexico 87117
Attn: WLRPH, MAJ W. Whitaker, CAPT R. E. Langsdale 5

Headquarters
Air Force Systems Command
Andrews AFB, Washington, D. C. 20331
Attn: SCPSL, Technical Library

AF Cambridge Research Laboratories, OAR
L. G. Hanscom Field
Bedford, Massachusetts 01730
Attn: CRMXLR, Research Library, Stop 29

AF Institute of Technology, Au
Wright-Patterson AFB, Ohio 45433
Attn: Technical Library

Air Force Special Weapons Center, AFSC
Kirtland AFB, New Mexico 87117
Attn: R. Bunker

Commander
Air Research & Development Command
Andrews AFB
Washington, D. C. 20331

Commanding Officer, Air Force Armament Laboratory, RTD
Eglin AFB, Florida 32542
Attn: (Mr. C. Kyselka, Weapons Division
Technology Branch (ATWT)

DISTRIBUTION (Con'd)

	Copies
Air University Library, Au Maxwell AFB, Alabama 36112 Attn: Documents Section	
Rome Air Development Center, AFSC Griffiss AFB, New York 13440 Attn: Documents Library EMLAL-1	
Space & Missile Systems Organization, AFSC Norton AFB, California 92409 Attn: SMQN	5
Director of Defense Research and Engineering Washington, D. C. 20330 Attn: Tech Library, R. D. Geckler	2
Defense Documentation Center Cameron Station Alexandria, Virginia 22314	12
Defense Intelligence Agency Washington, D. C. 20301 Attn: DIAAP-8B	
Commander Defense Nuclear Agency, Headquarters, Field Command Kirtland AFB, New Mexico 87115 Attn: FCWT, FCTG	2
Director Defense Nuclear Agency Washington, D. C. 20305 Attn: SPAS, SPSS	10
Civil Defense Research Project Oak Ridge National Lab P. O. Box X Oak Ridge, Tennessee 37830 Attn: Dr. Carsten Haaland	
Director Advanced Research Projects Agency Washington, D. C. 20301 Attn: NMR Nuclear Monitoring Res. Office	
Commandant Industrial College of the Armed Forces Ft. McNair, Washington, D. C. 20315 Attn: Document Control	

DISTRIBUTION (Con'd)

Copies

Commandant
National War College
Fort Lesley J. McNair
Washington, D. C. 20315
Attn: Class Rec. Library

Assistant to the Secretary of Defense
Atomic Energy
Washington, D. C. 20301
Attn: Document Control

Director of Defense Research & Engineering
Washington, D. C. 20301
Attn: Assistant Director Nuclear Programs

Director Weapons Systems Evaluation Group
Washington, D. C. 20305
Attn: Library

Director
Institute for Defense Analysis
400 Army-Navy Drive
Arlington, Virginia 22202
Attn: Dr. R. Fox
Dr. B. Tucker
Dr. R. Mollander
Dr. L. Schmidt 4

Asst. General Manager for Military Application
Atomic Energy Commission
Washington, D. C. 20543
Attn: Document Control for R&D

Atomic Energy Commission
Albuquerque Operations Office
P. O. Box 5400
Albuquerque, New Mexico 87116
Attn: Technical Library

Los Alamos Scientific Laboratory
P. O. Box 1663
Los Alamos, New Mexico 87544
Attn: LASL Library, Serials Librarian

University of California
Lawrence Livermore Laboratory
P. O. Box 808
Livermore, California 94551
Attn: J. Kury
E. James
M. Wilkins
D. L. Ornellas
H. C. Hornig 7

DISTRIBUTION (Con'd)

	Copies
National Aeronautics and Space Administration Goddard Space Flight Center Greenbelt, Maryland 20771 Attn: Technical Library	
President Sandia Corporation, Sandia Base Albuquerque, New Mexico 87115 Attn: Dr. M. L. Merritt W. B. Bendick W. Roberts J. W. Reed Dr. C. Broyles Dr. J. E. Kennedy	6
Director U. S. Bureau of Mines Division of Explosive Technology 4800 Forbes Street Pittsburgh, Pennsylvania 15231 Attn: Dr. Robert W. Van Dolah Dr. R. W. Watson	2
Chairman Department of Defense Explosives Safety Board NASSIF Bldg., 5616 Columbia Pike Washington, D. C. 20315 Attn: Mr. R. G. Perkins, Dr. T. A. Zaker	2
Department of Physics Stanford Research Institute Menlo Park, California 94025 Attn: Library	
Southwest Research Institute 8500 Culebra Road San Antonio, Texas 78206 Attn: Dr. Robert C. Dehart, Dr. W. Baker	2
Space Technology Laboratories, Inc. 5500 West El Segundo Blvd. Los Angeles, California 90000 Attn: Dr. Leon Via: BSD, Norton AFB, California 94209	
GE-TEMPO P. O. Drawer QQ 816 State Street Santa Barbara, California 93102 Attn: DASA Information and Analysis Center Mr. Warren W. Chan Dr. C. M. Schindler	3

DISTRIBUTION (Con'd)

	Copies
President Kaman Nuclear Colorado Springs, Colorado 80900 Attn: Dr. Frank Shelton	
IIT Research Institute 10 West 35th Street Chicago, Illinois 60616 Attn: D. Andersen H. Napadensky A. Weidermann E. V. Gallagher	4
Denver Research Institute Mechanics Division, University of Denver Denver, Colorado 80210 Attn: Dr. Rodney F. Recht	2
Falcon Research and Development 1225 South Huron Street Denver, Colorado 80223 Attn: Mr. D. K. Parks	
Director New Mexico Institute of Mining Technology Socorro, New Mexico 87801 Attn: Dr. M. Kempton	
URS Corporation 1700 S. El Camino Real San Mateo, California 94401 Attn: Dr. Kenneth Kaplan, Mr. C. Wilton	2
DBS Laboratories High Ridge Road Stamford, Connecticut 06905 Attn: A. J. Rosenheck, A. L. DiMattia, B. B. Bauer	3
U. S. Geological Survey Center of Astrogeology 601 East Cedar Avenue Flagstaff, Arizona 86001 Attn: Dr. D. J. Roddy	
Atlas Chemical Industries Reynolds Experimental Laboratories Tamaqua, Pennsylvania 18252 Attn: N. M. Junk	

DISTRIBUTION (Con'd)

Copies

Bell Telephone Laboratories, Inc.
Whippany Road
Whippany, New Jersey 07981
Attn: M. F. Stevens

The Boeing Company
P. O. Box 3707
Seattle, Washington 98124
Attn: W. Crist

Engineering Physics Company
12721 Twinbrook Parkway
Rockville, Maryland 20852
Attn: Dr. Vincent J. Cushing

General American Transportation Corporation
General American Research Division
7449 North Natchez Avenue
Niles, Illinois 60648
Attn: Dr. T. Schiffman

Kaman Avidyne Division of Kaman Sciences Corporation
83 2nd Avenue Northwest Industrial Park
Burlington, Massachusetts 01803
Attn: N. P. Hobbs

The Rand Corporation
1700 Main Street
Santa Monica, California 90406
Attn: Technical Library

TRW Systems Group
One Space Park
Redondo Beach, California 90278
Attn: H. J. Carpenter

Commanding Officer
Naval Construction Battalion Center
Port Hueneme, California 93041
Attn: Civ Engr Corps Ofc

Commanding Officer & Director
Naval Electronics Lab
San Diego, California 92152

President
Naval War College
Newport, Rhode Island 20840

DISTRIBUTION (Con'd)

Copies

Commandant
U. S. Marine Corps
Washington, D. C. 20380
Attn: Code A03H

AFATL (ATB, PGOW, PGBPS)
Eglin AFB, Florida 32542

Commandant
Armed Forces Staff College
Norfolk, Virginia 23511
Attn: Library

Commanding Officer
Harry Diamond Laboratories
Washington, D. C. 20438
Attn: AMXDO-TD/002

Director
Army Aeronautical Research Laboratory
Moffett Naval Air Station
California 94035

Director of Civil Defense
Department of the Army
Washington, D. C. 20310
Attn: RADLMON

Director
Applied Physics Laboratory
John Hopkins University
8621 Georgia Avenue
Silver Spring, Maryland 20910
Attn: F. K. Hill
L. F. Welanetz
Tech Library

Commanding Officer
U. S. Army Aviation Materiel Laboratories
Fort Eustis, Virginia 23604
Attn: SAVFE-SO, Tech Library Branch

Commanding Officer
U. S. Army Edgewood Arsenal
Edgewood Arsenal, Maryland 21010
Attn: SMUEA-W

Commanding Officer
U. S. Army Materiels and Machanics
Research Center
Watertown, Massachusetts 02172

DISTRIBUTION (Con'd)

Copies

Commanding Officer
U. S. Army Cold Regions Research and
Engineering Laboratories
Hanover, New Hampshire 03755
Attn: Mr. R. Frost, Mr. H. Smith 2

Commanding General
U. S. Army Natick Laboratories
Natick, Massachusetts 01762
ATTN: AMXRE, Dr. Dale H. Sieling

Office of Project Manager
NIKE-X
Redstone Arsenal, Alabama 35809
Attn: Mr. H. Solomonson

Lovelace Foundation
4800 Gibson Blvd., S. E.
Albuquerque, New Mexico 87100
Attn: Dr. D. Richmond

University of Illinois
Talbot Laboratory, Rm. 207
Urbana, Illinois 61803
Attn: Dr. N. Newmark

University of Michigan
Institute of Science and Technology
P. O. Box 618
Ann Arbor, Michigan 48104
Attn: Mr. G. Frantti

Massachusetts Institute of Technology
77 Massachusetts Avenue
Cambridge, Massachusetts 02139
Attn: Dr. R. Hansen

St. Louis University
221 North Grand
St. Louis, Missouri 63100
Attn: Dr. C. Kisslinger

Edgerton, Germeshausen and Grier, Inc.
933 Bradbury Drive, S. E.
Albuquerque, New Mexico 87106
Attn: B. Collins

Sandia Corporation Livermore Lab.
P. O. Box 969
Livermore, California 94550

DISTRIBUTION (Cont'd)

	Copies
Department of Physics Princeton University Princeton, New Jersey 08540 Attn: Profs. J. Wheeler, George Reynolds	1
University of Idaho College of Mines Moscow, Idaho 83843 Attn: Prof. J. Newton	
Edgerton, Germeshausen and Grier, Inc. Crosby Drive Bedford, Massachusetts 01730 Attn: D. Seacord	

Unclassified

Security Classification

DOCUMENT CONTROL DATA - R & D

(Security classification of title, body of abstract and indexing annotation must be entered when the overall report is classified)

1. ORIGINATING ACTIVITY *(Corporate author)*

Naval Ordnance Laboratory
Silver Spring, Maryland 20910

2a. REPORT SECURITY CLASSIFICATION

Unclassified

2b. GROUP

3. REPORT TITLE

Introduction to a Unified Theory of Explosions (UTE)

4. DESCRIPTIVE NOTES *(Type of report and inclusive dates)*

5. AUTHOR(S) *(First name, middle initial, last name)*

Francis B. Porzel

6. REPORT DATE	7a. TOTAL NO. OF PAGES	7b. NO. OF REFS
14 September 1972	271	35

8a. CONTRACT OR GRANT NO.	9a. ORIGINATOR'S REPORT NUMBER(S)
b. PROJECT NO. ORD 332-001/092-1/UF20-354-310	NOLTR 72-209
c.	9b. OTHER REPORT NO(S) *(Any other numbers that may be assigned this report)*
d.	

10. DISTRIBUTION STATEMENT

Approved for public release; distribution unlimited.

11. SUPPLEMENTARY NOTES	12. SPONSORING MILITARY ACTIVITY
	Naval Ordnance Systems Command Washington, D. C. 20360

13. ABSTRACT

The unified theory of explosions offers simple methods for analyses of blast and absolute hydrodynamic yield of explosions in general and similar energy releases. The concepts and techniques apply at any shock strength, in virtually any medium and ambient conditions, and are adaptable to a gamut of burst geometries and warhead configurations. The methods are conveniently summarized by two separate BASIC machine programs, with complete instructions for prediction and evaluation of explosions in air; machine time and research effort are many times more cost effective than with present machine or hand calculations. The methods are illustrated with nuclear and TNT data. Present results indicate that the concepts and techniques are probably valid within a few percent for measuring yield, predicting peak pressure and distance; results are well within the natural variations of blast and well-suited to diagnose non-ideal explosions.

14. KEY WORDS	LINK A		LINK B		LINK C	
	ROLE	WT	ROLE	WT	ROLE	WT
Blast						
Shock Waves						
Nuclear Explosions						
Chemical Explosions						
Scaling						
Yield						
Mass Effect						
Dissipation						
Entropy						
Non-linear Hydrodynamics						
Free Air						
Cased Explosives						
Energy Partition						
Weapon Effects						
Equivalent Weight						

U15